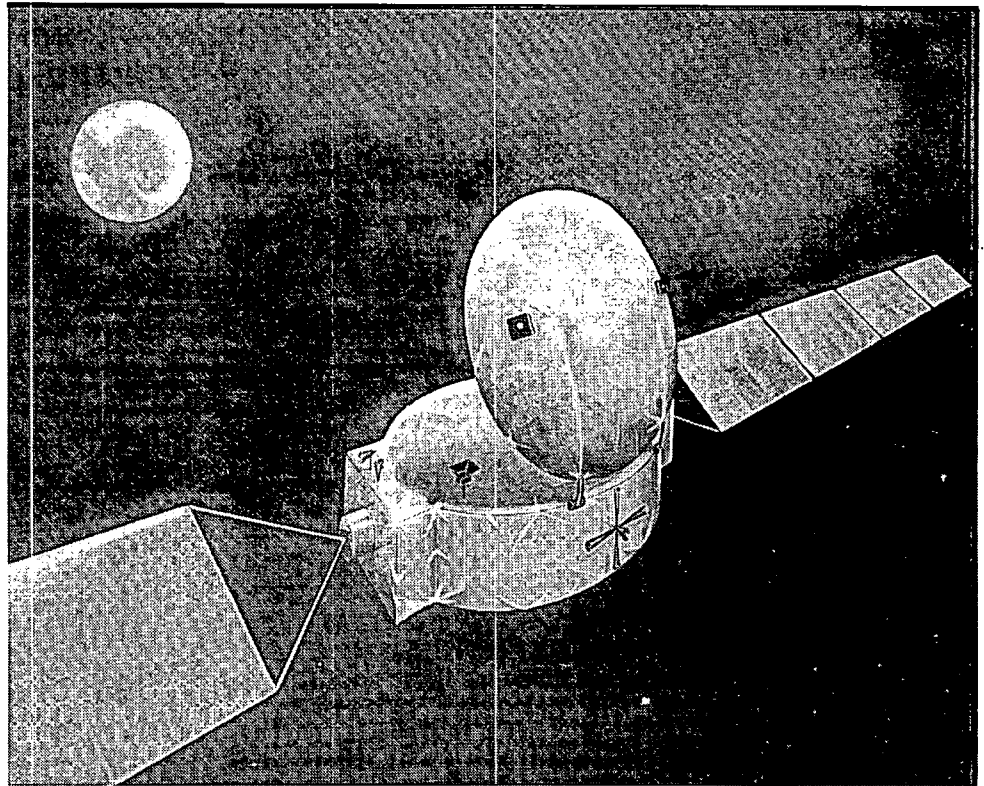Report
LR-644

PROJECT HITCH HIKER

A feasibility study for a small
telecommunication satellite

September 1990

Space system design team of ir. M.P. Nieuwenhuizen

TUDelft

Delft University of Technology

Faculty of Aerospace Engineering

PROJECT HITCH HIKER

A feasibility study for a small
telecommunication satellite

Space system design team of ir. M.P. Nieuwenhuizen
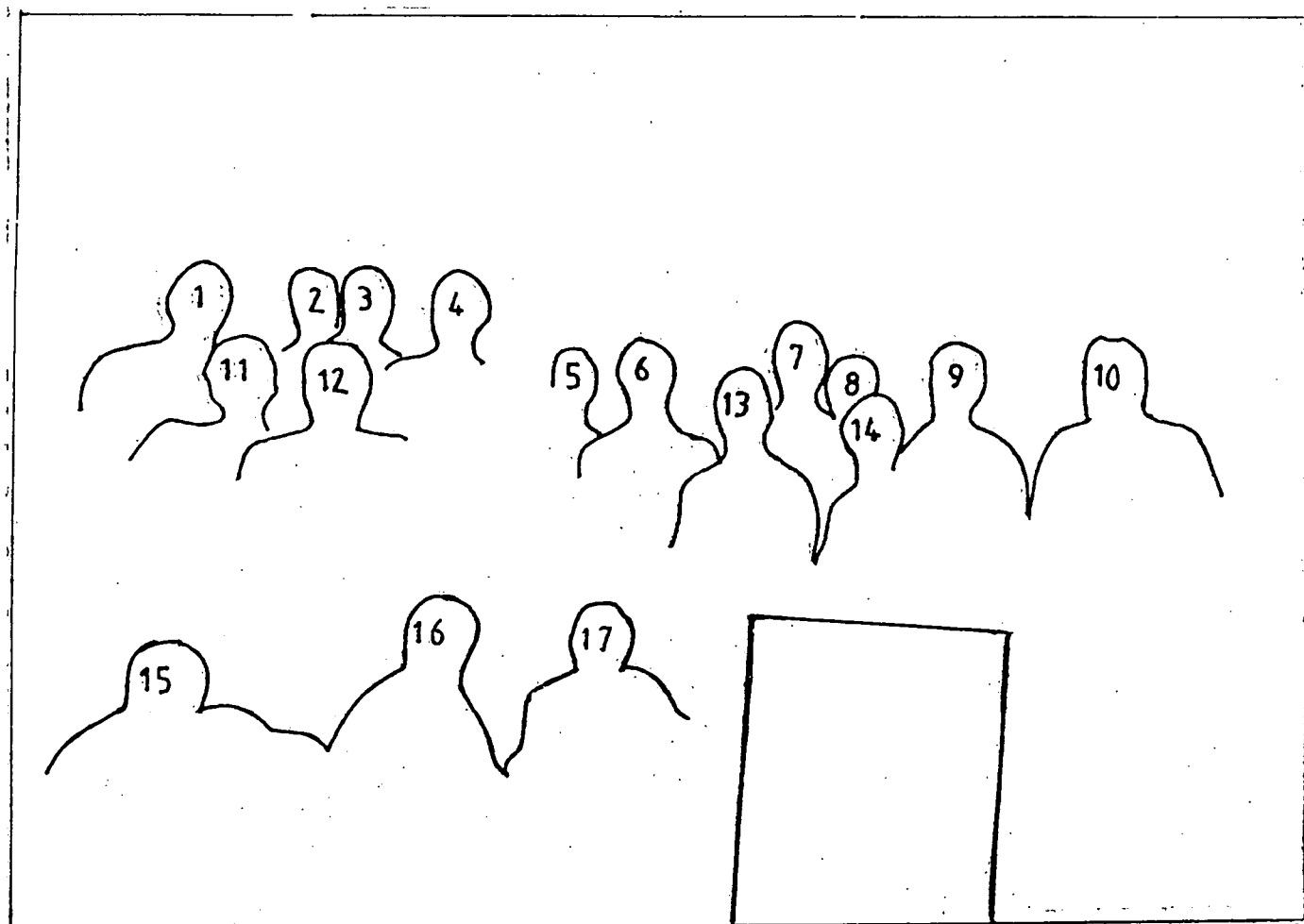
PROJECT HITCH HIKER

A feasibility study for a small telecommunication satellite

By the space system design team of ir. M.P. Nieuwenhuizen

September 1990

Cover Drawing: HANS MAREE

Participants of the hitch-hiker project.

1.	Albert-Jan Bunt	9.	Bas J. Theelen
2.	Steven P. Verhagen	10.	Ir. M.P. Nieuwenhuizen
3.	Dirk de Waart	11.	Guido V. Nierop
4.	Marcel J. Belien	12.	Darwan Shawalli
5.	Erik P. de Heer	13.	Arthur J. Smith
6.	Bryan P. Ho	14.	Renate v Drimmelen
7.	Mark J. v Dijk	15.	Marc Dubbeldam
8.	Eduard P. v d Heuvel	16.	Anton G. Maree
		17.	John L. Mensink

Foreword to Hitch-Hiker.

One of most interesting areas which have recently emerged in the communication satellite business are small satellites for developing countries. It all started some 2 years ago when Arianespace announced that they would launch such satellites as auxiliary payloads for a special promotional price; why would they do this? Because such is the capacity of Ariane 4 these days that they often have spare capacity after taking care of their major passenger(s) satellites.

The other part of the story concerns the developing countries who have been renting satellite communications capacity through the INTELSAT system and are gradually realizing that a tailor made satellite takes care of their increasing requirements. We should also not forget that ownership of one's own satellite system shown that you have reached a certain technical maturity, particularly with respect to the neighbors.

One of the most challenging aspects of designing such a satellite is to pack the satellite into a very compact configuration for launch because, although the spare kilogrammes may be available, the remaining volume is always very tight. It also goes without saying that the major fare paying passengers want to be released from the launch vehicle first, so the Hitch-Hiker goes off last from the bottom of the stack, which means that he has to support the launch loads of the upper passengers which is quite a challenge. The remaining challenge is to design the satellite on a modular basis, so the manufacture and test of the sub-systems can be performed in parallel, this saves valuable time and enables the manufacturer to take advantage of the launch opportunities that appear at short notice, e.g. when launch manifests are being reworked.

Looking at the work described here on Hitch-Hiker, I am impressed by the team's quick response in arriving at a design to the challenging specification and statement of work that we supplied. The degree of detailed work that was produced in some of the sub-systems was also surprising considering the very limited amount of time that they had available for the study. As a training exercise for their future in Industry I am sure the TU DELFT Team will have benefited greatly from this experience.

Dennis L. Brown
ESTEC (ESA)

Table of contents.

Appendices

SUMMARY.

1   Management.

To divide the 16 participating students several clusters are formed in which different sub-systems are worked out. Not all the sub-systems can be covered.

Following an ESA-Statement Of Work (SOW) the project is divided in four tasks. In the first task a stabilization system is chosen. In the second a trade-off is made between launchers and a launch configuration is chosen. In the third task the actual design of the sub-systems takes place. The final task is the writing of a final report.

No manufacture & test programmes are conducted, neither a cost-analysis.

Every week several separate meetings are held and one plenary meeting with all the students.

To support the design-project, a room, a PC and CAD-possibilities are arranged.

To make a planning of the phase A study, three stages are made. The first stage is an orientation of the systems. In the second stage the requirements are defined and in the third stage details are worked out and a verification is performed.

2   System engineering.

The task for the System Engineering group was to establish the requirements for the project and to make sure all the changes were in accordance with these requirements.
Most of the requirements are copied from an ESA specification. Because this specification concerns an innovative modular spacecraft some adjustments are made.
This chapter only consists of an enumeration of the requirements and a mass budget analysis.

3   Launcher and orbit dynamics.

After reviewing the advantages and disadvantages of the Ariane IV and Titan III, the choice of the launcher became the Ariane IV. This choice also determines the separation sequence.

Also is defined the two velocity changes (1.488 km/s and 0.021 km/s) needed to bring the Hitch-Hiker in its operational longitude. Between the two velocity changes the Hitch-Hiker drifts to his operational longitude. This drift orbit lasts for about 23 days.

4 Configuration.

For the optimal functioning of the Hitch-Hiker satellite a good configuration design is required. To match the requirements of the different subsystems four guidelines are made.

Since there are many different designs for the configuration possible, some trade-off's are made which are described in this chapter.

All the subsystems interact with each other, so the whole satellite forms a complete system. In the configuration design this approach is achieved as much as possible.

5 Payload.

The Hitch-hiker satellite communications system is capable of relaying various types of signals with different quality and information density requirements, at only a very small percentage of outage. The satellite can be shared among many users, which are expected to be (major) companies in the main part of Europe, on a TDMA basis and can directly be addressed with small and medium large domestic earth stations. The quality and capacity of the link can be varied according to the customers needs, by adapting the dimensions of the ground station's antenna and equipment. Four standard types of ground stations are available.

The maximum transmission capacity can be achieved with a 4.90 meters ground station, which is capable of transmitting 60 Mbits of digital information per second - which is equivalent with about 1680 one way telephone channels - over one transponder. The bit-error-rate (BER) is 10^{-8}, which is sufficient for high quality purposes. The smallest earth station with a 2.00 meters antenna provides half that capacity and is only capable of transmitting low quality signals (BER = 10^{-5}), like telephony.

The satellite's communications payload employs an antenna of 1.80 meters diameter and uses TWTAs for final amplification. Ten transponders will be operational.

For the TT&C subsystem, 10.0 meters ground stations are required, whereas SSPAs are used for the final amplification.

6 The Electrical Power Subsystem.

For the power supply of the Hitch-Hiker, an electrical power subsystem (EPS) has been designed. The power is obtained by photovoltaic conversion of sunlight in electric power. The EPS consists of a solar array (two wings), two batteries, a power conditioning unit, a power control and distribution unit, two Bearing and Power Transfer Assemblies (BAPTA) and a wiring harness. The main requirements for the EPS are:
- providing 24 hours of communications
- low mass
- low volume (compact)
- high reliability $_\sigma$
- power dump possibility

7 Structure.

The structure subsystem must provide a sufficiently strong and stiff support for all the subsystems. In the structure chapter several structure subsystems are designed and analysed to fulfill this requirement as good as possible.

The different subsystems are cylinder, separation mechanisms, extra rings, platforms, extra support structure, tank support structure and solar array. All of these are described one by one.

The depth of the analysis varies. Most of the time some rough estimations are made, which are nevertheless very valid for a first design study.

8 AOCS.

For the attitude and orbit control system, a configuration has been designed. In the design, a trade off has been made for the stabilization in the transfer orbit and in the normal mode.

For the transfer-orbit a spin stabilization has been chosen. For the normal mode, a three axis stabilized system with reaction wheels has been chosen.

The desaturation of the wheels and the NS/EW station keeping maneuvers will be done by bi-propellant thrusters.
The NS/EW station keeping maneuvers will be done by ground control command. During the station keeping the attitude control will be done by thrusters also.

An acquisition procedure has been worked out.

For measuring the attitude of the S/C, there has been made use of sun sensors, an infrared earth sensor and rate integrating gyros.

The system control will be done by the on board computer (OBC).

For the verification of the designed system, the normal mode and he desaturation mode have been simulated.

9 Thermal control.

A thermal subsystem to keep the Hitch-Hiker spacecraft within the required temperatures has been designed. Calculations of the maximum and minimum temperatures where made with the aid of models. These calculations show that the satellite temperature and the subsystem temperatures are within the required temperature limits without using more heaterpower and mass than the budget allows.

10 Telemetry and telecommand.

A subsystem to provide the Hitch-Hiker spacecraft with capabilities for handling computer generated and TTC data is studied.

The subsystem which has to be developed should perform the following functions:
- station keeping
- telemetry data formatting
- interpretation and distribution of groundcommands
  whereas it should also meet certain requirements specified by ESA.

To realize the two most important goals of reliability and flexibility, the on-board computer is microprogrammable and provided with an expandable structure, while the encoder and decoder allow for "manual control" from Ground Segment.

Some figures characterizing the subsystem are:
-total mass of 26,5 kg
-total power consumption of 32,5 Watts
-code and modulation techniques used are split phase code,
 pulse code modulation, and phase modulation
-bit rate varies from 256 b.p.s. in case of normal mode, up to 1024 b.p.s. when memory is being unloaded

During the design an effort has been made to combine this subsystem with the Payload subsystem.

11 Propulsion.

Worked out is a unified propulsion system (UPS) containing MMH and NTO as propellants. The feedsystem contains helium as pressurizing gas. The apogee engine produces a constant force of 490 N during the apogee kick, which takes 30 minutes.

The attitude control system consists of 12 similar 4.45 N thrusters. Four of them are used for the orbit control, i.e. for east-west and north-south station-keeping, as well. However, in spite of the similarity of these thrusters, the specific impulses are different, because the time of operation of the attitude control thrusters is very short. Therefore they have a lower specific impulse.

The total mass of the propulsion system is 467 kg, which is 58% of the total satellite mass (the 15% overall mass margin excluded).

NOTATIONS.

3 Orbit dynamics.

V_{c_a}	circular velocity at the apogee point	[km/s]
V_{c_p}	circular velocity at the perigee point	[km/s]
V_a	velocity at the apogee point	[km/s]
V_p	velocity at the perigee point	[km/s]
V_b	the apogee velocity in the ellipse	[km/s]
ΔV_a	velocity change in the apogee point	[km/s]
ΔV_p	velocity change in the perigee point	[km/s]
ΔV_{a_1}	the first apogee kick	[km/s]
ΔV_{a_2}	the second apogee kick	[km/s]
ΔV	the full apogee kick	[km/s]
h_p	perigee altitude	[km]
h_a	apogee altitude	[km]
r_p	radius of the perigee	[km]
r_a	radius of the apogee	[km]
R_e	radius of the earth (=6378)	[km]
Λ_o	earth longitude of injection point	[deg]
i	inclination	[deg]
a	semi major axis	
e	eccentricity	
α	angle	[deg]
$\Delta \lambda$	movement of the sub satellite point to the west	[deg]
$\Delta \lambda'$	movement of the subsatellite point to the east	[deg]
Ω	the right ascension of the ascending node	[deg]
ζ	position of the earth in the ecliptic	[deg]
β	the movement from $180°W$ to $12°E$	[deg]
T	orbital period	[s]
T_t	transfer period from perigee to apogee	[h]
P	the period of the drift orbit	[h]
ψ	the period in which the apogee moves from $180°W$ to $12°E$	[h]
μ	earth's gravitational constant	[km³ sec⁻²]

5   Payload.

A	Aperture area of antenna	[m²]
B	Bandwidth	[Hz]
C	Capacity	[bps]
C	Carrier power	[dBW]
c	Speed of light = $3.00 \cdot 10^8$ m/s	
C/I	Carrier-to-interference ratio (CIR)	[dB]
C/N	Carrier-to-noise ratio (CNR)	[dB]
D	Diameter of the antenna	[m]
d	Distance ground station - satellite	[m]
E	EIRP of wanted satellite	[dBW]
E_b	Power per transmitted bit	[dBW/bit]
e	EIRP of interfering satellite	[dBW]
f	Frequency	[Hz]
f	Focal length of the paraboloid	[m]
G	Amplifier gain	[dB]
G_a	Antenna gain	[dB]
G/T	Figure of merit for receiving station	[dB]
I	Intensity	[dBW]
k	Boltzmann's constant = $1.38 \cdot 10^{-23}$ J/K	
L	Loss	[dB]
L_s	Path loss	[dB]
M	Margin	[dB]
N	Noise power	[dBW]
N_0	Noise power per unit bandwidth	[dBW / Hz]
N	Number of sun outages	[days/year]
NF	Noise figure	[dB]
P	Power	[W]
P_b	Probability of bit error	
R	Transmitted symbol-rate	[baud]
R_b	Transmitted data-rate	[bps]
R_c	Transmitted bit-rate	[bps]
r	Code-rate	
T	Effective noise temperature	[K]
T_r	Receiver noise temperature	[K]
T	Maximum duration of sun interference	[minutes]
α	Deviation angle from boresight	[degrees]
β_0	Beamwidth of antenna	[degrees]
δ	Angle of elevation	[degrees]
λ	Wavelength	[m]
η	antenna efficiency	
σ	R.M.S. Antenna surface error	[m]

Indices

a	Antenna
d	Downlink
i	Internal
i	Interference
out	Output
r	Receiver
t	Threshold
t	Transmitter
t	Total
u	Uplink
0	Reference

6   Power.

C	Capacity	[Ah]
I	Current	[I]
I_{sc}	Short circuit current	
N_p	Number of cells in parralel	
N_s	Number of cells in series	
P	Power	[W]
V_{bus}	Bus Voltage	
V_{pm}	Maximum power point voltage	
V	Voltage	[V]
V_{cd}	Battery charger voltage drop	
V_{oc}	Open circuit voltage	
V_{db}	Minimum discharge voltage	
V_{ca}	Boost voltage of charge array	
W	Watt	[W]

7   Structure.

A   cross section area of one pitch of the cylinder
        cross sectional area of ring
        width of the solar panel
        constant dependent of the sort of support and the number of waves
        cross section area of the cylinder
a_{max} maximum acceleration
a(1)   dimensionless frequency
a   width of the platform
        dimensionless width of the solar panel
α   angle of separation parts
        dimensionless distance in X-direction on the solar panel
B   length of the solar panel
b   dimensionless length of the solar panel
        width of the plate of the cylinder
        length of the platform
β   dimensionless distance in Y-direction on the solar panel
D   stiffness of the platform
        stiffness of the solar panel per unit length
d_1 distance from the top of the SPELDA to the center of gravity of the upper

        satellite
d_2 distance from the top of the SPELDA to the center of gravity of the

        adaptor

d_3 distance from the top of the SPELDA to the center of gravity of the

        Hitch-Hiker
E   modulus of elasticity
F   maximum panel buckling load
        load on the cylinder
F(1)   lowest resonance frequency
g   number of which compose the composite section, plus the number of cuts g
        necessary to devide the sectio into a series of flanges

h	thickness of the solar panel
I_r	area momentum of inertia of the cylinder frame
I_{cg}	area momentum of inertia of one pitch
I	area moment of inertia
k_{lb}	local buckling factor
L	length of the cylinder
l	length of a panel of the cylinder
	length of the beam
	distance between the frames of the cylinder
ω	resonance freqeuncy
ω_n	resonance frequency of the beam
M	moment acting on the cylinder at the clamped interface
m	mass of the stiffeners
	mass of clampband
	mass of the cylinder
m_1	mass of upper satellite
m_2	mass of adaptor
m_3	mass of the Hitch-Hiker satellite
m_{tot}	mass of the upper satellite, the adaptor and the Hitch-Hiker together
μ	coefficientof fricfion on the contact surface between the structure and the Marman clamp band
	mass per unit length of the beam
N_{cr}	desired classical buckling load
ν	Poisson's ratio
ρ	mass density of CFRP face sheets
	mass density of solar panels
	mass density of aluminum core
	mass density
	mass density of adhesive
	mass per area
p	pitch
Q	amplification factor
γ	mass density
R	radius of the cylinder
σ	stress
σ_{occ}	occurring stress
σ_{cy}	compression yield stress
σ_{all}	allowable stress
σ	yield stress
$\sigma_{c_{cr}}$	critical compression stress
σ_{cs}	crippling stress
$T_{clamping}$	clamping force of the clampband on the separation parts
$T_{release}$	release force of the clampband on the separation parts
t_c	thickness of core
t	thickness of a plate of the cylinder
t_f	thickness of the face sheets
t	thickness of the hat-stiffeners
	thickness of a CFRP sheet
	wall thickness of the cylinder
t_{eq}	equivalent wall thickness
W	section modulus

8   AOCS.

A   Area
AZ   Azimuth of ground target
α orbit angle measured from S/C local noon
α, β angles, see figure 8.13
ψ yaw error
Φ latitude of ground target
ϕ roll error
EL   Elevation of ground target
λ longitude of the S/C
H   Height of the spacecraft from earth surface
h   angular momentum of the reaction wheel
I_{zz} principal moment of inertia about z-axis
I_{yy} principal moment of inertia about y-axis
I_{xx} principal moment of inertia about x-axis
I_w moment of inertia of the wheel
K   gain
Ω right ascension of the ascending node
ω_0 orbital rate
ω angular speed of the wheel
M_c Control torque

M_s Solar radiation pressure torque

M_g Gravity-gradient torque

$\bar{n}$ normal vector of the area
P   Solar radiation pressure
ρ_d diffuse reflection coefficient

ρ_s specularly reflection coefficient

Re   Radius of the earth
R   Radius of the spacecraft orbit
θ pitch error

$\bar{r}$ vector from center of mass of S/C to the center of pressure of area

$\bar{S}$ unit vector along the direction of the incoming photons
T   Time between two east-west corrections
t   time contant
V   orbit velocity of the S/C
$\Delta\phi$ roll error
ΔEL elevation error
ΔAZ azimuth error
$\Delta\lambda$ east-west orbit error
$\Delta\theta$ pitch error
δ declination of the sun

x,y,z components of vector $\bar{r}$

9   Thermal control.

A   total battery surface
a   Solar absorption coefficient
Ar   radiator surface
As   Radiated surface
ε emmision coefficient
I   Intentity
k_{eff} conductivity

l   length
P   Dissipated heat   [W]
Q   transferred heat
Q_b dissipated heat of the batteries

R   Radius of the earth
r   Distance from earth's center to the satellite
S   Solar flux   [W/m²]
σ Stephan Boltzmann constant = 5.6703e-8 W/km²
T   Temperature
$T_{C,H}$ boundary temperatures

t   thickness
ΔT temperature difference in/outside radiator

ABBREVIATIONS.

1   Management.

AOCS   Attitude and Orbital Control Subsystem
CAD   Computer Aided Drawing
ESA   European Space Agency
ESTEC   European Space Research and Technology Center
OBS   Organizational Breakdown Structure
SOW   Statement Of Work
TT&TC   Telemetry and Telecommand
TU   Technical University
WBS   Work Breakdown Structure
WP   Work Packages

2   System Engineering.

ACS   Attitude Control System
GTO   Geostationary Transfer Orbit
RF   Radio Frequency
SPELDA   Ariane Dual Launch External Bearing Structure
TTC   Telemetry and Telecommand

3   Launcher and Orbital Dynamics.

ESA   European Space Agency
GMT   Greenwich Mean Time
SCAR   Attitude and Roll Control System
SPELDA   Ariane Dual Launch External Bearing Structure

4   Configuration.

SPELDA   Ariane Dual Launch External Bearing Structure
AOCS   Attitude and Orbital Control Subsystem
IRES   InfraRed Earth Sensor
ESS   Extra Support Structure
BAPTA   Bearing And Power Transfer Assembly
TTC   Telemetry and Telecommand
PCDU   Power Control and Distribution Unit
PCU   Power Conditioning Unit
TWT   Travelling Wave Tube
QSS   Quadrant Sun Sensor
SAS   Sun Aquisition Sensor
RIG   Rate Integrating Gyro
WDE   Wheel Drive Electronics
FOV   Field Of View

5   **Payload.**

ADPCM   Adaptive differential pulse-code modulation
ALC   Automatic level control
AM   Amplitude modulation
BDF   Beam deviation factor
BER   Bit-error-rate
BPF   Bandpass filter
BPSK   Binary phase-shift keying
CCIR   International radio consultative committee
CCITT   International telephone & telegraph consultative committee
CDMA   Code-division multiple access (= SSMA)
CIR   Carrier-to-interference ratio
CNR   Carrier-to-noise ratio
CP   Communications payload
D-   Differential detection
DE-   Coherent detection
DSI   Digital speech interpolation
EIRP   Equivalent isotropic radiated power
EPC   Electric power conditioner
FDM   Frequency-division multiplex
FDMA   Frequency-division multiple access
FET   Field-effect transistor
FM   Frequency modulation
HPA   High power amplifier
IF   Intermediate frequency
ITU   International telecommunications union
LNA   Low noise amplifier
MCPC   Multiple channel per carrier
M-PSK   Multiple phase-shift keying
PCM   Pulse-code modulation
PFD   Power-flux density
PM   Phase modulation
QPSK   Quaternary phase-shift keying
RF   Radio frequency
SCPC   Single channel per carrier
SNR   Signal-to-noise ratio
SSMA   Spread spectrum multiple access
SSPA   Solid state power amplifier
TASI   Time-assigned speech interpolation
TDM   Time-division multiplex
TDMA   Time-division multiple access
TT&C   Telemetry, tracking & command
TWT   Traveling wave tube
TWTA   Traveling wave tube amplifier
%EFS   Percent error-free seconds

6 The Electrical Power Subsystem.

AMO	Air Mass Zero
BAPTA	Bearing And Power Transfer Assembly
BOL	Begin Of Life
BSR	Back Surface Reflecting
DOD	Depth Of Discharge
EOL	End Of Life
EPS	Electrical Power Subsystem
GaAs	Gallium-Arsenide
NiCd	Nickel-Cadmium
NiH_2	Nickel-Hydrogen
PCDU	Power Control and Distribution Unit
PCU	Power Conditioning Unit
Si	Silicium

7 Structure.

CFRP	Carbon Fiber Reinforced Plastics
SPELDA	Ariane Dual Launch External Bearing Structure
QSL	Quasistatic Load
TWT	Travelling Wave Tube
EPC	Electronic Power Converter
ESS	Extra Support Structure
BAPTA	Bearing And Power Transfer Assembly
MS	Margin of Safety
EOL	End Of Life

8 Attitude and Orbital Control Subsystem.

ABP	Antenna Beam Pointing
ACT	Attitude Control Thrusters
AEF	Apogee Engine Firing
AOCS	Attitude and Orbital Control Subsystem
CASS	Coarse Analog Sun Sensor
CMG	Control Moment Gyros
EW	East-West
FOV	Field Of View
IRES	InfraRed Earth Sensor
NS	North-South
OBC	On Board Computer
QSS	Quadrant Sun Sensor
RW	Reaction Wheels
RIG	Rate Integrating Gyros
S/C	Spacecraft
SAS	Sun Acquisition Sensor
TTC	Telemetry and Telecommand
WDE	Wheel Drive Electronics

9	Thermal Control.
AOCS	Attitude and Orbital Control Subsystem
BAPTA	Bearing And Power Transfer Assembly
BOL	Begin Of Life
EOL	End Of Life
EPC	Electronic Power Convertor
IRES	InfraRed Earth Sensor
MLI	MultiLayer Insulation
OSR	Optical Solar Reflector
PCDU	Power Control and Distribution Unit
PCU	Power Conditioning Unit
TWT	Travelling Wave Tube

10	Telemetry and Telecommand.
CMD	Command
CMOS	Complementory MOS
CPU	Central Processing Unit
DMA	Direct Memory Access
EPROM	Erasable Programmable Read Only Memory
ESA	European Space Agency
FET	Field Effect Transistor
GTO	Geosynchronous Transfer Orbit
MOS	Metal Oxide Semiconductor
OBC	On Board Computer
PCM	Pulse Code Modulation
PM	Pulse Modulation
RF	Radio Frequency
ROM	Read Only Memory
SPC	Split Phase Code
TLM	Telemetry
TTC	Telemetry and Telecommand
VCXO	Voltage Controlled Crystal Oscillator

11	Propulsion.
AMF	Aapogee motor firing
AOCS	Attitude and orbit control system
CPS	Combined propulsion system
MBB	Messerschmidt-B lkow-Blohm
MEOP	Maximum expected operating pressure
MMH	Mono methylhydrazine, CH_3NHNH_2
NC	Normally closed
NO	Normally open
NTO	Nitrogen tetroxide, N_2O_4
PMD	Propellant management device
RCS	Reaction control system
UPS	Unified propulsion system

Introduction.

Why a system design exercise?

A spacecraft is a system consisting of a payload and a spacecraft bus. The spacecraft bus and the payload can be divided into a number of subsystems. For each subsystem a lot of technology knowhow is necessary. The application of all kinds of sciences is the work of the engineers involved. No scientific development but the application of developed sciences is the main activity for the designers and manufacturers of spacecraft. A thorough knowledge of a number of basic scientific achievements in many fields is necessary. This principle is valid for the design of an aircraft but certainly this is also the case for the design of a spacecraft. However a spacecraft is in general much smaller than an aircraft which intensifies the number of the interface problems between one subsystem and the others. An example may be the shift of an equipment box from one location to a nearby location.

This relocation of a piece of equipment influences:

- vibrational characteristics and may lead to a change of the structure.
- vibration environment changes for the equipment
- mass moments of inertia which might have an influence on the attitude control system. In case the spacecraft is spinning it will also necessitate a change of the mass balance
- the temperature distribution because the view factors of the equipment boxes mutually are changed
- electromagnetic interference might be influenced because the electromagnetic field of the subject box is interfering with that of other boxed
- influences might be in cabling interference, etc., etc.

The interfaces between the subsystems can be demonstrated by doing a system conceptual design. But a system is always designed by a number of experts. The concept of the Hitch-Hiker/Ariane was designed by all participating students. Working together on one project is a challenge for students who in general are not used to have a common interest in one project. After it was decided by the Delft Technical University to start a preliminary design program for spacecraft, it was also necessary to choose a study project. The design of a complete new project was not considered to be feasible due to the jump in technology, which is only possible if a considerable amount of experience is present. It was therefore decided to have an evolutionary design project. In the literature, a great amount of data and characteristic parameters are given for telecommunication satellites. Moreover at ESTEC there where ongoing activities for a small innovative telecommunication satellite.

The manager of this project at ESTEC was Mr. D. Brown. With the cooperation of Mr. D. Brown it was possible to select as a study project also a small telecommunications satellite. The ESTEC work statement for a small communication satellite was followed to a great extend. Moreover in a later stat of the study also Mr. Kletzkine of ESTEC assisted the project team in a very helpful manner.

Fokker supported also in the field of power supply, thermal control and attitude control. This industrial support improved the design considerably. Staffmembers of the Delft University were consulted for several expertises but in some areas the knowledge was not available such as spacecraft electrical architecture and space telecommunication. The lack of experience in those areas was certainly of influence.

The unexperienced students with only limited support from the staff able to bring forward an acceptable design. No real innovation was aimed for in this project. It must be realized that the project lasted only two dimesters of a study year and each student should nominal spent about 250 hours on this project. The design and the verification is only performed to the level in accordance with the number of hours available for the project. Suggestions how to improve a similar project in the future will be welcome.

M.P. Nieuwenhuizen.

1 Management.

1.1 Introduction.

One of the intentions of the project is to simulate the actual procedures of designing a spacecraft as this is performed in the industry. To provide the necessary coordination it is needed to have a management team. The task of the management team is to organise the project (group division, working methods etc.), to arrange facilities and to make a planning.

1.2 Group division.

In the first introductory plenary meeting a start was made to divide the students in different groups: sub-system clusters.

Some of the clusters were joined together to combine the personal expertises and interests of the students. The managing tasks were combined in the Management cluster: System-Engineering, Launcher, Operations and Final Report. The sub-systems dealing with electronic equipment and data management were combined: Payload, Telemetry & Telecommand and Data Handling. The other subsystems are: Propulsion, Attitude and Orbital Control System (AOCS) and Power. Finally, the structure cluster was combined with Thermal Control and Materials. Later on, the necessary orbital mechanics calculations were made by the management cluster because two of the students are graduating in orbital mechanics.

The amount of students in each cluster was shifted in such a way that the cluster could deal with the expected amount of work. After a few weeks, 3 students left the design study and 2 other students joined it.

The final group division is:

Cluster	Sub-cluster	Persons
Management	System-Engineering	Albert-Jan Bunt
	Operations	
	Launchers	Bryan P. Ho
	Orbital Dynamics	
	Final Report	Darwan A. Shawalli
Payload	TT&TC	Marc Dubbeldam
	Data Handling	Arthur J. Smith
Propulsion		Marcel J. Belien
		Steven P. Verhagen
		Dirk de Waart
A.O.C.S.		Ton G. Maree
		Guido V. Nierop
Power		Mark J. v Dijk
		Eduard P. v d Heuvel
Structure	Thermal Control	Renate v Drimmelen
	Materials	Erik P. de Heer
		John L. Mensink
		Bas J.C. Theelen
Total:		16

The configurational design of the satellite was done mainly by the clusters structure and management.

In the course of the project it turned out that not all the tasks were divided correctly, so some adjustments were made. Structure took over the design of the solar arrays and the structural design of the dish-antenna. Propulsion designed the thrusters for attitude-control and station keeping.

Some of the tasks could not be worked out precisely. Firstly because it is out of the scope of the project, which has a more educational task than an innovative study. Secondly because the knowledge of the students is limited to the available reports and literature in the libraries. The partly neglected tasks are: Operations, Materials and some smaller tasks in the sub-systems such as cabling.

1.3   Task-definition.

In the first meeting an ESA-specification and Statement of Work (ref 1.1) was handed over a study of an innovative modular communication satellite design, author D. Brown of ESTEC. The tasks described in the report were copied and partly adjusted.

The first task in the SOW was a trade-off study between alternative system design concepts for the satellite and the launch system. This included a trade off for the attitude control by means of spin stablisation, dual spin and conventional three axis stabilization systems. Because the necessary expertise to make such a trade-off was not available and to maximize the time spent on designing the satellite it was decided not to perform a trade-off between the stabilization systems. Our coordinator suggested to choose the option of a three-axis stabilized system because this was applied most in geostationary-satellite designs. In this way, more literature would be available on this subject. No objections were made.

The third task described in the ESA-SOW was a study of the launch-configurations. The SOW stated that the satellite should be fully compatible with at least two different launchers, in particular the Ariane IV and the TITAN III. Because of reasons mentioned later in chapter 3 it was decided to use the Ariane IV launcher, so just a single study had to be performed.

We shifted this task before the actual design study of the spacecraft because we would have to integrate the satellite as a piggy-back payload in the Ariane IV. This meant that the choice of the launcher defined the primary configuration of the satellite.

The second task also included the following phases:
- launch
- orbit injection
- orbit manouvre and control
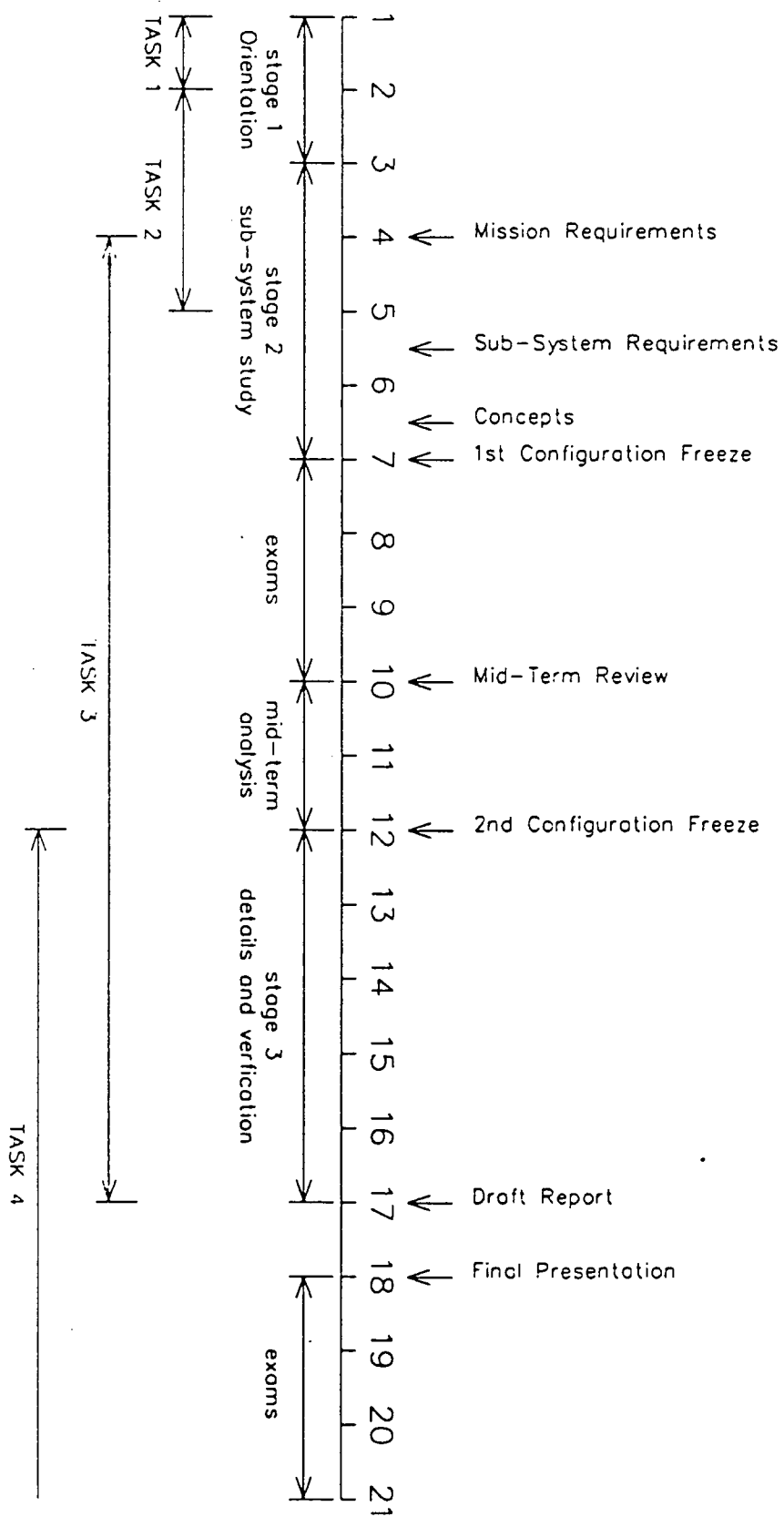- in-orbit storage and reactivation

figure 1.1
Planning scheme.

The third task in our study was to perform a system design to sub-system level, against the range of system performance specifications. It incorporated the following items:
- Drawings of the spacecraft configuration, including all the major structural elements.
- Design and analysis of the Thermal Control sub-system for the principal phases of the mission, assuming a 70% payload power dissipation.
- Design and analysis of the Electrical sub-system, including estimates of the solar array characteristics for all phases of the mission and a typical battery operating profile.
- A mass budget analysis.
- A Reaction Control sub-system design and analysis for the required mission lifetime.
- An Attitude Control sub-system design and analysis including estimates of the satellite pointing errors.
- A design of the Telemetry and Telecommand sub-system required for satellite control and operation.
- A design of the propulsion sub-system.

The fourth task in the ESA-SOW describes a manufacture & test programme, in which all the significant phases of a typical programme should be examined, including Parts Procurement, Engineering Model, Qualification Model, etc. This task was not performed because it was expected that there was no time available.

On the University of Delft no particular lectures are given on cost analysis which formed the main reason not to perform the fifth task as described in the SOW: A budgetary cost estimate for the satellite.

The final task is to prepare a comprehensive final report which incorporates the task reports and clearly explains the reasons for the selected design approach. Conclusions have to be made on the feasibility of using a low cost satellite together with a viable launch concept for the specified mission.

1.4   Working method.

Once a week a plenary meeting was held.
The main purposes are:
- A presentation of the work done in the past week.
- A presentation and motivation of chosen concepts.
- To solve incertainties.
- Questions to other clusters.
- Planning aspects.

Of all the plenary meetings minutes were made and given to all participants and the TU-coordinator.
Besides this, several seperate meetings of the sub-system groups were held and, where cooperation was needed, between two or more clusters.
The total time to be spent on a TZ-exercise is prescribed: 250 hours. This meant that about 15 hours a week had to be spent on the project. In this way, the normal procedure of attending lectures could be maintained.
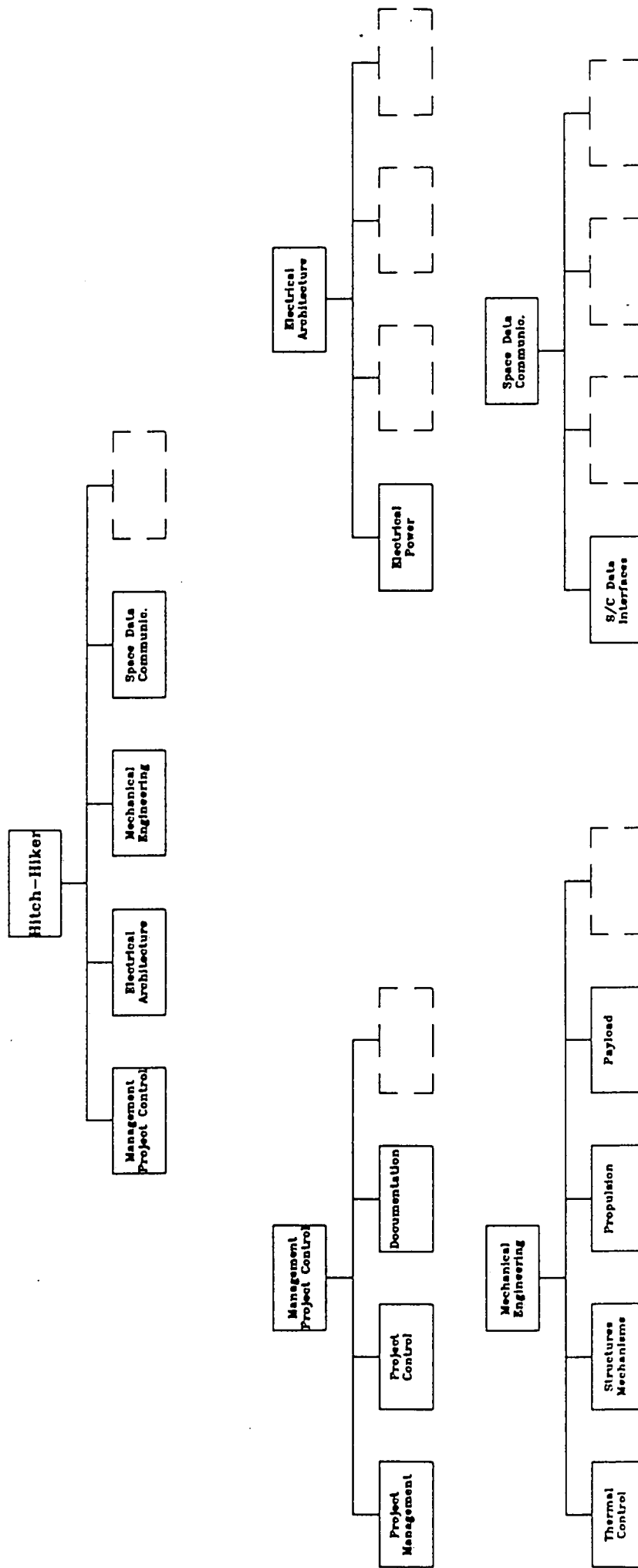
figure 1.2

Organisational Breakdown Structure (OBS)

The information which was needed for the project was mainly extruded from the University libraries. Secondly, the industry was consulted. To avoid double-questioning and confusions it was decided to use a single channel to the industry. The questions had to be approved after which our coordinator would inform the local Aerospace industry. Also, some foreign industries were consulted for specific information on sub-systems.

Because it is possible that the space-design study is repeated in the next year(s) it was decided to set up a database with all the literature which included information of the design of a communications satellite and the sub-systems.

1.5   Facilities.

Because every week a general meeting was held it was necessary to have a meeting-room. Also a room was needed to store all the produced results and literature.

After some meetings with the TU-personal we got a room assigned which was big enough to be used as meeting room. The room was filled with two chests, some tables, bureau's and chairs and an overhead projector.

To be able to make the necessary drawings we had several possibilities. First a drawing board, which could be arranged quite easily. Second, because most of the student had CAD-expertise, we would like to use a computer drawing programma. The SUN-computers of the TU were not available because of two major CAD-exercises performed by undergraduate students in the same period. We could also use the mainframe of the TU but the choice of applications programs proved to be limited.

The third option was a PC for the project, but it was not sure if the budgets would be approved. After several discussions the faculty council decided to approve the purchase of an IBM PS/2 Personal Computer with additional programs.

Five weeks after the start of the project the PC was delivered, together with a color monitor and a printer.

The programs used were:
- AutoCad10, with a 3D-modeller
- WordMark
- Profort, a FORTRAN compiler
- PSI, a simulation programme
- TurboPascal, a Pascal compiler
- Jason, programm for thermal control

Also for copying the group was authorised.

1.6   Organisation.

1.6.1 Planning.

The study performed was a phase A study. A phase A study globally exists of a preliminary design and a feasibility study. We defined three stages in the study (figure 1.1).

The first stage is an orientation of the systems. Since most of the students are undergraduate there was no detailed knowledge of the different subsystems. No particular lectures are given on the design of system elements, so literature had to be found to provide this knowledge. Of course, during the whole project literature was consulted to expand the knowledge, but the first two weeks were spent mostly on this orientating phase.

PROJECT WORK BREAKDOWN STRUCTURE (WBS)

| WP | WP | WP | WP | WP |

ORGANIZATIONAL BREAKDOWN STRUCTURE (OBS)

WP MANAGER

PROJECT MANAGER

WP MANAGER

WP MANAGER

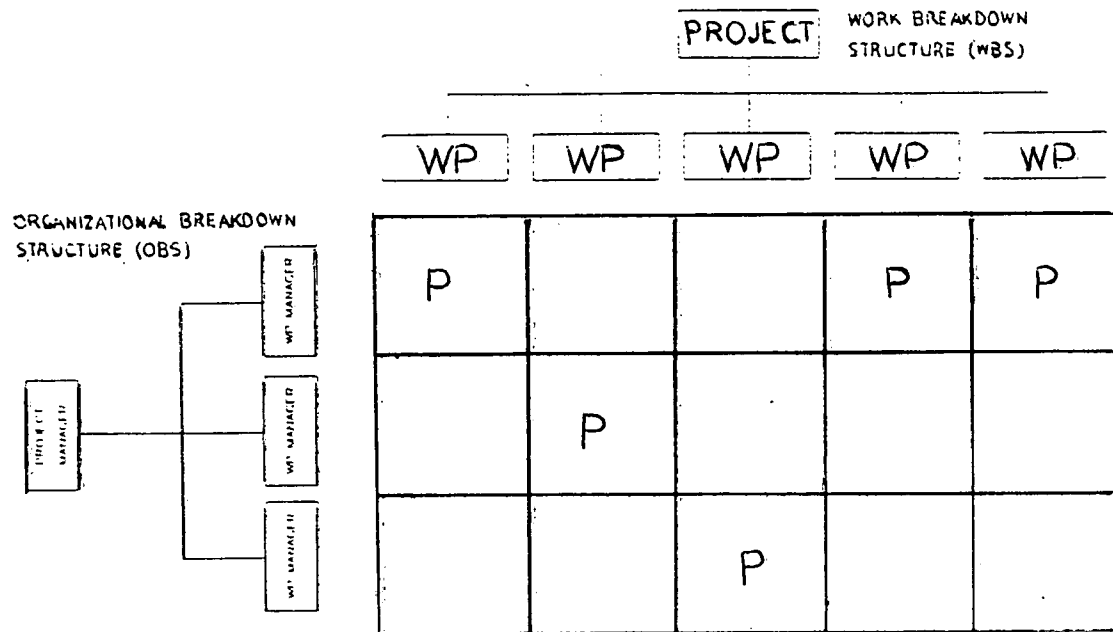|				
P			P	P
	P			
		P		

figure 1.3
Work Breakdown Structure (WBS)

The second stage consists of the definition of the mission requirements and the system requirements and a study of the sub-systems in which the needed equipment was examined and a few concepts had to be performed. A concept is chosen to make a first configuration freeze.

The third stage consists of a more detailed study of the sub-systems in which a final concept was chosen and a verification of the concept was worked out, like simulations and calculations.

To review the work and to come to a more viable concept our coordinator proposed to organize a Mid-Term Review. In this review some experts of the sub-systems are invited to give their opinion and critics of the configuration and the definitions.

To analyze the criticism given on this review two weeks are inserted in which configuration and sub-system changes could be performed. After this a second configuration freeze occurred and further verification was performed.

In between the project two exam-periods occur. These exams last three weeks and no work on the project has been performed during these periods.

After the first exam-period the Mid-Term-Review is planned.

The writing of the draft report will begin after the mid-term analysis. The draft report has to be finished before the Final Presentation, so at least a week before the Final Presentation all the cluster reports has to be finished.

After the Final Presentation and the second exam-period the management team has to adapt the draft report to a final report, which has to be finished in September.

Finally, in September an evaluation of the project is planned with the TU-board to discuss the project and the possibility of repeating or expanding the project.

1.6.2 Work Breakdown Structure.

For the realisation of a project, it is of importance to have a Work Breakdown Structure (WBS) because it determines the form and contents of a project (ref 1.2).

A WBS is divided in levels. Every level means a more detailed description of the previous level. This entering into details has to go on till it is possible to describe the tasks. These tasks form the Work Packages (WP).

Together with the Organizational Breakdown Structure (OBS) (figure 1.2), it is possible to divide the work between the project teammembers.

For the Hitch-Hiker project the WBS is given in figure 1.3. The WBS is worked out till level 2. The reason for this is the lack of experience of how the sub-systems interact. There was no time available for further analysis.

2   System Engineering.

2.1   Introduction.

The system engineering was approached in the Hitch-Hiker project as follows. Major decisions were taken by the system group such as :
- The definition of the specification for the satellite.
- The launcher choice.
- The position of the satellite on the launcher.
- The allowable satellite mass.
- The way of separation of the satellite from the launcher.
- The type of stabilisation of the satellite (spinners versus 3-axis stabilisation.

However a number of system decisions were taken by a kind of bottom-up approach.

Analysis of the design possibilities for the major sub-system have lead to a system decision. The general meeting each week was merely a system review meeting. This approach necessitated consideration of all participants on the system work. The depth of the sub-system work was therefor less than if the system design requirements were directly handed to the sub-system designers.

This chapter only consists of an enumeration of the requirements and a mass budget analysis. The elements you are used to find in the system chapter can be found in the sub-system chapters.

2.2   Requirements.

Most of the requirements in this chapter are copied from the ESA-spec of D. Brown (ref 2.1). Because the ESA-spec concerned an innovative modular spacecraft some adjustments are made.

2.2.1 Launch and mission requirements.

1. The spacecraft shall be geostationary to provide 24 hours communications. The operational longitude shall be $12°$
2. The spacecraft missionlife shall be 10 years.
3. The total mass of the spacecraft in G.T.O shall not exceed 800 kg.
4. The spacecraft shall be fully compatible with Ariane 4, as a piggy-back load for the Ariane 4.
5. Full eclipse operation is required.
6. The antenna pointing accuracy is required to be within $0.3°$ longitude and $0.3°$ latitude.
7. The spacecraft shall be designed to meet all performance requirements specified after exposure to the launch environments.
8. The spacecraft shall survive without degradation for periods of up to 24 hours without any RF uplink.
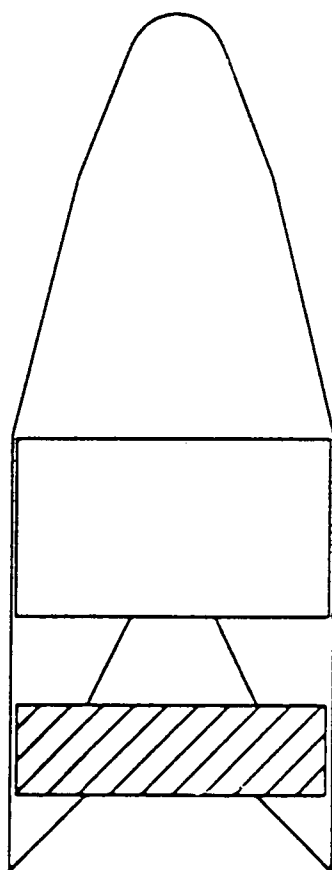
figure 2.1
Usuable volume of the Hitch-Hiker

ad.1 The operational longitude is chosen to cover most of Europe.
ad.3 The spacecraft will be launched by Ariane 44P Spelda (chapter 3). With
      the addition of the Hitch-Hiker concept it is a triple launch instead of
      a double launch. The spacecraft be integrated between the SPELDA and the
      adaptorand will interfere the normal dual launch as less as possible. The
      spacecraft is able to use all the usable volume in a cylinder which
      height may not exceed 1000 mm (see figure 2.1).
ad.4 This requirement is added to keep a commercial attractive launch
      configuration for the primary satellites.
ad.5 It was proposed to maintain just a partial payload operation during
      eclipse periods. This was rejected because of commercial reasons.
ad.6 The initial requirement stated an accuracy of 0.1° longitude and
      latitude. This proved to be too strict to accomplish. Also, because no
      beam-shaping concept is used, the antenna pointing does not have to be of
      extreme accuracy, so the required accuracy was decreased to 0.3°.

2.2.2 Space segment requirements.

9. For communications a minimum of 12 multi-purpose channels will be used in
    the total power/mass ratio of 600 Watts/ 60 kg.
10. The maximum space-antenna diameter shall be 1,80 meters.
11. The spacecraft shall have a three-axis stabilized Attitude Control System.

ad.10 Since the antenna will be stowed inside the adaptor (diameter 1920mm), a
      maximum antenna diameter of 1800 mm can be used.
ad.11 As described in chapter 1, no trade-off was performed, but a three-axis
      stabilization system was chosen.

2.2.3 Sub-system requirements.

PROPULSION

12. The spacecraft shall have a propulsion unit to provide transfer into a
    geostationary orbit, for station keeping and for attitude control.

STRUCTURE

13. The spacecraft shall consist of a cylinder-structure to support the upper
    spacecraft and adaptor.
14. The satellite structure shall create a mechanical environment which is
    guaranteing the defect free launch of the equipment.
    However in orbit the structure is responsible for guaranteing the proper
    functions of the equipment.
15. The structures of the spacecraft shall have adequate strength to resist
    all loads without failing.

THERMAL CONTROL

16. The satellite thermal control design shall be such that satisfactory
    temperature environments shall be maintained for all components during
    pre-launch operation, launch, separation sequences, pre-operational and
    operational stages of the mission including eclipse periods.

MATERIALS

17. The design and application of spacecraft parts and materials shall be such
    as to ensure all performance specifications are met throughout the mission
    of the spacecraft when operated in all the expected environments.

Table 2.1: The mass budget.

	Mass [kg]
Payload	70
TTC/Datahandling	26
AOCS	26
Power	116
Propulsion	36
Thermal control	20
Structure	80
Dry Mass	374
Propellant and pressurizer	427
Satellite Mass	801
Separation mechanism & Separation rings	45
Margin of 15%	85
Total Launch Mass	931

POWER

18. During the transfer-orbit into geostationary orbit the power supply shall be sufficient for the necessary subsystems.
19. During eclipse the batteries will supply enough power for full operations.
20. The power during normal mode shall be provided by solar cells.
21. The ACS shall remain operational and shall maintain satellite stability during one power bus fault clearance.

ATTITUDE AND ORBITAL CONTROL SYSTEM

22. The ACS shall sense the spacecraft orientation for attitude determination and shall provide attitude control to ensure that the spacecraft meets all attitude and orbit performance requirements throughout the mission.
23. The ACS shall provide attitude sensor data via the telemetry system for ground processing to determine the satellite orientation about all three axis.
24. The ACS shall provide orientation control and stabilization during transition from the pre-operational to the operational configuration including acquisition of the operational attitude.
25. The ACS shall provide antenna earth capture.
26. The AOCS shall provide the necessary pointing accuracy.
27. AOCS shall provide a station keeping tolerance of 0,1° North-South/East-West.
28. The ACS shall provide recovery from predictable failure modes.
29. There shall be no obstruction in the field of view of the attitude sensors.

PAYLOAD

30. The spacecraft communications subsystem comprises of either L, C, Kμ or Ka-Band transponders capable of supporting a variety of communication signals between fixed ground stations and/or mobiles over western Europe.

TELEMETRY

31. The TTC sub-system shall provide the necessary monitoring and control of the spacecraft throughout all mission phases including ground system testing, injection into orbit, and operation. The system shall be designed to permit the detection of spacecraft degradation and anomalous performance during all phases of the mission.
32. The frequencies for the TTC system shall be within the payload frequencies.

ad.13 Since the spacecraft will be placed between the SPELDA an the upper spacecraft, all the loads due to the upper spacecraft and adaptor during launch and separation will have to be transferred through the spacecraft, so a cylinder structure with the same diameter as the adaptor will have to be provided to transfer these loads.

ad.29 This requirement shall have to be provided by the configuration-group.

2.3 Mass budget.

After the first stage in the design study it was necessary to have a mass budget for the sub-systems. Again, the inexperience caused some problems. Some mass-budgets of other satellites were compared but none of them could be identified as the same kind of spacecraft we would design. A rough calculation was made to scale the usual mass-budget of a geostationary telecommunications satellite. The original total mass limit of 500 kg showed to be much to low so it was increased to 800 kg, including margins. As can be seen in table 2.1,

also this limit could not be achieved. A decrease of the total mass would ask for a different design-approach.

The following definitions are used:
- **Dry Mass:** The mass of all the structural elements which have to be taken into geostationary orbit.
- **Satellite Mass:** Dry Mass increased by the mass of the propellant and pressurizer needed to provide the apogee boost.
- **Total Launch Mass:** Satellite Mass increased by the mass of all the structural elements which are needed to launch the spacecraft, but which do not have to be taken into geostationary orbit.
  The Total Launch Mass is increased with a margin.

To account for unexpected changes in the design in a phase B study and to take account of uncertainties, a margin of 15% is used.

3   Launcher and orbit dynamics.

3.1   Introduction.

In this chapter the difference between two launchers are considered: the Titan III and the Ariane IV. After these considerations a choice of launcher is made.

Considerations concerning the orbit, which brings the Hitch Hiker into his operational longitude, is one of the important phases of a satellite design project. The choice of the orbit is especially of importance for the power- and propulsion group.

These phases are part of the task 3 mentioned in chapter 1.

3.2   Choice of the launcher.

One of the specification, in the SOW of ESA is that the satellite must be designed as part of a multiple launch on Ariane IV or any other comparable launch systems. This means that for the launch configuration not only the Ariane IV should be considered, but also at least one other launcher. The one launcher that can be compared with Ariane IV is the Titan III, which has the same fairing diameter as the Ariane IV. The Titan III, used for military purposes has been commercialised and is used often as second launch option besides the Ariane launcher.

In the trade-off some serious disadvantages of the Titan launcher are found:
1. The Titan III does not provide the injection into transfer orbit, so the satellite is required to have more propellant. The extra mass will exceed the maximum mass as required.
2. The Titan III is launched from Cape Caneveral which has a latitude of 28.5°. The satellite has to decrease this inclination to 0°. Compared with the Ariane IV, which has a launch inclination of 8°, a velocity change of 122% is needed.
3. In our libraries there is no literature available about the Titan III launcher. On the Ariane IV several documents are to our disposal, including the Ariane manual.
4. When using the Titan III there is no ESA-involvement.

Because of the above mentioned reasons, it is decided not to study the integration in a Titan III launcher, but to focus on a Ariane IV.

3.3   Spacecraft orientation and seperation.

The spacecraft separation discussed in the manual of the Ariane 4 are more of less standard procedures. The introduction of a third satellite will therefore cause some considerable problems. After a long discussion it was concluded that there were two possible spacecraft separation scenarios involving the Hitch-Hiker. The scenarios are:

figure 3.1
Possible separation sequences.
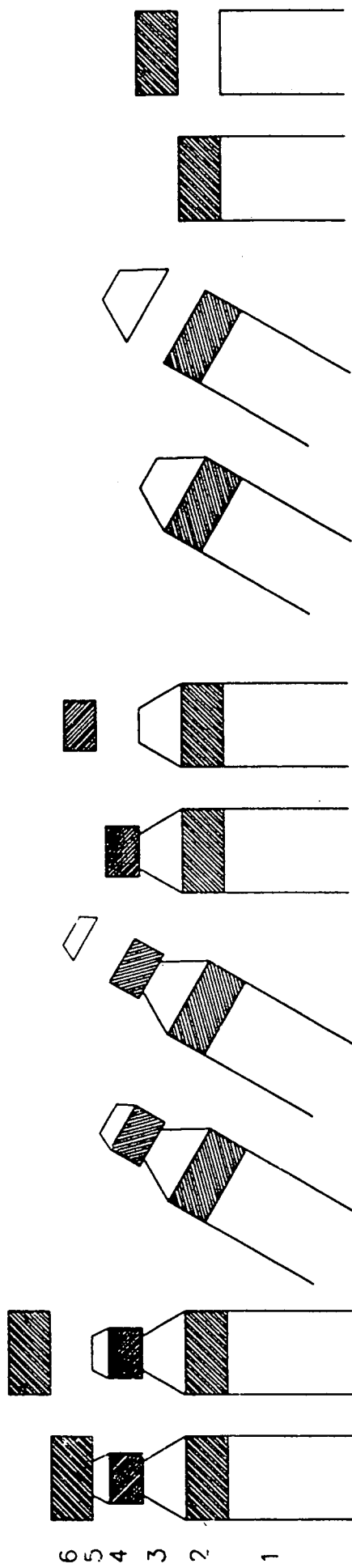
1. ARIANE 4PP LAUNCHER
2. SHORT SPELDA + LOWER SPACECRAFT
3. ADAPTOR
4. HITCH–HIKER SPACECRAFT
5. ADAPTOR
6. UPPER SPACECRAFT
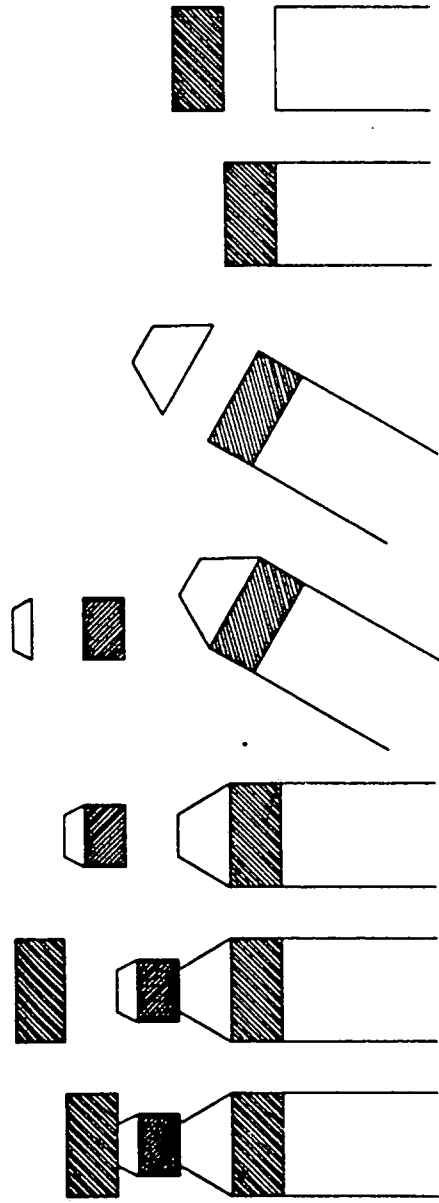
SCENARIO A

SCENARIO B

Scenario A:
(1) An orientation of composite (3rd stage+payload) by 3rd stage roll and attitude control system(SCAR).
(2) A spin up by action of SCAR.
(3) Separation of the upper s/c. Then a spin down and attitude deviation.
(4) Separation of the adaptor. Reorientation as requested by the Hitch-Hiker.
(5) Spin up and separation of the Hitch-Hiker. Then a spin down and attitude deviation.
(6) Separation of the upper SPELDA. Reorientation as requested by inner s/c.
(7) Spin up and separation of the inner s/c.
(8) Finally the 3rd stage avoidance maneuver to avoid collision.

Scenario B:
(1) An orientation of composite by 3rd stage roll and attitude control system.
(2) A spin up by action of SCAR.
(3) Separation of the upper s/c.
(4) Separation of the adaptor and the Hitch-Hiker. Then a spin down and attitude deviation.
(5) Separation of the upper SPELDA. Reorientation as requested by inner s/c.
(6) Spin up and separation of the inner s/c.
(7) Finally the 3rd stage avoidance maneuver to avoid collision.

The two scenarios are displayed in figure 3.1.

Considering the two scenarios it is clear that scenario B has a few advantages above scenario A. For example scenario A demands an extra spin down and a extra spin up. These extra maneuvers are probably not possible. The choice is therefore scenario B.

3.4   Velocity requirements for a geostationary satellite.

After the launch from Kourou at a time compatible with the launch-window constraints, the Ariane achieves a circular orbit with an altitude of about 200 km at an inclination angle of approximate 8°. At the equatorial crossing a perigee-kick is given by the Ariane that puts the Hitch-Hiker in a transfer orbit. Finally, at the apogee, a kick is given that places the Hitch-Hiker into an geosynchronous orbit.

For the calculations values are given to some of the orbital parametres. These are:

perigee altitude: $h_p = 200$ km

apogee altitude: $h_a = 35786$ km

radius of the earth: $R_e = 6378$ km

earth's gravitational constant: $\mu = 3.986*10^5$ km³ sec⁻²

earth longitude of injection point: $\Lambda_o = 0°$

inclination: $i = 8°$

Parking orbit:

The circular velocity V_{c_p} of a satellite along the parking orbit is:

$$V_{c_p} = \sqrt{\frac{\mu}{r_p}} = \sqrt{\frac{\mu}{Re+h_p}} \qquad (3.1)$$

$$V_{c_p} = 7.784 \text{ km/s} \qquad ; \quad r_p = 6578 \text{ km}$$

Geostationary orbit:

The circular velocity V_{c_a} of a satellite along the geostationary orbit is:

$$V_{c_a} = \sqrt{\frac{\mu}{r_a}} = \sqrt{\frac{\mu}{R_e+h_a}} \qquad (3.2)$$

$$V_{c_a} = 3.075 \text{ km/s} \qquad ; \quad r_a = 42164 \text{ km}$$

Transfer orbit:

The transfer period from perigee to apogee is given by:

$$T_t = \pi \sqrt{\frac{a^3}{\mu}} \qquad (3.3)$$

$$T_t = 5.259 \text{ h} = 5^h 15^m 32^s.$$

The eccentricity of the transfer orbit is given by:

$$e = \frac{r_a - r_p}{r_a + r_p} \qquad (3.4)$$

$$e = 0.730$$

$$V_p^2 = V_{c_p}^2 (1+e) \qquad (3.5)$$

$$V_p = 10.328 \text{ km/sec}$$

$$V_a^2 = V_{c_a}^2 (1-e) \qquad (3.6)$$
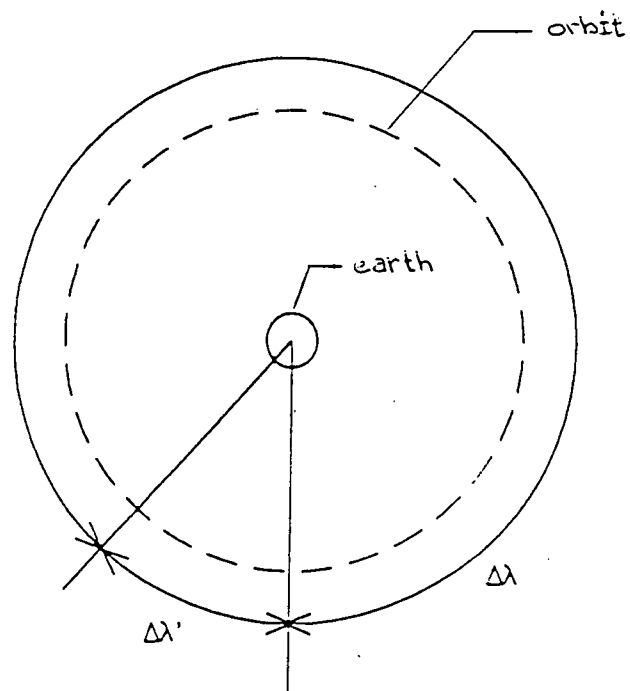
$$V_a = 1.598 \text{ km/sec}$$

figure 3.2
The movement of the subsatellite point alongside the equatorial plane.

<u>Velocity change:</u>

The velocity change needed in the perigee is:

$$\Delta V_p = V_p - V_{c_p} \tag{3.7}$$

$$\Delta V_p = 2.454 \ km/sec$$

This perigee kick is given by the Ariane IV.

Besides providing the necessary velocity change, the apogee kick also has to reduce the inclination of $8°$ to $0°$.
The velocity change needed in the apogee is:

$$\Delta V_a{}^2 = V_{c_a}{}^2 + V_a{}^2 - 2V_{c_a} V_a \cos(i) \tag{3.8}$$

$$\Delta V_a = 1.509 \ km/sec$$

The apogee motor is required to provide the velocity change at an angle α with respect to the equatorial plane.

$$\alpha = \arctan \frac{V_a \sin(i)}{V_{c_a} - V_a \cos(i)} \tag{3.9}$$

$$\alpha = 8.475°.$$

3.5 Drift orbit.

The perigee kick is given at a longitude of $0°$. This means that the apogee shall be at a longitude of $180°W$. If the full apogee kick is given at this longitude the Hitch-Hiker will have an operational longitude of $180°W$. The requirement however, demands an operational longitude of $12°E$.

One of the possibilities, to bring the Hitch-Hiker from a longitude of $180°W$ to $12°E$, is by using a drift orbit. This means that at the apogee not the full velocity change is given. The orbit will therefore not be circular but elliptical. The result is that the projection of the apogee on the earth (sub satellite point) will move alongside the equatorial plane.

Consider figure 3.2.

The earth needs 24 hours to complete a full $360°$ turn in the east direction. The subsatellite point will move $\Delta\lambda$ degrees to the west

$$\Delta\lambda = \left(\frac{360}{24}\right)P = 15P \tag{3.10}$$

P : the period of the drift orbit

The $\Delta\lambda'$ degrees mentioned in figure 3.1 are the movement of the sub satellite point to the east.

$\Delta\lambda'$ [°]	P [h]	Ψ [days]	a [km]	r_p [km]	e [$*10^{-3}$]	ΔV_{a_1} [km/s]	ΔV_{a_2} [km/s]	α [°]
2	23.867	95.468	42085	42006	1.88	1.506	0.003	8.486
4	23.733	47.466	41927	41690	5.65	1.500	0.009	8.526
6	23.600	31.467	41770	41376	9.43	1.494	0.015	8.560
8	23.467	23.467	41613	41062	13.23	1.488	0.021	8.717
192	11.200	0.467	25414	8664	660	0.095	1.28	46.297

table 3.1
The results for different choices of $\Delta\lambda'$.

The calculations for $\Delta\lambda'=8°$ are given:

(1) $\Delta\lambda'= 360°-\Delta\lambda= 360°-15P$ (3.11)

      P : the period (h)
      $\Delta\lambda'$: the movement of the subsatellite point to the east

      $P=23.467$ h

(2) $(\beta/\Delta\lambda')*P=\Psi$ (3.12)

      β : 192°
      Ψ : the period in which the apogee moves from 180°W to 12°E (h)

      $\Psi=563$ h (=23.467 days)

(3) $T= P*60^2 = 2\pi \sqrt{\dfrac{a^3}{\mu}}$ (3.13)

      T : orbital period (s)
      a : semi major axis
      μ : earth's gravitational constant

      $a= 41613$km

(4) $a= \dfrac{r_a+r_p}{2}$ (3.14)

      $e= \dfrac{r_a-r_p}{r_a+r_p}$ (3.15)

      r_a : radius of the apogee
      r_p : radius of the perigee
      e : eccentricity

      $r_p= 41062$km; $e= 13.23*10^{-3}$

(5) $V_b^2 =\mu \left[\dfrac{2}{r_a} - \dfrac{1}{a} \right]$ (3.16)

      $\Delta V_{a_1}^2 =V_b^2 + V_a^2 - 2V_b V_a \cos i$ (3.17)

      V_b : the apogee velocity in the ellipse
      ΔV_{a_1} : the first apogee kick
      V_a : the apogee velocity in the transfer orbit
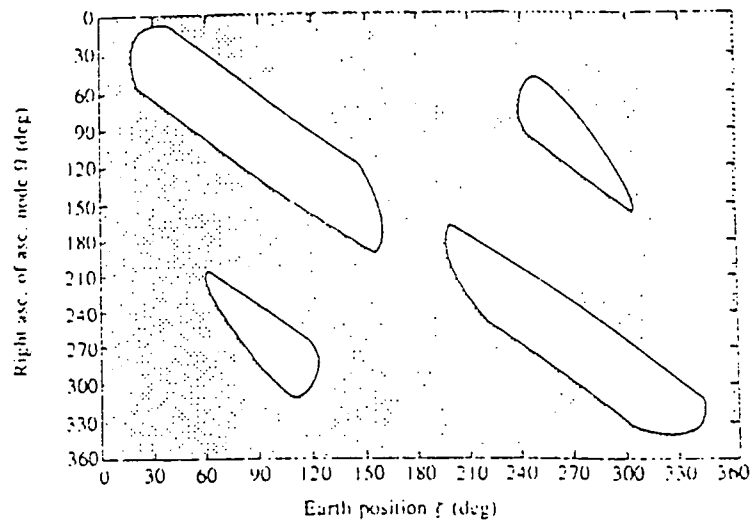 i : inclination

      $\Delta V_{a_1} = 1.488$ km/s
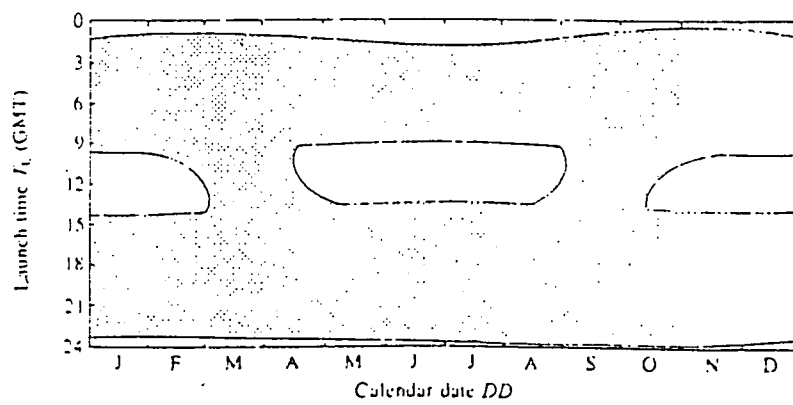
figure 3.3
Launch window in term of Ω and ζ

figure 3.4
Lauch window in terms of launch date DD and launch time T_1

(6) $\Delta V_{a_2} = \Delta V - \Delta V_{a_1}$ (3.18)

ΔV_{a_2} : the second apogee kick

ΔV : the full apogee kick

$\Delta V_{a_2} = 0.021$ km/s

(7) $\alpha = \arctan \left[\dfrac{V_a \sin i}{V_b - V_a \cos i} \right]$ (3.19)

α: angle for the velocity change with respect to the equatorial plane

$\alpha = 8.717°$

These calculations can be made for every value of $\Delta\lambda'$.

In table 3.1 the results for different choices of $\Delta\lambda'$ are given.
Before the choice of the $\Delta\lambda'$ can be made, some considerations have to be taken into account.
Two values are of interest namely the time the Hitch-Hiker needs to drift to the operational longitude and the velocity changes.
The drift period has to be as short as possible because when the Hitch Hiker is still in the drift orbit it can't be used for the purpose it is made for. A drift orbit that last for a maximum of 30 days is considered acceptable.
The duration of the first and second velocity change is also of importance. The reason for this is that after the transfer orbit the solar arrays have to be defolded. Because there are two velocity changes, the solar arrays have to be defolded after the first apogeekick. If the solar arrays are defolded after the second velocity change there won't be enough battery power to provide the sub-systems. The acceleration during the second velocity change has to be low enough for the solar arrays to withstand.
The values belonging to a choice of $\Delta\lambda'=8°$ meets our demands. Those values are taken for further calculations.

3.6   Orbit description.

The orbit that takes the Hitch-Hiker from the perigee point to the apogee point is an elliptical orbit with an eccentricity of 0,730. The total duration of the transfer orbit is $5^h15^m32^s$.
This transfer period puts demands for the powersupply. During this transfer orbit the satellite is spin stabilized. This means that the solar arrays are folded. The necessary power has to be supplied by the batteries.
Furthermore it is important that in the transfer orbit there is an adequate power supply and an acceptable thermal environment.
The Hitch-Hiker must be maintained within a specified sun angle and must avoid eclipses longer than a certain duration. The sun angle has to be maintained within typically 60°-120° (ref. 3.2) because in the transfer orbit the Hitch-Hiker is spin-stabilized. The choice for the maximum tolerable eclipse duration is 22 min.
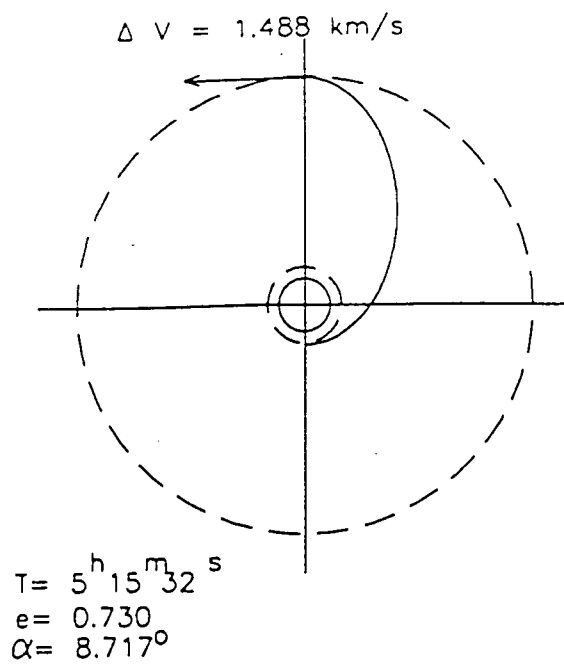
$\Delta V = 1.488$ km/s

T= $5^h15^m32^s$
e= 0.730
α= 8.717°

figure 3.5
The transfer orbit of the Hitch Hiker
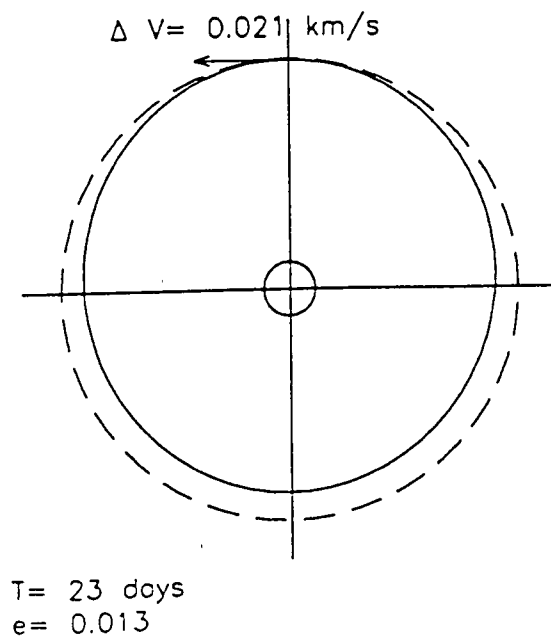
$\Delta V= 0.021$ km/s

T= 23 days
e= 0.013

figure 3.6
The drift orbit of the Hitch Hiker

When we take this in consideration we obtain figure 3.3 In the figure the launch window is plotted in terms of the right ascension of the ascending node Ω and the position of the earth in the ecliptic ζ. It is also possible to use the launch date DD

instead of ζ and the launch time T_1 (GMT) instead of Ω. This is plotted in figure 3.4.

At the end of the transfer orbit the first velocity change is given (ΔV_{a_1} = 1.488 km/s) at an angle with respect to the equatorial plane of $8.717°$ (see figure 3.5). The first velocity change last for about 25 minutes. After the Hitch-Hiker starts the despin maneuver and becomes three axis stabilized the solar panels can then be defolded.

The drift orbit that follows is still elliptical with an eccentricity of 0.013. For the Hitch-Hiker to arrive at the operational longitude, it has to drift for about 23 days and 11 hours. Finally at the operational longitude ($12°$) the second velocity change is given of about 0.021 km/s (see figure 3.6). This last for about 20 minutes. The disc antenna can then be opened. Finnaly the Hitch-Hiker is in an geostationary orbit.
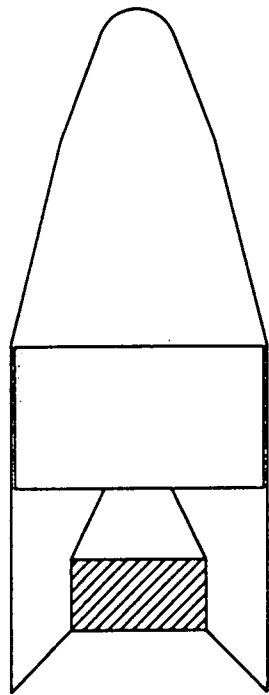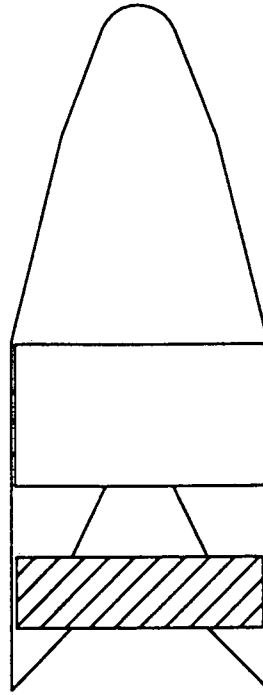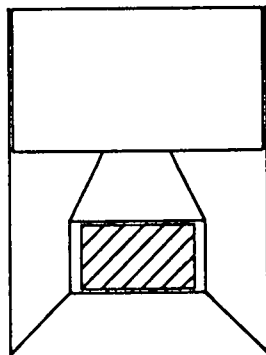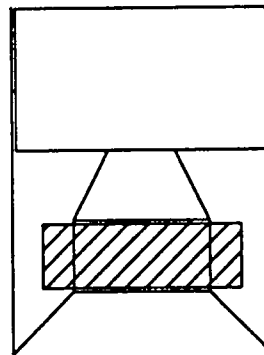
figure 4.1
Launch configuration.

figure 4.2
Available volume for the Hitch-Hiker.

First Option

Second Option

figure 4.3
Location of the Hitch-Hiker.

4   Configuration.

4.1   Introduction.

This chapter deals with the configuration of the spacecraft. It describes the location of the different subsystem elements and the motivation for this location. To get a better understanding of the design process, the interaction and trade-offs between the different subsystems are given.

4.2   Location in the Ariane IV.

The satellite is situated between the SPELDA and the assembly of the adaptor 937B and the upper spacecraft (figure 4.1 and ref. 4.1). The area that is available is a cylinder with a diameter of the outer fairing (3600 mm), see figure 4.2. The height of this cylinder may not exceed 1000 mm (chapter 2).

To support the upper satellite and the adaptor, forces must be transferred trough this area. Since the adaptor is a cone, the most optimal design to transfer these loads is a cylinder with the same diameter as the bottom of the adaptor 937B (1920 mm).

The cylindrical structure which carries the adaptor and the upper spacecraft must be designed in such a way that the upper spacecraft does not encounter higher environmental loads than are foreseen in the Ariane IV Users Manual. Thereby, the upper spacecraft is lifted to a maximum of 1000 mm, so there is less space available in the fairing for the upper spacecraft. Another problem is that the loadings and vibrations for which the upper satellite must be designed change due to the presence of the Hitch-Hiker satellite. The consequences of this approach have to be negotiated with the launch authorities.

Moreover, the extra separation mechanism which is needed must be designed by the Hitch-Hiker-project. The qualification of the separation system shall be performed under CNES/Arianespace authority because the SPELDA functions can be influenced by the extra separation. The separation mechanism has to be designed in such a way that the adaptor 937B and the SPELDA interfaces are not modified.

4.3   Support structure.

4.3.1 Cylinder structure.

To locate the Hitch-Hiker there are two possibilities (figure 4.3). The first is to place a whole satellite in the cylinder mentioned above. The second option is to use this cylinder as the main load carrying subassy for the Hitch-Hiker-satellite, so the cylinder is an important part of the satellite itself.

The disadvantage of the second option is that the dry mass of the satellite increases and with this, the satellite mass increases even more because extra propellant is needed.

For all the elements between the adaptor and the SPELDA interfaces has to be paid. Since for the second option no extra supporting structure is needed, this will decrease the total cost of the project.

The total launch mass of this option is expected to be lower than that of the first option because now no separate load carrying subassy for the Hitch-Hiker-satellite is needed.
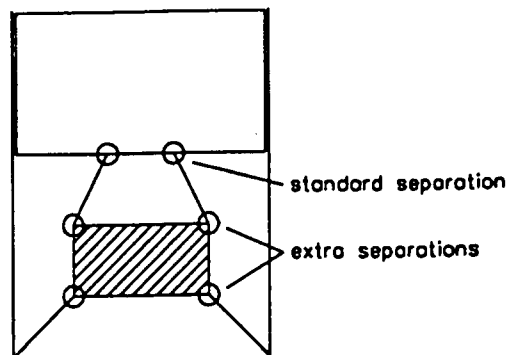
figure 4.4
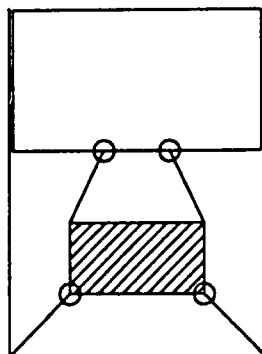Separation points.

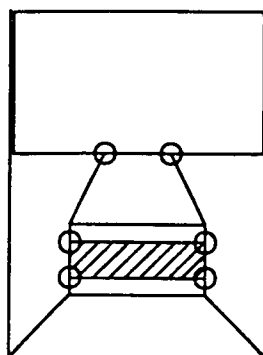figure 4.5
Adaptor attached to the Hitch-Hiker.

figure 4.6
Separation mechanism with extra rings.

Besides that, this option has the extra advantage that when the area around the cylinder is used, the height of the cylinder decreases so the environment of the upper spacecraft is less influenced. Thereby it is not sure wether it is possible to place all the equipment into the cylinder of the first option, even when using the maximum allowable height.

In the first stage of the design study it shows that the Payload subsystem needs an antenna with a diameter of 1800 mm. This antenna takes too much volume so not enough room inside the cylinder is available for the other subsystems like solar arrays and tanks.

For the reasons mentioned above, the cylinder structure is a part of the Hitch-Hiker-satellite, serving three main purposes. It transfers the loads of the upper satellite trough the available area for the Hitch-Hiker, it provides stiffness for the upper satellite and it is the outer side of the Hitch-Hiker satellite.

4.3.2 Separation mechanisms.

In the conventional configuration, without the Hitch-Hiker-satellite, the adaptor is attached directly to the SPELDA so no separation is needed. In our configuration there have to be two extra separations; the first to separate the adaptor from the Hitch-Hiker, the second to separate the Hitch-Hiker from the SPELDA (figure 4.4).

Separation mechanisms are very heavy and an alternative for using two separation mechanisms is to leave the adaptor attached to the Hitch-Hiker satellite (figure 4.5). This has the advantage of having one separation mechanism less, but it also increases the reliability of the system as a whole. Nevertheless two separation mechanisms are used for the reasons mentioned below:

- The adaptor represents an extra mass of 48 kg, for which approximately 50 kg extra propellant is needed during the apogee boost.
- The adaptor will function as a very big surface to radiate energy to the outer environment. The thermal isolation to take care of this problem is extremely complicated.
- It is possible that the adaptor interferes with the burning of the apogee engine. It is sure that the apogee burning heatens the adaptor and introduces a second thermal problem.

The interface of the adaptor and SPELDA cannot be modified so the extra separation mechanisms cannot be attached to these interfaces. The only solution is to use two extra rings on the upper and lower side of the satellite (figure 4.6). The rings are attached to the adaptor and the SPELDA on a conventional way (bolted interface) and contain a separation mechanism on the other side. Since the separation mechanisms are situated on the extra rings and not on the satellite itself, no extra propellant is needed. Nevertheless these extra rings do in fact contribute to the launch mass of the Hitch-Hiker satellite.

To provide the spacecraft the necessary energy during pre-launch for the Hitch-Hiker and the upper satellite an umbilical system is needed. In dual launch configuration the power cables are transported through the adaptor and directely connected to the upper satellite by an umbilical link (ref. 4.1).

In the present configuration the power cables must be lead through the Hitch-Hiker. This is not designed but there is enough room to situate the umbilical connection.

figure 4.7
Tanks of the Hitch-Hiker.

figure 4.8
Another location for the tanks.

figure 4.9
Tank support structure.

figure 4.10
Two cylindrical spherical tanks.

figure 4.11
Toroidal tank.

figure 4.12
Four cylindrical spherical tanks.

Besides that, this option has the extra advantage that when the area around the cylinder is used, the height of the cylinder decreases so the environment of the upper spacecraft is less influenced. Thereby it is not sure wether it is possible to place all the equipment into the cylinder of the first option, even when using the maximum allowable height.

In the first stage of the design study it shows that the Payload subsystem needs an antenna with a diameter of 1800 mm. This antenna takes too much volume so not enough room inside the cylinder is available for the other subsystems like solar arrays and tanks.

For the reasons mentioned above, the cylinder structure is a part of the Hitch-Hiker-satellite, serving three main purposes. It transfers the loads of the upper satellite trough the available area for the Hitch-Hiker, it provides stiffness for the upper satellite and it is the outer side of the Hitch-Hiker satellite.

4.3.2 Separation mechanisms.

In the conventional configuration, without the Hitch-Hiker-satellite, the adaptor is attached directly to the SPELDA so no separation is needed. In our configuration there have to be two extra separations; the first to separate the adaptor from the Hitch-Hiker, the second to separate the Hitch-Hiker from the SPELDA (figure 4.4).

Separation mechanisms are very heavy and an alternative for using two separation mechanisms is to leave the adaptor attached to the Hitch-Hiker satellite (figure 4.5). This has the advantage of having one separation mechanism less, but it also increases the reliability of the system as a whole. Nevertheless two separation mechanisms are used for the reasons mentioned below:

- The adaptor represents an extra mass of 48 kg, for which approximately 50 kg extra propellant is needed during the apogee boost.
- The adaptor will function as a very big surface to radiate energy to the outer environment. The thermal isolation to take care of this problem is extremely complicated.
- It is possible that the adaptor interferes with the burning of the apogee engine. It is sure that the apogee burning heatens the adaptor and introduces a second thermal problem.

The interface of the adaptor and SPELDA cannot be modified so the extra separation mechanisms cannot be attached to these interfaces. The only solution is to use two extra rings on the upper and lower side of the satellite (figure 4.6). The rings are attached to the adaptor and the SPELDA on a conventional way (bolted interface) and contain a separation mechanism on the other side. Since the separation mechanisms are situated on the extra rings and not on the satellite itself, no extra propellant is needed. Nevertheless these extra rings do in fact contribute to the launch mass of the Hitch-Hiker satellite.

To provide the spacecraft the necessary energy during pre-launch for the Hitch-Hiker and the upper satellite an umbilical system is needed. In dual launch configuration the power cables are transported through the adaptor and directely connected to the upper satellite by an umbilical link (ref. 4.1).

In the present configuration the power cables must be lead through the Hitch-Hiker. This is not designed but there is enough room to situate the umbilical connection.
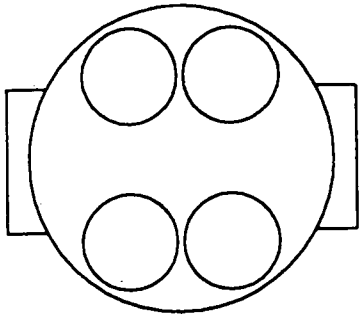
figure 4.7
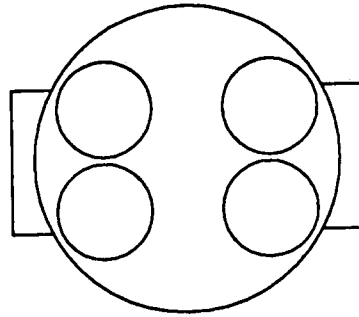Tanks of the Hitch-Hiker.

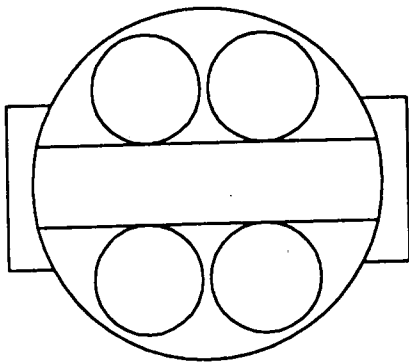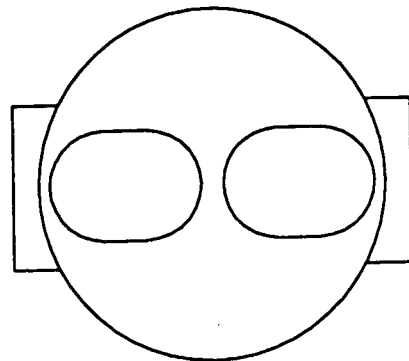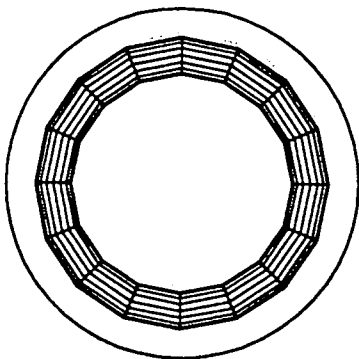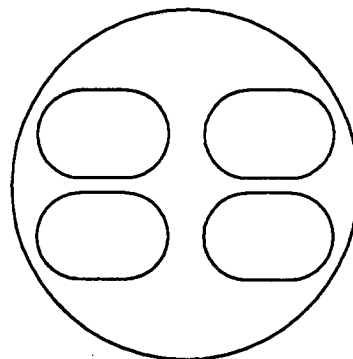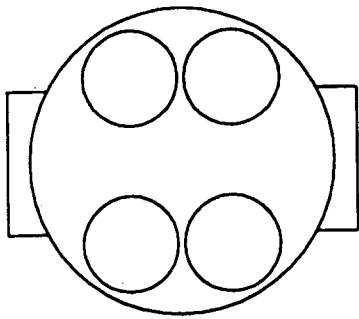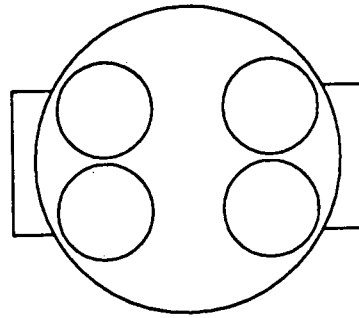figure 4.8
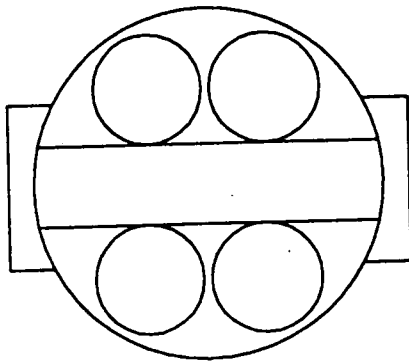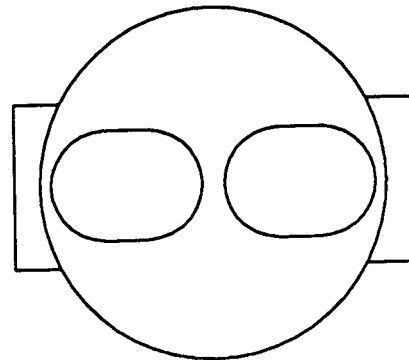Another location for the tanks.

figure 4.9
Tank support structure.

figure 4.10
Two cylindrical spherical tanks.

figure 4.11
Toroidal tank.

figure 4.12
Four cylindrical spherical tanks.

4.4   Configuration design guidelines.

In order to locate the different subsystem elements some general guidelines are applied. In order of importance these are:

1. During the spinning in transfer orbit and apogee boost the center of gravity must be in the center of the satellite so a symmetric design is required. In normal mode one of the axis of inertia must correspond with the rotation axis of the solar array (ref. 4.2). During the apogee boost, most of the propellant is used, so the center of gravity will shift. Therefore it is difficult to keep the center of gravity in the middle of the satellite.
2. The surface used by the equipment is 30% of the total surface. The remaining 70% is used by the wiring and pipes (ref. 4.2).
3. For some equipment, the thermal requirements are very severe, so a good thermal environment must be created.
4. To obtain a stiff structural support, the heavy equipment elements are placed near the cylinder wall (as far as this is possible).

In the following part of this chapter these design guidelines are mentioned frequently to explain some designs.

4.5   Propulsion.

4.5.1 Tanks.

The largest and heaviest elements in the satellite are the propellant tanks. The diameter of the tanks defines the total height of the cylinder and has a great influence on the main design of the configuration.

In the Hitch-Hiker four spherical tanks are used (figure 4.7). These are located around the center. It is assumed that the tanks empty uniformly so the center of gravity remains in the middle before and after the apogee boost (guideline 1). The tanks are spherical because this is the optimal shape for pressurized tanks.

The exact location is chosen to create sufficient room for the other equipment. The batteries must be near to the plane perpendicular to the solar array so the option of figure 4.8 is abandoned (chapter 4.7.1.).

The tank support consists of struts so the forces introduced by the tanks are transferred to the cylinder wall (figure 4.9 and chapter 7.3).

Some other solutions are considered, but abandoned:

-<u>Two cylindrical spherical tanks</u> (figure 4.10).

The propulsion interface is less complicated when two tanks are used. To reduce the height of the satellite, cylindrical spherical tanks can be used. The disadvantages of this option are that the cylindrical spherical tank is not an optimal shape for a pressurized tank and that the center of gravity can never be in the middle before, during and after apogee boost (guideline 1).

-<u>Toroidal tank</u> (figure 4.11).

This solution has the great advantage that the height of the cylinder can be reduced to approximately 200 mm, although in this configuration there might be unsufficient room for the other equipment. In this way the tanks don't define the height of the cylinder anymore. The disadvantages of this option are that the mass of such a tank is far higher than the mass of four tanks because the surface is much bigger. Besides that, some compartments must be designed to get the center of gravity in the middle of the satellite (guideline 1). This solution introduces a very complicated system, and the Hitch-Hiker is not meant to be innovative.

-<u>Four cylindrical spherical tanks</u> (figure 4.12).

The solution of four cylindrical spherical tanks reduces the height of the satellite. The disadvantage is that there is not enough room anymore for the remaining equipment (guideline 2).
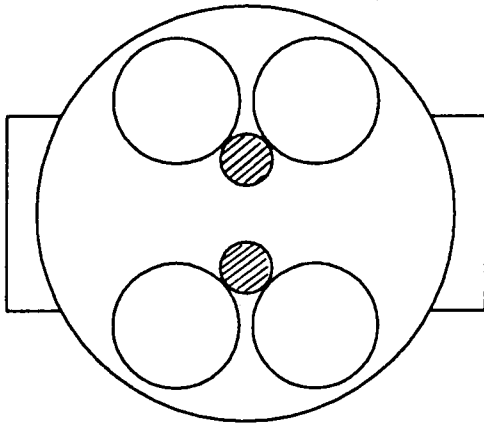
figure 4.13
Helium tanks.
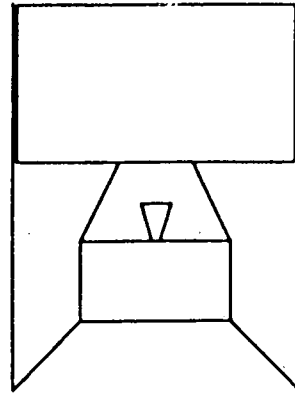
figure 4.14
Nozzle penetrating the adaptor.

A B A

A B A

C C
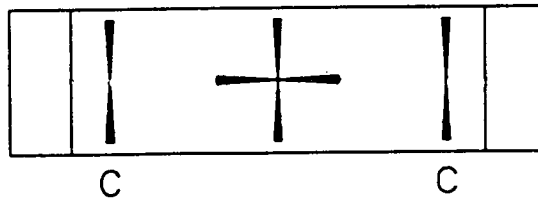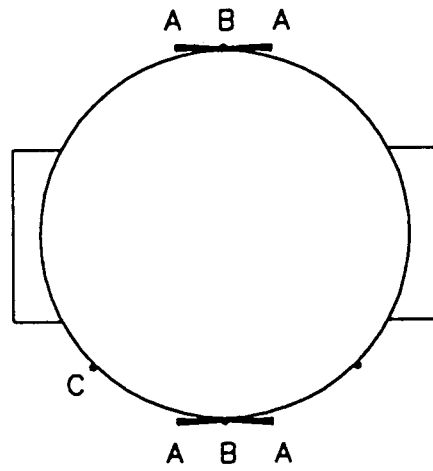
figure 4.15
Position of the AOCS thrusters.

The propulsion subsystem also uses two small helium tanks to provide the required pressure. These tanks are located on the lower platform near to the propellant tanks to shorten the pipe lines (figure 4.13).

Both propellant and helium tanks must be isolated. The tanks have restrictions to the storage temperature of the propellant and the helium (chapter 11.6).

4.5.2 Apogee engine.

The chosen propulsion system consists of one apogee boost engine with a diameter of 180 mm and a height of 400 mm. Since a single engine is used it has to be placed on the spinning axis, being the mayor axis of inertia.

The engine is placed below the lower platform. In launch configuration the Hitch-Hiker-satellite is placed upside-down in the Ariane IV (figure 4.14), so the nozzle of the engine penetrates the adaptor over 400 mm. This solution has to be discussed with Arianespace because it is not sure whether the empty space of the adaptor can be used. About 400 mm of the upper side of the adaptor is defined as usuable volume for the upper spacecraft so in principal, it must be possible to use 400 mm of the lower part of the adaptor.

The advantage to place the engine in this location is the much improved thermal environment in the cylinder structure. When placed inside the cylinder, the engine radiates a great percentage of its heat to the surrounding equipment.

An incidental advantage of using the rings for the separation mechanism is that the total height of the nozzle penetrating the adaptor is reduced.

Another solution studied is the use of more than one engine, placed outside the cylinder wall. This has the advantage that the loadings due to the thrust of the engines are in the same direction as the main loads during launch. Also, less volume inside the cylinder is used and the thermal radiation can be handled easier and there is no penetrating of the nozzle in the adaptor.

There are also some serious disadvantages. First, a simultaneous ignition of the engines requires a complex valve-system. Also, the pipe-system has to be doubled or even quadrippled which increases the launch mass. Second, there must be made more cut-outs in the cylinder wall which lowers the maximum allowable loads on the cylinder. Third, the burning times are enlarged because the four engines are smaller so possibly more apogee kicks are needed which can result in a longer transfer orbit and the additional problems that arise with this. A final problem is that the reliability of the system would be insufficient so the design of a single engine is chosen (chapter 11.2.3).

4.5.3 Thrusters.

The AOCS subsystem needs 12 thrusters to provide rotation about the three major axis of inertia. These are placed on the outside of the cylinder wall (figure 4.15).

Thrusters A provide rotation about the X-axis.
Thrusters B provide rotation about the Y-axis.
Thrusters C provide rotation about the Z-axis.
Thrusters C have a shorter arm to the major axis of inertia.

For each rotation four thrusters are used because a moment in both directions has to be produced. The thrusters are packed together so only four cut-outs in the cylinder wall are needed.

The thruster radiate much heat, so to protect the cylinder wall the direction of the thrust vector is facing outwards and the cylinder wall is locally isolated. Special care is taken not to interfere with infrared equipment (IRES) and the solar array.

Four of these thrusters are also used for station keeping. In this way, no extra four thrusters are needed (chapter 8.6.1, 11.3).
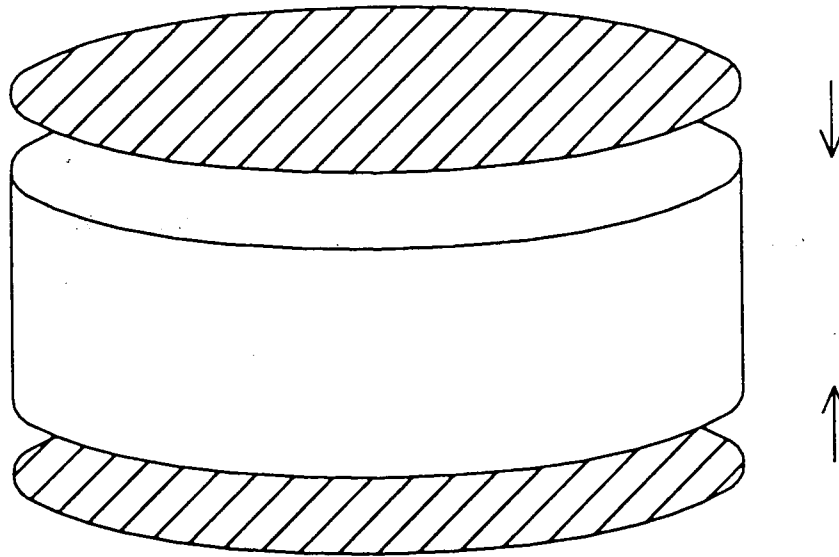
figure 4.16
Platforms.
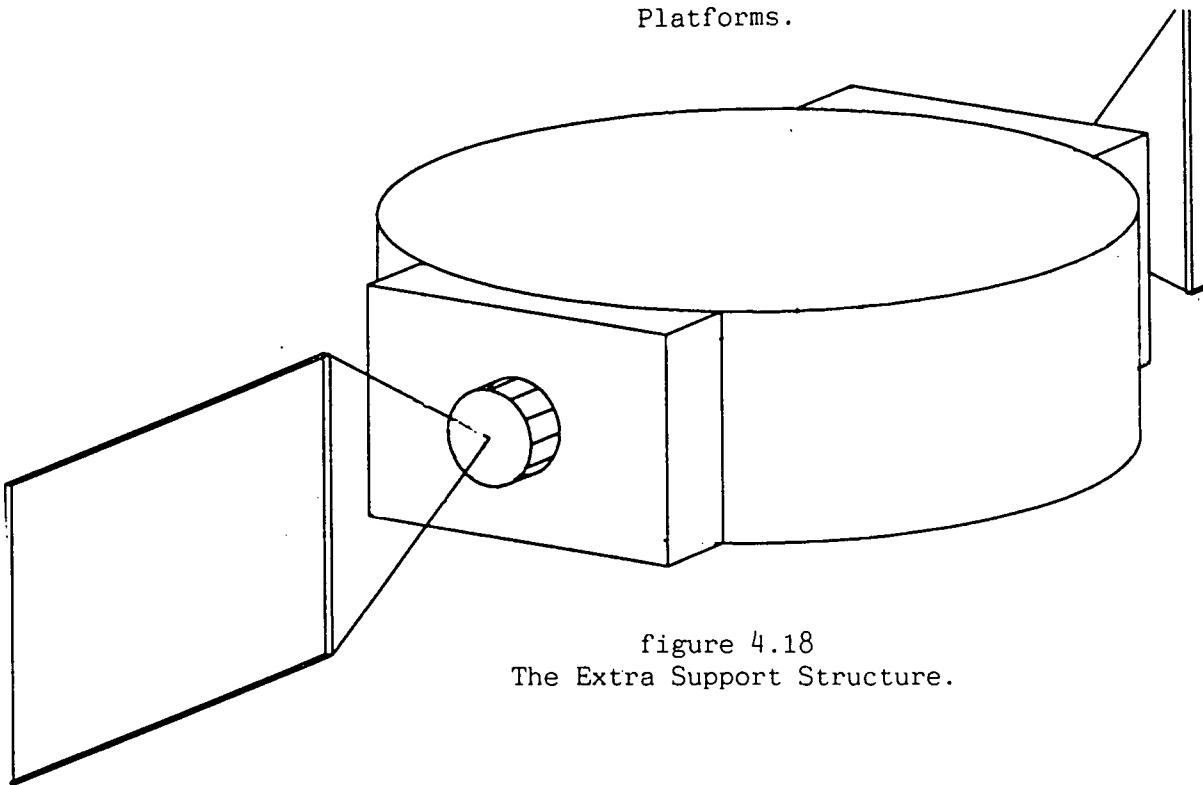
figure 4.18
The Extra Support Structure.
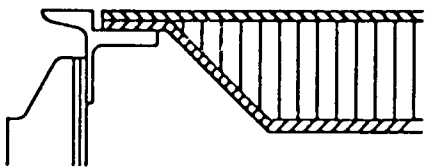
figure 4.17
Support of the platforms at the cylinder edge.
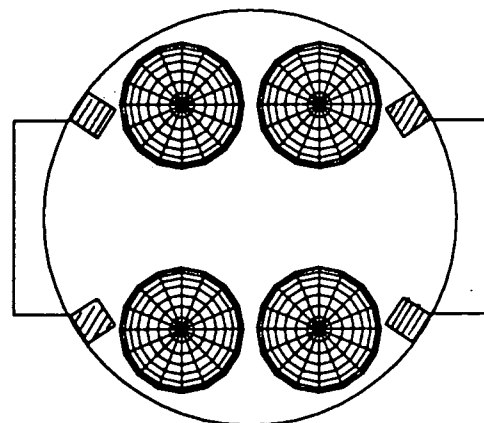
figure 4.19
Position of the batteries.

4.6 Structure.

4.6.1 Platforms.

To provide enough room for the equipment (guideline 2), two platforms are placed on both ends of the cylinder (figure 4.16). The upper platform is used mainly for the payload and TTC equipment. The lower platform supports the housekeeping equipment and the apogee engine. To give the platforms enough stiffness the tank support structure is sufficient. For detailed design information see chapter 7.4.2.

The platforms are simply supported at the cylinder edge (figure 4.17) so a ring of approximately 50 mm next to the edge of the platform cannot be used to place equipment.

4.6.2 Tank support structure.

During launch, the tanks introduce the most severe loads. To transfer these loads to the cylinder wall a tank support structure is needed (figure 4.9). In this way the loads are carried by the cylinder, something for which it is designed. It is assumed that the platform are no part of the main load path of the forces introduced by the tanks.

The tank support structure is made of a milled aluminum structure. An extra advantage of the tank support structure is that it also supports the platforms. In this way, it provides a stiff support for the platforms. This is necessary because the great diameter of the platforms would else require very thick and heavy platforms to obtain the required stiffness.

4.6.3 The extra support structure.

The amplifiers of the payload subsystem radiate much unwanted heat (chapter 7.9.2, 5). To radiate this heat into space a flat surface is created in such a way that it catches very little sun radiation (figure 4.18). This surface is orientated perpendicular to the solar arrays. The cylinder itself cannot provide this surface because it has a curved surface.

The ESS is made completely of aluminum honeycomb structure because the aluminum has a high coefficient of thermal conduction. In this way it is able to radiate the heat quickly (chapter 7.4.5.).

The ESS supports the BAPTA's and the solar wings. Also, the horns of TTC are placed on the ESS. This introduces some loading cases which must be met. It is considered to place the BAPTA into the ESS but this is not possible because there is not enough room and the thermal environment is too severe for the BAPTA.

An advantage in the scope of manufacturing is that the ESS with all the equipment inside can be assembled as a whole subassy.

4.7 Power.

4.7.1 Batteries.

The heavy batteries are split into four boxes (chapter 6). Because the operating temperature is stricktly limited, a stable thermal environment has to exist in the location of the batteries. Another requirement is that the batteries must be able to radiate a lot of energy during charging and decharging. The other equipment may not be influenced by this radiation, so the batteries are placed against the cylinder wall.
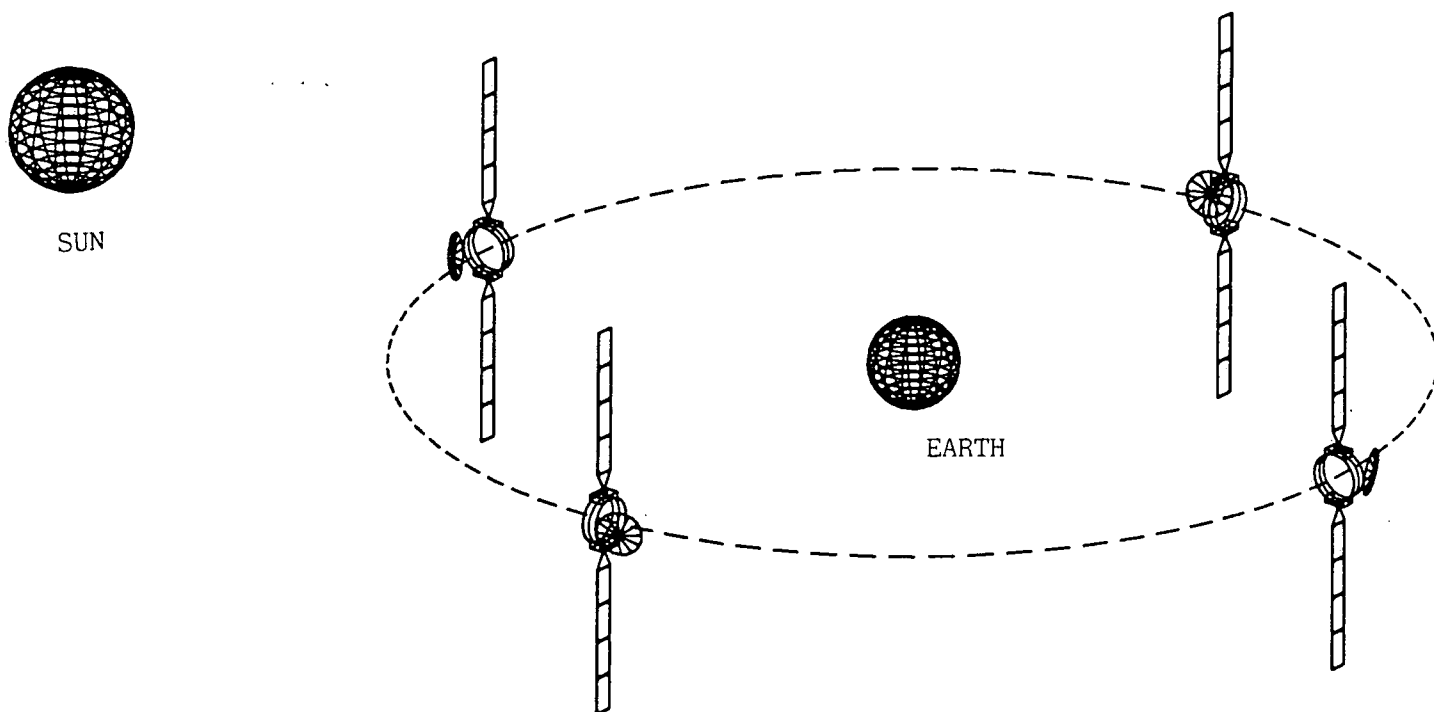
figure 4.20
Configuration of the Hitch-Hiker in orbit.
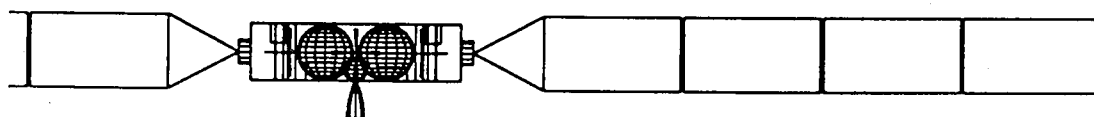
figure 4.21
Solar array.
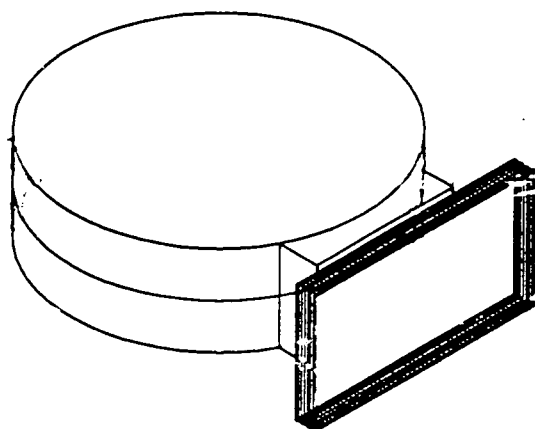
figure 4.22
Solar panals packed to the ESS.
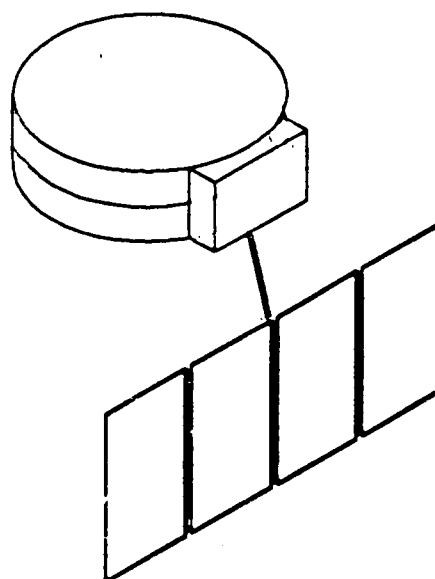
figure 4.23
Configuration using one wing.

The batteries cannot be placed against the ESS because the power radiation cannot be handled. The location for the batteries is now between the tanks and the ESS (figure 4.19). Special care must be taken for the isolation of the tanks.

The batteries have a contact surface with the cylinder wall, but the weight of the batteries is carried by both platforms. The platforms are stiffest near the edge of the cylinder, so in this configuration the location of the batteries is also optimal from structural point of view.

4.7.2 Solar array.

In figure 4.20 the configuration of the satellite in orbit is shown. The solar array is placed perpendicular to the equatorial plane. In this way, the solar cells will catch the most possible sun radiation. It is not possible to place the array perpendicular to the sun radiation without an extra mechanism, because the inclination between the equatorial plane and the ecliptic is 23°.

The solar array consists of two wings with each four rigid panals (figure 4.21). The choice for this kind of array and its location is explained in chapter 7.4.6. The wings are packed against the ESS, on the outer side of the cylinder. During transfer orbit, one panal on each side faces outward so it is possible to obtain energy (figure 4.22). This reduces the battery power needed in transfer orbit.

The panals are held down on four points and will be deployed by a thermal-knife system. The deployment must be controlled and no heavy shocks may occur.

To provide rotation of the solar array, two BAPTA's are used. The BAPTA functiones with a solar cell so it has to be placed outside the cylinder wall. The connection with the solar array is provided by a yoke. The dimensions of the yoke depend on the shadow effects of the satellite. This is analysed in chapter 7.4.6.

Another solution considered consists of a solar array with one wing, totally deployed under the satellite (figure 4.23). This solution could save mass, but an extra mechanism has to be developed taking care of rotating the BAPTA. Moving parts have to be avoided as much as possible so it is abandoned.

Besides rigid panels it is also possible to use a foldable array of a roll-up system. In this way there can also be obtained energy during transfer orbit, but it has to be partial deployed so there are moving parts and extra demands to the solar array being able to resist the forces during the apogee boost.

The advantage of using a roll-up of foldable array is that it takes up less volume in the satellite. However, this only accounts for big panels. The Hitch-Hiker's solar array has a surface area of approximately 9 m² so it is not convenient to use a roll-up system or a foldable array.

4.7.3 Equipment.

The additional equipment of the Power sub-system consists of a Power Conditioning Unit (PCU), a Power Control Distributing Unit (PCDU) and BAPTA-electronics.

The PCDU and PCU have no requirements on the location so these are placed opposite to each other to keep the location of the center of gravity in the middle of the satellite (guideline 1).

The BAPTA-electronics are placed in the cylinder, on the upper platform near the BAPTA's themselves. It was impossible to place the electronics box into the ESS because of lack of room, and the thermal enviromnent created by the TWT might be too severe for the BAPTA-electronics.

In this phase of the study the wiring and its exact location is not taken into account.
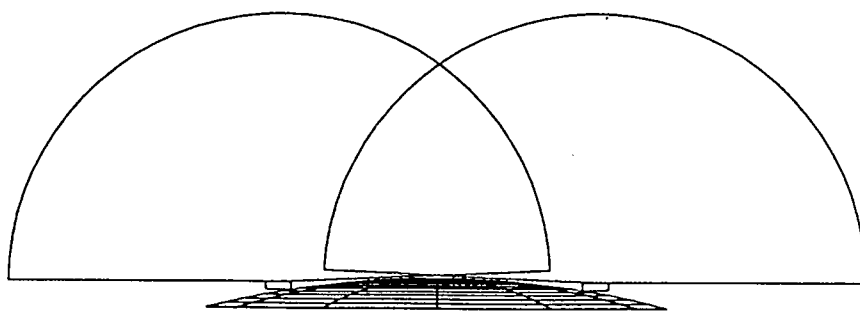
figure 4.24
Field of view of the upper SAS's.
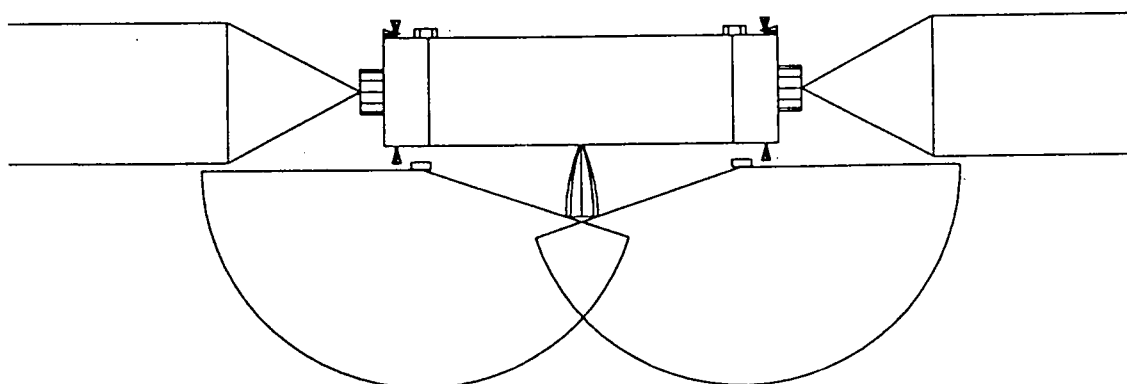
figure 4.25
Field of view of the lower SAS's.

Lower Platform
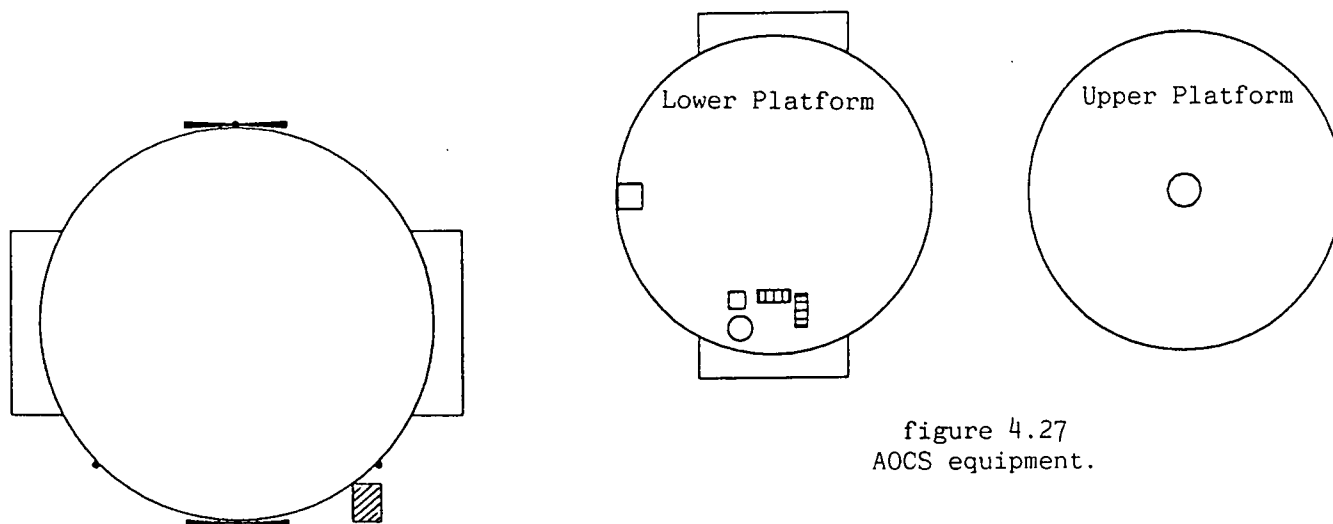
Upper Platform

figure 4.27
AOCS equipment.
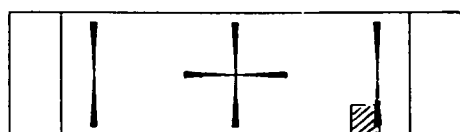
figure 4.26
Position of the IRES.

upper platform

hinge

7°

reflector

hold down points

ribs
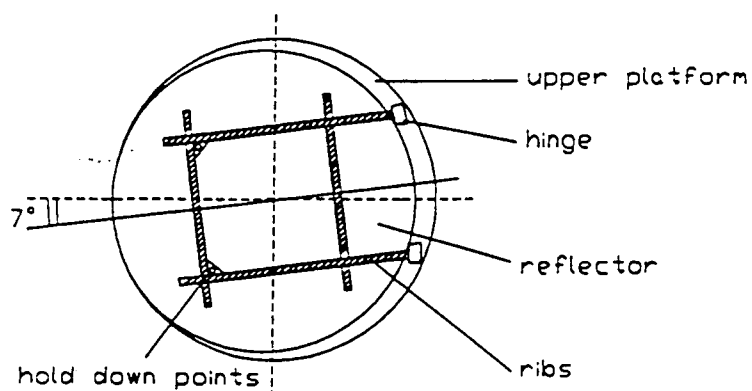
figure 4.28
Position of the antenna on the upper platform.

4.8 Attitude and Orbital Control.

4.8.1 Sensors.

The AOCS equipment consists of four Sun Aquisition Sensors (SAS), 3 Quadrant Sun Sensors (QSS), an InfraRed Earth Sensor (IRES), 3 reaction wheels, Rate Integrating Gyro's (RIG) packed in a Ferranti-box, a RIG-electronics box and a Wheel Drive Electronics box (WDE) (chapter 8.6.).

The SAS must have a Field Of View (FOV) of $\pm 90°$ in both positive and negative X-direction. The SAS is an aquisition sensor. As the dish-antenna deploys in orbit, the SAS is only active when the dish antenna is in retracted position. Because of this it can be placed on top of the dish antenna. It is possible to use only one SAS on top of the dish antenna, but in this way the height of the satellite increases, so it is chosen to use two SAS's (figure 4.24).

On the bottom of the satellite also two SAS's are needed because the FOV is blocked by the nozzle. Also, the solar panels are higher than the height of the cylinder, so the SAS's must be places on a picket (figure 4.25). Special care must be taken for the interference during apogee burning.

The QSS needs a FOV of $\pm 30°$ in both positive and negative X-direction. Placed on top of the satellite, the deployed dish antenna blocks the FOV so again, two QSS's are used. On the bottom this problem does not occur, so only one QSS is used.

The IRES must be placed in the +Z-direction with a FOV of $\pm 15°$ in Y-direction and $\pm 11°$ in X-direction. Also, the IRES cannot be placed near an element which radiates too much heat for reasons of interference. To obtain this requirements, the IRES is placed against the cylinder wall, as shown in figure 4.26. Assumed is that in this configuration there is no interference with the thrusters.

4.8.2 Equipment.

The axis of the reaction wheels are placed in the same direction as the axis of inertia. There are no further requirements so the location of the wheels is free to choose. Two reaction wheels are placed on the lower platform, the third is placed in the middle of the upper platform (guideline 1 and figure 4.27).

The WDE is placed between the tanks on the lower platform in order to compensate the TTC-computer (guideline 1 and chapter 4.10.2)'.

The Ferranti-box and the RIG-electronics are placed on the lower platform. These are placed near the reaction wheels to compensate the high mass of the PCDU and are placed close to each other to shorten the wires.

The thrusters used for station keeping and orbit control are described in chapter 4.5.3.

4.9 Payload.

4.9.1 Dish antenna.

The main antenna is a deployable dish antenna with a diameter of 1800 mm, which is the maximum allowable antenna diameter. The payload sub-system uses a filter duplexer, so a single dish antenna can be used for up- and down-link. The feed is located on the upper platform and is not deployable.

The deployment system and hold-down mechanism take up some room so the antenna is shifted a bit to the cylinder wall (figure 4.28).

Another solution considered is to use a rigid antenna and a deployable feed. In this way, the antenna can be supported very stiff. However, the deployable feed has to be placed next to the antenna, where there is not enough room for a deployment arm.

Lower Platform

Upper Platform
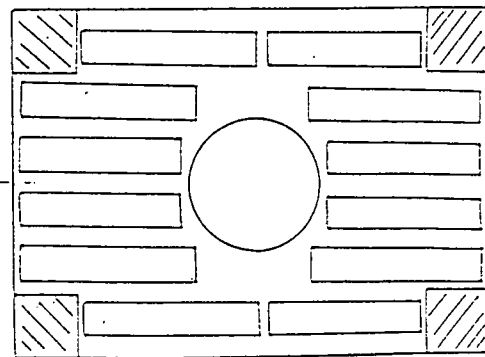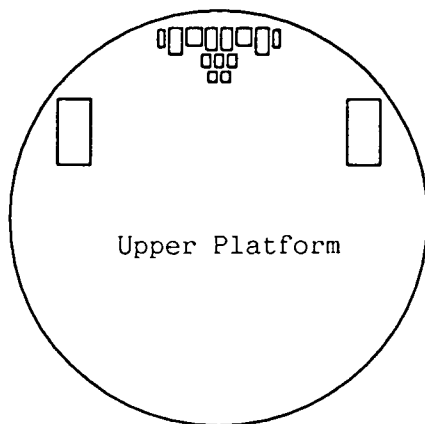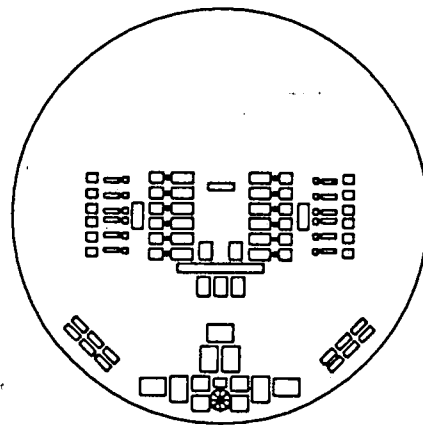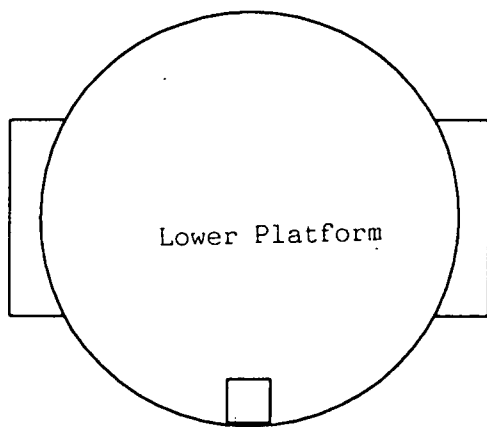
figure 4.31
TT&C equipment.

figure 4.29
Payload equipment.
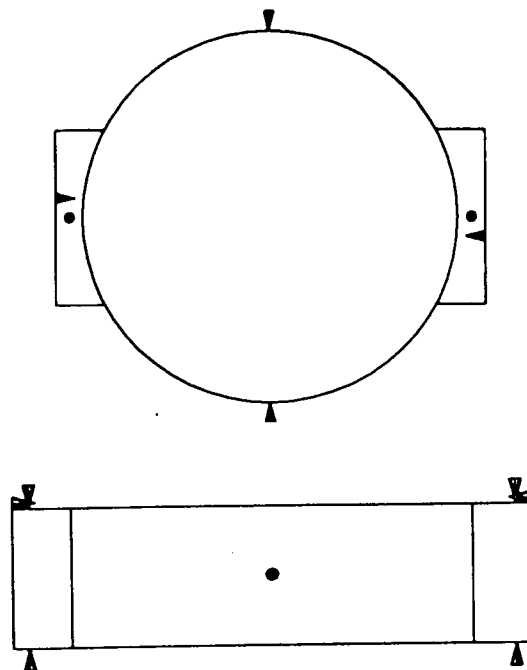
figure 4.30
Position of the telemetry horns.

In the retracted position the antenna coveres the feed. Since the feed is about 100 mm high, it has to be lowered inside the platform. This reduces the stiffness of the platform, but otherwise the height of the cylinder increases too much.

The antenna is stowed in one of the extra rings of the separation mechanism just above the lower SPELDA, so an enlargement of cylinder is not needed. This means that the lower ring is heigher than the upper ring, so these cannot be produced in the same way which increases the costs.

The design of the dish-antenna is such that it takes as less volume as possible is order not to increase the height of the cylinder too much (chapter 7.4.7). Again, special care must be taken for a good isolation (chapter 9).

4.9.2 Equipment.

The payload equipment consists of an amplifier-system which is duplicated 12 times. The only requirement to the location of the equipment is that the wiring between the duplexer and the feed must be as short as possible.

The upper platform is used mainly for the payload equipment. The equipment is placed in accordance with the wiring diagram of payload (figure 4.29 and chapter 5.11). This is not true for the EPC and TWT. These two elements radiate much heat. In order not to influence the equipment inside the satellite, these are placed inside the ESS (chapter 7.4.5 and 9).

The equipment is placed as symmetrical as possible to keep the center of gravity in the middle of the satellite (guideline 1). Still, more equipment is placed on the side of the feed. This is done to compensate the mass of the dish antenna.

The equipment is placed partially under the tanks.

4.10   Telemetry and telecommand.

4.10.1 Antenna's.

To provide communication the Hitch-Hiker needs an omnidirectional transmission capability (chapter 10). An omnidirectional transmitter cannot be used because there is not enough space available. To meet this problems, eight individual horns are used, 6 in every direction and 2 for reliability (figure 4.30). The horns on the ESS are placed such that they do not interfere with the Marman clampband when the separation takes place.

4.10.2 Equipment.

The TTC equipment consists of two amplifiers and one on-board computer. The electronical equipment of the amplifiers is placed on the upper platform. There are no severe requirements to the location of this equipment, so mainly guideline 1 is used (figure 4.31).
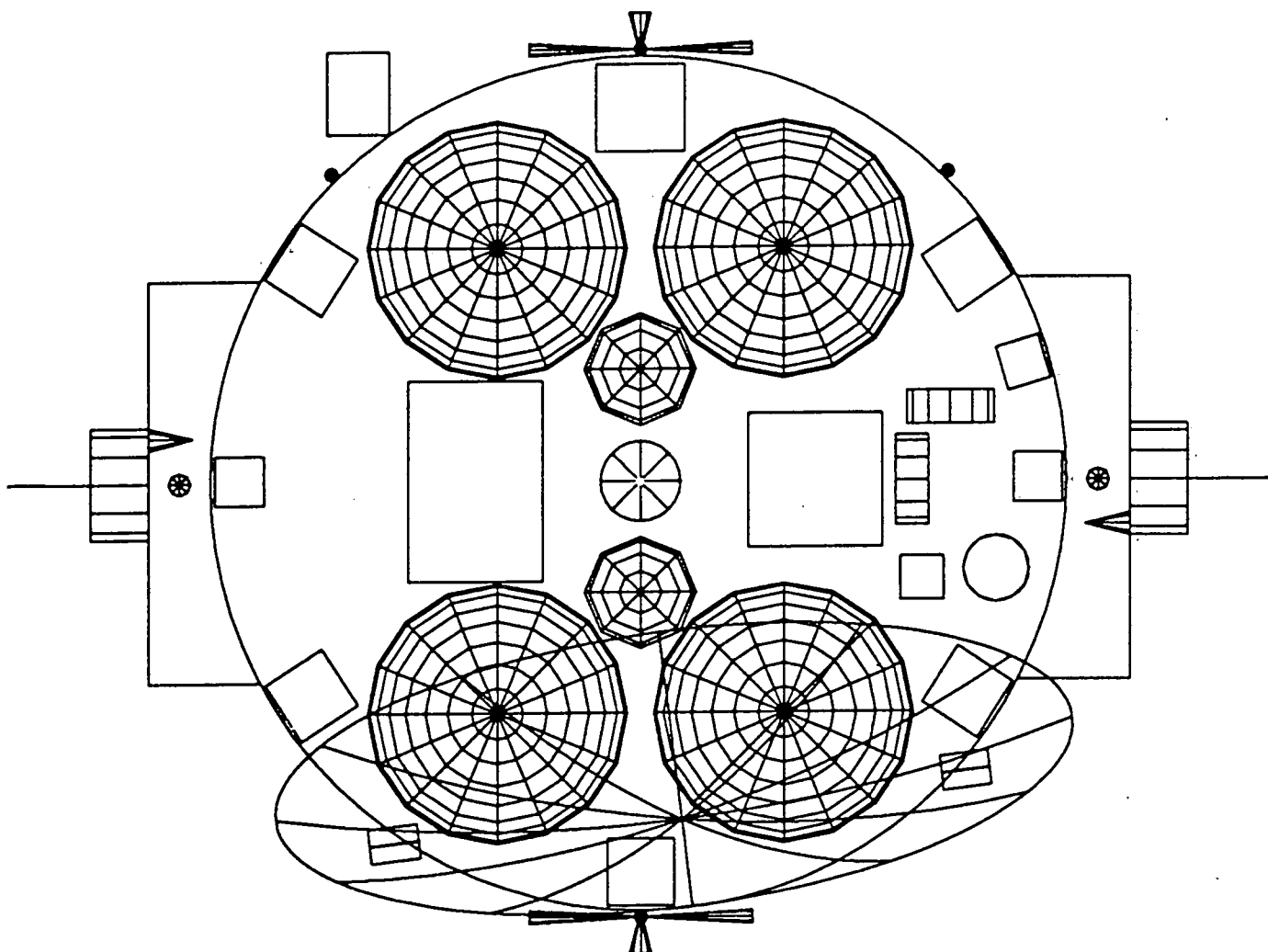
figure 4.32
Overview of the total equipment.

The moments of intertia about the center are:

Ix = 2.5514321997 E 8
Iy = 3.1834836401 E 8
Iz = 3.9352262543 E 8
Cxy = 3.5109307983 E 12
Cyz = 9.1845032435 E 6
Cxz = 7.1730670934 E 5

The position of the center of gravity about the center is:

x   = 3.052765 E 4 mm.
y   = 4.010855 E 4 mm.
z   = 2.858470 E 2 mm.

The moments of inertia about the center of gravity are:

Ix = 1.1530625852 E 12
Iy = 6.6849752926 E 11
Iz = 1.8214972983 E 12
Cxy = 8.7775071963 E 11
Cyz = 3.8820682523 E 6
Cxz = 6.7939381403 E 5

Table 4.1: Moments of inertia and position of center of gravity.

4.11 Moments of inertia.

After the first configuration freeze, which occured before the Mid-Term Review, a rough calculation was made by hand to provide the AOCS-subsystem with data to perform simulations.
Two different configurations were calculated:
1. In transfer orbit, with retracted dish antenna, full tanks and undeployed solar panals.
2. In normal mode: deployed dish antenna and solar panals and the tanks almost empty.
It showed that: - in transfer orbit: $I_{xx} = 350$ kgm²

- in normal mode : $I_{xx} = 760$ kgm².

After the second configuration freeze, a PASCAL programma was made to get more precize data of the moments of inertia and the location of the center of gravity. In this programma, all the equipment can be input as simple elements, namely:
- a solid box, dimensions length, width, height (almost all equipment).
- a sphere-shell, dimension radius (empty tanks)
- a solid sphere (fuel)
- a solid cylinder, placed perpendicular to the three major axis (platforms, antenna, reaction wheels)
- a cone, placed in the x-direction (nozzle)

All equipment is simplified to one of these elements. The output of the program is table 4.1. The location of the center of gravity is almost in the middle of the cylinder and the requirements concerning the moments of inertia are satisfied (chapter 8).

4.12   Remarks and conclusions.

Figures 4.32 and 4.33 show an overview of the total equipment of the Hitch-Hiker. It shows a symmetrical design due to guideline 1.
In table 4.2 an equipment list is presented. In this table all dimensions and masses (per element) of the various elements are given.

The configuration as a whole seems to be an appropriate one, although some aspects like magnetic fields and potential differences are not taken into account.
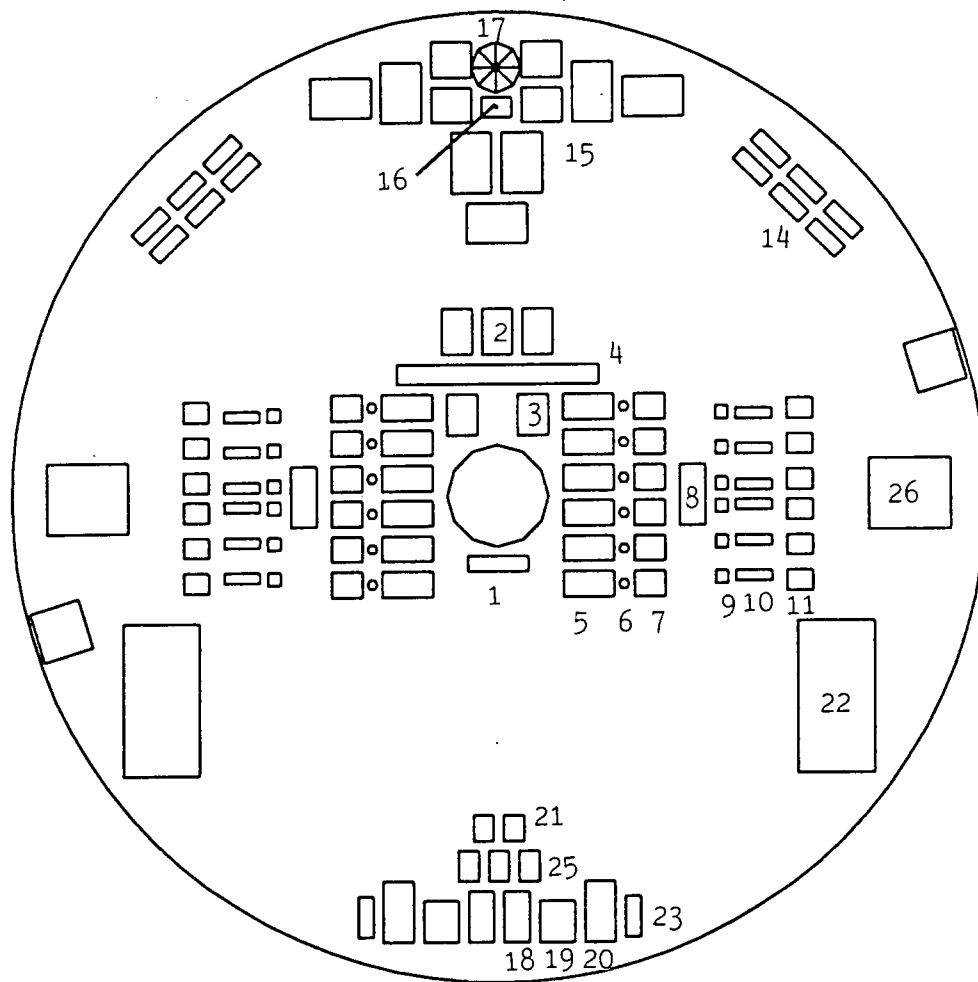
payload	number		TT&C	
1 duplexer	1		18 band pass filter	2
2 switch	3		19 attenuator	2
3 receiver	2		20 main amplifier	2
4 branching network	1		21 drive	2
5 bandpass filter	12		22 SSPA	2
6 attenuator	12		23 isolator	2
7 main amplifier	12		24 max. filters	2
8 control box	2		25 switch	3
9 ALC	12		26 computer	2
10 FET amplifier	12			
11 drive adjust	12			
12 TWT	12			
13 EPC	12			
14 isolator	12			
15 multiplexing filter	11			
16 harmonic filter	1			
17 feed	1			

figure 4.33
Overview of the total equipment (contined)

EQUIPMENT LIST

	Dimensions	Mass (kg) per element
AOCS.		
SAS 4x	110x110x42	0.155
QSS 4x	100x100x50	1.8
IRES 1x	137x190x158	2.55
Reaction wheel 3x	d=200 h=75	3.0
Ferranti	d=150 h=100	2.5
WDE	210x150x150	3.5
RIG electr	200x100x100	2.0
POWER.		
PCU	300x300x150	8.0
PCDU	400x250x300	17.3
Batteries 4x	450x300x200	10.0
BAPTA 2x	d=250 h=130	3.5
BAPTA elec 2x	203x145x158	2.0
Harness		10.0
Solar Arrays	9m²	26.0
PROPULSION.		
Nozzle	d=180 h=400	
Tanks 4x	d=580	
Pressurizer 2x	d=252	
Thrusters 12x	d=30 h=250	
TT&TC		
Computer 2x	200x200x200	5.0
Horns 8x	d=50 h=100	0.8
BPF 2x	200x100x 50	0.75
Attenuators 2x	d=20 h=20	0.005
Main Ampl. 2x	120x 50x 60	0.175
BPF 2x	200x100x 50	0.75
drives 2x	40x 50x 15	0.10
SSPA 2x	300x150x100	1.50
Isolators 2x	80x 30x 30	0.10
Max filters 2x	120x 80x 70	0.30
Switches 3x	90x 60x 40	0.20
Cabling		0.50

Payload.

Duplexer 1x	400x 60x 40	0.30
Switch 3x	90x 60x 40	0.20
Receiver 2x	130x 80x 60	2
Branching netw	120x 30x 30	0.15
BPF 12x	200x100x 50	0.75
Attenuators 12x	d=20 h=20	0.005
Main Ampl. 12x	120x 50x 60	0.175
Control Box 2x	150x120x 50	0.50
ALC 12x	70x 25x 25	0.10
FET amps. 12x	70x 40x 20	0.12
Drive Adjust 12x	40x 50x 15	0.10
TWT 12x	50x 60x300	0.60
EPC 12x	330x 60x150	1.60
Isolator 12x	80x 30x 30	0.10
Multipl filt 11x	120x 80x 70	0.30
Harm Filt	120x 60x 40	0.20
Cabling		3.00
Antenna	d=1800	12.5
Support		3.0
Mechanism		2.0
Feed	d=100 h=100	1.0

Structure

Platform 2x	d=1800 h=35	11.9
Cylinder	d=1920 h=600	23.8
ESS 2x	t=220 l=800 h=600	7.0
Sep mech 2x		20.0
Tank support 2x		6.5
Extra rings (tot.)		10.0

Table 4.2:   Equipment list
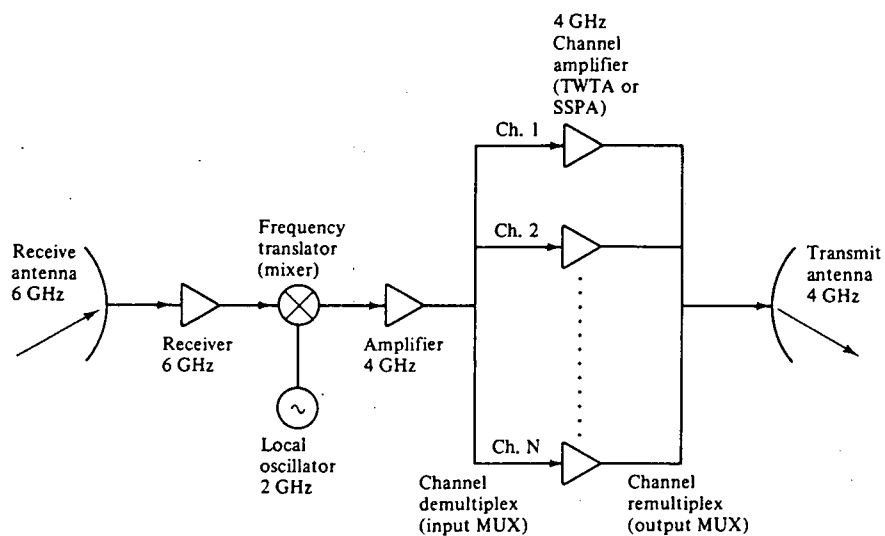
figure 5.1
Simplified block diagram of a satellite communications subsystem.
(ref. 5.1)
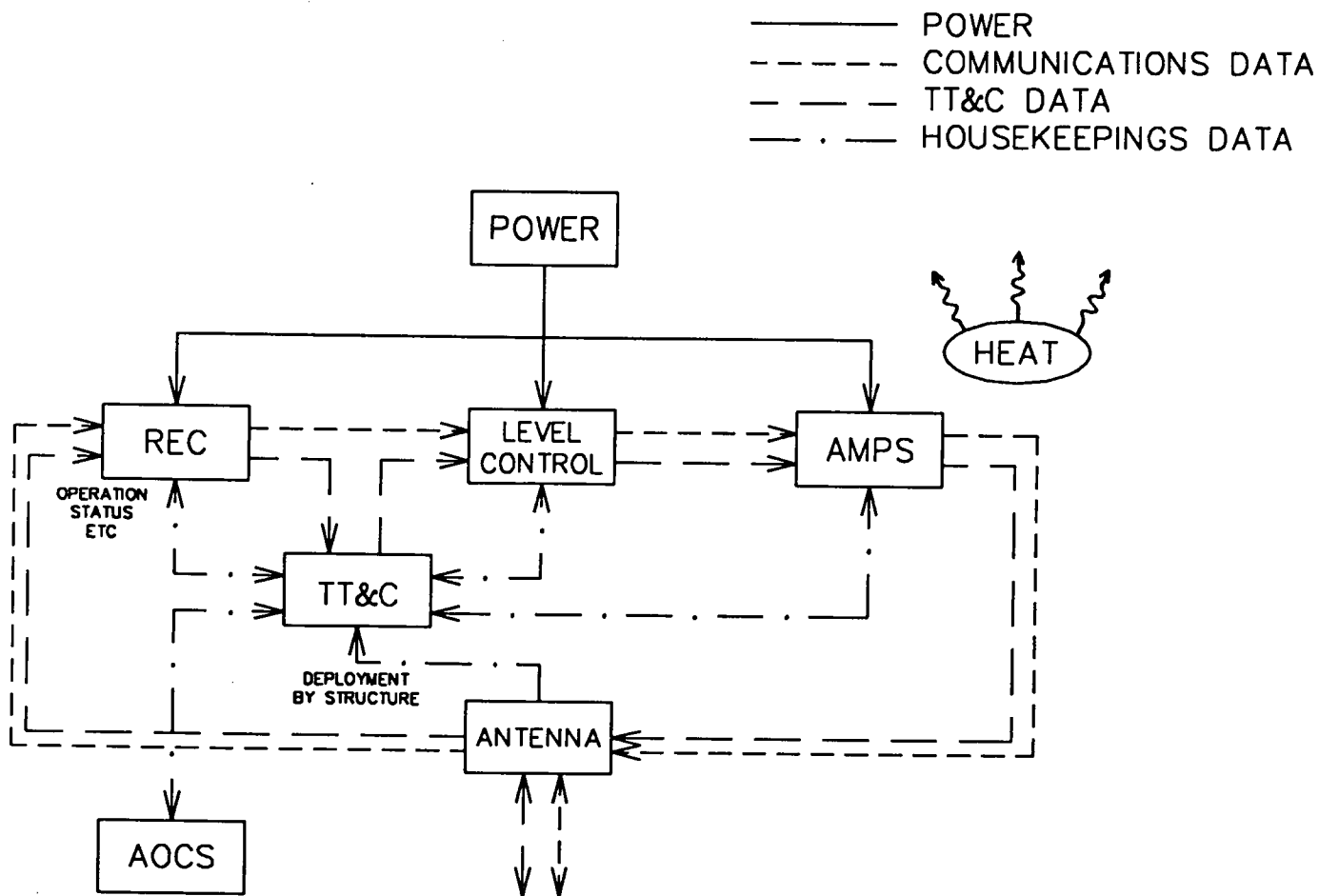
figure 5.2
Relations of the communications subsystem with other subsystems.

5   Payload.

5.1   Introduction.

In this chapter an overview of the design of the communications payload (for convenience abbreviated as CP) will be given. Unfortunately the know-how for the design of a communications subsystem was not available in the Hitch-hiker design team, when the project was started, nor was it provided during the study at the aerospace department in Delft. Therefore, it was necessary to keep the design of the CP relatively simple.

The task of a CP is to provide communications between several ground stations, which may be mobile. In order to provide communications the payload must receive the signals transmitted by the transmitting ground stations (uplink). Then the weak communications signals must be downconverted to the downlink frequency, amplified and retransmitted to the receiving ground stations (downlink). Reception and retransmission of the communications signals is usually provided by passive elements: the antennas. Conversion and amplification of the signals however is done by active elements: the repeater or transponders, see figure 5.1. The designation "active" means that these elements consume power which is generated by the power subsystem.

As mentioned above, the CP depends on the power supply subsystem, which produces the power consumed by the CP. This relation and the relations with other subsystems are shown in figure 5.2. As can be seen from this figure, the operation of the CP is controlled by the telemetry and telecommand (TT&C) subsystem, which on its term uses the payload repeater and antenna for the transmission of data. The structure must provide firm support of the payload equipment and must deploy the antenna. Again, this deployment is controlled by the TT&C subsystem. The attitude control system has to ensure that the antenna will be pointed towards the right spot on earth with sufficient accuracy, whereas the thermal control subsystem has to deal with the huge amount of heat, produced by the amplifiers.

5.2   Requirements.

The goal of the mission is to provide all weather communications capability in the main part of western Europe. The capacity, quality and grade of service of the link must be sufficient to meet the needs of the customers. The main customers are expected to be (major) companies, expected to relay telephone calls, business video, file transfer, high speed fax, computer graphics etc., which will, according to the latest trends, be transmitted in digital format. Each type of signal requires a minimum channel quality and capacity, which can be translated into a minimum carrier-to-noise ratio (CNR). According to ref 5.4, telephony requires a capacity of 32 kilobits per second (kbps) and a BER of 10^{-4}, whereas file transfer may require up to 6 Mbps and a BER of 10^{-8}, see table 5.1. The space segment CP, together with the ground stations that will be used must be able to provide the required quality and capacity under all conditions, excluding outage due to sun interference. In order to achieve this, both the ground stations and the CP transmitter must provide sufficient amplification of the weak signals. Because the customers are expected to be companies in the main part of Europe, a large number of domestic ground stations will be required. Therefore moderately low ground station costs, leading to higher space segment costs are preferred. The spacecraft, operating in a geostationary orbit will provide a fixed service communications link, which means that a fixed portion of the earth will be covered.

Application	Transmission Rate	Required BER Performance	Typical Connect Time
Digital voice	19.2–64 kb/s	10^{-4}	3–4 min
Business video	56 kb/s–1.544 Mb/s	10^{-5}	30 min–1 h
File transfer	56 kb/s–6.312 Mb/s	10^{-8}	2–30 min
Electronic mail and high-speed fax	4.8–56 kb/s	10^{-8}	2–10 min
Data-base "refresh and downline loading"	9.6–56 kb/s	10^{-8}	2–10 min
Cad/cam	56–224 kb/s	10^{-7}	1-h session intermittent use
Remote job entry station	9.6–56 kb/s	10^{-8}	10–30 min
Computer graphics	9.6–56 kb/s	10^{-8}	30 min–1 h intermittent use

table 5.1
Performance requirements for various digital system applications.
(ref. 5.4)
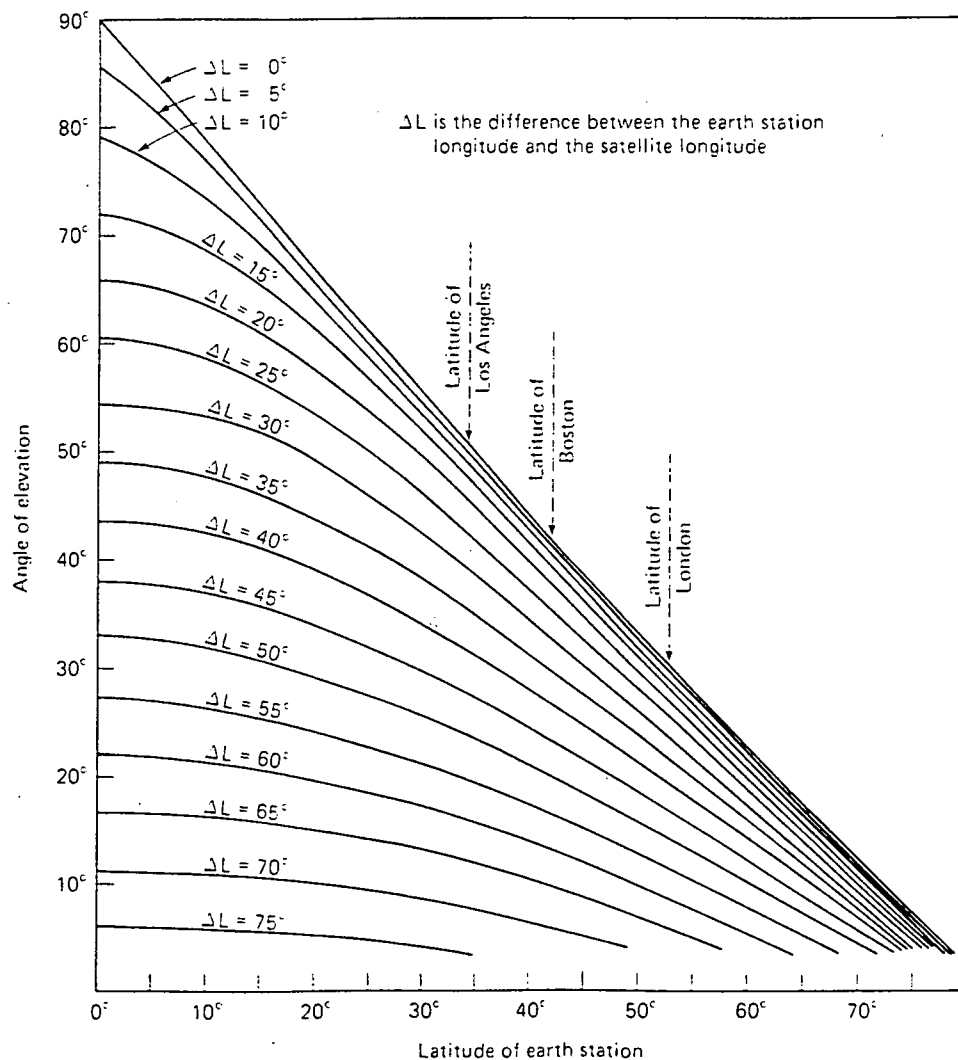
figure 5.5
A chart giving the satellite angle of elevation.
(ref. 5.5)

To allow several customers, scattered across the earth's surface to use the satellite simultaneously, the system must provide multiple access capability.

In order to provide the customers maximum grade of service the spacecraft must be fully operational during eclipses. The main drawbacks are the high requirements concerning the batteries, which must provide power during the eclipses. An advantage is the production of heat during eclipses, which prevents the temperature from dropping too badly.

The maximum allowable spacecraft antenna diameter is 1.80 meters.

The required operational lifetime is 10 years.

According to the ITU Radio Regulations (see ref. 5.1), the maximum power-flux density (PFD) on the earth's surface is -148 dBW per 4 kHz.m² .

5.3   Orbits.

For communications satellites many possible orbits are available. The most convenient however is the geostationary orbit, in which the satellite rotates around the earth in 24 hours, which exactly equals the earth's rotation time. If its orbit is over the equator and it travels in the same direction as the earth's surface, then the satellite appears to be stationary over one point on earth.

For this reason the geostationary orbit has some great advantages over other orbits, which - according to ref. 5.5 - are:
1.   The satellite remains stationary relative to the ground stations' antennas. Therefore the ground stations do not require tracking systems, which are very costly.
2.   The satellite will not disappear over the horizon, so there is no necessity to switch from one satellite to another.
3.   The satellite is permanently visible, so there are no breaks in transmission.
4.   The satellite is in line of sight from 42.4% of the earth's surface and thus covers a large number of ground stations.
5.   There is no Doppler shift in the signals because the satellite has no radial velocity relative to the ground stations.
6.   Three satellites could provide global coverage.

The disadvantages are (ref. 5.5):
1.   Latitudes greater than 81.25° north and south are not covered. However there is little other than polar ice in these regions.
2.   Because of the distance of the satellite (between 35,860 km and 41,756 km) the received signals are very weak and the signal propagation delay is 270 milliseconds. This means that, in a two-way communications link answers arrive after 540 milliseconds. Additional to this propagation delay the system is also subjected to echoes arriving after 540 milliseconds. This however can easily be corrected by the use of suitable electronics; a so called echo suppressor. This device inserts an impedance into the reverse path, when signals are being transmitted, and removes it when no signals are transmitted.

These disadvantages may not be underestimated; the advantages however are so important that a geostationary orbit is preferred for the Hitch-hiker mission. Considering operational and launch constraints, the satellite will be stationed at a longitude of 12° east, as will be explained in the chapter on system engineering.
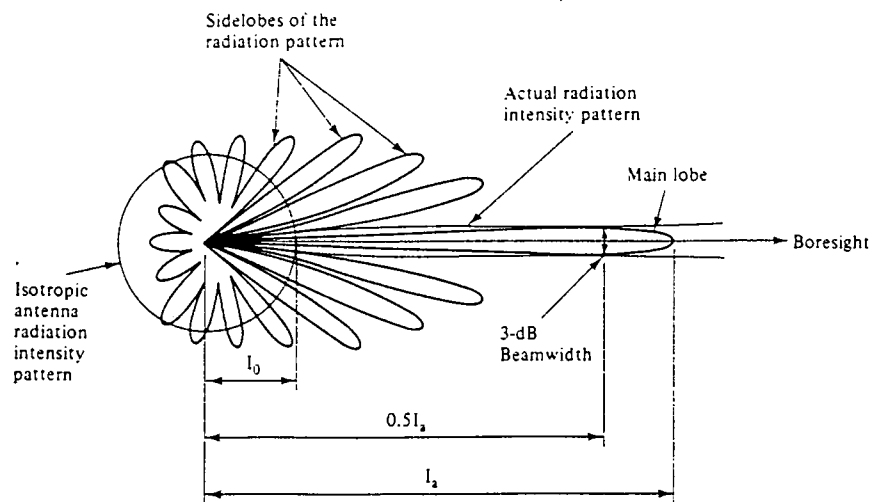
figure 5.3
Polar radiation pattern of an antenna.
(ref. 5.1)
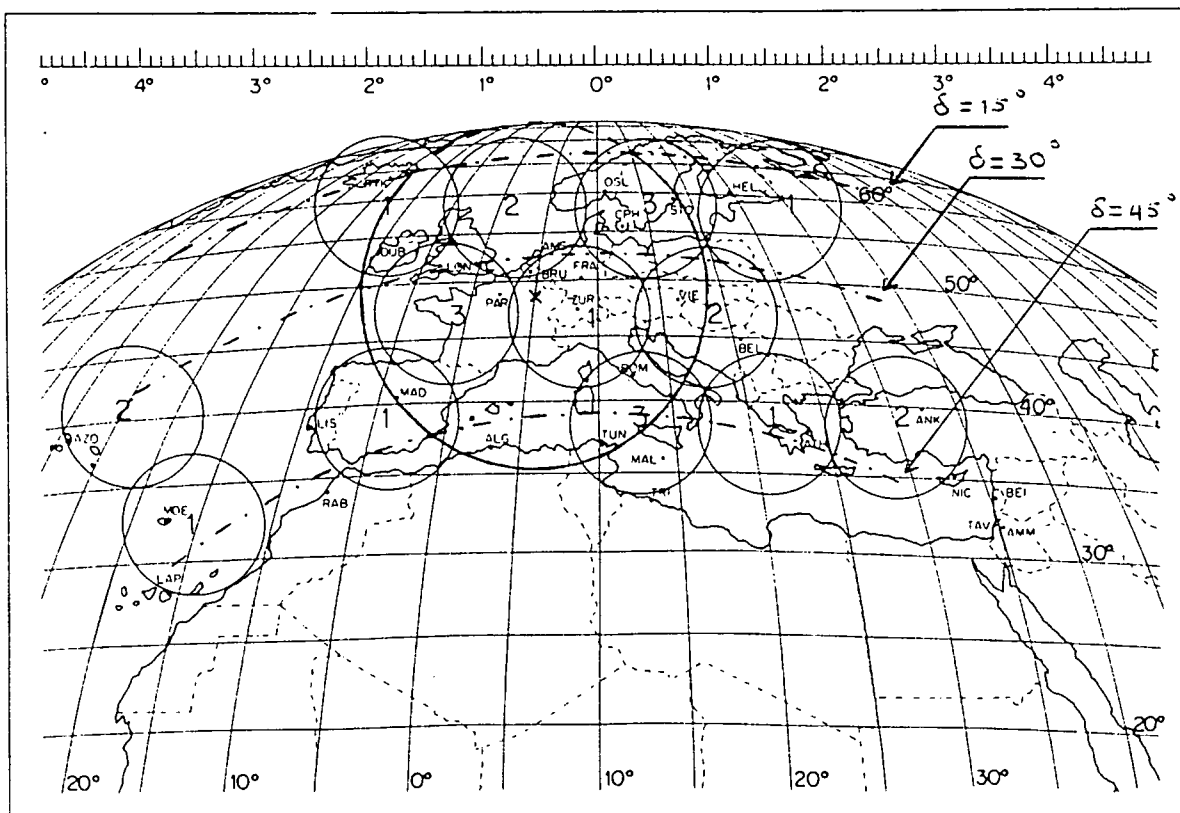
figure 5.4
Coverage area and lines for equal angles of elevation.

5.4 Sun and moon interference.

On very rare occasions the direction of the spacecraft, when observed from earth coincides with the direction of the sun. Because of its high noise temperature the sun causes very high noise levels in the communications link, causing severe link degradation; the downlink signal "drowns" in the noise caused by the sun. During these short periods of sun outage the spacecraft cannot be used for communications purposes, so then another spacecraft has to be used.

The moments when sun outage will occur depend on the date, the geographic position and the dimensions of the ground station antennas and the position of the spacecraft in its orbit (longitude), which means that a general calculation of the moments of sun outage can 't be performed. The maximum duration of the sun outage depends on the beamwidth of the receiving ground station antenna which is $2.86°$ for a 2.00 meters C-band antenna and $1.17°$ for a 4.90 meters antenna (calculated for a frequency of 3.70 GHz, giving the largest beamwidth; see section 5. 5, equation 5.3.b.), which are two of the types of ground stations that will be used for the Hitch-hiker project. According to ref. 5.4 the maximum duration T is

$$T = 8 \beta \quad \text{(minutes)}, \tag{5.1 a}$$

in which $\quad \beta = 0.54 + \beta_0 \quad \text{(degrees)}, \tag{5.1 b}$

in which β_0 is the beamwidth of the receiving antenna. For a 2.00 meters C-band antenna the maximum duration is 28 minutes and for the 4.90 meters antenna it is 14 minutes. The number of sun outages per year, N, according to ref. 5.4 is

$$N = \frac{2 \beta}{0.4} \quad \text{(days a year)}, \tag{5.2}$$

which, for the considered ground stations of 2.00 resp. 4.90 meters means 18 resp. 10 days a year (nine resp. five days, twice a year). The performed approximations are less accurate for wide beam antennas, which is the case for the smaller types of possible Hitch-hiker ground stations, but then the link degradation due to sun interference also becomes less severe and the increase of noise level may be tolerable. Nevertheless, the foregoing calculations provide a reasonable indication of the importance of sun interference.

Another form of sun interference occurs when the sun shines into the spacecraft's antenna or is reflected into the antenna by the spacecraft body. This causes severe uplink degradation. However, this does not degrade the overall link quality too badly because communications links are usually downlink critical, which is also the case for the Hitch-hiker system. The calculation of the moments at which this type of sun interference occurs is much more complex and less important and hence these calculations have not been performed.

On occasion the moon can also pass directly behind the spacecraft, causing moon interference. The moon shining directly into the earth antenna does not blot out the transmission, as does the sun, but it does increase the received noise level and so degrade the quality of satellite transmission.
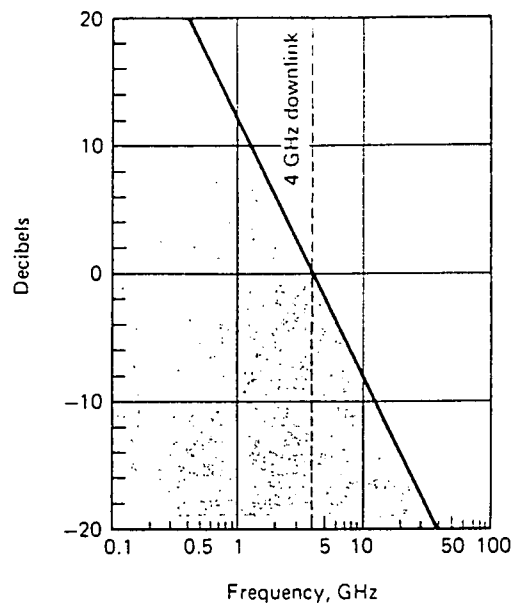
1. Relative loss in the space link (taking into consideration the gain of the transmitting and receiving antennas).
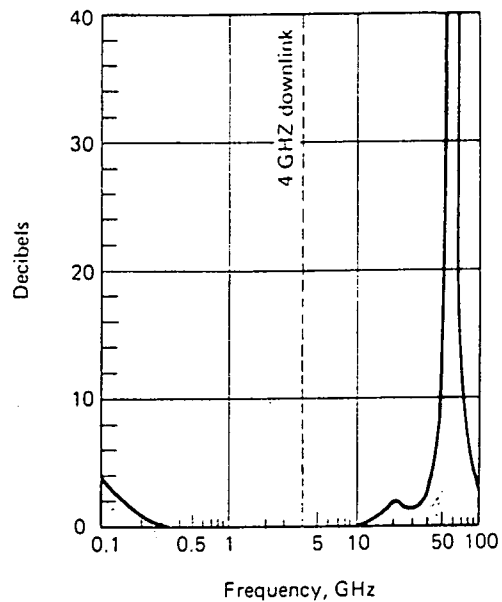
2. Relative attenuation in the earth's atmosphere.
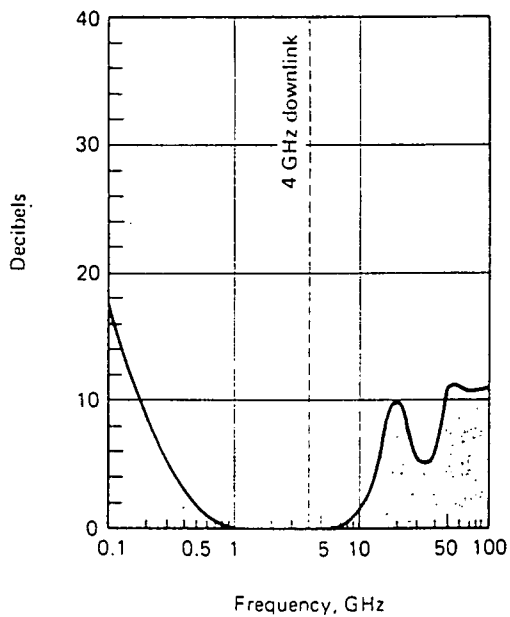
3. Relative power of atmospheric noise
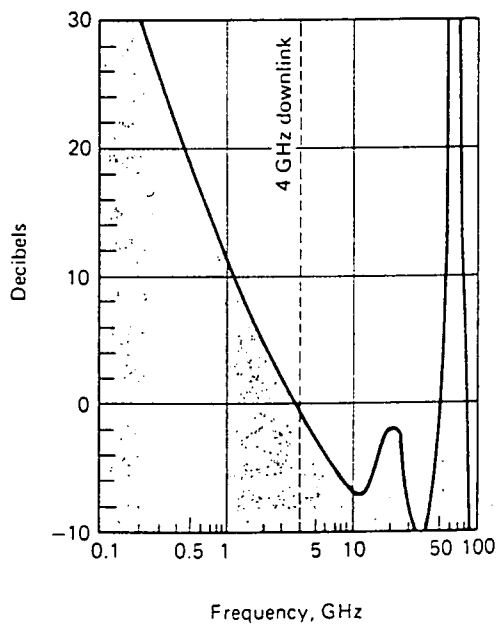
4. Composite effect of link loss, atmospheric attenuation and atmospheric noise

figure 5.6.a

Charts drawn to compare how the relative effects of different types of loss and noise vary with frequency. All charts are drawn relative to the loss or noise power of a 4 Ghz downlink. All charts are for a 15° elevation.

(ref. 5.5)

5.5 Coverage area.

The coverage area (operational area) of a satellite must be as large as possible in order to reach the largest possible number of customers. The coverage area of the CP depends on the station (operational longitude) of the spacecraft and on the 3-dB beamwidth of the transmitting spacecraft antenna. As mentioned before, the operational longitude is 12.0° east. According to ref. 5.1 the 3-dB beamwidth of the antenna is defined by the two points on either side of the boresight where the gains are 3 dB below (i.e. half power) the maximum gain of the antenna (boresight gain), see figure 5.3. The 3-dB beamwidth is usually considered as a boundary of the operational area of the satellite.

The beamwidth depends on the operational frequency and the size of the transmitting antenna. For a circular antenna beam, when no beam shaping will be used, the 3-dB beamwidth - according to ref. 5.7 - is:

$$\beta_0 = \sqrt{\frac{(32,000)}{G_a}} \quad \text{(degrees)}, \tag{5.3 a}$$

where an antenna efficiency η of 65% is assumed. When equation 5.10, giving the gain G_a of the antenna is substituted, the beamwidth becomes:

$$\beta_0 = \sqrt{\frac{(32,000)}{\eta}} * \frac{c}{\pi\, D\, f} \quad \text{(degrees)}, \tag{5.3 b}$$

in which D is the antenna diameter, f the operational downlink frequency and c the velocity of light, which is $3.00\ 10^8$ meters per second. For the antenna that will be operational on the Hitch-hiker spacecraft, an 1.80 meters C-band antenna, the beamwidth is 2.80° (calculated for a frequency of 4.20 GHz, giving the minimum beamwidth), which is the maximum allowing maximum gain.

For the fixed service Hitch-hiker CP the coverage area is very roughly sketched in figure 5.4, when the boresight is directed towards a point at a latitude of 48° north and a longitude of 5° east. Also lines for equal elevation angles are sketched, using figure 5.5. Figures of signal strength contours, which are important for ground station design purposes are more difficult to draw and lie beyond the scope of this project.

For telemetry and telecommand omnidirectional coverage is required, because the spacecraft must be able to receive commands and to transmit data under all conditions and possible attitudes.

5.6 Frequencies.

The ITU have allocated several frequency bands which may be used for space telecommunications (ITU Radio Regulations, Geneva, 1982). The most common are the C-band (4 GHz downlink / 6 GHz uplink) and the Ku-band (12 GHz downlink / 14 GHz uplink), both providing a bandwidth of 500 MHz. For future satellites, bands allocated at even higher frequencies may be used, but these are not considered here.
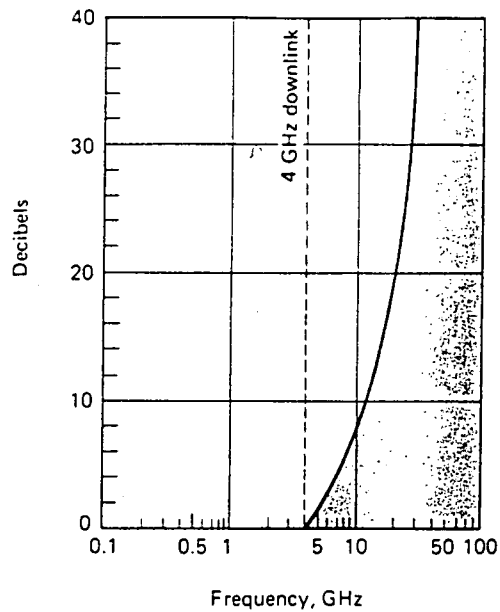
5. Relative attenuation caused by very
   heavy rain
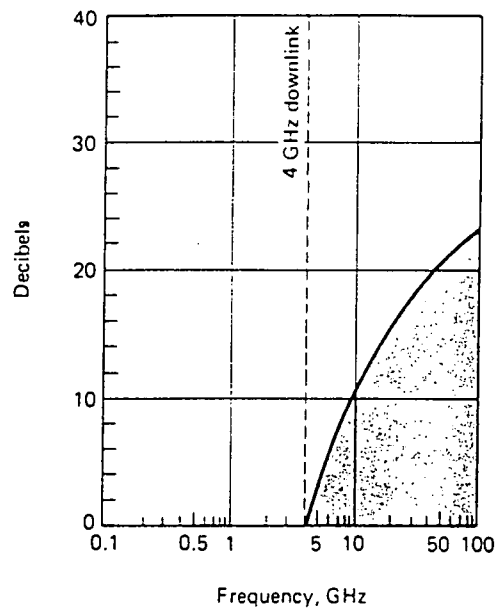
6. Relative power of noise from very
   heavy rain
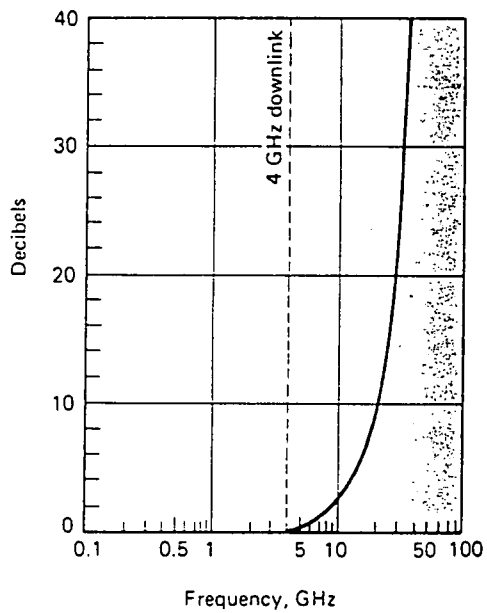
7. Relative attenuation caused by very
   . thick fog or cloud cover
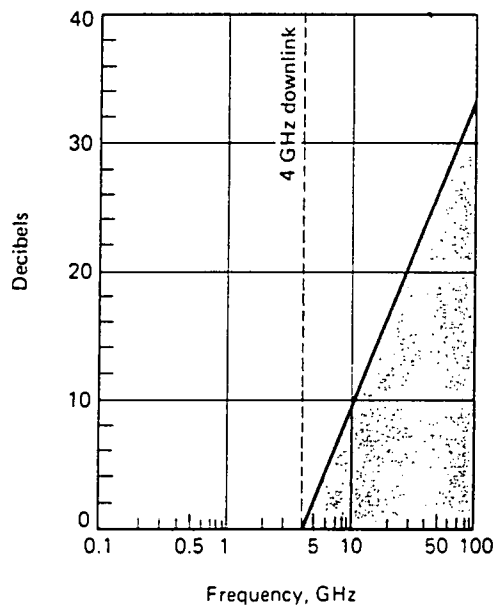
8. Relative noise power of very thick fog
   or cloud cover

figure 5.6.a

The C-band has some great advantages over other bands at higher frequencies, namely:

1. The C-band has been used since the early beginning of space communications and therefore uses established technology.
2. Atmospheric losses, which attenuate the already very weak communications signals are very low in the C-band. This also holds for losses due to precipitations and clouds, which may be up to 50 times smaller than in the Ku-band.
3. An intermediate frequency (IF) stage, for efficient processing of the communications signals at low frequencies is not required. This also holds for the Ku-band.
4. Using the same CP antenna diameter, the C-band provides a larger coverage area. Consequently, the attitude control error limits, which usually are 10% of the 3-dB beamwidth, may be less strict.
5. Using the C-band requires the smallest ground stations, mainly because of the small atmospheric losses, see figures 5.6 a and b.

The C-band also has some important disadvantages, which are:

1. The C-band is severely congested, which means that a lot of geostationary communications satellites and terrestrial links use the C-band, causing major interference problems, which degrade the quality of the communications link. Due to terrestrial interference, the nearest possible antenna site may be many miles away from the locations of the customers, which usually are located in urban centers. The cost of moving the wideband signals over common carrier facilities between the location of the user and the antenna site may be very high. The problem of interference also occurs when the Ku-band is used, although at a much smaller extent. This is because the K-band is not used for terrestrial links and therefore interference with terrestrial links doesn't occur.
2. Because of the lower frequencies either larger or else lossier components need to be used, because the dimensions of the components increase when the operating frequency decreases. When larger dimensions are not acceptable, lossier components need to be used, because the ohmic losses of the passive elements increase as the dimensions of the components decrease.

Considering both the pros and cons, using the C-band appears to be the best choice. It covers the 5.925 - 6.425 GHz band for the uplink and the 3.700 - 4.200 GHz band for the downlink, providing 500 MHz bandwidth for transmission.

5.7 Payload description.

The CP is equipped with 10 operational channels, providing a bandwidth of 36 MHz each, when no polarization or other means of frequency re-use is used. A bandwidth of 36 MHz per channel is the maximum allowing good CNR performance, because the noise level is proportional to the bandwidth (see section 5.10.2.1). Two redundant channels are used as backup in case failure of one of the other channels occurs. When a channel spacing of 4 MHz is used, 20 MHz bandwidth is available for data relay (Telemetry, tracking & command; TT&C). Two separate transponder channels, one of which is used as backup, are reserved for this purpose. The grouping of the separate channels over the frequency band is shown in figure 5.7. The frequencies used for TT&C are within the payload frequencies. Therefore the communications hardware of this data relay subsystem, containing antennas, receivers, amplifiers etc. was designed by the payload team. Computers and other data handling equipment were designed by the data handling team.
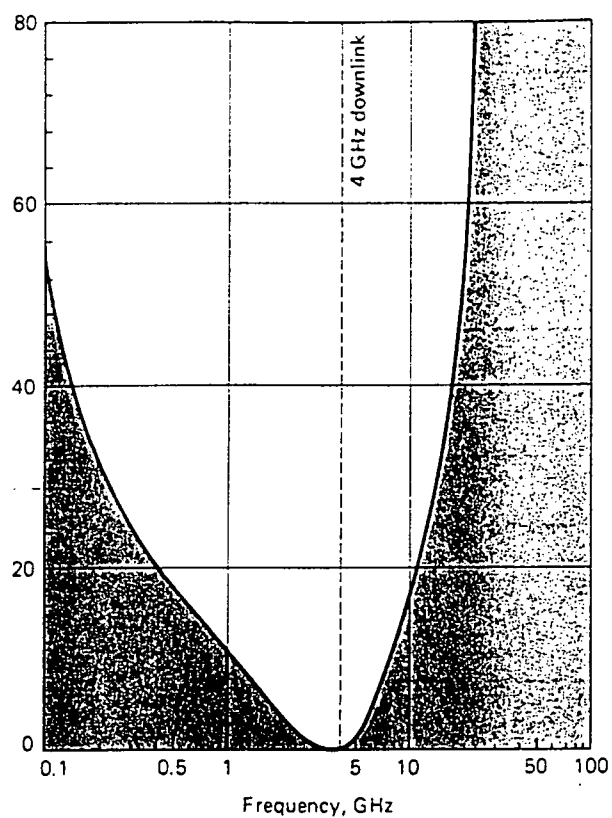
figure 5.6.b
A composite diagram showing the combined effects of all the types
of loss and noise shown in fig 5.6.a. (i.e. assuming both very heavy rain and
very heavy cloud cover, and an angle of elevation of 15°).
(ref. 5.5)
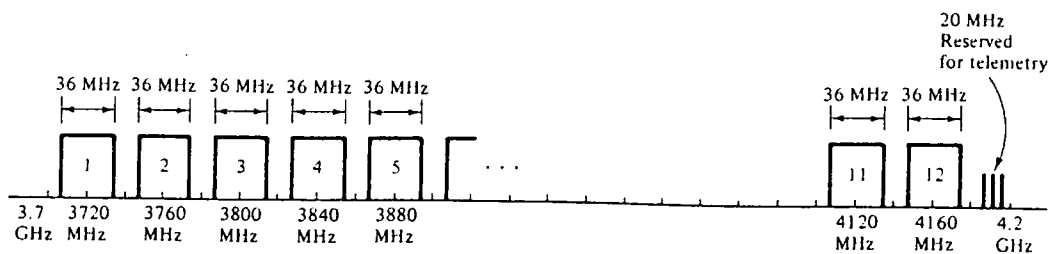
figure 5.7
Downlink channelization.

The total radio frequency (RF) power present in the communications signals is 17.8 W per channel (transmitting system losses taken into account), requiring a total DC input power of 455 W. The total efficiency of the payload subsystem is 39.1 %. The total mass of the CP, including antenna and antenna support will be 70.0 kg, of which 13.0 kg is reserved for the antenna subsystem.

For the data handling signals a RF power of 5.0 watts is required, providing a CNR better than 23.0 dB which is sufficient for a BER superior to 10^{-7} when PCM/FM modulation is used and 6 dB (de)modulation losses are included (for more details please see the chapter on TT&C). The TT&C link provides a bandwidth of 3.0 kHz, sufficient for a bit-rate of 1024 bits per second (bps). A DC input power of 18.5 watts is required. Eight horn antennas of 0.7 kg each will be used to provide omnidirectional coverage. The total mass of this subsystem, including the horn antennas is approximately 14.1 kg.

5.8   Antenna subsystem.

The function of the antenna subsystem is to receive uplink signals and to transmit the amplified downlink signals. In order to save expensive mass and launcher volume, one combined receive and transmit antenna will be used. Avoiding mechanical complexity, the electronic complexity will be raised, because a device which separates uplink from downlink signals will be required in order to avoid interference of these two signals.

The diameter will be the maximum allowable diameter, which is 1.80 meters, providing maximum gain. The antenna will be a simple offset fed parabolic dish reflector, having an f/D of 1.0 (where f is the focal length of the paraboloid), which, according to ref. 5.1 provides good scanning properties - which means that the beam can be displaced from its nominal boresight direction (i.e. the direction of maximum gain) simply by displacing the feed horn from the focal point, without much loss of performance - and avoiding a large and heavy support structure. This support structure must deploy the antenna and after that provide a firm and stable support insensible to mechanical and thermal distortions. The materials used for the reflector dish must have adequate thermal and electromagnetic properties. A very commonly used material is graphite epoxy. A detailed description of the design of the antenna subsystem is given in the chapter on structure. The geometry, calculated from ref. 5.4, is given in figure 5.8 and table 5.2. The mass of the communications antenna subsystem will be approximately 13.0 kg. A mass-breakdown for the antenna subsystem is given in table 5.3 and will be discussed in the chapter on structure.

As mentioned before the antenna subsystem must be highly insensitive to mechanical and thermal distortions. According to ref. 5.1, the main contributors to distortion are displacement of the feed relative to the dish antenna and distortion of the dish itself.

The displacement of the feed can be either lateral to or along the axis of the parabola, see figures 5.9 a and b. The first will cause displacement of the boresight (i.e. the direction of maximum gain) causing minor link degradation. Displacements along the axis of the parabola will cause defocusing of the antenna causing severe link degradation. However, this type of distortion is of minor importance when f/D equals 1.0 or larger, which is indeed the case for the Hitch-hiker antenna.
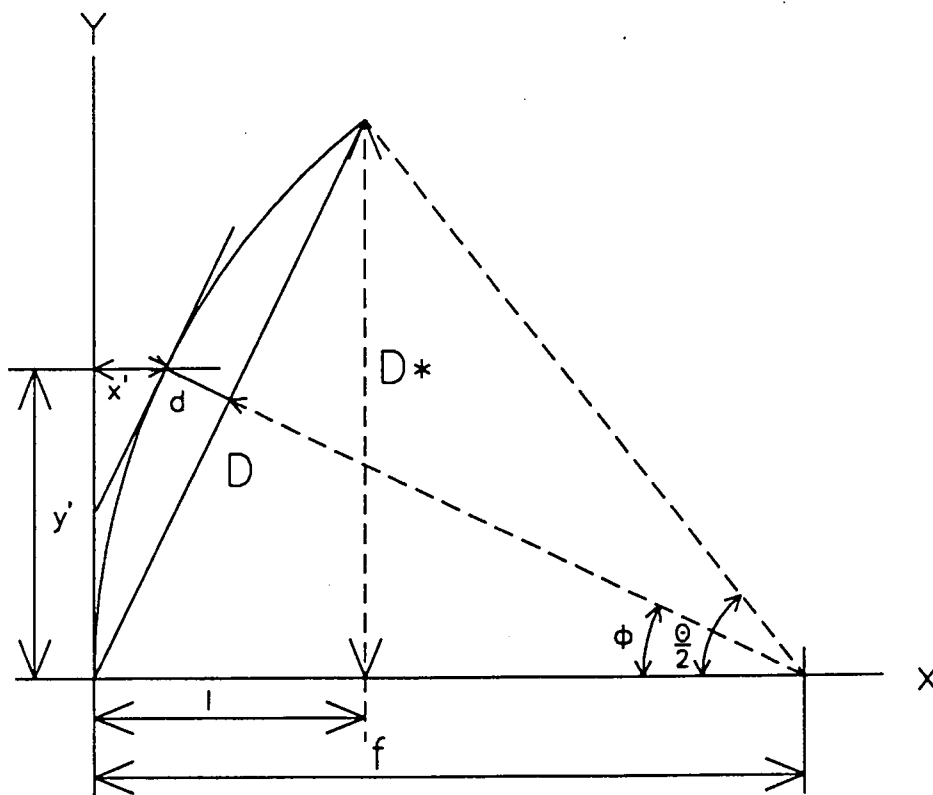
figure 5.8
Antenna geometry.

f	= 1.800 m	D	= 1.800 m
1	= 0.4249 m	D^*	= 1.7491 m
$y' = {}^1/_2 \, D^*$	= 0.8746 m	$x' = {}^1/_4 \, 1$	= 0.1062 m
d	= 0.1195 m	Φ	= 27.31°
$\theta/2$	= 51.83°		

Table 5.2: The dimensions of the payload antenna.

Reflector	Core	1.63 kg	
	Sheets	4.07 kg	
	Adhesive	0.51 kg	
	Subtotal		6.21 kg
Ribs	Core	0.33 kg	
	Sheets	1.90 kg	
	Adhesive	0.11 kg	
	Subtotal		2.34 kg
Hinges (2 units)			
	Subtotal		4.43 kg
Total mass			12.98 kg

Table 5.3: Mass-breakdown for the antenna subsystem.

Distortion of the dish itself can be treated by drawing a best fit parabola through the actual shape of the antenna, see figure 5.10. Differences of this best fit parabola relative to the ideal shape and attitude of the antenna can be treated as outlined before. Surface errors of the antenna can be characterized by a RMS value σ, which determines the gain degradation of the actual antenna relative to the ideal antenna as follows (ref. 5.1):

$$\frac{G_a}{G_{a_0}} = e^{-\frac{(4\pi\sigma)^2}{\lambda}} \quad (dB). \tag{5.4}$$

In order to cause less than 0.25 dB gain degradation, this RMS value must be less than 2% of the wavelength λ of the transmitted signals. This means that for a C-band antenna this RMS surface error must be less than 1.4 mm. The maximum allowable surface error is three times this RMS value, so 4.2 mm, even under very bad thermal loadings, varying from approximately -200° C to +100° C.

To avoid both transmit and receive interference with other satellites and groundstations communicating with an adjacent satellite, the antenna must have low sidelobe levels. This means it must be relatively insensible for signals coming from a direction outside the beamwidth. This is also important for the attainable efficiency of the antenna. The lower the sidelobes, the less signal power is spilt outside the beamwidth and the larger the efficiency will be. The efficiency of the antenna is defined as the ratio of the actual gain relative to the gain of an ideal (i.e. no losses) antenna with zero sidelobe gain.

The choice of the feed horn has large influence on the sidelobe levels. A circular horn with corrugated interior walls will be used as primary source antenna (feed horn), see figure 5.11. This type of feed horn has the following advantages (see ref. 5.1):
1. It has very low sidelobe radiation, causing very little spillover of the communications signals and therefore small losses.
2. The antenna beam is circularly symmetric.
The main drawback is that this type of horn is somewhat larger and heavier than a conventional circular conical horn. The important improvement of performance allows the use of this type of feed. The required (3 - dB) beamwidth of the feed horn is 52°.

For telemetry and telecommand omnidirectional antennas must be used because the spacecraft must be operable under all possible conditions and attitudes. For this purpose 8 horn antennas (very similar to feed horns) will be used, with a total mass of 5.6 kg, including support-brackets. A more comprehensive description of the TT&C subsystem is given in the chapter on this subject.

5.9   Modulation and multiple access.

Because the capacity of the satellite's CP is much larger than the capacity required by one customer, this capacity must be shared among many users. This is achieved by:
1. Multiplexing, where several channels are modulated upon one carrier.
2. Multiple access, which allows several ground stations to use the satellite's transponders simultaneously.
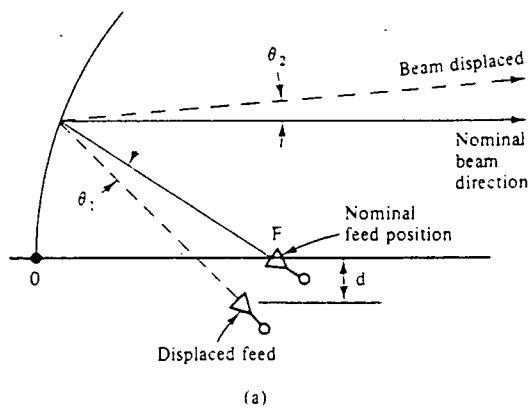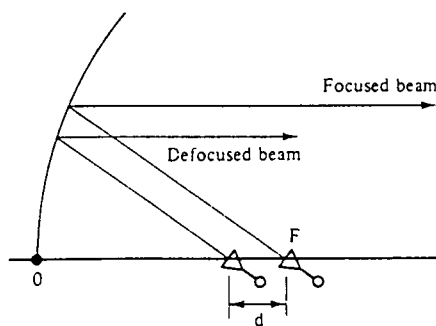
figure 5.9.a
Effects of lateral feed displacement.
(ref. 5.1)

figure 5.9.b
Effects of de-focussing.
(ref. 5.1)
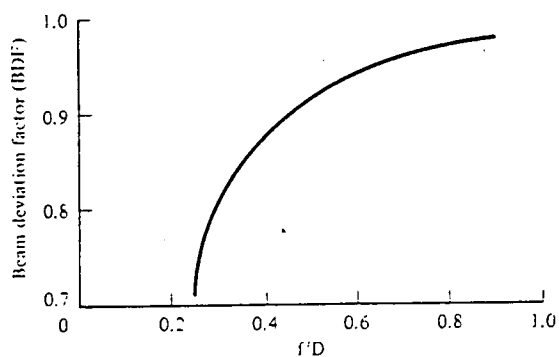
figure 5.9.c
BDF versus f/D. BDF = θ_2/θ_1.
(ref. 5.1)
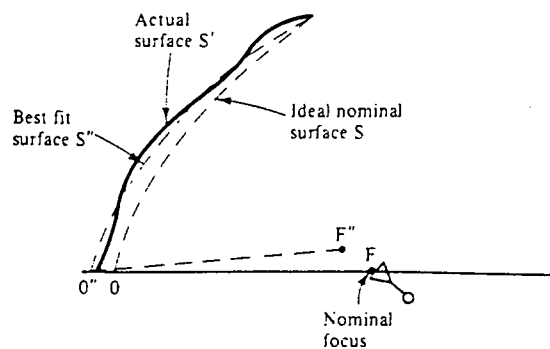
figure 5.10
Concept of a best fit paraboloid.
(ref. 5.1)

5.9.1 Modulation.

In the next section the carrier-to-noise ratio of the communications link will be determined, assuming certain specifications for the ground stations. This available CNR must match the required CNR, which depends on the required signal quality (channel performance) - which on its term depends on the type of signals that will be transmitted - in terms of a signal-to-noise ratio (SNR) or BER, the applied modulation and multiple access techniques and the required capacity of the link (data-rate).

The use of advanced modulation and coding techniques may reduce the required CNR and may consequently reduce the dimensions and the costs of the ground stations. However, they do not essentially change the design of the satellite's transponders. The specifications of the ground stations may vary, according to the needs of the customers. A general calculation, covering all the possible wishes of the customers is impossible. Therefore only a general treatment of the subject will be given.

Because of the nature of the signals that are projected to be transmitted, digital transmission appears to be a logical choice. This also has the advantage of raising the capacity of the link. However, real-time signals like telephony etc. require idle channels in order to prevent that too many channels will be busy at the same time. Therefore, most of the time 80 % of the satellite's capacity remains unused for real-time transmission. During these periods, the satellite may be used by non real-time traffic, which may be interrupted when extra capacity is required for real-time traffic.

Before the signal is ready for transmission, several stages of processing of the baseband signals are to be distinguished (figure 5.12):
1. Source coding and/or modulation, also called individual channel coding, where the source signal is prepared for transmission in a modem. For analog transmission the signal will either be amplitude or frequency modulated (AM or FM), whereas for digital transmission analog signals will be coded to digital format by a codec. The digital source signals may be processed in order to omit redundant information.
2. Because the capacities of the links are usually much larger than the capacity required for one signal, these signals are being multiplexed: several separate signals are combined to form one signal. Analog signals will usually be frequency-division multiplexed (FDM), a process which combines source coding (usually AM) and multiplexing. Digital signals are usually time-division multiplexed (TDM).
3. Channel coding, where redundancy is added prior to transmission of digital signals. It provides good operations at low CNR levels, but at the expense of consuming up bandwidth. When this technique is applied, it is possible to use smaller and thus cheaper ground stations, than without coding.
4. RF modulation: the multiplexed signals are modulated on a RF carrier for transmission. For analog signals FM will be used, whereas digital transmission commonly uses phase-shift keying (PSK).
5. Multiple access, which will be considered in section 5.9.2.

Because of the nature of the signals, the first stage may not always be necessary. However, analog signals like speech must first be converted into digital format. This is achieved by using a codec, which is designed to transmit the necessary information at the lowest possible data-rate R_b. Many possible coding techniques are available. Which will be selected depends on:
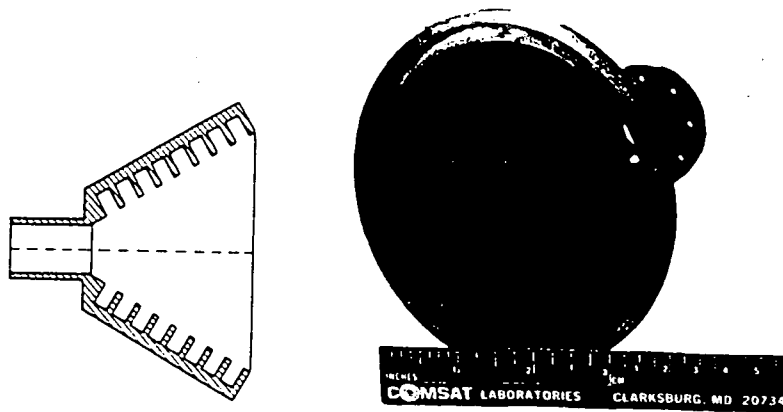
figure 5.11
Corrugated conical horn (Courtesey of COMSAT).
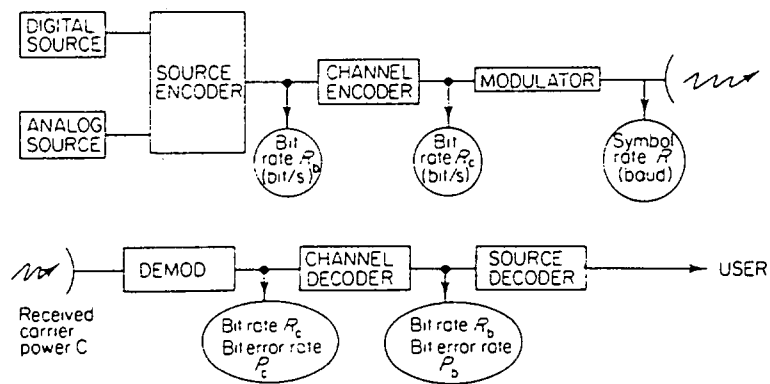
figure 5.12
Digital communications system model.
(ref. 5.7)

1. Equipment complexity.
2. Equipment efficiency.
3. Spectral occupation, i.e. the bandwidth consumed by the signal.
4. Information transfer efficiency.
5. Robustness, i.e. the insensitivity to varying CNR of the signal.

For example: AM is not commonly used for satellite transmission, because linear operation of the equipment is critical. Therefore, a large back-off will be required, which ruins the efficiency of the equipment. Furthermore, bandwidth can not be traded off with RF power, so it is not possible to save power by using up a larger bandwidth.

One of the most commonly used coding techniques for telephone transmission is pulse-code modulation (PCM). First, the signal is sampled, then the samples are quantized and finally the samples are coded. Using this basic technique, more efficient variants like adaptive differential pulse-code modulation (ADPCM) have been designed. The data rates vary from 64 kbps for PCM down to 32 kbps for ADPCM. The use of compandors, which reduce quantizing noise by means of an efficient quantizing process for low level signals, and digital speech interpolation (DSI), where telephony channels are swhitched off, when a person doesn't speak (i.e. voice activation) may enlarge the capacity of a transponder to a still further extent. Applying DSI - or time-assigned speech interpolation (TASI) for analog single channel per carrier (SCPC) signals - will:
1. Conserve satellite transmitter power, and
2. Reduce intermodulation levels.

For a large number of telephony channels, which usually have 40% activity this means a 3.5 dB increase of $(CNR)_i$ and a 4.0 dB gain in available

transmitter power per carrier (see ref. 5.4). These considerations only hold for two way communications links, not for one way links like data links. Furthermore, channel synchronization will be required, for which purpose some overhead info is added to the signal, which reduces the information carrying capacity of the link. The transmission of television signals usually requires 6 Mbps, whereas studio quality TV pictures require 25 up to 40 Mbps.
Not only the quantization process produces noise, also bits received in error will produce some noise. A figure of merit characterizing this type of noise is the bit-error-rate (BER).

After the individual source coding the signals may be time- division multiplexed (TDM), where each signal will occupy the assigned bandwidth for a small period of time (time slot). Accurate synchronization of the transmitting and receiving equipment is required. For this purpose, some synchronization bits are added to the signal. For telephony, several standards have been developed. An, in Western Europe commonly used standard is the CCITT standard, which uses PCM, where 30 speech channel are being multiplexed to form one signal of 2.048 Mbits per second.

For RF modulation several techniques are used, of which binary phase-shift keying (BPSK) and quaternary PSK (QPSK) are the most common ones. Either direct or differential coding is applied. When differential coding is used, the detection of the signals can either be coherent (designated as DE-M-PSK) or differential (D-M-PSK). When the latter technique is applied, no carrier recovery is required which simplifies the demodulator lay-out, but the performance decreases. For BPSK two different states are used to transmit the data, whereas QPSK uses four different states (i.e. the symbol rate R is the half of the bit rate R_c, because one symbol represents two bits), resulting

into a higher transmission speed within the same bandwidth and giving the same error rate, when coherently detected (see ref. 5.4). A still larger number of states will provide higher transmission speeds, but the error performance will deteriorate. Generally: the larger the number of states represented at one instant, the higher the transmission speed, but the lower the margin for errors in the detecting equipment will be. Sources of errors may be:

figure 5.14   Probability of bit error of various coding schemes.
(ref. 5.7)

figure 5.13   Probability of bit error of various digital modulation schemes.
(ref. 5.7)

1. Thermal noise, which spreads uniformly in time.
2. Hardware errors.
3. Software errors.
4. Interference, the latter three occurring in bursts.

Figures of merit which characterize the quality of the link are:
1. Bit-error-rate (BER). The theoretically determined value is usually called the probability of bit error P_b. It can be calculated analitically under the following assumptions:
   - Gaussian white noise.
   - Perfect synchronization of the receiving and transmitting equipment.
   - No error control coding is applied.
2. Block-error-rate.
3. Percent error-free seconds (%EFS).

The probability of bit error depends on the carrier-to-noise ratio (i.e. E_b/N_0) and is given in figure 5.13 for various modulation techniques. The E_b/N_0, required to achieve a given P_b value (i.e. the threshold E_b/N_0), determines the required CNR:

$$\frac{C}{N} = \left(\frac{E_b}{N_0}\right)_t \frac{R_c}{B} \quad (dB),\tag{5.5}$$

where E_b is the power per transmitted bit, R_c is the transmitted bit-rate, N_0 is the noise power per unit bandwidth and B is the bandwidth over which the signals are being transmitted. Figure 5.14 shows the P_b-performance when channel coding is applied for various coding techniques. As can be seen from the figure, the channel operates well at low CNR (i.e. E_b/N_0) levels. Then more bits will be received in error, than is the case when no coding is used, but this is compensated by the error correcting capability, which is provided by adding redundancy prior to transmission. However, this reduces the possible data-rate, when the symbol-rate, and thus the bit-rate is fixed. The latter is caused by the limited capacity of the modems and spacecraft transponders. The possible data-rate is:

$$R_b = R_c * r \quad (bps),\tag{5.6}$$

where r is the code-rate of the channel coder, which is always smaller than one.

Which coding technique will be applied depends on:
1. The degree of protection, that is: how much does coding improve the BER performance.
2. The code-rate, i.e. what portion of redundant bits is required.
3. Coding complexity.

Soft-decision coding techniques, which take into consideration what type of error is most likely to occur, which means that they are linked to the applied RF modulation technique (see ref. 5.5), perform better than hard-decision techniques. However, the are more complex and require more advanced computer technology.

The efficiency of digital modulation techniques can be expressed in terms of the bandwidth expansion factor, also called the spectral efficiency which is the ratio of the transmitted bit-rate, to the consumed channel bandwidth, for a fixed value of P_b, see figure 5.15. For QPSK, this ratio is 5/3.
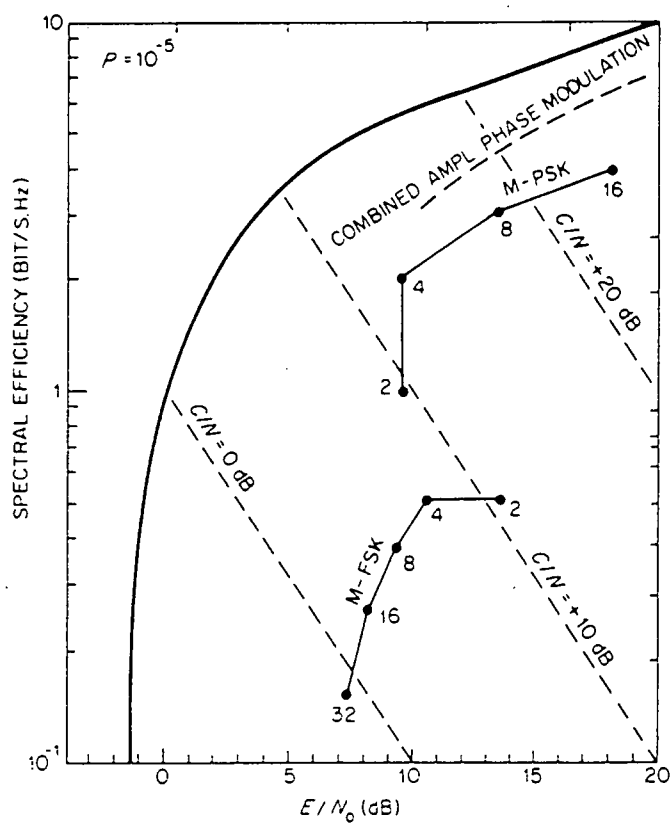
figure 5.15
Theoretical spectral efficiency of various digital RF modulation schemes at a
given probability of bit error.
(ref. 5.7)

5.9.2 Multiple access.

Multiple access systems allow many ground stations, which may be scattered across the earth's surface and may have varying demands, to be interconnected simultaneously by the same satellite. They make use of the fact that not all the users communicate at the same time, the well-known principle of concentration. Probability calculations must be performed in order to determine the required capacity to serve the projected number of customers. Demand assignment systems, which allocate communications capability according to the needs of the users on a flexible basis, are very useful in handling fluctuating traffic demands. This form of dynamic assignment may be up to 4 times more efficient than fixed assignment, where users have been assigned a fixed portion of the total communications capacity, regardless of the actual needs.

The operation of the multiple access system and the allocation of communications capacity is controlled by ground stations. This control may either be centralized or decentralized. The first option is rather vulnerable to the failure of one ground station, whereas the latter is a more costly solution. Another possible solution is called contention, where all ground stations transmit short bursts at random. These bursts may collide with bursts from other stations and damage each other and then these bursts have to be transmitted again.

There are three important multiple access systems available:
1. Frequency-division multiple access (FDMA), where each carrier continuously uses a limited portion of the total transponder bandwidth. It can be used for both analog and digital transmission.
2. Time-division multiple access (TDMA), in which each carrier uses the full transponder bandwidth for only a short period of time (burst). It is only applicable for digital signals.
3. Code-division multiple access (CDMA), also called spread spectrum multiple access (SSMA) where all carriers use the full transponder bandwidth simultaneously. This system has only been used for military purposes and not for commercial ones. It can only be used for digital transmission.
The first two systems will now be treated more extensively.

5.9.2.1 FDMA systems.

These systems operate a pool of frequencies, from which the user is assigned a suitable frequency band.
Two different forms of FDMA have been used for commercial purposes:
1. Single channel per carrier (SCPC). The second stage of signal processing, multiplexing, has been omitted.
2. Multiple channel per carrier (MCPC). This type of system is rather inflexible. It is only effective for high density point to point links, f.e. between two ground stations of a large telephone company.
Both forms are characterized by multiple carrier operation; one transponder transmits several carriers. This may cause intelligable interference, called cross talk. Because of the nonlinearities in the equipment also intermodulation of the carriers occurs, which forces the amplifiers to operate at less than the saturated output power (back-off). This means that the capacity of the satellite will be reduced, in order to maintain the required quality of the signal. The more carriers share a transponder, the lower the overall capacity will be because:
1. Guard bands are needed to separate adjacent carriers. The more carriers are used, the more guard bands will be required. These guardbands may occupy up to 10% of the transponder bandwidth.
2. The intermodulation level increases, as the number of carriers increases.

Because of the reduction of satellite capacity due to the multiple carrier operation of the satellite, FDMA will generally lead to higher space segment costs.

For example: A well known FDMA system is called SPADE, and is operated by INTELSAT. It is capable of transmitting 397 two way telephone links through a 36 MHz transponder. It employs QPSK, but makes no use of DSI. It requires large ground stations. A system which may be used for small domestic ground stations is the General Electric System ES-144.

5.9.2.2 TDMA systems.

In a TDMA system high speed bursts of data are transmitted through the satellite. Each burst occupies the full transponder bandwidth for a short period of time and the bursts may have variable length, according to the customers' needs. Therefore, at the ground stations data buffers will be required to collect the data. State-of-the art burst modems are capable of transmitting 60 Mbps over a 36 MHz transponder, using QPSK. Each burst contains control information and synchronization bits, the so-called preamble or header, which reduce the capacity by about 5%. This synchronization is very important because bursts from different ground station must not interfere. Synchronization systems also correct for:

1. The diverse locations of the ground stations, which may lead to different propagation times.
2. Drift of the satellite.
3. Tidal motions of the satellite.

The latter two not only change the position of the satellite, but also cause Doppler shift of the signals, which may affect the demodulators and demultiplexers. Because of the high synchronization requirements, the ground segment costs will be rather high, compared to the ground segment costs for an FDMA system. Still, according to ref. 5.5, TDMA has some large advantages over FDMA:

1. Because it is software controlled, TDMA is highly flexible.
2. The maximum throughput of a TDMA system is larger than for an FDMA system.
3. Because of the single-carrier operation, no intermodulation of carriers occurs. Therefore an efficient use of the available satellite power can be made, because no back-off will be required.
4. Less interference with other satellites occurs.
5. DSI can be employed for telephony in order to raise the capacity of the CP.
6. No guard bands will be required, so the useful bandwidth will not be reduced.

There also exists a type of TDMA called narrowband TDMA, which employs TDMA within an FDMA system. This may be highly efficient for users with small capacity demands. However, the large advantages of TDMA will not be exploited.

type	A	B	C	B
Required BER	10^{-8}	10^{-8}	10^{-5}	10^{-5}
Coding techn.	no	Viterby soft-dec.	no	Viterby soft-dec.
Capacity (Mbps)	60	30	60	30
(tel. ch.)	1680	840	1680	840
Required CNR (dB)	17.7	11.5	15.2	10.0
Antenna diameter (m)	4.90	2.40	3.65	2.00
RF power (W)	200	200	300	300
EIRP (dBW)	70.30	64.10	69.50	64.27
G/T (dB)	21.40	15.20	18.84	13.61

Table 5.4: Standard ground station specifications.

Which system will be used depends on several "engineering factors":
1. Capacity, which is defined as the number of voice channels of specified quality, that can be transmitted per transponder.
2. The required RF power and bandwidth.
3. Interconnectivity among many users at various data rates and quality levels.
4. Adaptability to growth.
5. Accommodation of multiple services, such as voice, data and images.
6. Terrestrial interface (availability).
7. Communications security.
8. Cost effectiveness.

Because of the large advantages, the Hitch-hiker system will operate TDMA.

5.9.3 Capacity.

Now an overview of the modulation and multiple access techniques has been given, the capacity of the link can be calculated. The capacity of the link depends on the carrier-to-noise ratio, as can be seen from Shannon's formula:

$$C = B \log_2 (\frac{C}{N} + 1) \quad (bps), \qquad (5.7)$$

where C is the capacity in bps and B is the available bandwidth. This value is an theoretical upperbound of the bit-rate at which data can be transmitted without error. For digital transmission the minimum required E_b/N_0 is -1.6 dB; below this theoretical value no error free coding systems are possible.

These equations however, do not consider the practical limits of the ground station's capacity and the capacity of the CP transponders. For QPSK, the spectral efficiency is 5/3 bit per Hz, so over one 36 MHz transponder, a bit-rate of 60 Mbits per second can be achieved. A formula for the CNR, which is required to achieve this transmission capacity, can be derived from equation 5.5 (see ref 5.4):

$$C/N = (E_b/N_0)_t - B + R_c + M_i + M_a \quad (dB), \qquad (5.8)$$

in which $(E_b/N_0)_t$ is the threshold E_b/N_0, that can be evaluated from figures. 5.13 and 5.14, B the bandwidth (36 MHz), R_c the bit-rate (60 mbps), M_i is a margin for the (de)modulation losses, which are about 3.0 dB and M_a is a margin for adjacent channel interference (0.5 dB). When no coding is used, the data-rate equals the bit-rate. When Viterby r = $^1/_2$, soft-decision coding is used, the data-rate is one half of the bit-rate, i.e. 30 Mbps.

Using equation 5.7 and 5.8, the specifications of the four types of ground station terminals can be calculated. The capacity is expressed as the number of telephone channels with a data-rate of 32 kbps (ADPCM), that can be transmitted, assuming a somewhat pessimistic reduction of capacity due to preamble of 10%. The results are summarized in table 5.4.

Projected
area A
(aperture)

Reflector

Direction of
maximum
radiation
(secondary
radiation)

Parabola

Primary
radiation

Feed
horn
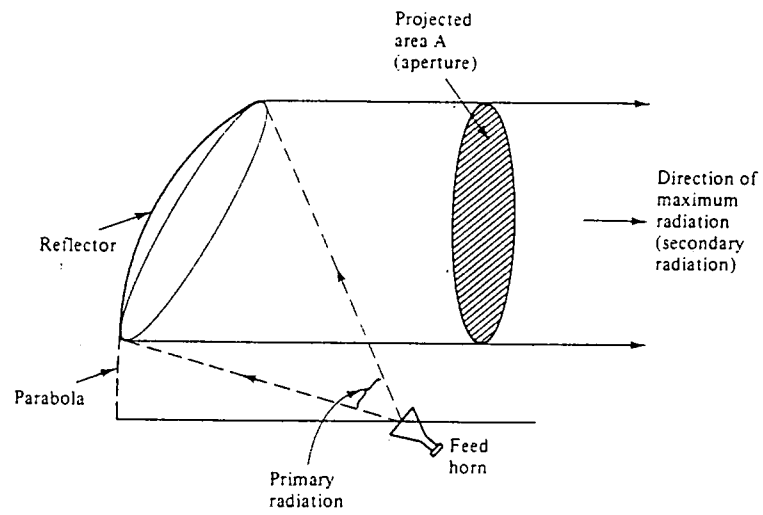
figure 5.16
Projected aperture area of an offset-fed parabolic reflector.
(ref. 5.1)

5.10 Link budget.

In the previous section, the required CNR has been determined for several types of signals. This figure depends on the required quality and capacity of the communications link. The available CNR, which depends on the type of ground station that will be used, must match the required CNR, according to the customers' wishes. In order to determine the available CNR (i.e. the ground station requirements), a link budget for the Hitch-hiker system has to be made. This is the first step when attempting to optimize a space communications system.

5.10.1 Ideal power transfer.

The power transfer between two microwave antennas depends on the antenna gains (i.e. the dimensions) of the both transmitting and receiving station, the power radiated by the transmitting station, the wavelength of the transmitted waves (and thus the frequency) and the line-of-sight distance between the two stations. The carrier power received by the receiving station, when both boresights of the antennas are collinear (no misalignment), can be expressed as (see ref. 5.1):

$$C_r = \frac{P_t \, G_{at} \, G_{ar}}{\left(\frac{4\pi \, d}{\lambda}\right)^2} \quad \text{(Watts)}, \tag{5.9}$$

where P_t is the transmitted power, G_{at} resp. G_{ar} the transmitting resp. receiving antenna gain, d the line-of-sight distance between the two stations and λ the wavelength of the signals. Usually, the product $P_t \, G_{at}$ is called the EIRP (Equivalent Isotropic Radiated Power), that is - following the definition of ref. 5.1 - the power that appears to have radiated from an isotropic antenna, which is an antenna that radiates uniformly in all directions. The term in the denominator is usually called the path loss L_s.

According to ref. 5.1, the peak or boresight gain of an antenna is defined as the ratio of maximum radiated power intensity of that antenna to the radiated power intensity of a hypothetical isotropic antenna fed with the same transmitting power as the actual antenna. For both receive and transmit antennas this gain is given by (ref. 5.1):

$$G_a = \eta \frac{4\pi \, A}{\lambda^2} \quad \text{(dB)}, \tag{5.10}$$

where η is the efficiency of the antenna and A the aperture area, when projected on the plane perpendicular to the line of maximum gain (boresight), see figure 5.16. The efficiency factor of the antenna, which is in the order of 0.6 up to 0.7 is caused by:
1. Blocking of the main reflector by the subreflector or feeds.
2. Nonuniform illumination of the main reflector.
3. Spillover of the signal.
4. Surface irregularities.
5. Ohmic efficiency.
For the Hitch-hiker antennas a total efficiency of 65% is assumed.
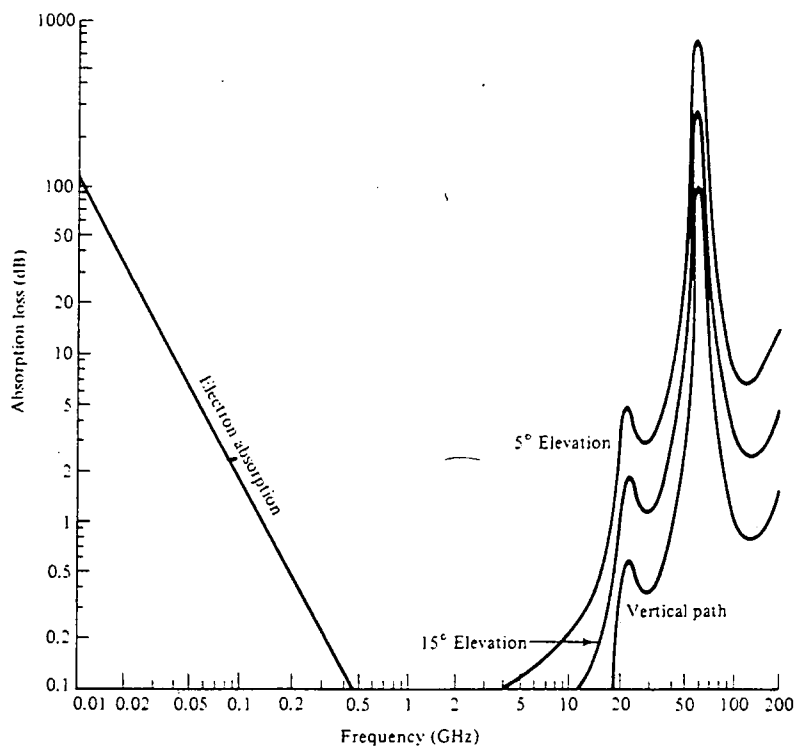
figure 5.17
Absorption in the atmosphere caused by electrons, molecular
oxygen, and uncondensed water vapor.
(ref. 5.1)

(a)

(b)
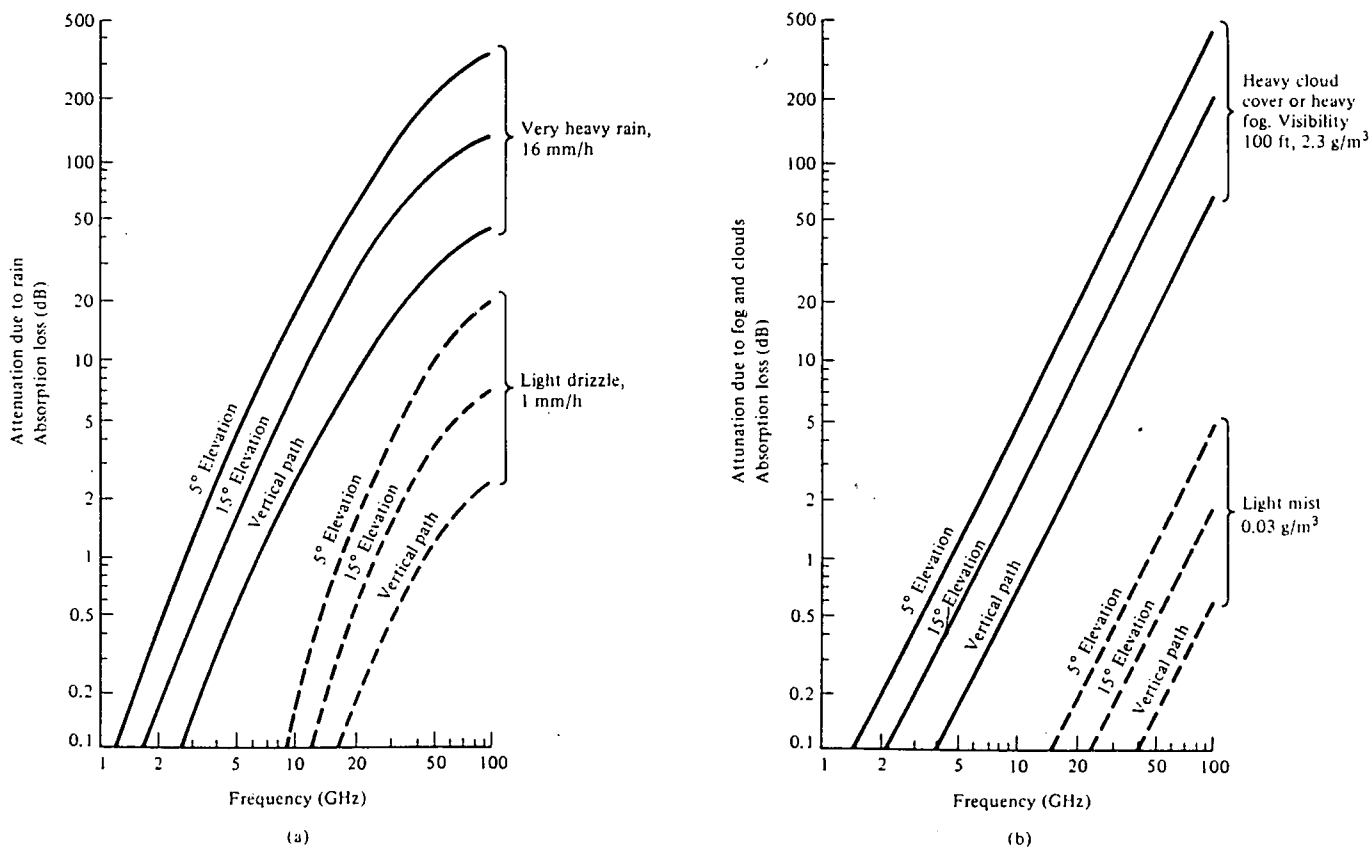
figure 5.18
(a) Absorption due to precipitations (rain).
(b) Absorption due to fog, mist and clouds.
(ref. 5.1)

5.10.2 Impairments.

Unfortunately, during transmission of communications signals losses occur and noise is added to the signal. The main contributors to these impairments are:
1. Thermal noise.
2. Transmission losses.
3. Nonlinearities in active devices and distortion (i.e. equipment noise). These two types of impairments can be treated in a thermal noise-like manner, simplifying the calculations.
4. Interference with other communications devices, which can also be treated in a thermal noise-like manner.

5.10.2.1 Thermal noise.

Thermal noise is one of the major contributors to link degradation, due to the random movements of electrons in the receiver which are of thermal origin. It is caused by:
1. Receiver noise, due to the physical temperature of the receiver.
2. External background noise, picked up by the antenna, of which the main contributors are noise caused by:
    - the sun, which may cause very severe link degradation.
    - the moon.
    - the earth, which is the main contributor to the noise temperature of the satellite's antenna.
    - the sky.
    - the atmosphere (clear sky noise).
    - precipitations and clouds.
    Both the atmosphere and precipitations and clouds absorb radio wave energy, which goes along with random transmission, causing an increase of noise power.
    - galactic noise.
    - cosmic noise.
    - man made noise, which may affect the reception of the communications signals by the ground station antennas.
    The latter three are of minor importance for the frequencies at which the Hitch-hiker system operates.

According to ref. 5.4, the noise power in a communications link operating at microwave frequencies is approximately given by:

$$N = k \, T_t \, B \quad \text{(Watts)}, \tag{5.11}$$

in which k is Boltzmann's constant (k = $1.38 \, 10^{-23}$ J/K), B the bandwidth of the link and T_t the total effective noise temperature of the receiving system. The total effective noise temperature is defined as the noise temperature which causes a noise level at the input of a noiseless receiver, which after amplification is equal to the noise level of the actual noisy receiving system, which means that the output noise power is:

$$N_{out} = k \, G \, T_t \, B \quad \text{(Watts)}, \tag{5.12}$$

where G is the gain of the receiver.
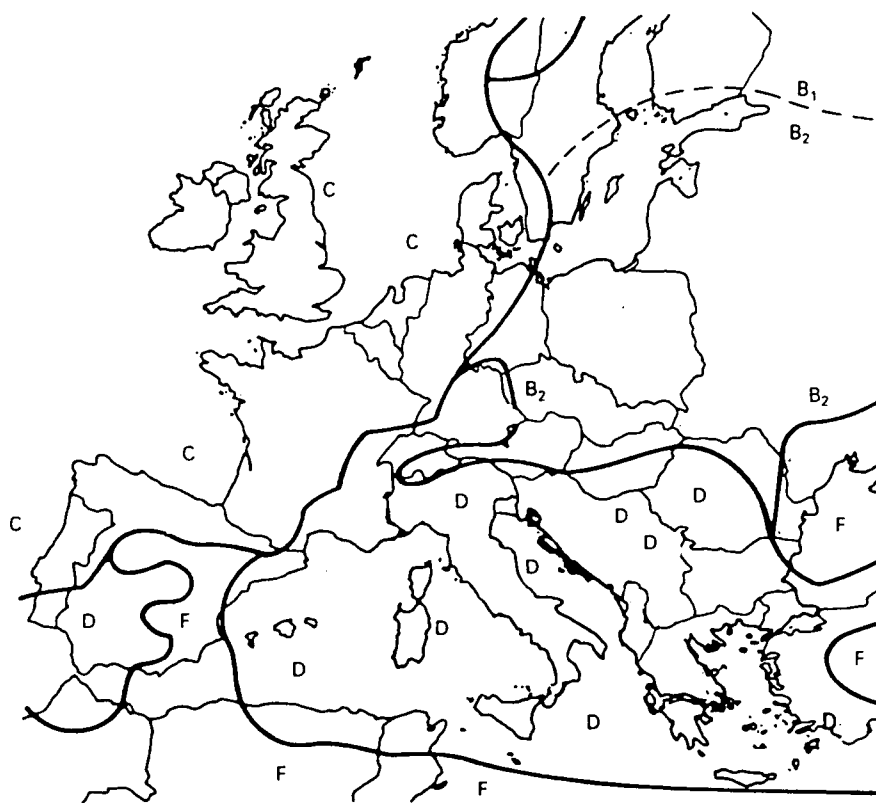
figure 5.19
Rain-rate climate regions for Europe.
(ref. 5.4)

Percent of Year	Rain Climate Region										Minutes per Year	Hours per Year
	A	B	C	D₁	D₂	D₃	E	F	G	H		
0.001	28	54	80	90	102	127	164	66	129	251	5.3	0.09
0.002	24	40	62	72	86	107	144	51	109	220	10.5	0.18
0.005	19	26	41	50	64	81	117	34	85	178	26	0.44
0.01	15	19	28	37	49	63	98	23	67	147	53	0.88
0.02	12	14	18	27	35	48	77	14	51	115	105	1.75
0.05	8	9.5	11	16	22	31	52	8.0	33	77	263	4.38
0.1	6.5	6.8	72	11	15	22	35	5.5	22	51	526	8.77
0.2	4.0	4.8	4.8	7.5	9.5	14	21	3.8	14	31	1,052	17.5
0.5	2.5	2.7	2.8	4.0	5.2	7.0	8.5	2.4	7.0	13	2,630	43.8
1.0	1.7	1.8	1.9	2.2	3.0	4.0	4.0	1.7	3.7	6.4	5,260	87.66
2.0	1.1	1.2	1.2	1.3	1.8	2.5	2.0	1.1	1.6	2.8	10,520	175.3

Source: NASA Propagation Effects Handbook for Satellite System Design, ORI TR 1679.

table 5.5
Point-rain-rate distribution values (mm/h) versus percent of year that the
rain-rate is exceeded for various rain-rate climate regions.
(ref. 5.4)

The total effective noise temperature of a receiving system at the receiver input is (ref. 5.4):

$$T_t = T_a / L + (1 - 1/L) T_0 + T_r \quad (Kelvin),$$ (5.13)

where T_r is the effective noise temperature of the receiver, which is an indication of the front-end quality, T_0 is the physical temperature of the surroundings, usually assumed to be 290 K, L is the loss between the receive horn and the receiver, which may boost the system's noise temperature, for every tenth of dB extra loss will cause a 7K increase of noise temperature and T_a is the noise temperature of the antenna. The latter depends on the radiation pattern of the antenna, the angle of elevation of the satellite, the physical temperature of the surroundings and the external background noise sources mentioned before. Ref. 5.1 shows that under normal conditions an acceptable engineering value for T_a is 70 K for ground station antennas, including additional noise due to precipitations and clouds. For the space segment antenna, which is pointed towards the earth, the average earth noise temperature determines the noise temperature of the antenna, which will be about 250 K.

In general, the receiver will be built up as a cascade of several devices, each having its own noise temperature. For a simple receiver, this may be an amplifier followed by a frequency translator (mixer). Ref. 5.4 shows, that for such a cascade, the effective noise temperature of the receiver is

$$T_r = T_1 + \frac{T_2}{G} \quad (Kelvin),$$ (5.14)

where T_1 is the amplifier noise temperature, T_2 is the mixer noise temperature and G is the amplifier gain.

The performance of a receiving ground station can be expressed in terms of the figure of merit G/T, which in fact is a measure of sensitivity. This is an important figure because the CNR of the link is directly proportional to the G/T figure of merit:

$$C/N = \frac{EIRP}{L_s \, k \, B} * \frac{G}{T} \quad (dB),$$ (5.15)

see ref. 5.1.

The ultimate quality of the link on its turn depends on the CNR at the receiver input, as outlined in section 5.9.

Another important quality indicator is the receiver noise figure, defined as (ref. 5.4):

$$NF = 1 + \frac{T_r}{T_0} \quad (dB),$$ (5.16)

where T_0 is a reference temperature of 290 K.

Other origins of noise are:
1. Equipment noise, considered in section 5.10.2.3.
2. Interference, considered in section 5.10.2.4.
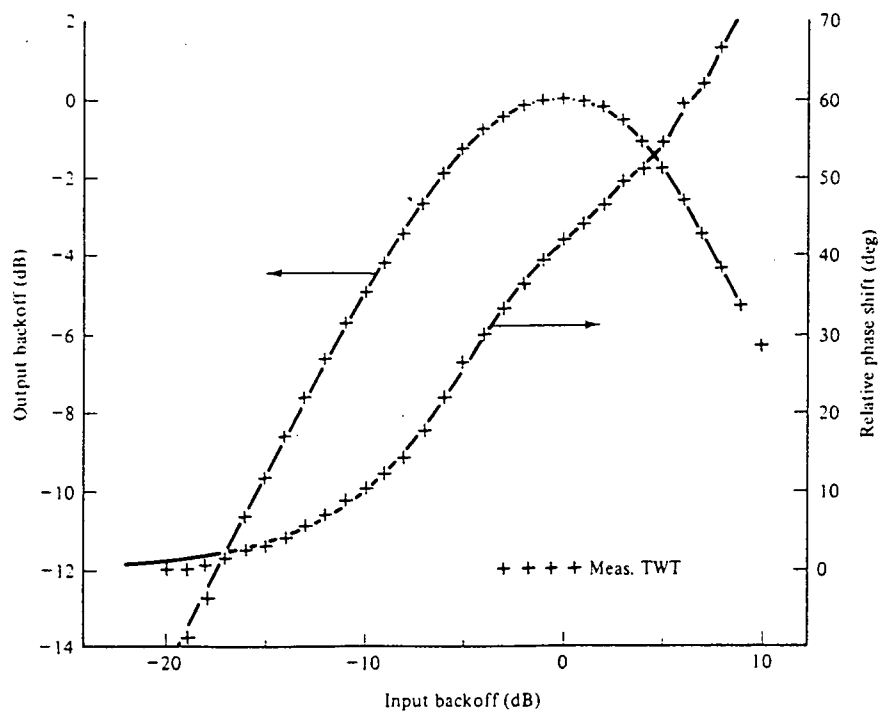
figure 5.20
TWTA transfer characteristics measured at 3.8 Ghz.
(ref. 5.1)
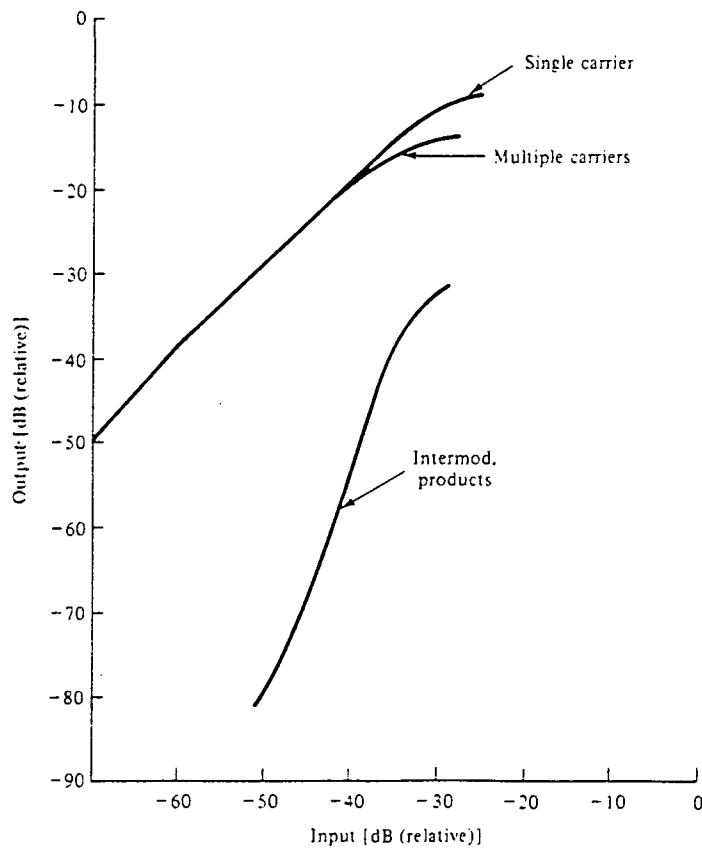
figure 5.21
HPA input-output characteristic and intermodulation levels versus drive level.
(ref. 5.4)

5.10.2.2 Transmission losses.

The communications signals have to travel through the earth's atmosphere, causing transmission losses and additional noise. These losses and noise depend on the path length of the signals through the atmosphere and thus on the elevation angle of the satellite. The transmission losses due to the atmosphere can be divided into two categories:
1. Absorption losses of the clear sky atmosphere, caused by molecular oxygen, uncondensed water vapor and free electrons, see figure 5.17.
2. Effects of rain, snow, hail and fog and clouds, which are much more severe than the clear sky absorption losses. These types of losses depend on the occurring rain rates, which are stochastic, which in their turn depend on the location on earth, the time of year and the elevation angle of the satellite. For a rainrate of 16 mm per hour (rather severe) these losses are given in figure 5.18. From figure 5.19. (Rain rate climate regions for Europe) and table 5.5 (probabilities of occurring rain rates) the grade of service of the satellite link can be determined. Even in the worst case of a D_1 rain rate climate region the grade of service is larger than 99.95%. In this case 4.38 hours per year outage due to bad weather may occur.

In general, the system can be organized such that for the larger types of Hitch-hiker ground stations the drop of capacity caused by a storm will merely delay the non-real-time transmission. Furthermore - since severe storms generally are limited to a small area - it may be beneficial to be able to switch the transmission line between ground stations some kilometers apart (diversity of ground stations).

Not only the atmosphere will cause transmission losses and additional losses may occur:
1. Between the transmitter output and the transmitting antenna (wiring, filters, duplexer).
2. Between the receiving antenna and the receiver input.
3. Due to antenna depointing which may be caused by:
    - pointing errors.
    - misalignment of the radio-electrical axis with the geometrical axis.
    - imperfect stabilization.
    - the fact that the ground station is near the coverage area boundary.

5.10.2.3 Equipment noise.

Equipment noise originates from nonlinearities in active devices and distortions in active and passive devices. The main contributor to equipment noise is the nonlinear behavior (due to saturation) of the high-power transmitter amplifiers (HPAs) like traveling wave tube amplifiers (TWTAs) and solid state power amplifiers (SSPAs), see figure 5.20. This nonlinear behavior results into intermodulation distortion when multiple carrier signals are transmitted as is the case for FDMA, see figure 5.21. This intermodulation distortion can be handled in a thermal noise-like way. The relative level of intermodulation increases as the amplifiers are operated at higher power levels. Therefore the amplifiers must be operated at less than the saturated output, this is called output back-off from saturation into the linear region, see figure 5.22. This output back-off can either be achieved by reducing the uplink transmitter power or by reducing the satellite transponder amplification. The last technique is preferred; it is mandatory when interference occurs, which almost always is the case.
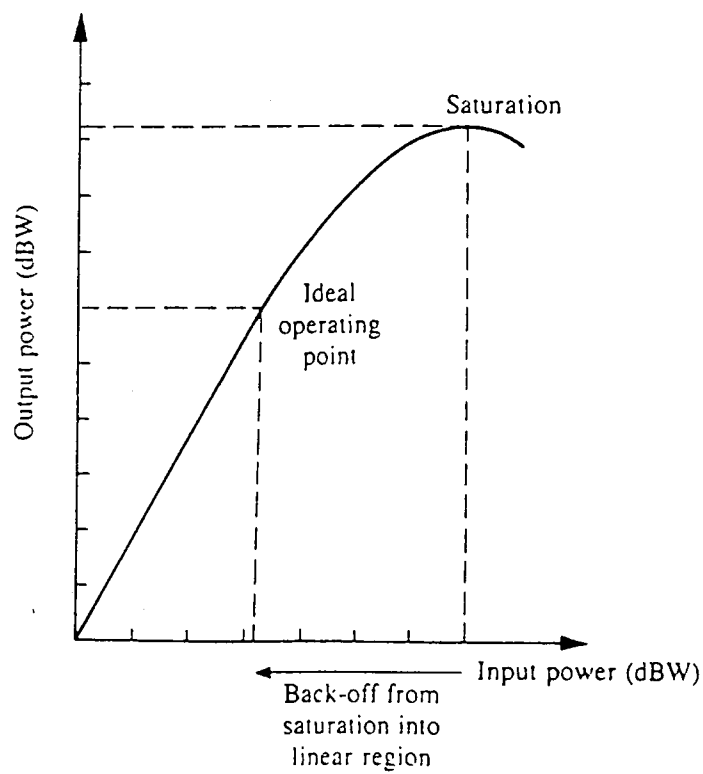
figure 5.22
The concept of back-off.
(ref. 5.2)
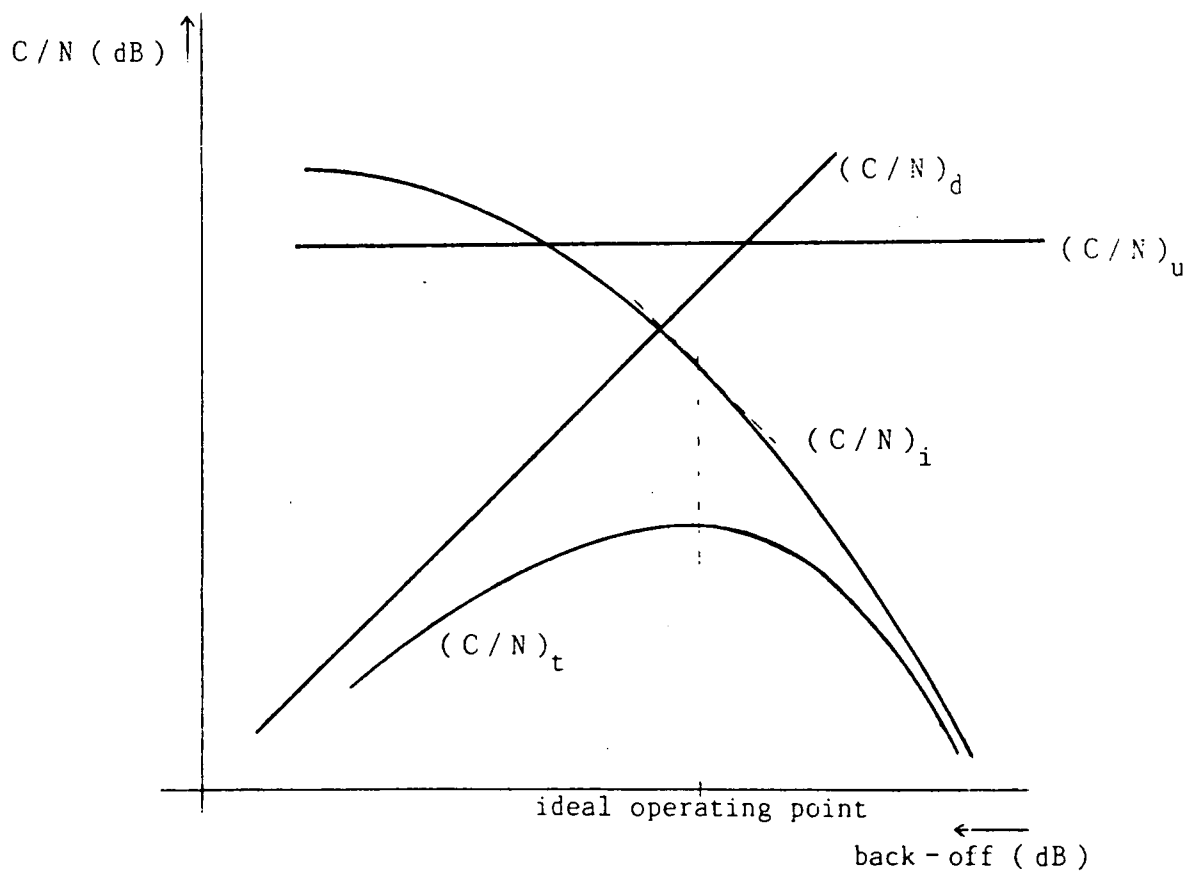
figure 5.23
Transponder performance versus back-off.

As mentioned before, the equipment noise can be treated in a noise-like fashion and therefore it appears to be logical to express this noise in terms of a carrier-to-noise ratio $(C/N)_i$. However, calculation of this figure is very difficult, for it depends on

1. The number of carriers that are used.
2. The modulation characteristics.
3. The amplitude and phase characteristics of the HPAs. Phase shifts lead to distortions like AM-to-PM conversion and intermodulation.

When calculating the total CNR for different values of the output back-off, an optimum value for the back-off appears. This is because the $(C/N)_i$ improves as the HPA power is reduced (decreasing intermodulation levels), but the downlink CNR deteriorates because of the lower output power. These effects are shown in figure 5.23. The optimization calculation can be performed when the transfer characteristics and data on   carrier-to-intermodulation levels of the HPA versus back-off are available. These calculations are beyond the scope of this study.

Noise can also originate from other equipment, for example the channelizing filters may suffer from interference from adjacent channels.

5.10.2.4 Interference.

For the C-band, which is very severely congested, also by terrestrial communications devices, interference is an important link impairment. It may even be necessary to place ground stations outside urban centers to avoid interference with terrestrial links. Because the uplink is not critical for the Hitch-hiker system, only downlink interference with adjacent satellites will be considered.

Interference is simply the effect of unwanted signals on the reception of the wanted signals. It depends on the signal and device characteristics. When only one satellite interferes with the wanted satellite (single entry interference), then, according to ref. 5.4, the carrier-to-interference ratio (CIR) at the receiver input is:

$$C/I = E - e - (L_s - L_{si}) + G_a(0) - G_a(\alpha) \quad (dB), \qquad (5.17)$$

where E is the EIRP of the desired satellite, e the EIRP of the unwanted satellite, L_s resp. L_{si} the path loss of resp. wanted and interfering satellite and $G_a(0)$ resp. $G_a(\alpha)$ the gain of the receiving antenna in the direction of the desired resp. interfering satellite. In general the polar radiation pattern of typical microwave antennas used in satellite communications is very complex, see figure 5.24. For the calculation of the gains, the CCIR have developed reference ground station antenna sidelobe radiation patterns, see ref. 5.4. For $(D / \lambda) < 100$, the off-axis sidelobe gain is:

$$G_a(\alpha) = 52 - 10\log (D / \lambda) - 25\log \alpha \quad (dB), \qquad (5.18a)$$

where α is the deviation angle from boresight in degrees. When $(D / \lambda) \geq 100$, the equation becomes:

$$G_a(\alpha) = 32 - 25\log \alpha \quad (dB). \qquad (5.18b)$$
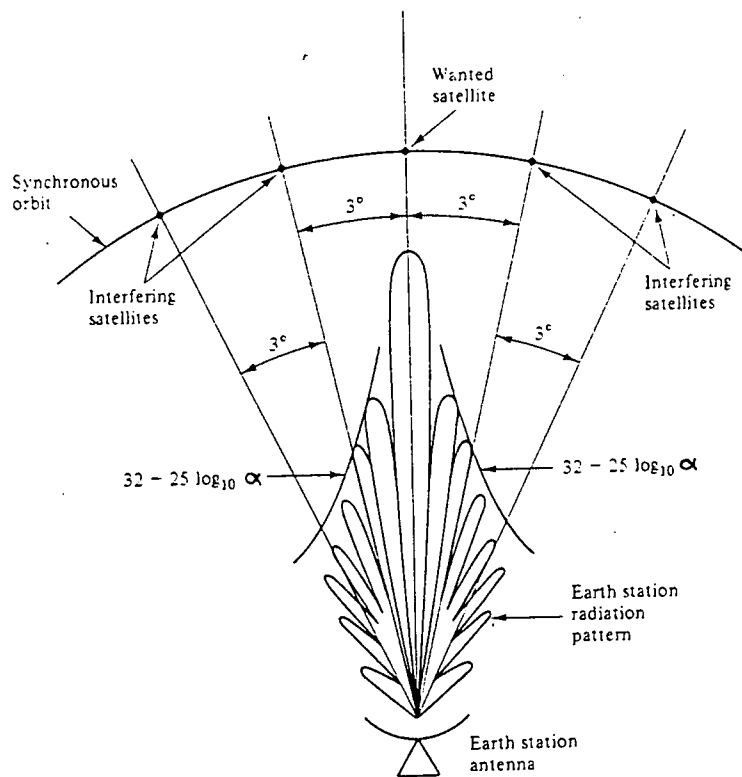
figure 5.24
Adjacent satellite interference.
(ref. 5.1)
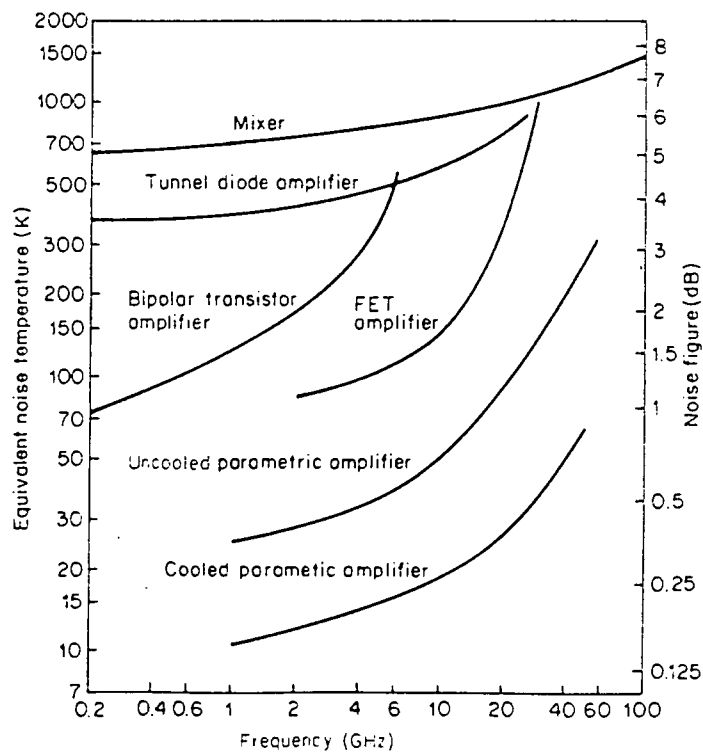
figure 5.25
Noise temperatures and noise figures for various devices.
(ref. 5.7)

When more satellites interfere with the desired satellite (total or multiple entry interference) the interferers may be added on a power basis when the following requirements are met:

1. The interferers are uncorrelated.
2. The interferers are sufficiently numerous, so that each contributes only a small portion to the interference power.
3. The interference power is small compared to the carrier power. Then (see ref. 5.4) the total CIR becomes:

$$(C/I)_t^{-1} = (C/I)_1^{-1} + .. + (C/I)_n^{-1} \quad (dB). \tag{5.19}$$

For each mission the effect of interference must be calculated, because no general prediction can be made. The CIR that is required to yield a chosen - subjectively determined - signal quality, is called the protection ratio, which is in the order of 30 dB for television transmission. However, it is difficult to predict the subjective effect of various combinations of noise and interference. Furthermore, the protection ratio depends on the type of signal and the applied modulation and multiple access techniques. Also, when the interfering carrier is displaced in frequency relative to the wanted carrier, the protection ratio can be reduced.

When both thermal noise, equipment noise and interference have the same characteristics (i.e. low level and additive), which often is the case, they can be treated in a similar fashion, which greatly facilitates the calculation of the overall CNR and thus the link quality and capacity. Then, according to ref. 5.4:

$$(C/N)_t^{-1} = (C/N)_u^{-1} + (C/N)_i^{-1} + (C/N)_d^{-1} + (C/I)_t^{-1} \quad (dB), \tag{5.20}$$

where $(C/N)_u$ resp. $(C/N)_i$ resp. $(C/N)_d$ is the uplink resp. equipment resp. downlink carrier-to-noise ratio. $(C/I)_t$ is the total carrier-to-interference ratio. This equation is very similar to that for resistors connected in parallel.

5.10.3 Link budget estimates.

In table 5.6 a to d and 5.7 the link budgets for both the payload and the TT&C subsystems are given. For the calculations of the overall carrier-to-noise ratios some assumptions, concerning equipment characteristics, losses, noise power etc. have been made, which will be explained in this section.

An important parameter is the noise temperature of the receivers that will be used. For the communications subsystem, low ground station costs are very important, and therefore an uncooled FET technology amplifier has been implemented, having a noise figure of 1.29 dB (figure 5.25). For the space segment a similar amplifier has been used, which, because of the higher frequency has a higher noise figure (1.40 dB). Because of the relatively large gain of the amplifiers (25 dB), the high noise temperature of the mixer will, according to equation 5.14 hardly affect the system noise temperature, which increases by 3 K.

ANTENNA

1 Duplexer
2 Switches
3 Receiver (including LNA and mixer)
4 Demultiplexer (Branching network)
5 Bandpass filter

6 Attenuator
7 Main amplifier
8 Control box (not drawn in this figure)
9 ALC unit
10 FET amplifier

11 Drive adjust
12 HPA (TWTA + EPC / SSPA)
13 Isolator
14 Multiplexing filter
15 Harmonic filter

RECEIVER

CHANNELIZING
NETWORK

PREAMPLIFICATION
& LEVEL CONTROL

POWER
AMPLIFI
CATION

MULTIPLEXING
NETWORK

P=POWER SUPPLY

figure 5.27
CP repeater lay-out.

For the TT&C subsystem, ground station costs are less critical, and therefore a cooled parametric amplifier, having an extremely low noise figure of 0.22 dB, has been used. When an amplifier gain of 20 dB is assumed, the mixer will raise the receiver noise temperature by 10 K, yielding a receiver noise temperature of 25K and a noise figure of 0.36 dB.

The minimum allowable elevation angle is 15°, in order to minimize atmospheric losses. For this elevation angle, the maximum distance from the satellite to the ground station can be calculated from (ref. 5.2):

$$d = \sqrt{(18.1839 - 5.3725 \cos \phi) * 10^7} \quad (m), \qquad (5.21a)$$

in which:

$$\phi \approx -0.9 \, \delta + 81 \quad (degrees), \qquad (5.21b)$$

where δ is the angle of elevation of the satellite above the local horizon. For $\delta = 15°$, the distance is 40,160 km.

As outlined before, the calculation of the equipment noise is very difficult. A rather pessimistic assumption is, that the noise generated in the CP equals the noise generated in the downlink. When the uplink noise and the interference level are sufficiently small - which will be the case when the CIR matches the protection ratio - follows from equation 5.20 that the total CNR decreases by 3.0 dB.

The ground stations are assumed to be pointed perfectly towards the satellite, so no misalignment losses occur.

The carrier-to-interference ratio is very important. However, no general calculations can be performed. Therefore the CIRs for the four types of ground stations have been calculated, assuming two adjacent satellites, having the same EIRP as the Hitch-hiker satellite, with an orbital spacing of 3°. When the differences in path losses are neglected, the CIRs will vary from 6.75 dB for the 2.00 meters antenna up to 18.43 dB for the 4.90 meters antenna, so the relative level of interference increases with decreasing ground station antenna dimensions. Satellites with larger spacing do not further affect these ratios. When interference with two satellites, having an EIRP of ten times the Hitch-hiker EIRP occurs, the minimum spacing is 7.5°, still yielding the same CIRs. These CIRs do exceed the protection ratio of 30 dB. If the CIR must match a protection ratio of 30 dB, in the considered interference case an antenna diameter of 14 meters will be required. However, the calculations may be rather pessimistic, because in general two adjacent satellites do not cover the same area or do not use the same frequency bands and hence do not interfere. According to IFRB circular No 1644 of 30. 10. 1984, the nearest satellite using the same frequency band was ARABSAT I, operating at a longitude of 19° east. However, this satellite covers the Middle-Eastern region, and hence does not interfere with the Hitch-hiker system. Still, careful calculations, requiring data of other satellites in the geostationary orbit, have to be made in order to verify the level of interference. When the CIR levels exceed the required protection ratio, interference will become the critical system design factor and the required dimensions of the ground station antennas may become much larger than the estimated ones.
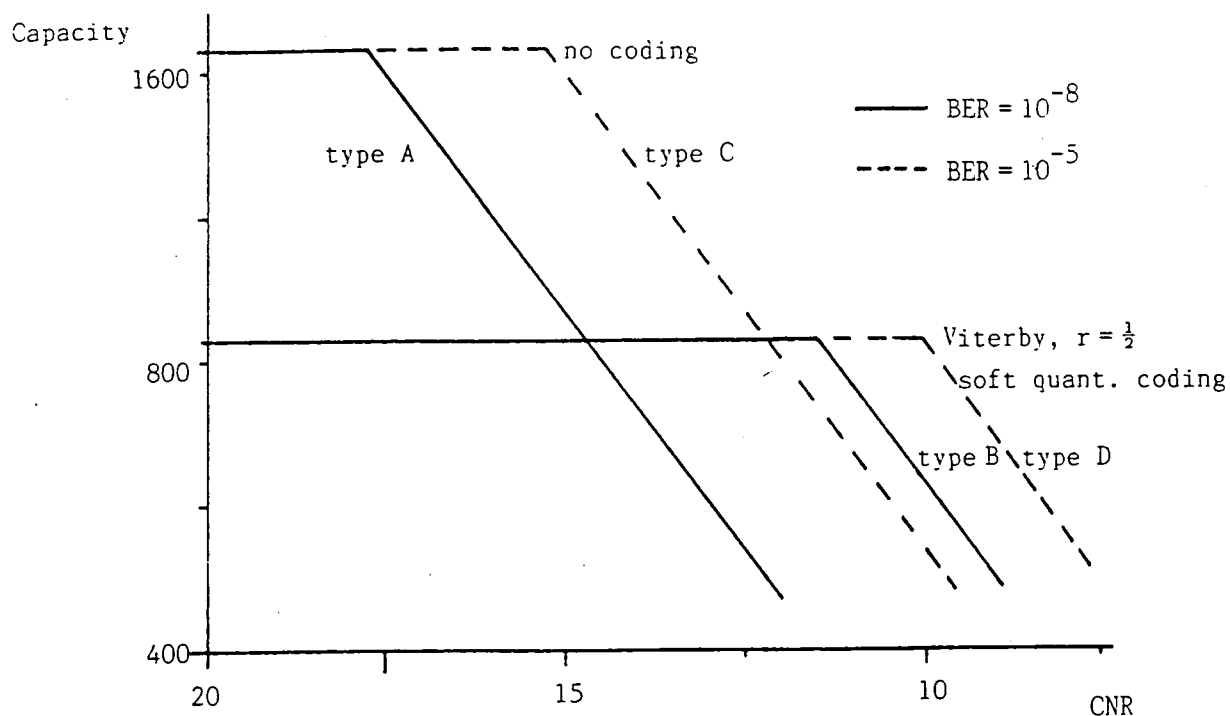
figure 5.26
The capacity (measured as the number of telephone channels with a data-rate of 32 kbps, that can be transmitted over one Hitch-Hiker transponder) of the four types of ground stations for varying overall CNR.
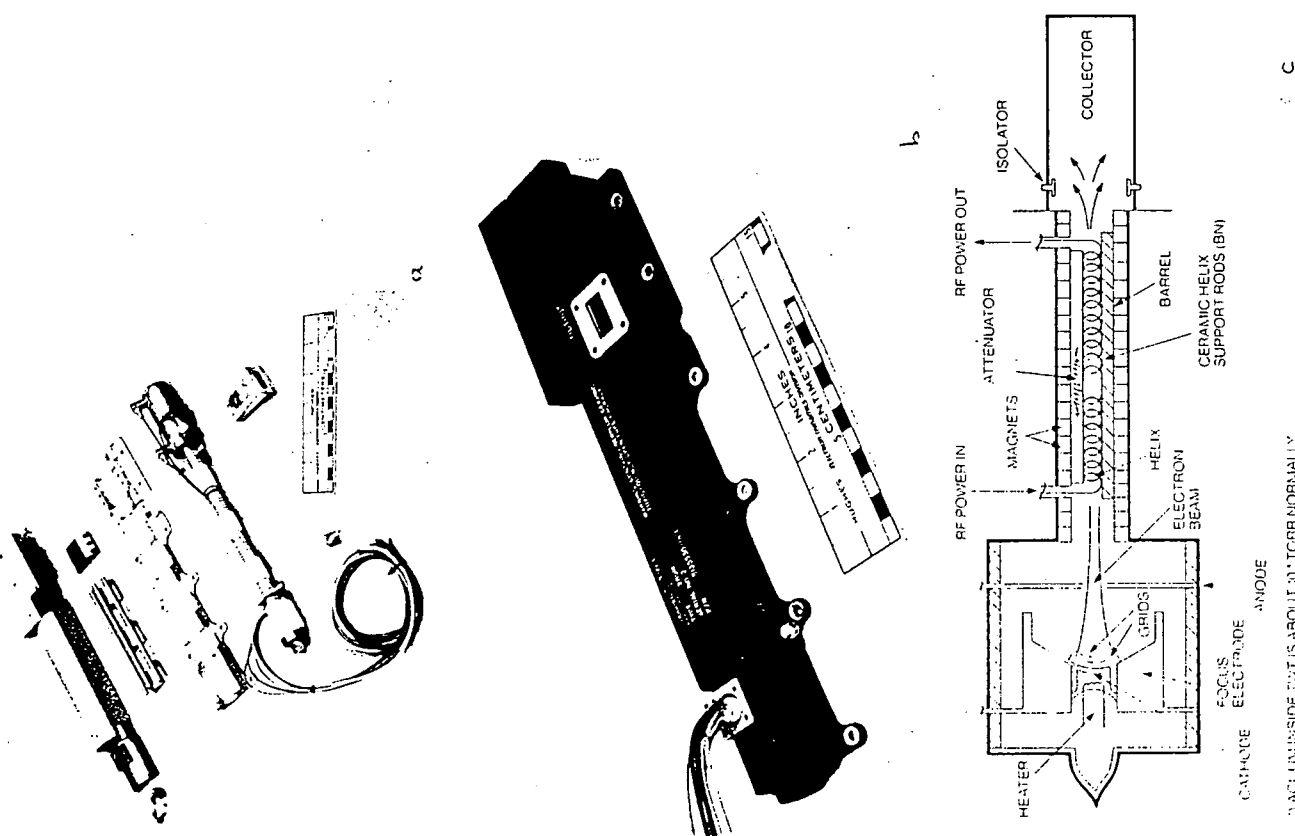
figure 5.28

For the TT&C subsystem, a large margin of 3.85 dB ($\approx$ 150 %) is included because interference has not been considered. During the transfer orbit, interference may be a major problem because of the small EIRP of the satellite. However, the small frequency band may possibly be allocated such that it doesn't coincide with the frequency bands over which other satellites transmit, and then the interference level decreases. During the operational phase the payload antenna will be used, providing a large gain. Then the margins will even be larger and interference may be of no concern.

For the payload subsystem, the margins over the required total CNRs, are about 0.40 dB, which is 10%. These margins may seem somewhat low. However, the estimations of the losses have been somewhat conservative and hence sufficient margin is available. The capacity (see section 5.9.3) of the transponders for varying CNR-levels is shown in figure 5.26 for the four types of ground stations.

For the communications signals, the maximum received power flux density on earth is -148.5 dBW per 36 MHz.m², that is -188 dBW per 4 kHZ.m², which is well below the maximum allowable PFD. Because of the lower output power, the maximum PFD for the TT&C subsystem will even be smaller.

5.11   Subsystem architecture.

In this section the properties of the payload equipment will be discussed. In order to avoid a complex lay-out, a single conversion, quasilinear repeater has been designed, leading to a simple and straightforward design, see figure 5.27. Other (more complex) options, which sometimes provide better signal quality, were rejected for simplicity reasons. In the early processing stages common equipment, employing FET technology, is used in order to save mass and power. Then the communications band is channelized for efficient amplification of the signals.

During the transfer and drift orbit, the TT&C subsystem uses omnidirectional antennas, because the spacecraft must be operable in every possible attitude. During the operational phase, it uses the payload antenna, providing better signal quality. Therefore the CP must contain switches to switch from one antenna system to another in case that unattended changes in attitude might occur. Three switches are used to provide redundancy. The payload uses a combined receive and transmit antenna. In order to avoid interference of the uplink and downlink signals, these signals are separated in the duplexer, providing an isolation of up and downlink signals larger than 110 dB, which also protects the subsystem against high uplink levels. Then the signals are led to two broadband receivers, controlled by three switches for redundancy reasons. Both one receiver and one switch may fail, without endangering the operation of the system. The receivers contain a low noise amplifier (LNA), using commercial FET technology to achieve low noise temperatures, and a local crystal oscillator with a stable, filtered output, to achieve the 2.225 GHz downconversion of the signals.

Then, for efficient amplification of the signals, the entire band is channelized into portions of 36 MHz bandwidth. This is done by the demultiplexer (branching network) and the channel filters (bandpass filters; BPF), which reject adjacent out-of-band frequencies from neighboring channels. Due to the different EIRP figures of the four possible types of ground stations and atmospheric changes, the uplink signals may vary in strength, whereas the transmitter amplifiers operate best at constant signal power levels. The attenuators account for these differences in received power flux density, which is assumed to be sufficient to produce saturated output power under all conditions.

RF INPUT
(COAX)

R.F. OUTPUT
(WAVEGUIDE)

T.W.T.

HEATER
5,2V

ANODE
+100V

CHASSIS
GROUND

COLLECTER
-1950V

CATHODE

-3300V

POWER SUPPLY

28V
BUS

ON/OFF
CONTROL

RF SWITCH
CONTROLS

TELEMETRY:
6 ANALOGUE
1 STATUS

COMMUNICATIONS
CONVERTER
CONTROL
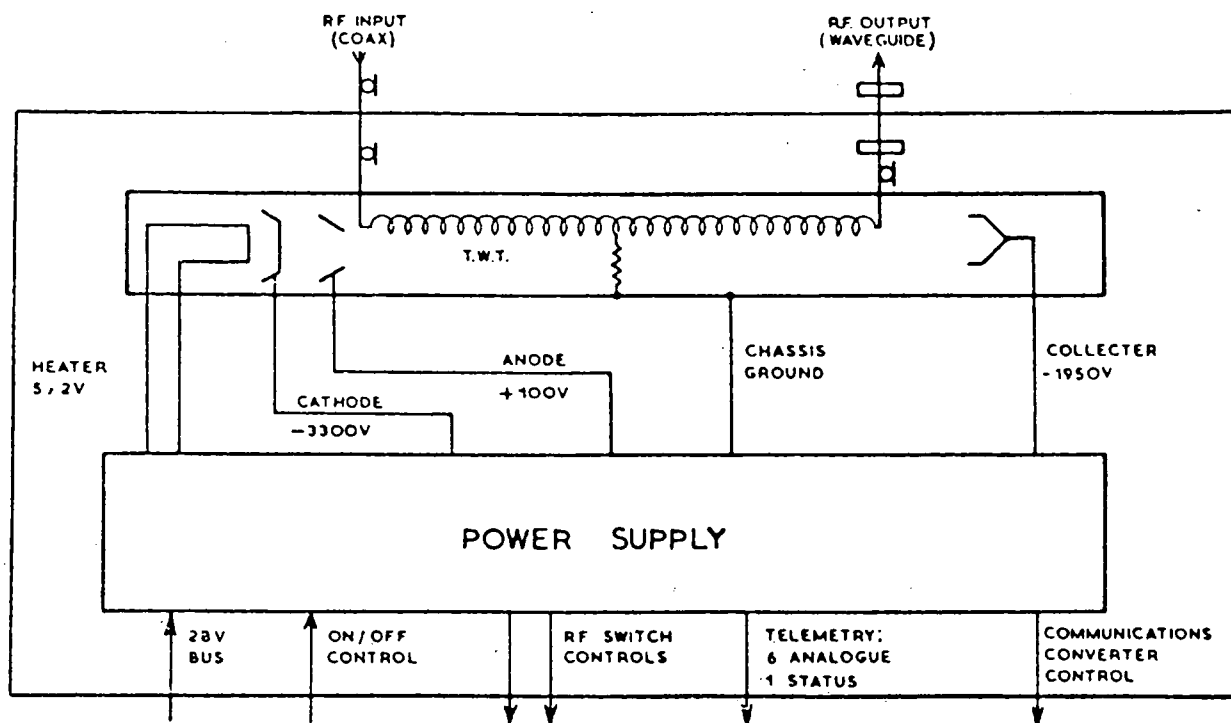
figure 5.28
(a) Unpotted HAC 289HP TWT (Courtesy of Hughes Aircraft Co.)
(b) Packaged HAC 289HP TWT (Courtesy of Hughes Aircraft Co.)
(c) Description of operation of a TWT (Courtesy of Hughes Aircraft Co.)
(d) TWTA configuration.
(ref. 5.3)
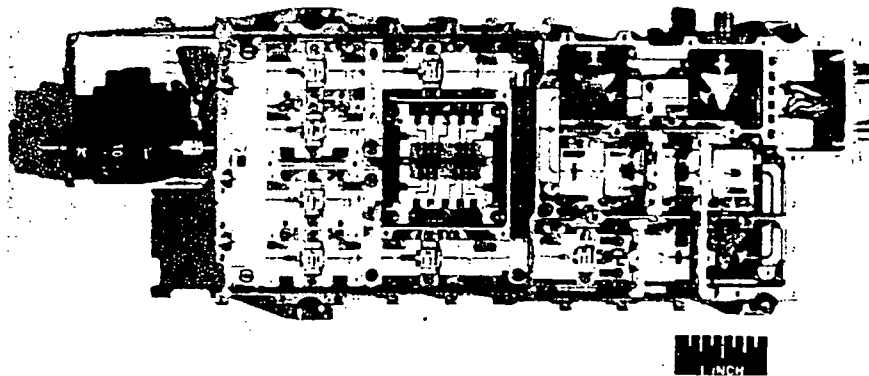
figure 5.29
C-band IOW SSPA.
(Courtesy of RCA)

As mentioned before, the high-power amplifiers (HPAs) suffer from saturation and hence are the main contributors to equipment noise. Therefore the entire gain in signal power can 't be provided by the HPAs alone and pre-amplification is required. This is achieved by using main amplifiers, FET amplifiers and driver amplifiers, the latter also regulating the HPA output back-off. The automatic level control (ALC) unit once more regulates and balances the power level of the signals. The closed loop, which is projected in the figure is somewhat tricky for stability reasons and a careful design is required.

After pre-amplification, the signals are amplified to the level required for downlink transmission in the HPAs, providing gains up to 60 dB. Two different technologies are available, namely traveling wave tube amplifiers (TWTAs), see figures 5.28 a - d, using acceleration of electron beams (see ref. 5.2) and solid state power amplifiers (SSPAs), see figure 5.29, using FET technology. TWTAs have been used since the beginning of telecommunications and hence are an established technology. They also provide the largest efficiencies, and therefore they require less power. SSPAs however have a smaller mass, cover less area in the spacecraft (area is scarce), provide better linear operation near the point of saturation and hence require less output back-off, and promise better reliability and have longer life, the latter being quite important, because the HPAs usually are the life-limiting components of a communications satellite. For the payload subsystem, which deals with large amounts of power, efficiency is very important and therefore TWTAs are preferred. For the TT&C subsystem, high reliability is required, but power is less critical and therefore GaAs FET SSPAs are used. The electric power conditioners (EPCs) provide the high voltages at which the tubes (TWTs) operate.

Finally, the signals are combined in the output multiplexer, which also rejects out-of-band frequencies generated by the HPAs. After passing through a harmonic filter and the duplexer the signals are retransmitted to earth.

The operation of the system is controlled by a control box, which is duplicated to provide redundancy.

5.11.1 Equipment characterizations and requirements.

In order to achieve the wanted output power, the amplifiers must provide sufficient gain. The internal link budget, which specifies the gains is given in table 5.8 a and b.
The dimensions, masses, power requirements and heat productions of the equipment units are given in table 5.9 a and b. These estimations are only very rough, but give a good insight into the characteristic properties of these units.

In order to achieve a certain quality level of the communications signals, the equipment units must meet rather tight specifications. However, as mentioned before, the knowledge to determine these requirements was not available in the design team. Therefore, these requirements will not be developed here. For a general discussion on this item, please see ref. 5.3.

Hyperboloid

$$\epsilon = \frac{f_h}{a} > 1$$

$$f' = \frac{\epsilon + 1}{\epsilon - 1} f$$
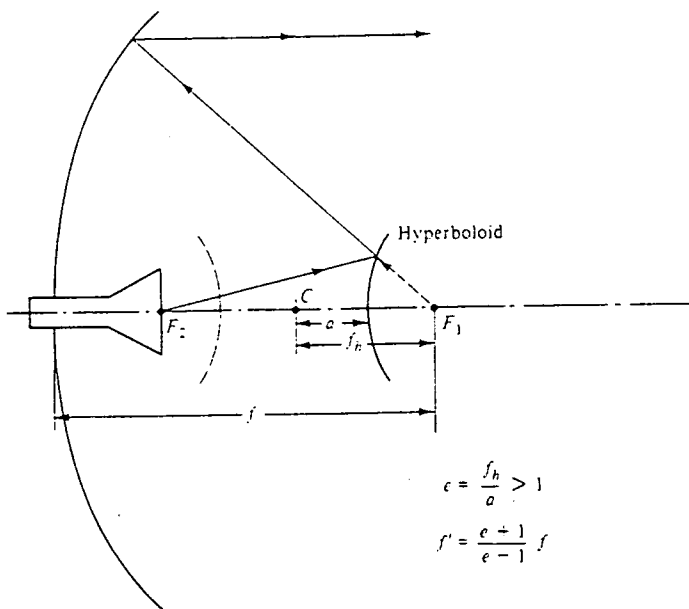
figure 5.31
Cassegrainian antenna.
(ref. 5.4)

DECLINATION AXIS

HOUR AXIS
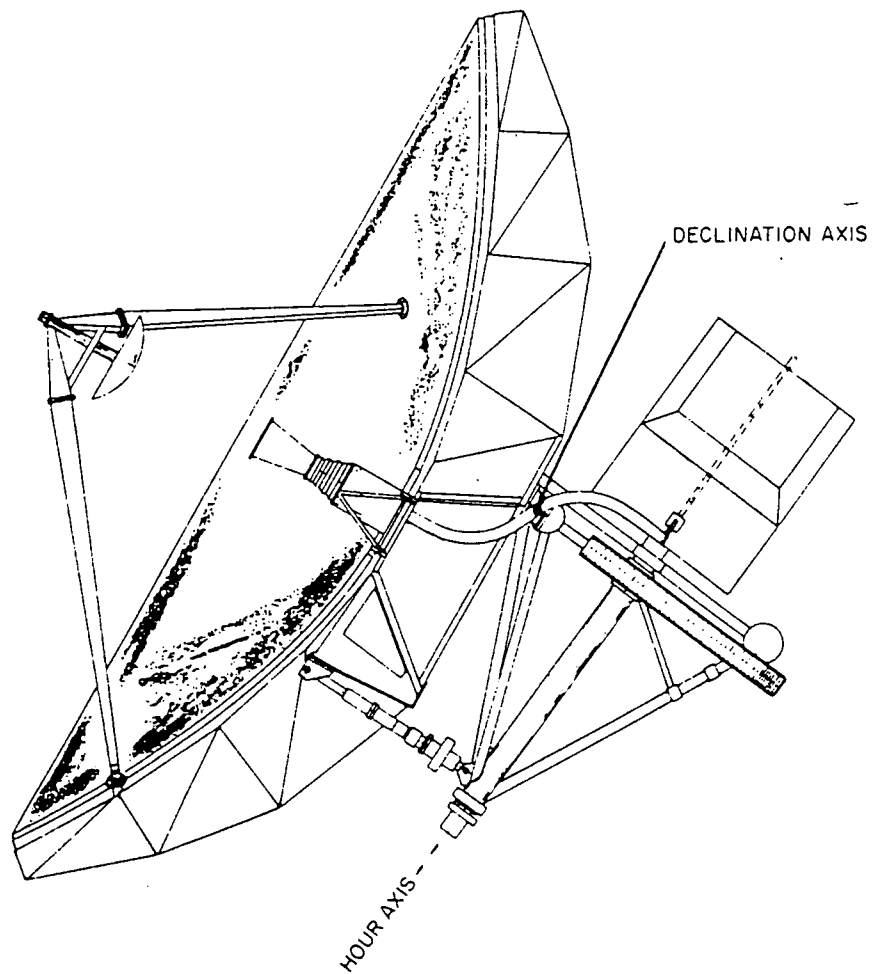
5.12   Ground stations.

For the Hitch-hiker project ground stations will be used, which have both receive and transmit capability. A typical ground station lay out is shown in figure 5.30. The following subsystems can be distinguished:
- Transmitter. In fact, the ground station transmitters do not essentially differ from the space segment transmitters. The main amplifiers are also TWTAs, which suffer from intermodulation distortion. However, transmitter power is not limited, as it is in space.
- Receiver. The receiver provides amplification and demodulation of the incoming signal and may prepare it for further transmission. The LNA of the receiver is very important for the overall performance of the ground station, which is characterized by the figure of merit G/T. Essential for a good performance are small losses in the transmission line between the antenna and the LNA, because these losses also boost the total system noise temperature of the ground station. Therefore a Cassegrainian antenna will be used, see figure 5.31. a and b.
- Antenna.
- Tracking system. The tracking system must point the antenna towards the satellite. It may be necessary to enable switching from one satellite to another and the antenna must be able to follow residual orbital motions of the satellite. Also the tracking system will allow for wind deflection of the antenna. Because of the quite large beamwidth of the ground station antennas (larger than 1^0), only occasional repointing, mainly to switch from one satellite to another, is required. Because of the dish dimensions this repointing is preferably motorized. When satellite operation from a 5^0 inclined orbit is required, continuous preprogrammed tracking will become necessary. The apparent satellite motion can be calculated and programmed.
- Terrestrial interface. This subsystem links the baseband signals, which may be generated at the ground station or are used for terrestrial links from the user to the ground station, with the RF signal, used for the satellite link. The techniques which are required to provide this interface have been discussed in section 5.9.
- Power subsystem. Very often commercial power is used as primary power supply. In order to continue the communications during commercial power outages, an emergency power system is required. In order to make the change over from one power system to another without any interruption in service, a no-break transition is applied.
- Test equipment.
- Control equipment, required for the multiple access operations of the system.

5.13   Conclusions.

The performance and capacity of the system is limited by several factors:
- limited CP transmitter power,
- interference,
- spacecraft mass,
- spacecraft area.
   Possible solutions for these problems may be:
1. To reduce the number of operational channels. Then a larger power will be available per transponder and both the downlink CNR and the CIR performance improve, which will lead to lower ground station costs. Furthermore, the spacecraft mass and the consumed area in the spacecraft will be reduced, leading to lower space segment costs. However, the capacity of the link will reduce, which may not be acceptable for the customers.
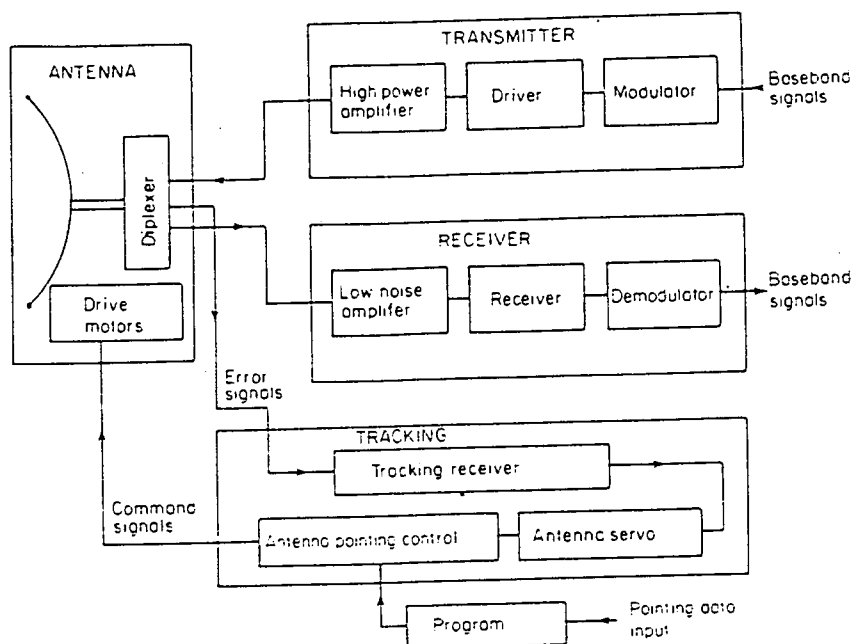
figure 5.30
Typical earth station lay-out.
(ref. 5.7)
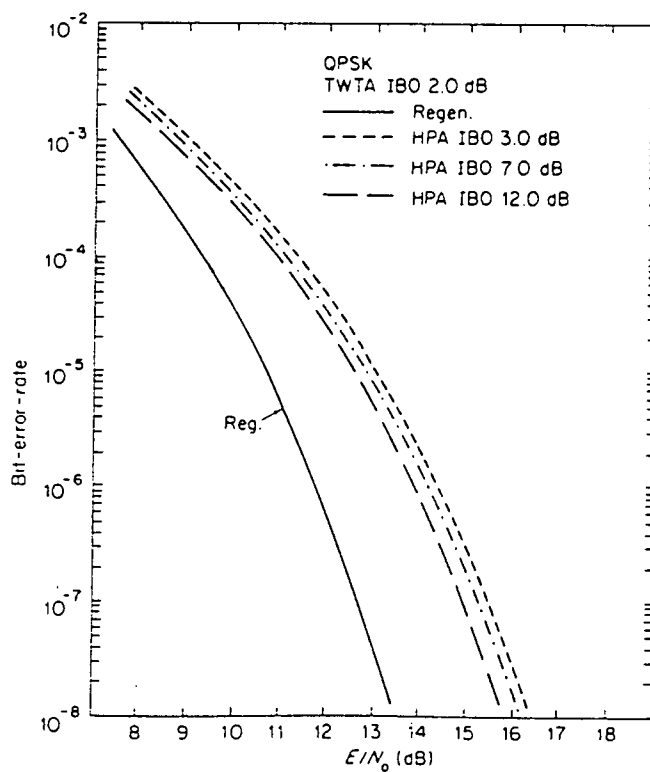
figure 5.32

Performance of a regenerative repeater compared to the performance of
conventional repeaters.
TWTA IBO: TWTA input back-off.
HPA IBO: ground station HPA input back-off.
(ref. 5.7)

2. Use the Ku-band instead of the C-band for transmission. Then, no interference with terrestrial links will occur and interference with other satellites will reduce because of the smaller beamwidth and larger gain of the ground station antennas, when the same antenna diameter will be used. A 5.00 meters antenna will be sufficient to match the 30 dB protection ratio, when two satellites, having the same EIRP as the Hitch-hiker satellite, with an orbital spacing of 3^0 interfere. However, as discussed in section 5.6, the Ku-band has large disadvantages, but when interference is a limiting factor, it may be profitable to switch to the Ku-band. A link budget for a 7.00 meters Ku-band ground station is given in table 5.10

3. Beamshaping will limit the amount of spillover of the signals outside Europe. Then the PFD on the earth's surface will increase, leading to smaller and cheaper ground stations. However, a beam forming network and a multiple feed array will be required, leading to a higher spacecraft mass and a more complex CP lay-out.

4. Use a regenerative spacecraft repeater, which separates the up and downlink performance by onboard de and remodulation and processing of the signals. This may improve the CNR performance by 2 - 5 dB, see figure 5.32. However, the mass and complexity of the system will increase.

5. Use SSPAs instead of TWTAs for the final amplification of the payload signals. Then the consumed spacecraft mass and area will be reduced. However, because of the lower efficiency the performance will reduce or the required DC power input will increase.

C-band: 500 MHz bandwidth available (no polarization).
   Uplink   : 5.925 - 6.425 GHz.
   Downlink : 3.700 - 4.200 GHz.

Space segment.

10 channels operational.
20 Watts RF power per channel.
36 MHz bandwidth per channel.
Combined receive / transmit antenna. Diameter 1.80 meters.
Noise temperature of the receiver: 110 K (uncooled).
Noise temperature of the antenna: 250 K.
Noise figure of the receiver: 1.40 dB, characteristic of
   commercial FET technology.

Ground segment.

Type A ground station.
Antenna diameter 4.90 meters.
Transmitter power 200 W.
Noise temperature of the receiver: 100 K (uncooled).
Noise temperature of the antenna: 70 K.
Noise figure of the receiver: 1.29 dB (commercial FET
   technology).

Link budget

	Uplink		Downlink	
Transmitter power	23.01	dBW	13.01	dBW
Transm. system loss	-0.50	dB	-0.50	dB
Transm. antenna gain (5.10)	47.79	dB	35.00	dB
Pointing loss, -3 dB	-		-3.00	dB
EIRP (Worst case) (5.9)	70.30	dB	44.51	dB
Path loss (5.9)	-199.97	dB	-195.88	dB
Atmospheric loss (worst case)*	< -0.10	dB	< -0.10	dB
Loss in bad storm *	-3.00	dB	-1.10	dB
Receiving antenna gain (5.10)	39.09	dB	43.70	dB
pointing loss, -3 dB	-3.00	dB	-	
Rec. system loss	-0.50	dB	-0.50	dB
Received power (5.9)	-97.18	dBW	-109.37	dBW
Noise temperature (5.13 & 5.14)	360	K	170	K
Figure of merit G/T	13.53	dB	21.40	dB
Received bandwidth	36.0	MHz	36.0	MHz
Noise power (5.11)	-127.48	dBW	-130.73	dBW
CP Noise	-		-3.00	dB
CNR (5.15)	30.30	dB	18.36	dB
CIR (5.17, 5.18 and 5.19)	-		18.43	dB

Overall CNR (worst case, no interference) (5.20): 18.09 dB

N.B. * : see fig. 5.17 and 5.18.

Table 5.6 a: Link budget for the communications payload, type A
         ground stations.

C-band: 500 MHz bandwidth available (no polarization).
   Uplink   : 5.925 - 6.425 GHz.
   Downlink : 3.700 - 4.200 GHz.

Space segment.

10 channels operational.
20 Watts RF power per channel.
36 MHz bandwidth per channel.
Combined receive / transmit antenna. Diameter 1.80 meters.
Noise temperature of the receiver: 110 K (uncooled).
Noise temperature of the antenna: 250 K.
Noise figure of the receiver: 1.40 dB, characteristic of
   commercial FET technology.

Ground segment.

Type B ground station.
Antenna diameter 2.40 meters.
Transmitter power 200 W.
Noise temperature of the receiver: 100 K (uncooled).
Noise temperature of the antenna: 70 K.
Noise figure of the receiver: 1.29 dB (commercial FET
   technology).

Link budget

	Uplink	Downlink
Transmitter power	23.01 dBW	13.01 dBW
Transm. system loss	-0.50 dB	-0.50 dB
Transm. antenna gain (5.10)	41.59 dB	35.00 dB
Pointing loss, -3 dB	–	-3.00 dB
EIRP (Worst case) (5.9)	64.10 dB	44.51 dB
Path loss (5.9)	-199.97 dB	-195.88 dB
Atmospheric loss (worst case)*	< -0.10 dB	< -0.10 dB
Loss in bad storm*	-3.00 dB	-1.10 dB
Receiving antenna gain (5.10)	39.09 dB	37.50 dB
pointing loss, -3 dB	-3.00 dB	–
Rec. system loss	-0.50 dB	-0.50 dB
Received power (5.9)	-103.38 dBW	-115.57 dBW
Noise temperature (5.13 & 5.14)	360 K	170 K
Figure of merit G/T	13.53 dB	15.20 dB
Received bandwidth	36.0 MHz	36.0 MHz
Noise power (5.11)	-127.48 dBW	-130.73 dBW
CP Noise	–	-3.00 dB
CNR (5.15)	24.10 dB	12.16 dB
CIR (5.17, 5.18 and 5.19)	–	9.13 dB

Overall CNR (worst case, no interference) (5.20): 11.89 dB

N.B. * : see fig. 5.17 and 5.18.

<u>Table 5.6 b:</u> **Link budget for the communications payload, type B**
         ground stations.

C-band: 500 MHz bandwidth available (no polarization).
   Uplink   : 5.925 - 6.425 GHz.
   Downlink : 3.700 - 4.200 GHz.

Space segment.

10 channels operational.
20 Watts RF power per channel.
36 MHz bandwidth per channel.
Combined receive / transmit antenna. Diameter 1.80 meters.
Noise temperature of the receiver: 110 K (uncooled).
Noise temperature of the antenna: 250 K.
Noise figure of the receiver: 1.40 dB, characteristic of
   commercial FET technology.

Ground segment.

Type C ground station.
Antenna diameter 3.65 meters.
Transmitter power 300 W.
Noise temperature of the receiver: 100 K (uncooled).
Noise temperature of the antenna: 70 K.
Noise figure of the receiver: 1.29 dB (commercial FET
   technology).

Link budget

	Uplink	Downlink
Transmitter power	24.77 dBW	13.01 dBW
Transm. system loss	-0.50 dB	-0.50 dB
Transm. antenna gain (5.10)	45.23 dB	35.00 dB
Pointing loss, -3 dB	-	-3.00 dB
EIRP (Worst case) (5.9)	69.50 dB	44.51 dB
Path loss (5.9)	-199.97 dB	-195.88 dB
Atmospheric loss (worst case)*	< -0.10 dB	< -0.10 dB
Loss in bad storm*	-3.00 dB	-1.10 dB
Receiving antenna gain (5.10)	39.09 dB	41.14 dB
pointing loss, -3 dB	-3.00 dB	-
Rec. system loss	-0.50 dB	-0.50 dB
Received power (5.9)	-97.98 dBW	-111.93 dBW
Noise temperature (5.13 & 5.14)	360 K	170 K
Figure of merit G/T	13.53 dB	18.84 dB
Received bandwidth	36.0 MHz	36.0 MHz
Noise power (5.11)	-127.48 dBW	-130.73 dBW
CP Noise	-	-3.00 dB
CNR (5.15)	29.50 dB	15.80 dB
CIR (5.17, 5.18 and 5.19)	-	14.58 dB

Overall CNR (worst case, no interference) (5.20): 15.62 dB

N.B. * : see fig. 5.17 and 5.18.

Table 5.6 c: Link budget for the communications payload, type C
            ground stations.

C-band: 500 MHz bandwidth available (no polarization).
    Uplink   : 5.925 - 6.425 GHz.
    Downlink : 3.700 - 4.200 GHz.

Space segment.

10 channels operational.
20 Watts RF power per channel.
36 MHz bandwidth per channel.
Combined receive / transmit antenna. Diameter 1.80 meters.
Noise temperature of the receiver: 110 K (uncooled).
Noise temperature of the antenna: 250 K.
Noise figure of the receiver: 1.40 dB, characteristic of
    commercial FET technology.

Ground segment.

Type D ground station.
Antenna diameter 2.00 meters.
Transmitter power 300 W.
Noise temperature of the receiver: 100 K (uncooled).
Noise temperature of the antenna: 70 K.
Noise figure of the receiver: 1.29 dB (commercial FET
    technology).

Link budget

	Uplink		Downlink	
Transmitter power	24.77	dBW	13.01	dBW
Transm. system loss	-0.50	dB	-0.50	dB
Transm. antenna gain (5.10)	40.00	dB	35.00	dB
Pointing loss, -3 dB	-		-3.00	dB
EIRP (Worst case) (5.9)	64.27	dB	44.51	dB
Path loss (5.9)	-199.97	dB	-195.88	dB
Atmospheric loss (worst case)*	< -0.10	dB	< -0.10	dB
Loss in bad storm *	-3.00	dB	-1.10	dB
Receiving antenna gain (5.10)	39.09	dB	35.91	dB
pointing loss, -3 dB	-3.00	dB	-	
Rec. system loss	-0.50	dB	-0.50	dB
Received power (5.9)	-103.21	dBW	-117.16	dBW
Noise temperature (5.13 & 5.14)	360	K	170	K
Figure of merit G/T	13.53	dB	13.61	dB
Received bandwidth	36.0	MHz	36.0	MHz
Noise power (5.11)	-127.48	dBW	-130.73	dBW
CP Noise	-		-3.00	dB
CNR (5.15)	24.27	dB	10.57	dB
CIR (5.17, 5.18 and 5.19)	-		6.75	dB

Overall CNR (worst case, no interference) (5.20): 10.39 dB

N.B. * : see fig. 5.17 and 5.18.

Table 5.6 d: Link budget for the communications payload, type D
            ground stations.

Frequency within C-band.
    Uplink   : 6.425 GHz.
    Downlink : 4.200 GHz.

Space segment.

5.0 Watt RF power.
3.0 kHz bandwidth.
Combined receive / transmit antenna. Omnidirectional coverage.
Noise temperature of the receiver: 110 K (uncooled).
Noise temperature of the antenna: 250 K.
Noise figure of the receiver: 1.40 dB, characteristic of
    commercial FET technology.

Ground segment.

Antenna diameter 10.00 meters.
Transmitter power 200 W.
Noise temperature of the receiver: 25 K (cooled parametric amp.)
Noise temperature of the antenna: 70 K.
Noise figure of the receiver: 0.36 dB.

Link budget

	Uplink	Downlink
Transmitter power	23.01 dBW	6.99 dBW
Transm. system loss	-0.50 dB	-0.50 dB
Transm. antenna gain (5.10)	54.69 dB	0.00 dB
Pointing loss, -3 dB	–	-3.00 dB
EIRP (Worst case) (5.9)	77.20 dB	3.49 dB
Path loss (5.9)	-200.68 dB	-196.98 dB
Atmospheric loss (worst case) *	< -0.10 dB	< -0.10 dB
Loss in bad storm *	-3.00 dB	-1.10 dB
Receiving antenna gain (5.10)	0.00 dB	50.99 dB
Pointing loss, -3 dB	-3.00 dB	–
Rec. system loss	-0.50 dB	-0.50 dB
Received power (5.9)	-130.08 dBW	-144.20 dBW
Noise temperature (5.13 & 5.14)	360 K	95 K
Figure of merit G/T	-25.56 dB	31.21 dB
Received bandwidth	3.00 kHz	3.00 kHz
Noise power (5.11)	-168.27 dBW	-174.05 dBW
CP Noise	0 dB	-3.00 dB
CNR (5.15)	38.19 dB	26.85 dB

N.B.: Uplink and downlink are not paired.
N.B. * : see fig. 5.17 and 5.18.

During the operational phase, the payload antenna is used,
providing larger gain and thus better CNR performance.

Table 5.7: Link budget for the TT&C subsystem.

	Signal levels	gain	loss
Input	-73 - -61 dBm		
Receiver	-48 - -36 dBm	25 dB	
Branching network	-54 - -42 dBm		6 dB
Bandpass filters	-60 - -48 dBm		6 dB
Attenuator	-65 dBm		5 - 20 dB (adjustable)
Main amplifiers	-40 dBm	25 dB	
ALCs	-50 dBm		10 dB
FET amplifiers	-30 dBm	20 dB	
Drives	-15 dBm	15 dB	
TWTAs	+43 dBm	58 dB	
Output mux & duplexer	+42.5 dBm		0.5 dB

Table 5.8 a: Internal link budget for the payload subsystem.

	Signal levels	gain	loss
Input	-100 - -94 dBm		
Receiver	-75 - -69 dBm	25 dB	
Branching network	-81 - -75 dBm		6 dB
Bandpass filter	-87 - -81 dBm		6 dB
Attenuator	-92 dBm		5 - 20 dB (adjustable)
Main amplifier	-67 dBm	25 dB	
Output data handling	-20 dBm		
Bandpass filter	-26 dBm		6 dB
Drive	-11 dBm	15 dB	
SSPA	+37 dBm	48 dB	
Output mux & duplexer	+36.5 dBm		0.5 dB

Additional 47 dB gain to be achieved in data handling subsystem.

Table 5.8 b: Internal link budget for the TT&C subsystem.

	dimensions (mm)	mass (kg)	Power (W) heat	consumption
1 Duplexer	400x 60x 40	0.30		
3 Switches	90x 60x 40	0.20		
2 Receivers	130x 80x 60	2.00	2.5	2.5
1 Branching netw.	120x 30x 30	0.15		
12 BPF	200x100x 50	0.75		
12 Attenuators	diam 20x 20	0.005		
12 Main amps	120x 50x 60	0.175	3.0	3.0
2 Control boxes	150x120x 50	0.50	1.2	1.2
12 ALC	70x 25x 25	0.10	0.6	0.6
12 FET amps	70x 40x 20	0.12	1.0	1.0
12 Drive adjusts	40x 50x 15	0.10	0.5	0.5
12 TWTs	50x 60x300	0.60	16.0	(36.0)
12 EPCs	330x 60x150	1.60	4.0	40.0
12 Isolators	80x 30x 30	0.10		
11 Multiplexing filters	120x 80x 70	0.30	2.2	
1 Harmonic filter	120x 60x 40	0.20		
Cabling		4.85	0.3	
total repeater		57.00	277.0	454.7
antenna		13.00		
Total Payload mass:		70.0 kg.		

Total efficiency: 39.1 %

Table 5.9 a: Payload equipment units specifications.

	dimensions (mm)	mass (kg)	Power (W) heat	consumption
3 Switches	90x 60x 40	0.20		
2 BPF	200x100x 50	0.75		
2 Attenuators	diam 20x 20	0.005		
2 Main amps	120x 50x 60	0.175	3.0	3.0
2 BPF	200x100x 50	0.75		
2 Drive adjusts	40x 50x 15	0.10	0.5	0.5
2 SSPAs	300x150x100	1.50	10.0	15.0
2 Isolators	80x 30x 30	0.10		
2 Multiplexing filters	120x 80x 70	0.30	0.1	
Cabling		<u>0.54</u>	———	———
total repeater		8.50	13.6	18.5
8 horn antennas		<u>5.60</u>		
Total TT&C repeater mass:		14.10 kg.		

Total efficiency: 26.5 %

Table 5.9 b: TT&C equipment units specifications.

Ku-band: 500 MHz bandwidth available (no polarization).
    Uplink   : 14.000 - 14.500 GHz.
    Downlink : 11.700 - 12.200 GHz.

Space segment.

10 channels operational.
20 Watts RF power per channel.
36 MHz bandwidth per channel.
Combined receive / transmit antenna. Diameter 1.80 meters.
Noise temperature of the receiver: 230 K (uncooled).
Noise temperature of the antenna: 250 K.
Noise figure of the receiver: 2.54 dB, characteristic of
    commercial FET technology.

Ground segment.

Antenna diameter 7.00 meters.
Transmitter power 500 W.
Noise temperature of the receiver: 180 K (uncooled).
Noise temperature of the antenna: 70 K.
Noise figure of the receiver: 2.10 dB (commercial FET
    technology).

Link budget

	Uplink		Downlink	
Transmitter power	26.99	dBW	13.01	dBW
Transm. system loss	-0.50	dB	-0.50	dB
Transm. antenna gain (5.10)	58.35	dB	45.00	dB
Pointing loss, -3 dB	-		-3.00	dB
EIRP (Worst case) (5.9)	84.84	dB	54.51	dB
Path loss (5.9)	-207.44	dB	-205.88	dB
Atmospheric loss (worst case)*	< -0.20	dB	< -0.15	dB
Loss in bad storm *	-20.00	dB	-12.00	dB
Receiving antenna gain (5.10)	46.56	dB	56.80	dB
pointing loss, -3 dB	-3.00	dB	-	
Rec. system loss	-0.50	dB	-0.50	dB
Received power (5.9)	-99.74	dBW	-107.22	dBW
Noise temperature (5.13 & 5.14)	480	K	250	K
Figure of merit G/T	19.75	dB	32.82	dB
Received bandwidth	36.0	MHz	36.0	MHz
Noise power (5.11)	-126.23	dBW	-129.06	dBW
CP Noise	-		-3.00	dB
CNR (5.15)	26.49	dB	18.84	dB
CIR (5.17, 5.18 and 5.19)	-		33.72	dB

Overall CNR (worst case, incl. interference) (5.20): 18.03 dB

N.B. * : see fig. 5.17 and 5.18.

Table 5.10: Link budget for the communications payload when the
            Ku-band is used.

```
┌─────────────────┐                    ARRAY
│     POWER       │                    SUBSYSTEM
│  GENERATION     │
└────────┬────────┘
         │
         │        ┌─────────────────┐  ORIENTATION
         └────────┤     ARRAY       │  SUBSYSTEM
                  │  ORIENTATION    │
                  └─────────────────┘

┌─────────────────┐                    POWER
│     POWER       │                    COLLECTION
│  COLLECTION     │                    SUBSYSTEM
└────────┬────────┘
         │        ┌─────────────────┐╮
         │        │  CHARGE AND     │
         └────────┤  DISCHARGE      │
                  │  CONTROL        │
                  └────────┬────────┘  ENERGY
                           │         ╮ STORAGE
                  ┌────────┴────────┐  SUBSYSTEM
                  │    ENERGY       │
                  │    STORAGE      │
                  └─────────────────┘╯

┌─────────────────┐                    POWER
│     POWER       │                    REGULATION
│ CONVERSION AND  │                    SUBSYSTEM
│  REGULATION     │
└────────┬────────┘
         │
┌────────┴────────┐                    POWER
│     POWER       │                    DISTRIBUTION
│  DISTRIBUTION   │                    SUBSYSTEM
└────────┬────────┘
         │        ┌─────────────────┐╮
         └────────┤  HOUSEKEEPING   │
                  │     LOADS       │
                  └─────────────────┘
                                     ╮ USERS
┌─────────────────┐
│                 │
│   USER LOADS    │
│                 │
└─────────────────┘
```
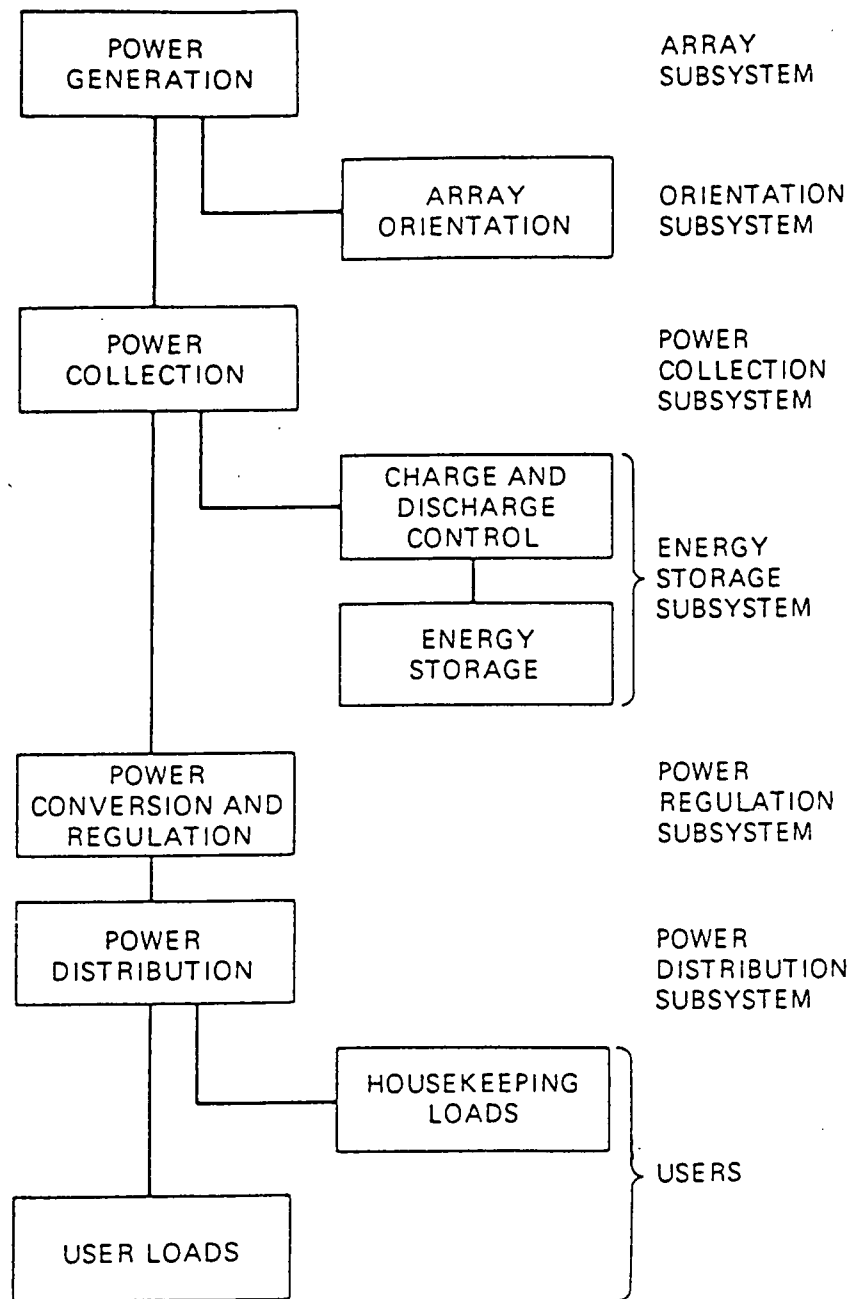
figure 6.1
The EPS.

6   The electrical power subsystem (EPS).

6.1 Introduction.

The electrical power subsystem (EPS) provides power to the satellite during all phases of the mission.

The power source is the photovoltaic conversion process of solar energy in electric power.

The main requirements for the EPS are:
- providing 24 hours of communications
- low mass
- low volume (compact)
- high reliability
- power dump possibility

The main subsystems of the EPS are (see figure 6.1):
- power generation subsystem
- energy storage subsystem
- power regulation subsystem
- power distribution subsystem

6.2 System description.

The EPS consists of the Power Conditioning Unit (PCU), the Power Control and Distribution Unit (PCDU), two Nickel-Hydrogen (NiH2) batteries for power supply during eclipses, the solar array, consisting of two wings of four panels each and the wiring harness (BAPTA).

The PCU and the PCDU contain all the electronics of the EPS.

	TRANSFER ORBIT	SUMMER SOLSTICE	AUTUMNAL EQUINOX	ECLIPSE
PAYLOAD	0	455	455	455
TM/TC	33	33	33	33
PROPULSION	53*	0	0	0
ELECTRIC POWER	18	18	18	18
AOCS	35	110	110	110
THERMAL CONTROL	20	20	20	20
BATTERY CHARGE	0	36	65	0
TOTAL	106	672	701	636
5% DESIGN MARGIN		33	35	
REQUIRED SOLAR ARRAY OUTPUT (10 % MARGIN INCLUDED)		775	809	

*) The 53 W for propulsion are needed for ignition of the apogee motor and control of the valves. This is only for a very short period (± 30 minutes). It is therefore not taken into account for the power need in the transfer orbit. The power will be delivered by the batteries.

figure 6.2
Power budget (W).

6.3   Power allocation.

6.3.1 The power budget.

The power needed during the mission can be divided in two groups:
- for the payload subsystem
- for the housekeeping subsystems

For designing an EPS it is important to know how much power every subsystem of the satellite needs at what time and for what period: the power profile. However it was not possible for the other subsystems to make such a profile of their subsystem due to lack of time, so the power budgets are based on peak power.

When the generated power exceeds the required power a power dump is used. This is a shunt located on the back side of the solar array.

The power budgets from the several subsystems of the satellite form an overall power budget (see figure 6.2).

A design margin of 5% is included and an extra 10% margin for uncertainty in the output of the solar array such as radiation degradation and other power prediction factors.

The power budget is divided in four periods:
- transfer orbit
- summer solstice
- autumnal equinox
- eclipse

This is done because of the different needs per subsystem per period and energy generation.

6.3.2 Transfer orbit.

During the transfer orbit the EPS has to generate 106 W (see figure 6.2). This will be provided partly by the solar array and the rest by the batteries.

For deployment of the solar array, antenna and for propulsion power is needed for a very short period. This will be delivered by the batteries.

During the transfer orbit short eclipse periods occur. In these periods power is delivered by the batteries.

There will be no battery charge during the transfer orbit.

After the transfer orbit the apogee-kick follows.

The solar array will be deployed when the satellite is in geostationary orbit.

6.3.3 Summer solstice.

Summer solstice occurs in the summer and winter season. In these seasons there are no eclipses so the batteries are kept on trickle charge. The solar array provides all the power which is 775 W (see figure 6.2).

6.3.4 Autumnal equinox and eclipse.

Autumnal equinox occurs in autumn and spring. In these seasons there will be a maximum eclipse period of 72 minutes in which the batteries will provide all the power.

After the eclipse the solar array has to deliver all power for communications, housekeeping subsystems and battery charging.

During this period maximum power need occurs so the solar array was designed to meet this power need (809 W).
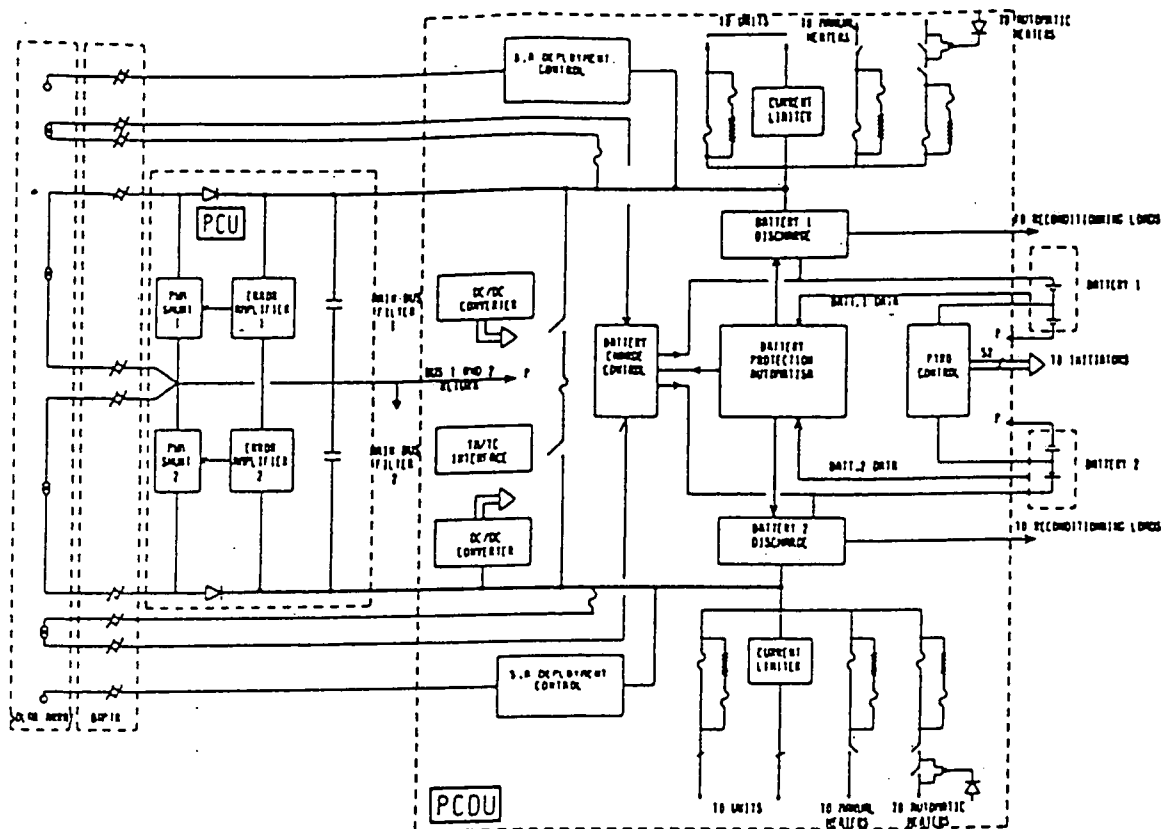
figure 6.3
Spacebus.

Dimensions   height 16 cm
                                  length 34 cm
                                  width   31 cm
Bus voltage   42 V in sunlight
                                  28 V in eclipse
Operating temperature   -10 - +50 degrees Celsius
Lifetime   > 10 years
Reliability   0.9986 (7 years)
Efficiency   96 %
Mass   8.3 kg

figure 6.4
PCU data.

Dimensions   height 26 cm
                                  length 42 cm
                                  width   29 cm
Operating temperature   -10 - +50 degrees Celsius
Lifetime   > 10 years
Reliability   0.9945 (7 years)
Efficiency (discharger)   97 %
Mass   17 kg

figure 6.5
PCDU data.

6.4   Power regulation and distribution.

6.4.1 Requirements.

The requirements for the EPS are low mass, compact subsystem, high reliability, a lifetime of 10 years and a high efficiency.

Due to the fact that the satellite is a piggy-back satellite, the first two requirements are very important.

The power regulation and distribution subsystem has to contain the following elements:
- shunt
- battery discharger
- battery charge controller
- dc/dc converter
- bus

These are just the main elements. Assembling and testing all these elements separately would cost a lot of money and a lot of time. Therefore the SPACEBUS system (see figure 6.3 and reference 6.3) from Aerospatiale has been chosen. This is a very compact, low weight reliable subsystem.

The SPACEBUS system consists of two boxes: Power Conditioning Unit (PCU) and the Power Distribution and Control Unit (PCDU).

6.4.2 The PCU.

The PCU has to condition the voltage of the EPS. It is a small box. For the data of the PCU see figure 6.4.

The PCU has two busses for reasons of redundancy. These busses have a voltage of 42 V (± 0,5 V) in sunlight and 28 V (± 0,5 V) in eclipses. It is a regulated bus subsystem. The voltage regulation is obtained by a shunt in combination with an error amplifier. Subsystem redundancy is achieved by duplicating all the main elements of the PCU and PCDU. The two busses are fully independent. Each bus is supplied from a solar array wing and a battery.

When the eclipse begins the bus voltage slowly drops to 28 V. At the moment the 28 V is reached the batteries are switched on automatically.

At the end of an eclipse the solar array currents recover their normal value and the batteries are switched off automatically.
The batteries are recharged during sunlight operation.

6.4.3 The PCDU.

The PCDU distributes the power to the various subsystems of the satellite. It is also a small box. For the data of the PCDU see figure 6.5. The PCDU contains the dc/dc converter, the battery charge controller, the battery discharger and the pyro controls.
All these elements are redundant.

The wiringharness for the satellite consists of a harness for the powerlines and a harness for the datalines. This is done to prevent possible interference between the signals.

Dimensions	height 60 cm
	length 15 cm
	width 15 cm
Operating temperature	0 - 25 degrees Celsius
Energy density	50 Wh/kg
Discharge voltage	1.1 V
Boost voltage	3.15 V
DOD	70 %
Charge rate	C/25 (equinox)
	C/45 (summer solstice)
Cell capacity	19 Ah
Mass	15 kg

figure 6.6
NiH2 battery data.
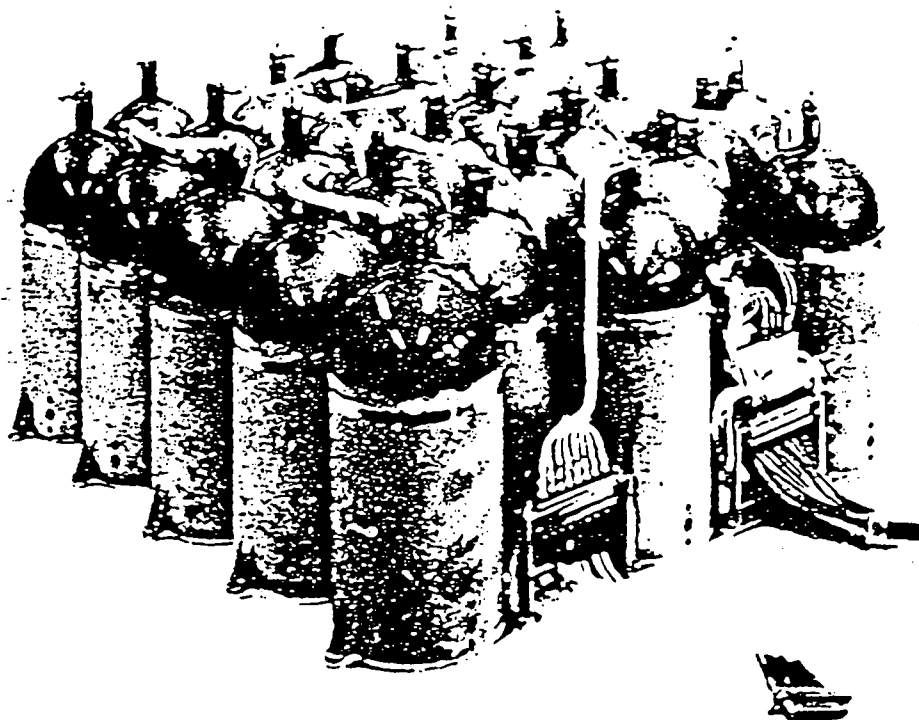
figure 6.7
NiH2 battery.

6.5 Energy storage.

6.5.1 Trade-off.

For power supply during eclipses batteries are needed. The two main possibilities are Nickel-Cadmium (NiCd) and Nickel-Hydrogen (NiH2) batteries. NiH2 batteries are chosen because :
- better energy/mass ratio
- longer lifetime
- higher depth of discharge (DOD)

The requirements are again low weight and a mission lifetime of ten years. NiH2 batteries have a considerable longer lifetime than NiCd batteries. The higher DOD of NiH2 batteries will lead to a lower mass compared to NiCd batteries.

6.5.2 NiH2 batteries calculations.

The data of the NiH2 batteries are given in figure 6.6.
Two batteries are used. Each battery is supplied by a wing of the solar array.
Each battery consists of 28 cells in series (see figure 6.7). It proved to be convenient for the configuration group to split each battery in two parts, each part containing 14 cells.
The battery load is 636 W (see figure 6.2). Each battery is connected to a bus, so the power required by each battery is half the total power: 318 W.
The maximum duration of an eclipse is 72 minutes (1.2 hrs).
The required capacity of a battery cell can be calculated with:

$$C = \frac{P * t}{V_{db} * DOD} \qquad (6.1)$$

where C = cell capacity (Ah)
  P = power (W)
  t = maximum eclipse period (1.2 hrs)
  V_{db}= minimum discharge voltage (28.6 V)
  DOD= depth of discharge

Substituting the values of the parameters above gives:

$$C = \frac{318 * 1.2}{28.6 * 0.7} = 19 \text{ Ah} \qquad (6.2)$$

After the eclipse the batteries are recharged. During charging the maximum allowable battery voltage V_{bc} is 42.9 V.

The main bus voltage is 42 V ($\pm$ 0.5 V). So the lower limit is 41.5 V. The battery charger voltage drop, V_{cd}, is 1.75 V.

The boost voltage required by the charge array, V_{ca}, is given by:

$$V_{ca} = V_{bc} - V_{bus} + V_{cd} = 42.9 - 41.5 + 1.75 = 3.15 \text{ V} \tag{6.3}$$

For charging the batteries a charge rate of C/25 is used for autumnal equinox and C/45 for summer solstice.

The power required for battery charging during autumnal equinox is:

$$P_{charge} = C/25 \text{ * voltage} = 19/25 \text{ * } 42.9 = 32.6 \text{ W} \tag{6.4}$$
(each battery)

The recharging time is:

$$t_{recharge} = \frac{P_{discharge} \text{ * } r_{discharge}}{P_{charge} \text{ * efficiency}} \tag{6.5}$$

where $P_{discharge} = 318$ W

$t_{discharge} = 1.2$ hrs

$P_{charge} = 32.6$ W

efficiency $= 0.9$

substituting these values gives:

$$t_{recharge} = \frac{318 \text{ * } 1.2}{32.6 \text{ * } 0.9} = 13 \text{ hrs} \tag{6.6}$$

The power required for battery charging during summer solstice is:

$$P_{charge} = C/45 \text{ * voltage} = 19/45 \text{ * } 42.9 = 18.1 \text{ W} \tag{6.7}$$
(each battery)

The batteries remain on trickle charge during the remaining time of an eclipse day.

```
Dimensions                diameter 225 mm
                          length   130 mm
Rate of rotation          15 deg/h normal
                          14 deg/min fast
Power consumption         3 W
Lifetime                  10.3 years
Reliability               0.985
Operating temperature     -40  -  +60 degrees Celsius
Mass            .         4 kg
```

figure 6.8
BAPTA data.

```
Dimensions                length 203 mm
                          width  145 mm
                          height 158 mm
Power consumption         7 W
Operating voltage         26 to 42 V
Lifetime                  10.3 years
Reliability               0.985
Operating temperature     -25  -  +60 degrees Celsius
Mass                      2 kg
```

figure 6.9
BAPTA electronics.

```
AEG              10 OHM-cm BSR cell
Dimension        49.8 * 56.2 mm2
Thickness        200 micron
Coverglass       100 micron CMX-100
M contact        Ti Pd Ag
P contact        Al
AR-coating       Ti Ox
I_sc             1063 mA
I_pm             1002 mA
V_oc             545 mV
V_pm             450 mV
Interconnector   35 micron mesh Ag
Cover adhesive   Dow Corning 93.500
```

figure 6.10
Solar cell data.

6.6 Solar array design.

6.6.1 Solar array description.

In this chapter the electrical performances of the solar array are described. The structural performances are described in chapter 7.4.4.

The solar array has to supply power to the satellite for all subsystems. It consists of two wings. Each wing consists of four panels. These panels are covered with solar cells. The solar cells convert energy from the sun into electrical energy by photovoltaic conversion.

The power generated by the solar cells is transferred to the satellite by the Bearing And Power Transfer Assembly (BAPTA).
Each wing has a BAPTA. The BAPTA is controlled by the BAPTA electronics. For the data of the BAPTA and the BAPTA electronics see figures 6.8 and 6.9. The BAPTA has to take care of the transfer of the power from the wings to the satellite. This is done by sliprings. The BAPTA also has to keep the solar array wings normal to the illumination of the sun (suntracking wings). A sun sensor is placed on the inner panel of each wing.

6.6.2 Trade-off between solar cells.

The two main choices for solar cells are Silicium (Si) or Gallium-Arsenide (GaAs) cells. GaAs cells are very expensive, still in development stages and not available in large quantities. Therefore there has been chosen for Si cells.
A wide variety of Si cells is available. A large area cell from AEG has been chosen. The data are pictured in figure 6.10.
A large area cell will lead to a high packing factor which yields to low mass.

The power performance is shown in the I-V curve in figure 6.11. In this figure current versus voltage is pictured. There are three significant points:

- point 1: I_{sc} = short-circuit current
- point 2: V_{oc} = open-circuit voltage
- point 3: I_{pm} and V_{pm} = maximum power point

At the maximum power point the product of I and V is the maximum power that can be reached. Calculations will be made at this point.
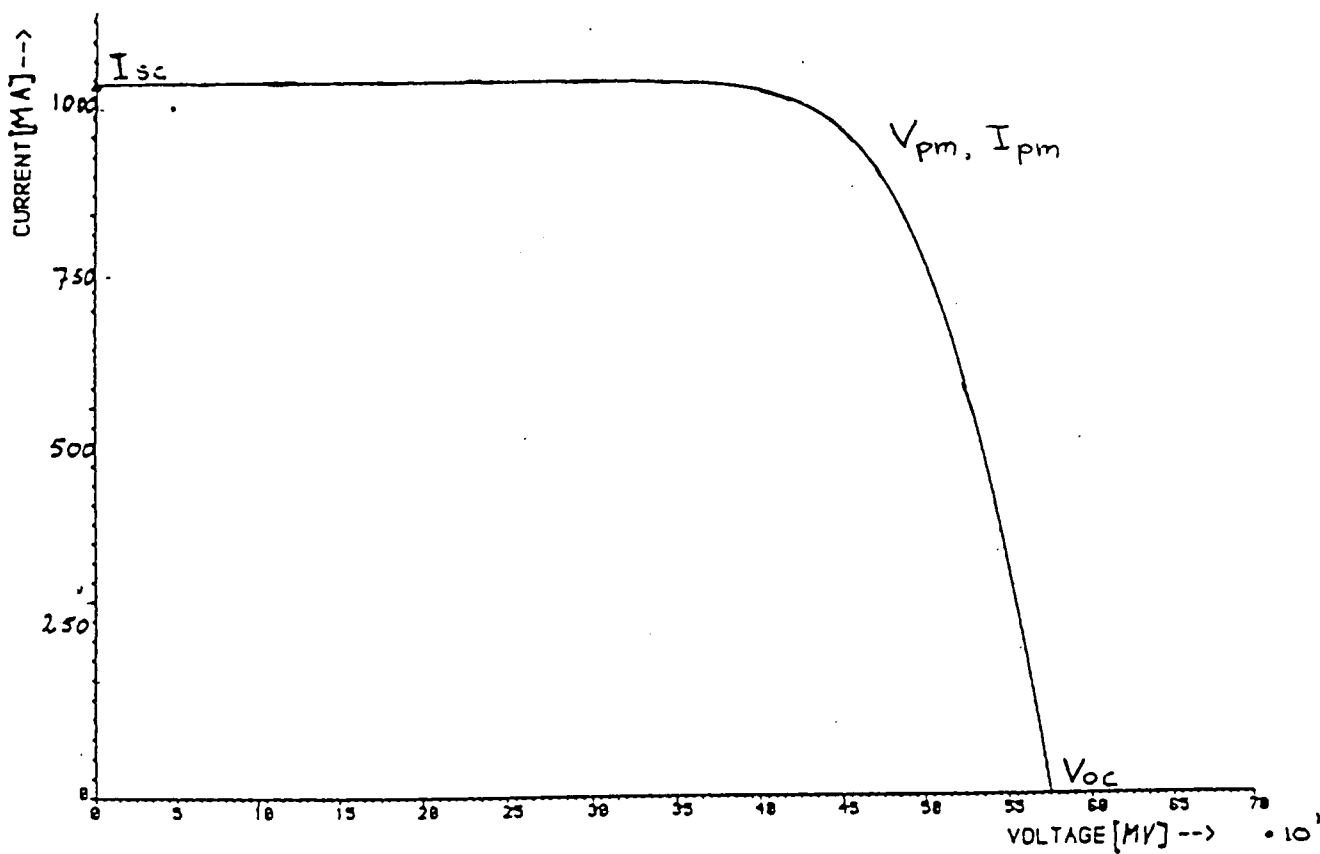
figure 6.11
I-V curve BOL.

	Summer solstice	Autumnal equinox
Sun intensity	0.965	1.000
Angle of incidence	0.917	1.000
UV + micrometeorites	0.965	0.965
Cell mismatch	0.990	0.990
Calibration error	0.980	0.980
Random failures	0.9755	0.9755
Total loss factor	0.808	0.913

figure 6.12
Losses (worst case EOL).

6.6.3 SI solar cell performances.

The solar array has to supply 809 W to the satellite at autumnal equinox. The autumnal equinox is the design driver for the solar array since the greatest amount of power is required at the least favorable conditions of solar cell efficiency and illumination.

The performances of the solar cell in figure 6.10 and 6.11 are at Beginning Of Life (BOL). This means under Air Mass Zero (AMO) conditions. Several effects cause loss factors which result in lower performances during the lifetime.

These losses are pictured in figure 6.12, both for summer solstice and for autumnal equinox.

First there is the variation of solar intensity at summer solstice and autumnal equinox. This is due to variation in the distance between earth and sun.

Secondly there is the influence of the angle of incidence. The power output of a solar cell is maximum when the angle of incidence of the illumination is zero, so normal to the solar cell surface. This is the case at autumnal equinox however not at summer solstice. The maximum angle of incidence at summer solstice is 23.5 degrees. Power decreases proportional to the cosine of the angle of incidence.

Thirdly there is an UV and micrometeorites loss factor. The UV radiation tends to darken the solar cell coverglass and its adhesive during life of the satellite and this reduces the transmission of the light through the cell.

On-station the solar array experiences a continuous micrometeorites bombardment. In time this may result in cells going open circuit because of a fracture or short circuit when a cell becomes electrically connected to the substrate.

Fourthly cell mismatch is a loss factor. This is due to the small differences in performance of cells in a string even though all the cells will be of the same current class.

Fifthly the calibration and measurement error causes a loss in predicted power. This is due to the problems with simulating AMO conditions when performing solar cell calibration. All solar cell performances are given for AMO conditions.
Random failures also result in a loss factor.

The overall loss factor is 0.808 at summer solstice and 0.913 at autumnal equinox.
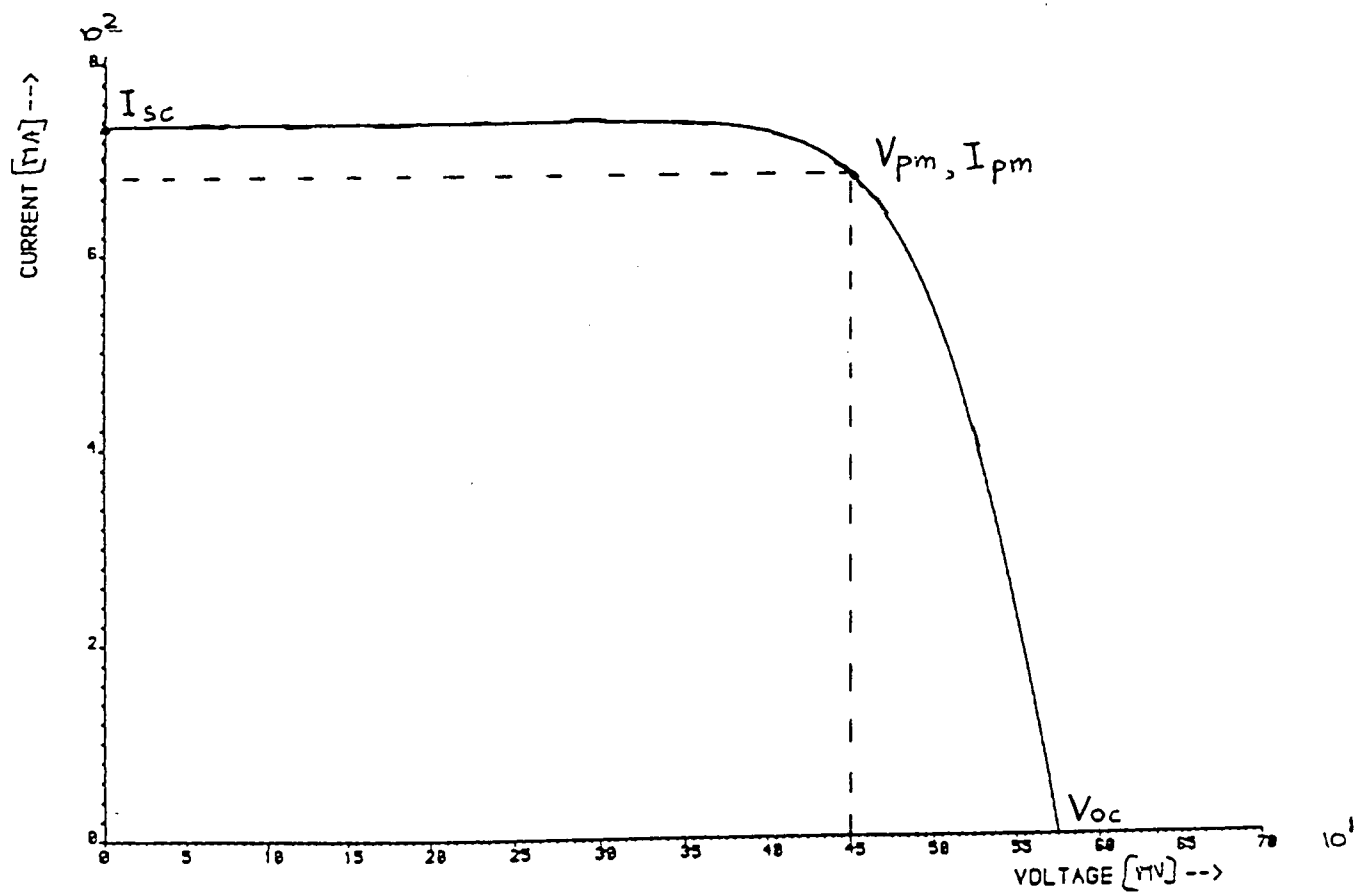
figure 6.13
I-V curve EOL.

6.6.4 Radiation losses.

Another loss factor is caused by degradation of the solar cells due to radiation. Both the voltage and current output are effected.
Radiation damage is caused by: solar flare protons on station, trapped electrons on station and trapped electrons and protons during transfer orbits.
To express the effect of radiation the 1 MeV electron fluence is used as a standard radiation environment.
The radiation dosis for this mission is equivalent to
1.4E+15 e/cm2.

6.6.5 Losses due to temperatures.

A change in temperature of the solar cells causes a change in the performances of the cells. The performances are obtained at AMO conditions: 28 degrees Celsius. At summer solstice the temperature of the cells will be 46 degrees and at autumnal equinox 56 degrees.
An increase in cell temperature causes a slight increase in the current and a significant decrease in the voltage of the cell.

6.6.6 Overall losses.

All loss factors mentioned above cause a decrease in the performances of the solar cells as pictured in figures 6.10 and 6.11. The performances in these figures are at AMO conditions.
A new I-V curve has to be made and the result is pictured in figure 6.13. In this figure current versus voltage is shown at autumnal equinox at End Of Life (EOL), 10 years. With this curve calculations can be made for the solar array.

6.7 Solar array calculations.

6.7.1 Main array.

Figure 6.13 showes the I-V curve at EOL autumnal equinox. At maximum power point the current and voltage are:

$$I_{pm} = 680 \text{ mA (one solar cell)}$$

$$V_{pm} = 450 \text{ mV (one solar cell)}$$

The power required at autumnal equinox is 809 W (see figure 6.2). The solar array consists of two wings. Each wing supplies half the total power required.
On a wing cells are connected to another in series and in parallel.
The number of cells in series can be calculated with:

$$N_s = \frac{\text{bus voltage drop + bus voltage}}{\text{cell voltage}} \tag{6.8}$$

The bus voltage drops are assumed to be 0.9 V in the blocking diode and 0.9 V in the array wiring harness and slipring of the BAPTA, hence 1.8 V.

$$N_s = \frac{42 + 1.8}{0.450} = 98 \tag{6.9}$$

The required current at autumnal equinox of each wing is:

$$I_t = \frac{\text{power}}{\text{bus voltage}} = \frac{809/2}{42} = 9.631 \text{ A} \tag{6.10}$$

The number of cells in parallel for each wing is:

$$N_p = \frac{I_t}{I_{pm}} = \frac{9.631}{0.680} = 15 \tag{6.11}$$

The current per wing is 15 * 0.680 = 10.2 A.
The voltage per wing is 98 * 0.450 - 1.8 = 42.3 V.
The output of the solar array is 2 * 10.2 * 42.3 = 863 W.
The power margin is 863 - 809 = 54 W.

So each wing of the solar array consists of 98 cells in series and 15 cells in parallel. The total amount of cells on the array is 2 * 1470 = 2940 cells.
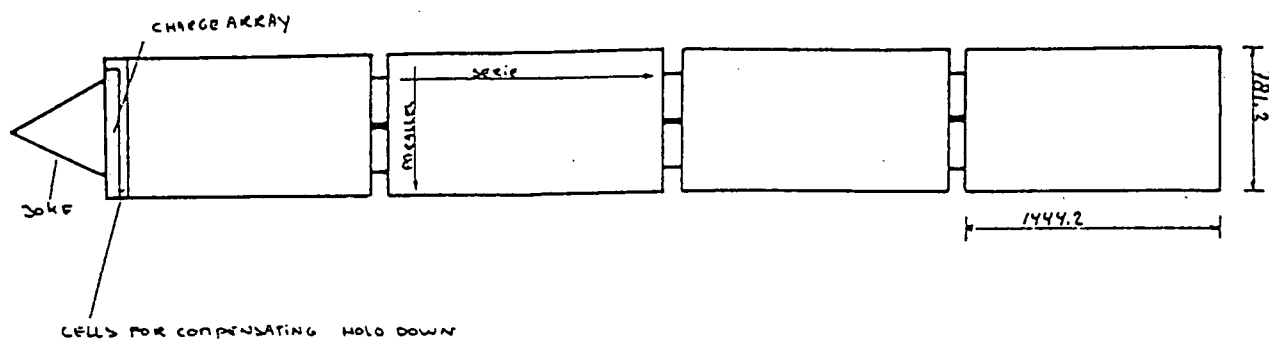
figure 6.14
Solar array design.
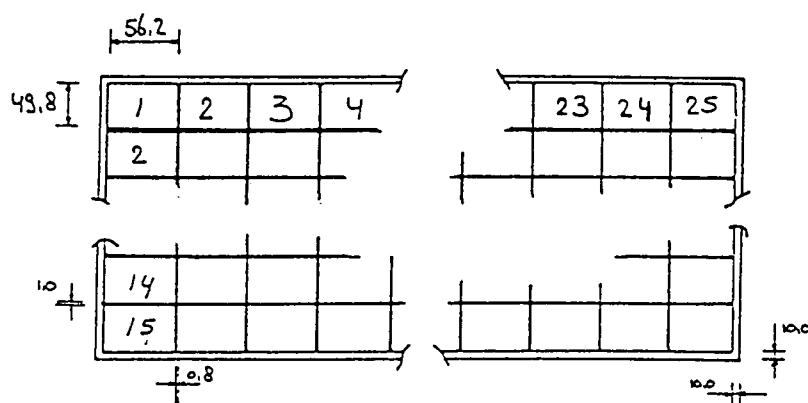
figure 6.15
Solar panel layout.
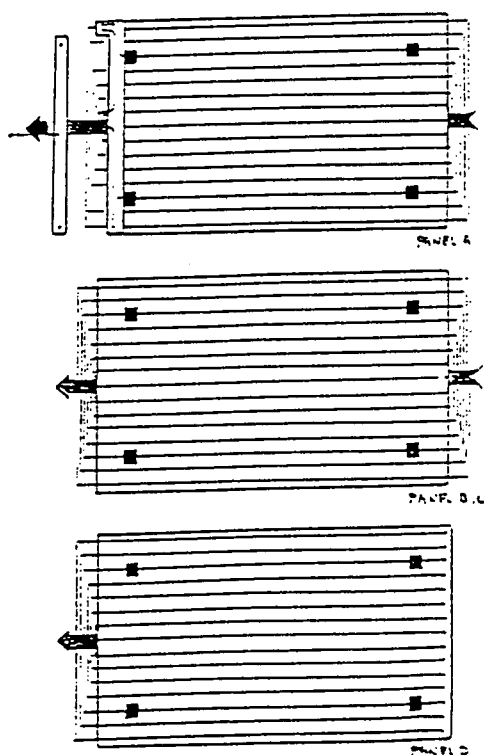
figure 6.16
Wiring schedule.

6.7.2 Charge array.

For charging the batteries a boost voltage of 3.15 V is required.

$$N_s = \frac{3.15}{0.45} = 7 \qquad (6.12)$$

The charge current at summer solstice is 0.422 A (C/45) and 0.76 A (C/25) at autumnal equinox for each battery.

The number of cells in parallel at summer solstice is:

$$N_p = \frac{0.422}{0.680} = 1 \qquad (6.13)$$

The number of cells in parallel at autumnal equinox is:

$$N_p = \frac{0.76}{0.68} = 2 \qquad (6.14)$$

So the charge array for each battery has to consist of 7 cells in series and 2 cells in parallel at autumnal equinox and 7 cells in series and 1 cell in parallel at summer solstice.

6.8   Solar array layout.

One solar array wing consists of four equal panels (see figure 6.14). The cells must be placed in series (98) and in parallel (15). Between the cells in series has to be a gap of 0.8 mm and 1.0 mm for cells in parallel. This is done to meet the thermal expansion requirements for thermal cycling.

One string consists of 25 cells in series and one in parallel. Four strings form a section of 98 (23 + 25 + 25 + 25) cells in series and 1 cell in parallel. Panels B and C are identical (see figure 6.15).

On panel A 13 strings of 23 cells in series and 1 cell in parallel are located plus 2 strings of 29 cells in series and 1 cell in parallel. These last two strings need to be 29 cells in series to compensate the 8 (4 * 2) cells in series missing due to the holddown points (see figure 6.14).

The charge array of 7 cells in series and 2 cells in parallel is also located on panel A (see figure 6.14).

The wiring layout is pictured in figure 6.16. Flat cables are used with interconnectors between the cells.

6.9 Power supply during the transfer orbit.

During the transfer orbit the EPS has to generate 106 W (see figure 6.2). The solar array is in stowed configuration during the transfer orbit. On each side of the satellite is a panel with 375 solar cells.

The performance of the solar cells is calculated at BOL conditions:

I_{pm} = 760 mA

V_{pm} = 480 mV

The output per cell is 760 * 480 = 0.3648 W.

During the transfer orbit the satellite is spinning. The effective illumination factor for a spinning satellite is $1/\pi$.

However this is for a satellite with a body totally covered with solar cells. The body of the Hitch-Hiker is covered for only 50 % so an extra reduction factor of 0.5 has to be taken into account.

The solar array output during the transfer orbit is:

$$750 * 0.3648 * 1/\pi * 0.5 = 43.5 \text{ W} \qquad (6.15)$$

The required output is 106 W. So the batteries have to deliver 62.5 W. The duration of the transfer orbit is 5.5 hrs.

Battery energy is 636 * 1.2 = 763.2 Wh.

During the transfer orbit 62.5 * 5.5 = 343.8 Wh is required.

So a margin of 419.5 Wh is available for ignition of the apogee motor, control of the valves plus antenna and solar array deployment on station.

```
Panel structure    1.0 kg/m2    (9.0 m2)          9.0 kg
Solar cells        1.2 kg/m2    (8.3 m2)          9.9 kg
Wiring harness                                    2.5 kg
Yoke (2)                                          4.0 kg
Panel hinges                                      1.0 kg
Hold-down/release mechanisms (8)                  3.8 kg
Miscellaneous                                     2.0 kg
Harness on yokes                                  2.0 kg

Subtotal                                         34.2 kg

Contingency 6 %                                   2.1 kg

Total                                            36.3 kg
```

figure 6.17
Solar array mass calculation.

```
PCU                                               8.3 kg
PCDU                                             17.0 kg
Batteries (2)                                    30.0 kg
BAPTA (2)                                         8.0 kg
BAPTA electronics (2)                             4.0 kg
Solar array                                      36.3 kg
Harness                                          12.0 kg

Total                                           115.6 kg
```

figure 6.18
EPS mass calculation

6.10 Mass calculation.

The mass calculation of the solar array is pictured in figure 6.17.
The masses of the elements of the EPS are pictured in figure 6.18.
The total mass of the EPS is 115.6 kg.

6.11 Concluding remarks.

Due to lack of information and time it was not possible to design and calculate every detail of the EPS. It was not possible to make a power profile, to do a reliability analysis of the solar array, to design a cable harness, wiring and diodes on the solar array, test, simulation and assembly possibilities.
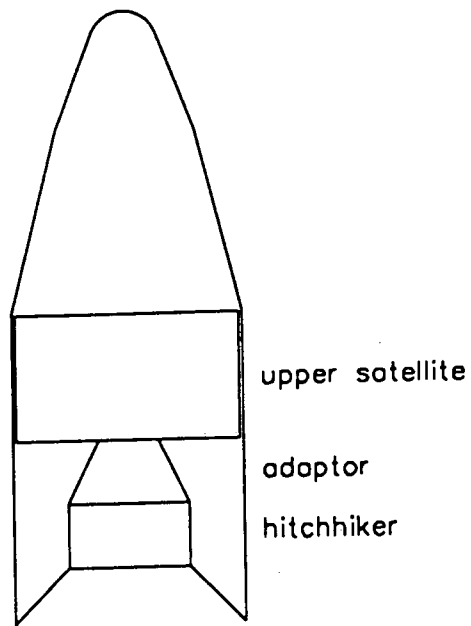
figure 7.1
Launch configuration.
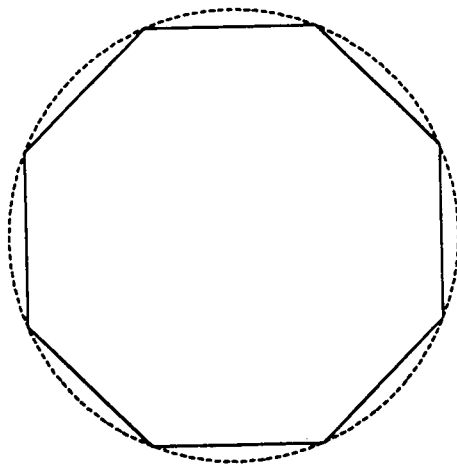
figure 7.2
A non-cylindrical structure.

7   Structure.

7.1   Introduction.

This chapter gives an overview of the design of the Hitch-Hiker structure subsystem. First the structure specification is given, followed by a description of the general layout of the structure system. Next the mayor individual structure subassys are dimensioned. Each of these chapters ends with some remarks and a conclusion. Finally a general conclusion is given.

7.2   Structure requirements.

The structure subsystem shall provide a stable mechanical support for the satellite subsystems under all expected environments over the life of the satellite. The structure shall have, and maintain, the necessary stability through all phases of the mission including the launch phase.

Due to the fact that the Hitchhiker is situated between the lower satellite and the adaptor an extra specification follows; there shall be provided a stable mechanical support for the adaptor and the upper satellite.

7.3   Structural design.

The Hitchhiker is situated between the lower satellite and the adaptor (figure 7.1). That is why a cylinder structure is placed below the adaptor. A cylinder will provide a good support for the adaptor and the upper satellite.

A non-cylindrical structure might simplify the positioning of the equipment (figure 7.2). This is difficult on a curved thin-walled aluminum plate. But this implicates that the forces introduced by the adaptor and the upper satellite are going through eight (or more) single points. This can never provide a better (stiffer) support than the cylinder support so this solution is abandoned.

The cylinder is a part of our satellite structure. This will gain weight compared to the alternative of an entire satellite inside the cylinder. (For a more detailed motivation of this design see the configuration chapter.)

An important consequence of this decision is that the satellite structure is exposed to a much more severe loading. Besides the general specifications, the satellite structure must also satisfy the extra specification mentioned above.

· Besides the cylinder the satellite consists of more important structure sub assys. These are:
    -equipment platforms
    -struts for the engine support
    -separate compartment boxes for the travelling wave tubes (TWT) and electronic power converters (EPC).
First an overview of the general design is given. This is followed by a more detailed design.
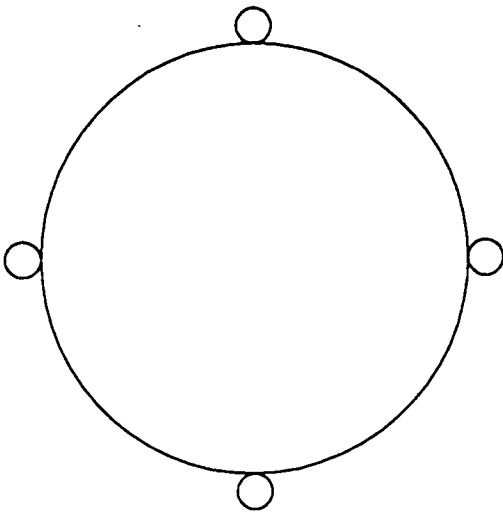
figure 7.3
More engines on the outside of the cylinder.

figure 7.4
Force induced by the nozzle on the cylinder wall.
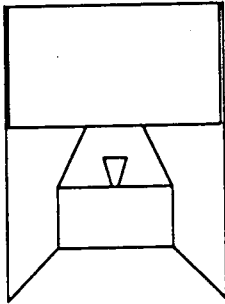
figure 7.5
The nozzle penetrates the adaptor.
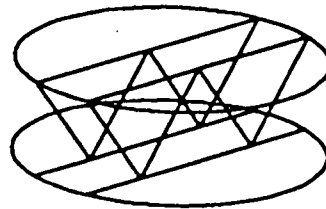
figure 7.6
The tank support structure.
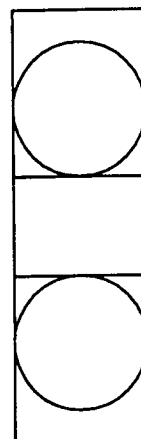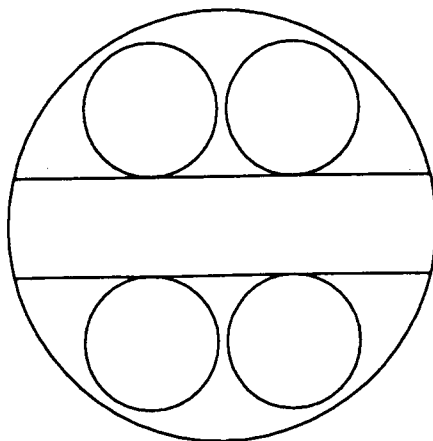
figure 7.7
The tank support structure with tanks.
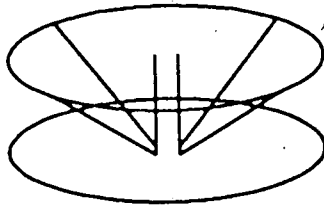
figure 7.8
Struts to support the platforms and the apogee engine.
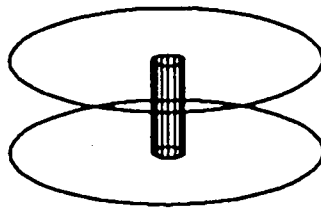
figure 7.9
A cylinder to support the platforms and the apogee engine.
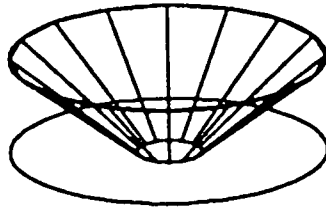
figure 7.10
A cone to support the apogee engine.
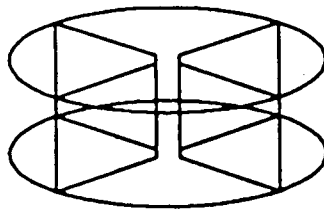
figure 7.11
Four plates to support the platforms and the apogee engine.
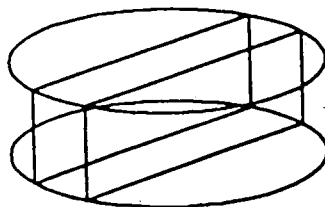
figure 7.12
Two vertical platforms instead of horizontal platforms.
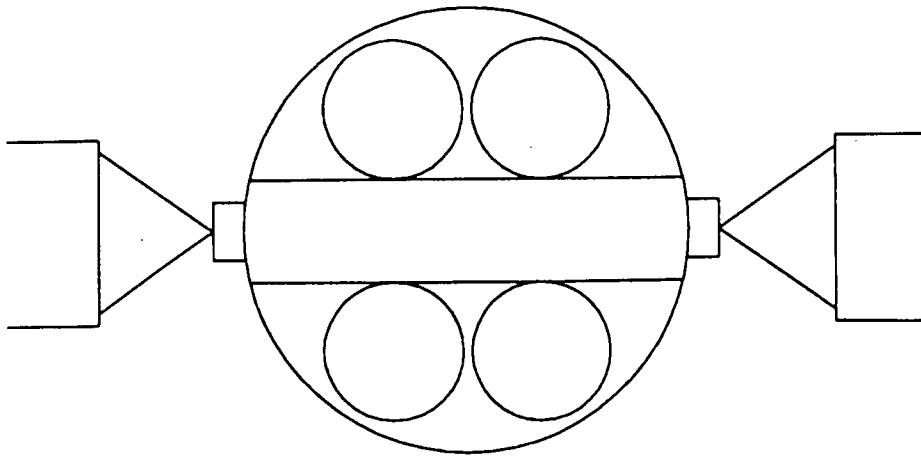
figure 7.13
The Hitch-Hiker without the extra support structure.
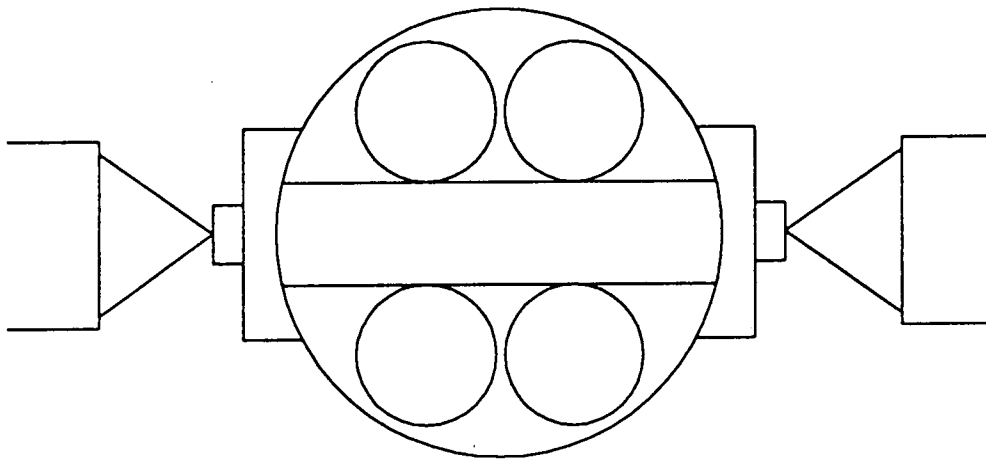
figure 7.14
The Hitch-Hiker with the extra support structure.
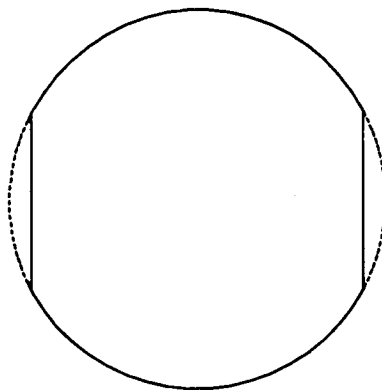
figure 7.15
A second alternative to create a plane instead of the ESS.

The position of the engine(s) is of great importance. From structural point of view it is a good solution to have more engines (two to four) placed on the outside wall of the cylinder (figure 7.3). These engines won't have to be in the direction of the cylinder axis (although that is preferred). In this way the forces are in the direction of the cylinder axis, something for which the cylinder is already designed (figure 7.4). One engine in the middle gives difficulties in providing a sufficient stiff support during launch and apogee burning.

For different reasons (see chapter configuration) one engine is chosen by the propulsion subsystem. The nozzle and throat of the apogee engine are placed outside the satellite (figure 7.5). The tank support structure is designed as follows (figure 7.6). To provide a sufficient support in the directions perpendicular to the cylinder axis a platform (honeycomb structure) is sufficient.

The great diameter of these platforms requires a very thick structure to obtain the required frequency. The tanks are located between the two platforms (figure 7.7). The tank support structure provides also a support for the two platforms by which a higher frequency is obtained so in this configuration no other structures are needed to provide the platform stiffness.

Some other possibilities to provide this stiff support for the platforms (especially the one with the apogee engine) were considered:

-struts (figure 7.8)

    The struts connect the center of the lower platform with the edge of the cylinder wall. So a higher resonance frequency of the platform is obtained and the apogee engine has a good support. To support the upper platform the two platforms are connected with each other by struts. The motivation not to choose this option is that the four tanks are not supported in this configuration.

-central cylinder (figure 7.9)

    This solution differs from the previous one in that the connection between the two platforms is achieved by a cylinder with a diameter of approximately 200mm. Beside the fact that there is still no support for the tanks there is another reason not to choose this option. That is the fact that the apogee engine is enclosed in this cylinder which will give a very good possibility to radiate unwanted energy into the satellite.

-a cone (figure 7.10)

    The advantage of such a structure is the high stiffness. But the shape is such that it takes too much room. Besides that some very big cut-out's have to be made in the cone for the apogee tanks.

-vertical platforms (figure 7.11):

    The advantage is again the high stiffness of such a support but these platforms take too much space, although some equipment can be attached to these platforms.

Perhaps vertical panels can be used instead of the horizontal panels (figure 7.12). In this way there are less problems with the "eardrum" effect. Another advantage is that the platforms are mainly loaded parallel to the platform itself because of the location of the equipment e.g. the tanks. Nevertheless also in this configuration the platforms aren't very stiff. But there are some other problems as well. When it isn't allowed to attach heavy equipment to the thin cylinder wall, these two platforms won't provide enough surface for the equipment because the area used for equipment is only 30% (ref. 7.1). Further some connections have to be made between the three compartments which damages the platform stiffness. And still the engine has to be supported in the middle of the satellite. Mainly because of these reasons this variation is abandoned (see chapter configuration for details).
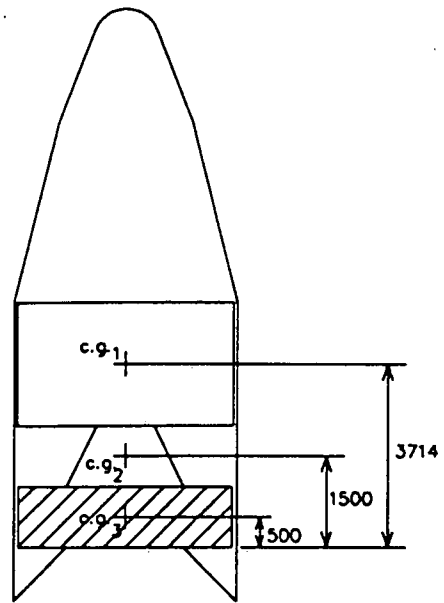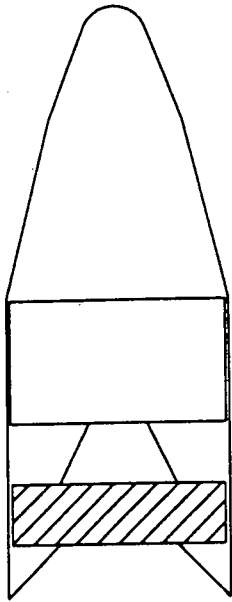
figure 7.16
The available area in the Ariane IV.

figure 7.18
The centers of gravity in launch configuration.

$c.g._1$

$c.g._2$

$c.g._3$

3714

1500

500
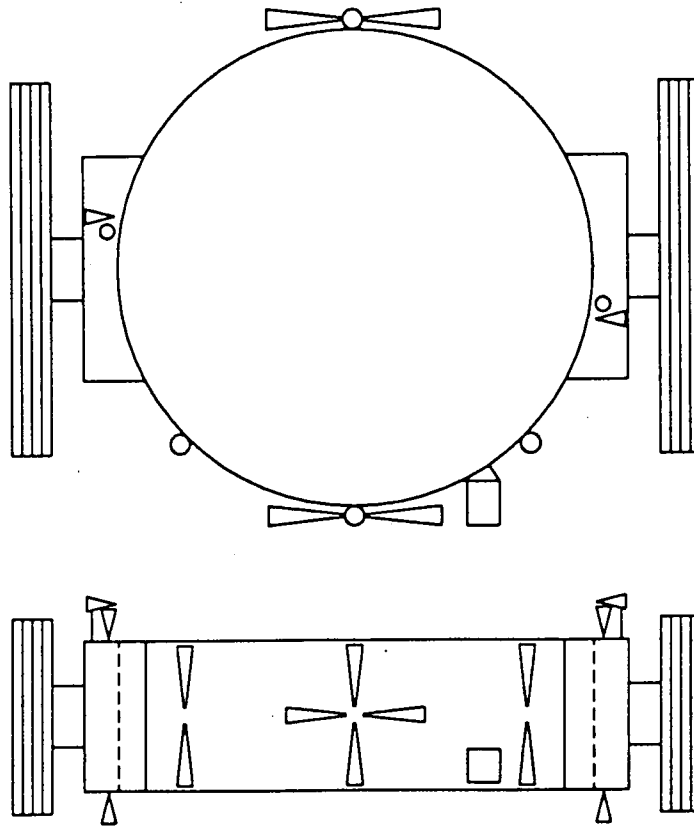
figure 7.17
The equipment outside the cylinder.
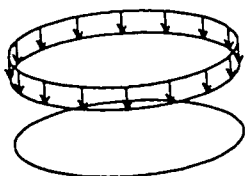
figure 7.19
The longitudinal load.
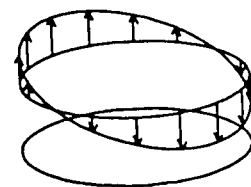
figure 7.20
The lateral load.

Due to a requirement of thermal control an extra structural part is designed. There has to be a plane out of the sunlight to be able to radiate the dissipated heat. This plane has to be perpendicular to the solar arrays because this plane receives the least sun radiation.

Since the satellite hasn't got such a plane (figure 7.13), this plane is created. An extra support structure (ESS) is placed outside the satellite (figure 7.14). From structural point of view this isn't a nice solution:

-The BAPTA and solar arrays are placed on a greater distance from the center of the cylinder. This creates a bigger momentum force on the cylinder wall.

-The ESS is attached to the cylinder,something which enlarges the structural weight of the cylinder

Nevertheless this is a severe requirement so it must be handled. For a moment the design of figure 7.15 is considered. The cylinder is partly flattened to create the necessary plane. But this reduces the stiffness of the cylinder a lot and the room inside the satellite is less, so this solution isn't a good alternative.

7.4 Structural parts, including materials.

7.4.1 Introduction.

In this chapter, the structural subassys are analyzed. In this analysis only the launch mode is considered because usually, this gives the critical loadings. The handling-, transport- and testloads are not taken into account. This takes too much time for this project.

7.4.2 The cylinder.

The cylinder structure is made of thin aluminum plate material because of the low mass per volume of aluminum and is stiffened on the outside. An alternative design is a honeycomb structure but since we didn't have enough time to analyze both of the options the simplest design is chosen. This certainly counts for a cylinder with cutouts and attachment points. So the alternative of the honeycomb cylinder structure is not yet studied.

It is permitted to use the space around the satellite as well for equipment (figure 7.16). This is done for the solar arrays, thrusters and some sensors (figure 7.17). Thus some connections are made through the cylinder wall. This has to be taken into account because the strength and stiffness of the cylinder reduces due to these cut outs.

A rough calculation follows:

Loads

The main static loads are the flight limit loads and the low sinusoidal frequency vibration acceptance levels. To ascertain these loads acting on the cylinder tables 4.2 and 4.6.1.2 of reference 7.2 are used (see table 7.1 and 7.2). From this it shows:

- the maximum longitudinal load a_{max} = 7g

- the maximum lateral load a_{max} = 1g

These two loads are assumed to act at the center of gravity of the spacecraft. When these loads are combined they give the so called "worst case" at the bottom of the cylinder. In the analysis a margin is included for cutouts, imperfections and the error in the methods used.

flight event	loads	longitudinal	lateral axis
max. dynamic pressure	QSL	-3.0	±1.5
	S+D	-2±1.0 (5 to 100Hz)	±0.2 ±0.4 (5 to 100Hz)
Before thrust termination	QSL	-7.0	±1.0
	S+D	-4.5±1.0 (5 to 100Hz)	±0.8 (5 to 18Hz) ±0.6 (18 to 100Hz)
During thrust tai-off	QSL	+2.5	±1.0
	S+D	±1.0 (5 to 100Hz)	±0.8 (5 to 18Hz) ±0.6 (18 to 100Hz)

Table 7.1 : maximum longitudinal loads

	Freqeuency range (Hz)	Qualification levels (O-peak) (recommended)	Acceptance levels (O-peak)
longitudinal	5-6	8.6 mm	1 g
	6-100	1.25 g	1 g
lateral	5-18	1 g	0.8 g
	18-100	0.8 g	0.6 g
Sweep rate		2 oct./min	4 oct./min

Table 7.2 : maximum lateral loads
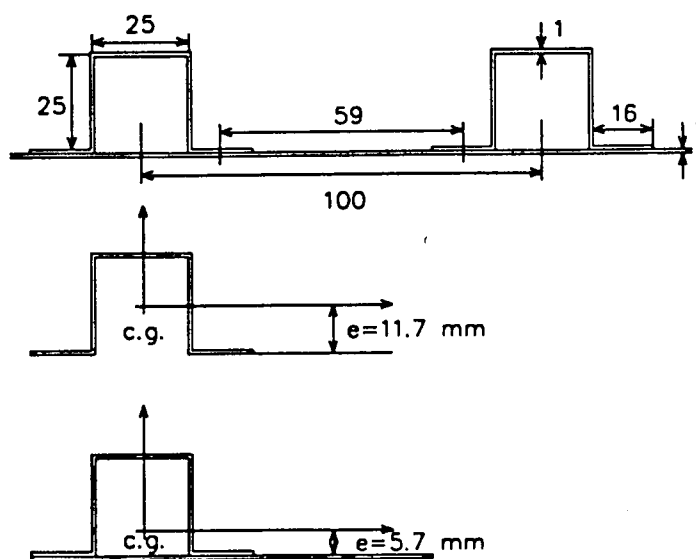
figure 7.21
The design of the stiffeners.

Running load

The running load is the force per running millimeter along the wall of the cylinder. To obtain this running load the next data are used in figure 7.18 (see chapter launch configuration):

$m_1 = 822$ kg $d_1 = 3714$ mm
$m_2 = 48$ kg (ref. 7.2) $d_2 = 1500$ mm
$m_3 = 800$ kg $d_3 = 500$ mm

-longitudinal load (figure 7.19)

$$\sigma = F/A = (m_{tot} a_{max})/(2\pi R t) \tag{7.1}$$

So $\sigma * t = (1670*7*9.81)/(2*\pi*960) = 19.0$ N/mm

Where: F = load on cylinder
       A = cross section area of the cylinder
       m_{tot} = $m_1 + m_2 + m_3$: total mass
       R = radius of the cylinder = 960 mm
       t = wall thickness of the cylinder

A uniform load is assumed to act all over the area of the cylinder.

-lateral load (figure 7.20)

$$M = Q(m_1 d_1 + m_2 d_2 + m_3 d_3) = 10(822*3.71 + 48*1.5 + 800*0.5) = 35250 \text{ kgm} \tag{7.2}$$

Where: M = moment acting on the cylinder at the clamped
           interface
       Q = amplification factor

$$Q = 1/(2(c/c_c)) = 1/(2\xi) \tag{7.3}$$

         with $\xi = 0.05$ (ref. 7.1) this yields Q=10

Since $\sigma = M/W$ with $W = I/R = (\pi R^3 t)/R$ this yields $\sigma t = M/(\pi R^2)$ (7.4)

So $\sigma t = 35.25*10^6 *9.81/(\pi*960^2) = 119.4$ N/mm

Where: W = section modulus
       I = moment of inertia

Combining these two loads yields $\sigma t = 19.0 + 119.4 \approx 140$ N/mm. For the design running load a safety factor and a design factor have to be taken into account:

$$(\sigma t)_{max} = (\sigma t)_{tot} * \text{safety factor} * \text{design factor} \tag{7.5}$$

Where (ref. 7.1) : -safety factor is 1.25
                -design factor is 1.2

This yields: $(\sigma t)_{max} = 140*1.25*1.2 = 210$ N/mm. This is the running load which is the basis of the analysis that follows. It must be noted that this load is acting only along one generatrix. However in the analysis it is assumed that the load is uniform distributed over the full cylindrical cross section.

Dimension choice

The dimensions chosen for this cylinder are given in figure 7.21. The thickness of the cylinder wall is 1 mm. The hat stiffener is 25 mm high, has a width of 25 mm and a thickness of 1 mm. The contact surface of the hat stiffener is 16 mm on each side. The pitch between the stiffeners is 100 mm. The equivalent thickness due to the area is approximately 2 mm. This choice is based on reference one. In this case the maximum occurring stress is 105 N/mm².

The momentum of inertia per pitch for this design is given in figure 7.21, together with the center of gravity.

Dimension analysis

The occurring running load is much too high for a homogeneous unstiffened thinwalled cylinder. So stiffeners are attached on the outside of the cylinder wall, because the stiffeners have more effect when these are placed on the outside of the cylinder. Besides that, all room inside the satellite is needed to place the equipment.

Two different configurations are analyzed. The first without an extra ring shaped frame, the second with this frame. In both cases the next four buckling criteria are considered:

1. classical buckling
2. panel buckling
3. local buckling
4. crippling (of the stiffeners)

1.classical buckling

To analyze the cylinder on classical buckling a homogeneous wall thickness is assumed having the same moment of inertia as a section with one stiffener.This yields:

$$I = b(t_{eq})^3/12 \quad \text{from which follows} \tag{7.6}$$

$$t_{eq} = \sqrt[3]{(12*I/b)} = \sqrt[3]{(12*20600/100)} = 13.5 \text{ mm}$$

To obtain the maximum allowed buckling stress figure C.8.8a from reference 7.3 is used which gives $\sigma_{c_{cr}}/E$ for values of R/t and L/R with a 99% probability and a confidence level of 95%.

With values of $R/t_{eq}=71.1$ and L/R=0.68 this gives a $\sigma_{c_{cr}}$ of 504 N/mm².

Since the running load induces a stress of 105 N/mm² the cylinder will not fail due to classical buckling. The margin of safety is here M.S.=504/105-1=3.8.

2.Panel buckling

For panel buckling the next equation is used (ref. 7.3):

$$F=k_{pb}\pi^2 EI/l^2 \hspace{4cm} (7.7)$$

Where: F = the maximum panel buckling load

k_{pb} = panel buckling factor = 0.7 (taken into account

the local buckling and yielding, see ref. 7.1)

E = modulus of elasticity = 70000 N/mm²

I = area momentum of inertia = 20600 mm⁴

l = length of the panel = 650 mm

Using equation (7.7) with the values mentioned above yields:

$$F=0.7*\pi^2 *70000*20600/650^2 =23580 \text{ N (per pitch)}$$

With $\sigma=F/A$ and A=207 mm² this results in a maximum panel buckling stress of 114 N/mm². In this case the margin of safety is 114/105-1=0.08 so the cylinder doesn't fail due to panel buckling.

3.Local buckling

For local buckling the next equation is used (ref. 7.3):

$$\sigma=(k_{lb}\pi^2 E)/(12(1-\nu^2))(t/b)^2 \hspace{3cm} (7.8)$$

Where: k_{lb} = local buckling factor

ν = Poisson's ratio= 0.3

t = thickness of the plate

b = width of the plate

Figure C.5.2 (ref. 7.3) gives the value of k_{lb}=4.0. This gives

$$(k_{lb}\pi^2)/(12(1-\nu^2)=4\pi^2/(12(1-(0.3)^2)=3.6$$

so $\sigma=3.6E(t/b)^2$ \hspace{5cm} (7.9)

For the stiffener this yields $\sigma=3.6*70000(1/25)^2 =403$ N/mm²
For the cylinder wall this yields $\sigma=3.6*70000(1/59)^2 =72$ N/mm²

Wether this stress is accepted depends on the criteria. When no local buckling is accepted before the limit load the value of 72 N/mm² is too low and the pitch between the hat stiffeners must be decreased. When the pitch is 47mm the local buckling load is 114 N/mm². This gives a margin of safety of M.S.= 114/105-1= 0.09.

However, when the local buckling is allowed before limit load, the design is accepted because the structure can withstand a stress that is approximately two times higher than the local buckling stress, in this case approximately 140 N/mm². The pitch can even be increased a bit.
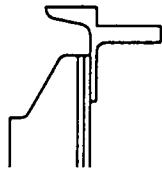
·figure 7.22
The design of the edge of the cylinder.
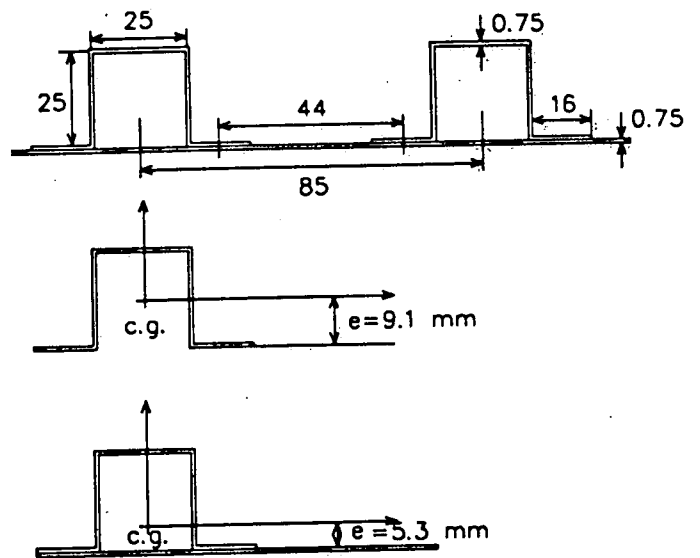
figure 7.23
The modufied design of the stiffeners.

- cylinder: t=1 mm
- hat stiffeners: t=1 mm
- pitch: p=100 mm
- cross sectional area per pitch: A= 205 mm²
- momentum of inertia: I_{cg}= 20600 mm⁴

- occurring stress: σ_{occ}= 105 N/mm²

	σ_{all}	M.S.
1	504	3.8
2	114	0.08
3	140	0.033
4	1138	--

cylinder:	m= 10.6 kg
stiffeners:	m= 11.2 kg
extra:	m= 2 kg
	23.8 kg

Table 7.3 : Design of the cylinder (alternative 1).

- cylinder: t= 1 mm
- hat stiffeners: t= 0.75 mm
- pitch: p= 85 mm
- cross sectional area per pitch: A= 164 mm²
- momentum of inertia: I_{cg}= 9650 mm⁴

- occurring stress: σ_{occ}= 120 N/mm²

	σ_{all}	M.S.
1	364	2.0
2	270	1.25
3	124	0.033
4	881	--

cylinder:	m= 10.6 kg
stiffeners:	m= 9.8 kg
extra:	m= 2.0 kg
frame:	m= 1.2 kg
	23.6 kg

Table 7.4 :Design of cylinder (alternative 2).

4. crippling

Crippling occurs after local buckling and the construction fails like a harmonica. The expression used to calculate the crippling stress is the Gerard Equation (p.C.7.2 and fig. 7.C.7.22, ref. 7.3):

$$\sigma_{cs}/\sigma_{cy}=3.2(gt^2/A\sqrt{(E/\sigma_{cy})})^{0.75} \tag{7.10}$$

Where σ_{cs} = crippling stress

σ_{cy} = compression yield stress = 300 N/mm² (ref. 7.1)

g = number of which compose the composite section, plus the number of cuts necessary to divide the section into a series of flanges =17 (ref. 7.3, fig. C.7.22).

t = thickness of the used sheet

A = cross section area

With these values equation (7.10) yields:

$$\sigma_{cs}=300*3.2(17*1^2/207\sqrt{(70000/300)})^{0.75}=1138 \text{ N/mm}^2$$

This stress goes far beyond the elastic allowable stress. Actually, a plastic calculation must be made but since the occurring stress never increases to this level, this is not done. Also, it has no use to calculate the margin of safety in this case because the answer is not reliable.

mass of the cylinder.

The parts of the cylinder give a certain mass for the total cylinder.

cylinder: m= 10.6 kg
stiffeners: m= 11.2 kg
               21.8 kg

This is of course no exact mass. There must be a way to attach the platforms and the separation mechanisms to the cylinder. A design of this is given in figure 7.22. This increases the weight of the cylinder. Besides that some extra weight for paint and nails must be taken into account. The design of figure 7.22 is not checked, so the extra mass is assumed to be 2 kg. This gives an estimated total mass of 23.8 kg for the cylinder.

remarks

-The result of the analysis is given in table 7.3.
-When local buckling is not allowed before limit load , the cylinder is not sufficiently dimensioned. The pitch has to be decreased.
-The calculations are very rough, so this analysis can only function as a guideline. For example, no cut-outs are taken into account. In any case, a reasonable mass estimation is made.
-To get a more optimal design, more different alternatives must be compared and a finite element program must be used to obtain more reliable results.
-When the thickness of the hat stiffeners is reduced to 0.75mm and the pitch is reduced to 85mm the allowable stresses change (figure 7.23). In this case also a frame is used to prevent local buckling (see below). For this alternative, the allowable stresses and the margins of safety are given in table 7.4.
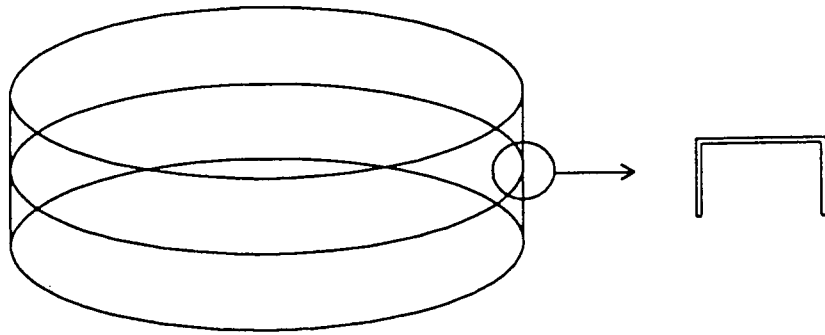
figure 7.24
The frame in the cylinder.
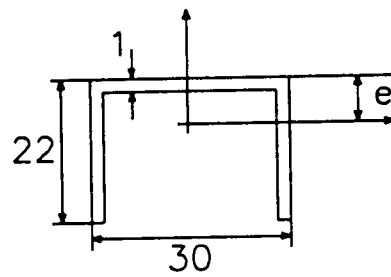
figure 7.25
The design of the frame.
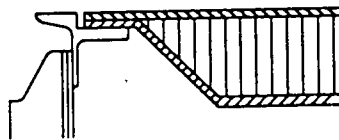
figure 7.26
Connection of the platforms to the cylinder wall.

-In the area of vibrations the requirements are given in chapter 3 of reference 7.1. No study to meet these requirements is done due to a lack of time. To get some idea of the resonance frequencies, reference 7.4 can be used.

the frame

The frame is made of aluminum and is placed in the middle of the height of the satellite (figure 7.24). To get an idea of the dimension of the frame, the next calculation is made with the expression of Shanley (ref. 7.1):

$$I_r = N_{cr} R^4 / (1273*1E) \tag{7.11}$$

Where N_{cr} = desired classical buckling load (in N/mm)

      1 = distance between the frames= 650 mm

The desired classical buckling load is the load that satisfies the calculated running load which is 210 N/mm² .The radius of the cylinder is 960 mm. Using equation (7.11) this yields:

$$I_r = 210*960^4 / (1273*650*70000) = 3079 \text{ mm}^4$$

The frame showed in figure 7.25 has an $I_r = 3664$ mm⁴ so it is used in the cylinder. The mass of this frame is approximately 1.15 kg. The margin of safety for this frame is calculated below:

$$\sigma_{all} = 3664*650*70000*1273/960^4 = 250 \text{ N/mm}^2$$

So the M.S. is $\sigma_{occ}/\sigma_{all} - 1 = 250/210 - 1 = 0.19$

conclusions.

Comparing tables 7.3 and 7.4 it shows that both alternatives have approximately the same mass. However, in the first design, local buckling is allowed. When this is not the case, the pitch must be reduced to 85mm and this increases the weight of this alternative with 1.8 kg.

The second alternative is already designed in such a way that no local buckling appears before the limit load. Since this design is less heavy, it is used in the Hitch-Hiker.

7.4.3 The platforms.

The platforms are made of a aluminum honeycomb structure with CFRP face sheets which provides a high resonance frequency. The resonance frequency of the platforms has to be higher then 80Hz to avoid coupling with resonance frequencies of reaction wheels or other parts of the satellite (ref. 7.1). To meet this requirement the exact dimensions are calculated. The platforms are supported by the tank support structure. This increases the resonance frequency so the platform thickness can be reduced.

In figure 7.26 the assembling of the platforms to the cylinder is shown This is a simply supported connection. The best solution is a clamped support to gain a high frequency. But this is too expensive and because of the great diameter of the platforms (1920 mm) it is not certain that it is possible to create a rigid support.
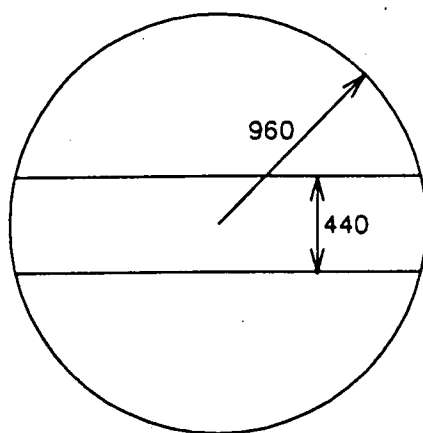
figure 7.27
The platform support.
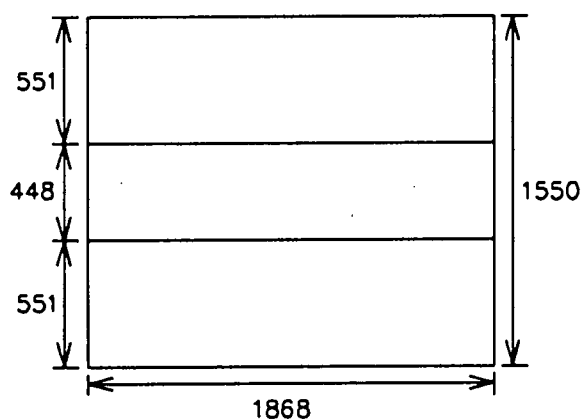
figure 7.28
The model of the platform support.

t_f	t_c	ρ_f	EI	ρ_c	ρ_{tot1}	ρ_{tot2}	(D/ρ_1)	(D/ρ_2)
mm	mm	kg/m²	Nm	kg/m²	kg/m²	kg/m²	m⁴/s²	m⁴/s²
1	15	3.2	6181	0.525	26.23	56.53	236	109
	20		10989	0.70	26.40	56.70	416	194
	25		17170	0.875	26.58	56.88	646	302
	30		24725	1.05	26.75	57.05	924	433
	40		43956	1.40	27.10	57.40	1622	766
	50		68681	1.75	27.45	57.75	2502	1189
	80		175824	2.80	28.50	58.80	6196	2990
2	20	6.4	21978	0.70	29.60	59.90	743	367
	30		49450	1.05	29.95	60.25	1651	821
	40		87912	1.40	30.30	60.60	2901	1451
	50		137362	1.75	30.65	60.95	4482	2254
	70		269231	2.45	31.35	61.65	8588	4367
	80		351648	2.80	31.70	62.00	11093	5672

Table 7.5 : Values of t_c, t_f, D, ρ_f, ρ_c, ρ_{tot1}, ρ_{tot2}, (D/ρ_{tot1}) and (D/ρ_{tot2}) for the platforms.

In figure 7.27 the platform support is shown. It is assumed that the platform is simply supported at the edges and at the tank support structure.

The requirement for the platforms is that the lowest resonance frequency must be larger than 80 Hz. To get an idea of the resonance frequency of the platform a model is used. The platform is split in three parts, each having a rectangular shape (figure 7.28). The areas of the three parts is the same as the areas of the three parts in figure 7.27. The biggest part has the dimensions of 1868x551 mm. The smallest part has the dimensions of 1868x448 mm. To make some calculations it is assumed that the equipment is spread smoothly over the surface and that the platforms are no part of the load path of the tanks. The next values are assumed to calculate the mass:

-CFRP face sheets ρ_{plate}= 1600 kg/m³

-aluminum core ρ_{core} = 35 kg/m³

-adhesive ρ_{adh} = 0.1 kg/m² (per area)

For the calculation reference 7.6 is used. For a simply supported plate the lowest resonance frequency is:

$$\omega = \sqrt{(D/\rho)((\pi/a)^2 + (\pi/b)^2)} \tag{7.12}$$

Where ω = the lowest resonance frequency
 D = stiffness of the platform
 ρ = mass per area of the platform
 a = width of the platform
 b = length of the platform

The resonance frequency now only depends on the stiffness and the mass per area of the platform. In table 7.5 these values are given for different values of the thickness of the face sheets and the thickness of the aluminum core. The value of E for the CFRP sheets is 50000 N/mm² and Poisson's ratio v=0.3.

The smallest surface has a maximum mass of equipment of 44 kg. This is 52.6 kg/m². The bigger surface has a maximum mass of equipment of 23 kg. This is 22.3 kg/m². In table 7.5 the total mass per area is given for the bigger surface (subscribt nr.1) and for the smaller surface (subscribt nr.2).

For the bigger surface the desired D/ρ is calculated with expression (7.12):

$$D/\rho = (\omega/((\pi/a)^2 + (\pi/b)))^2 = (80*2\pi/((\pi/0.551)^2 + (\pi/1.868)^2)))^2 = 202.3 \ m^4/s^2$$

From table 7.5 it shows that a thickness of the core of 15 mm and a thickness of the face sheets of 1 mm give a sufficient D/ρ. With expression (7.12) the lowest resonance frequency is calculated:

$$F(1) = \sqrt{(236)((\pi/0.551)^2 + (\pi/1.868)^2))}/(2*\pi) = 86 \ Hz$$

For the smaller surface the desired D/ρ is calculated with expression (7.12):

$$D/\rho = (\omega/((\pi/a)^2 + (\pi/b)))^2 = (80*2\pi/((\pi/0.488)^2 + (\pi/1.868)^2)))^2 = 128.9 \ m^4/s^2$$

From table 7.5 it shows that a thickness of the core of 15 mm and a thickness of the face sheets of 1 mm give a sufficient D/ρ. With expression (7.12) the lowest resonance frequency is calculated:

$$F(1) = \sqrt{(194)((\pi/0.488)^2 + (\pi/1.868)^2))}/(2*\pi) = 98 \ Hz$$
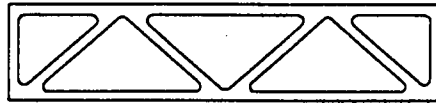
figure 7.29
Design of the tank support structure.
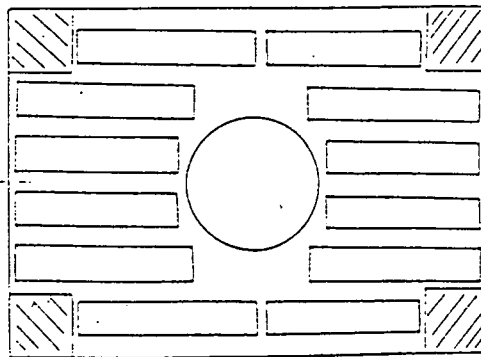
figure 7.30
The extra support structure.

remarks
-The severest loaded platform is the smaller one so these dimensions have
    to be taken for the whole platform of figure 7.28. Both platforms have
the same dimensions because this reduces the cost price. This results in   a
mass per platform of 11.9 kg.
-This mass is too high (ref. 7.1). This is caused by the choice of a wrong
    model. The assumption that the platform consists of three individual
parts is not trustworthy. In this way there is no interference between   the
three parts.
    The lowest resonance frequency of the platform with t_c = 15 mm and t_f = 1

mm is higher than the calculations above predict.

7.4.4 The tank support structure.

The tanks are the heaviest parts of the satellite (before apogee boost).
Therefore a special structure is needed to support the tanks. The forces
introduced by the tanks must be transferred to the cylinder wall. In the
satellite the design of figure 7.29 is used. It consists of a milled
strutlike shape, made of aluminum. The exact dimensions of this structure are
not designed because of a lack of time.
    Remarks
- An extra advantage of this design is that this structure also provides a
    stiff support for both equipment platforms, so no extra structure to
    provide stiffness for the platforms is needed (see paragraph 7.4.2).
- The reason for not using struts is that these don't provide enough
    stiffness. This option is shown in figure 7.8. In the first option the
    platform itself is used as a part of the tank support structure. In the
    second option the aluminum milled structure is used, so the platform is no
    part of the tank support structure. This latter design provides a better
    support.
- The design of figure 7.11 also is considered. Four plates are situated
    between the tanks. In this design however there is not enough room for the
    equipment.
- The design of figure 7.12 is considered. In this design platforms are used
    instead of the strutlike milled shape. This however divides the satellite
    in three different parts which has the disadvantage that connections
    between these part must be made.

7.4.5 The extra support structure.

This extra support structure (ESS) functions as a radiator. It is made of
aluminum honeycomb structure with aluminum face sheets because aluminum has a
very high coefficient of thermal conductivity. There is a severe thermal
environment because the TWTs and EPCs are positioned in the ESS (figure 7.30).
    The BAPTA and solar arrays are attached to the ESS. This creates a great
momentum force for which the ESS has to be designed. In the design process of
the Hitch-Hiker this is not done because there is no time to handle this
problem
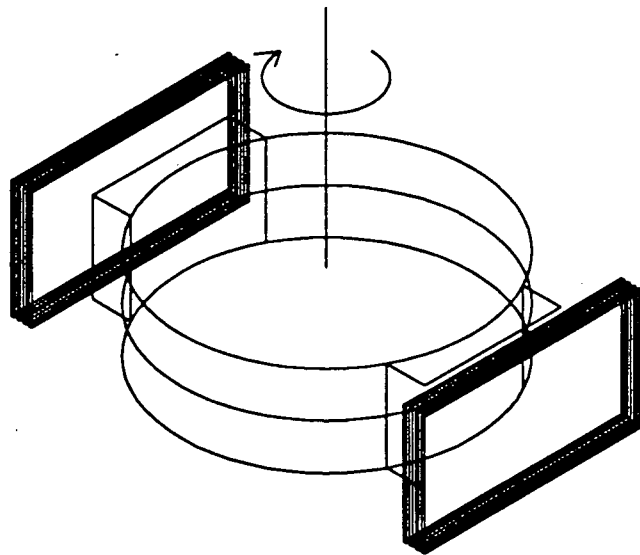
figure 7.31
The spinning configuration.
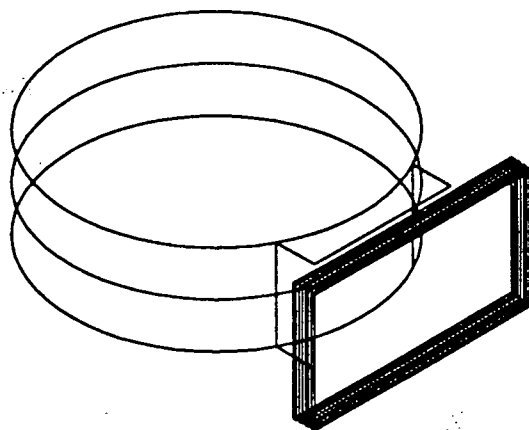
figure 7.32
The solar panels in stowed configuration.
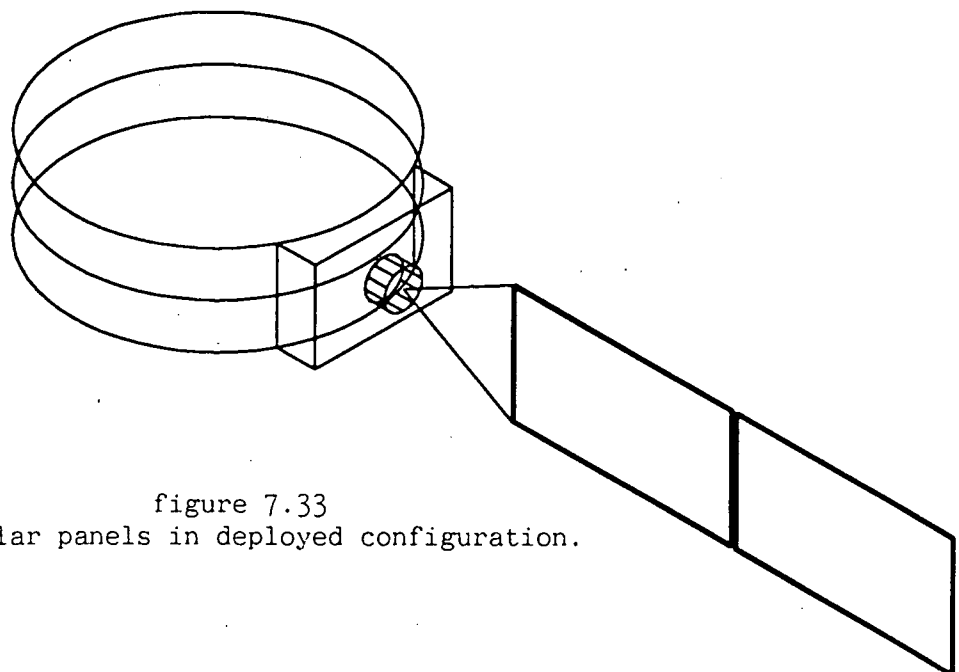
figure 7.33
The solar panels in deployed configuration.
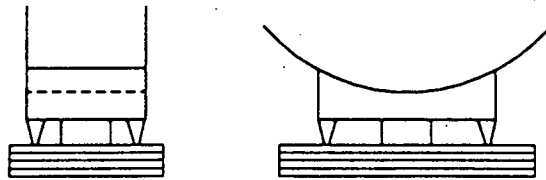
figure 7.34
The hold-down points.
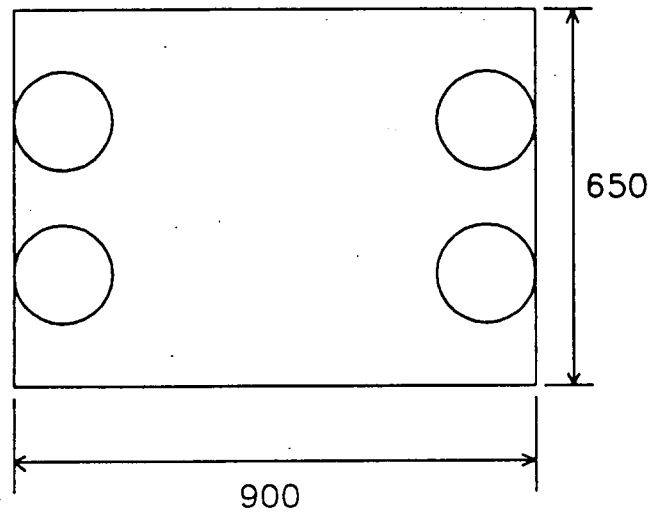
figure 7.36
The area of the extra support structure.
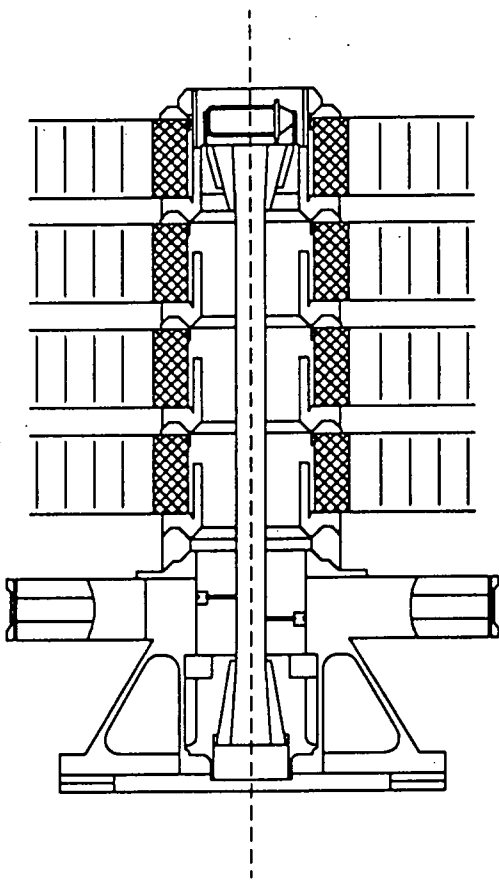
figure 7.35
The hold-down mechanism.
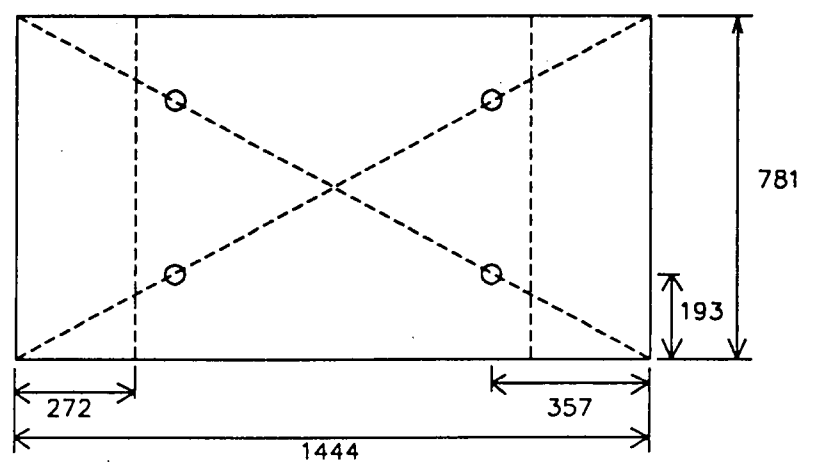
figure 7.37
The solar panel design with hold-down points.

	Flexible blankets	Rigid panels
Max power	> 10kW	till ± 10kW
Development costs	high	reasonable
Ability to repair	bad	good
Area for stowage	smaller	big
Mechanical behavior after deploying	not linear	longer linear
Mechanisms	complex	less complex

Table 7.6 : Comparison between flexible versus rigid solar arrays
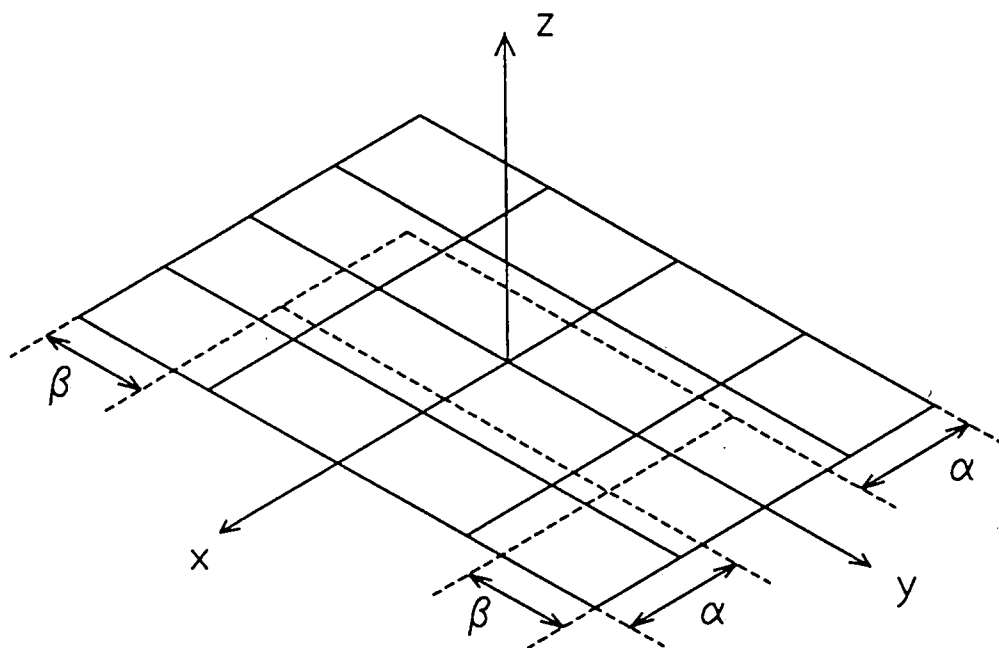
figure 7.38
Model of a plate to calculate the lowest natural frequency.

7.4.6 The solar array.

The total area of the solar array is approximately 9 m² to provide the required 850 W (EOL, see chapter 6). To make a trade off table 7.6 is used (ref. 7.1). For the Hitch-Hiker satellite a rigid array is used because this is cheaper than a flexible array. Besides that a flexible array is used mainly for a bigger power supply.

An extra advantage of this configuration is that it provides energy in transfer orbit without the necessity of a partial deployment of the array. This is so because one panel at each side of the satellite is faced outward so it catches sunlight during spinning (figure 7.31).

The rigid array is stowed on the extra support structure (figure 7.32). The deployed configuration is shown in figure 7.33. The panels are hold down on four points (figure 7.34) with the thermal knife system of Fokker (figure 7.35). Some specifications on the available height of the panels are given in the configuration chapter.

The frequency requirements are as follows:
- f>35 Hz in stowed configuration
- f must be between 0.1 and 0.2 Hz in deployed configuration

The first requirement comes from the satellite construction. The second must prevent interference with the attitude control system which has resonance frequencies that are around 0.01Hz.

To have a maximum power supply during transfer orbit the solar panels must be as big as possible. When six panels are used (three on each side) the panels are 781 x 1800 mm. Using these dimensions the solar panels are too thick. This is caused by the fact that the hold down mechanism is attached to the extra support structure and this extra support structure is not larger than 900 mm (figure 7.36). In this way the four hold down points can not be located in the optimal way and to obtain the required minimum resonance frequency of the panels a very thick panel must be used.

To obtain a thinner structure eight panels (each of 781x1444mm) are used. The hold down points are situated on the diagonals of the solar panels (figure 7.37). This configuration provides the highest possible resonance frequency (ref. 7.1).

For the calculation reference 7.6 is used. In this method the Raleigh-Ritz method is applied to calculate the fundamental frequencies of a panel which is hold down at four points. The method is very accurate for the lowest fundamental frequency.

The panel is considered to be dimensionless (length and width axb) with the four hold down points symmetrically located on the panel (figure 7.37). In this case the coordinates of the supports are:

$$(a/2-\alpha , b/2-\beta)$$
$$(-a/2+\alpha , b/2-\beta) \qquad\qquad (7.13)$$
$$(-a/2+\alpha , b/2+\beta)$$
$$(a/2-\alpha , b/2+\beta)$$

These coordinates have no dimensions because all the values are divided by the width of the panel. In the case of the Hitch-Hiker this yields (figure 7.38):

the width A=0.781 m
the length B=1.444 m
a =1
b =1444/781=1.85
a/b=781/1444=0.541
α =193/781 =0.247
β =357/781 =0.457

t_f mm	t_c mm	ρ_f kg/m²	ρ_c kg/m²	ρ_{tot} kg/m²	EI Nm	D/ρ m⁴/s²
0.15	15	0.48	0.24	3.72	927	249.2
	20		0.32	3.80	1648	433.7
	25		0.40	3.88	2576	663.9
	30		0.48	3.96	3709	936.6
0.12	15	0.384	0.24	3.624	741	204.5
	20		0.32	3.704	1319	356.1
	25		0.4	3.784	2060	544.4
	30		0.48	3.864	2967	767.9

Table 7.7 : Values of t_c, t_f, E, I, ρ for the solar panels.

Solar cells 1.0 kg/m²	9.9 kg
Wiring harness	2.5 kg
Yoke (2)	4.0 kg
Panel hinges	1.0 kg
Holddown/release mechanisms (8)	3.8 kg
Miscallaneous	2.0 kg
Harness on yokes	2.0 kg
Subtotal	25.2 kg

Table 7.8 : Mass of the solar panel equipment
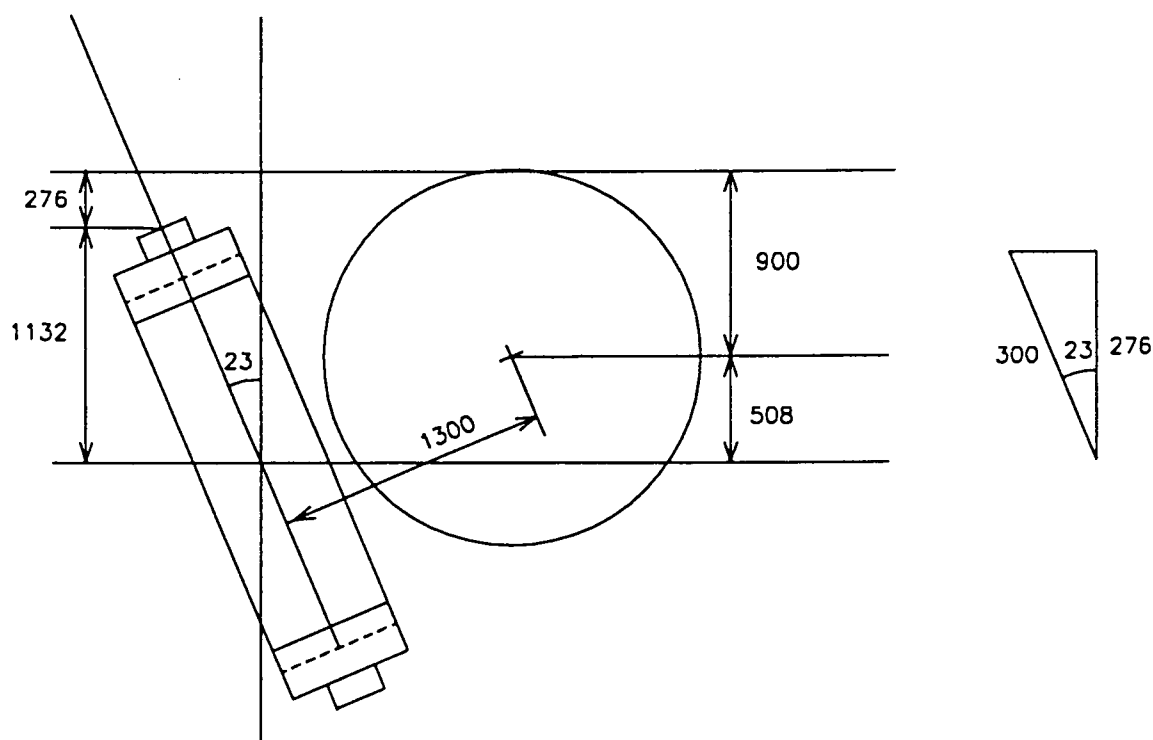
figure 7.39
Determination of the minimum length of the yoke

From tables 9 and 10 of reference 7.8 the dimensionless frequency can be determined. This dimensionless frequency can be converted to a non-dimensionless frequency with the next expression;

$$F(1)=(A(1)/2\pi AB)\sqrt{(D/\rho h)} \qquad (7.14)$$

Where: A(1) = dimensionless frequency
      A   = width of the panel
      B   = length of the panel
      D   = the stiffness of the panel per unit length
      ρ = the mass density of the panel
      h   = the thickness of the panel

However for a honeycomb structure this expression is slightly modified to take into account the core:

$$F(1)=(A(1)/2\pi AB)\sqrt{(D/\rho)} \qquad (7.15)$$

The modification is that now the mass density must be taken per unit area. Also the $D=EI=E(t_c)^2 t_f/(2(1-v^2))$ instead of $Eh^3/(12(1-v^2))$ for a homogeneous

plate.
In this case the next values of A(1) are found:
A(1)=11.318 (for A=1.0, B=1.8, α=0.25 and β=0.486)
A(1)=11.051 (for A=1.0, B=1.9, α=0.25 and β=0.475)
With expression 7.18 the D/ρ can now be calculated

$$D/\rho= (F(1)*2\pi AB/A(1))^2 = (35*2\pi*1.444*0.781/11.051)^2 =$$
$$503.65 \text{ m}^4/\text{s}^2$$

For different values of t_c and t_f the values of D, ρ and D/ρ are given in table 7.7. The value of E for the CFRP sheets is 50000 N/mm² and Poisson's ratio is 0.3. The equipment is assumed to be distributed homogeneous over the area. From table 7.8, which is made with the help of reference 7.5, the mass of the equipment on the solar panels is estimated to be 25.5 kg. This results in 2.8 kg/m². For the other masses is assumed (ref 7.1):
   -aluminum core: ρ= 16 kg/m³
   -CFRP face sheets: ρ= 1600 kg/m³
   -adhesive ρ= 0.2 kg/m² (mass per area)

From table 7.7 the option with t_c=25 mm and t_f=0.12 mm shows to be an appropriate one. In this case the ρ_{tot}=3.784 kg/m² and D=2060 Nm. The lowest resonance frequency is calculated with expression (7.18):

$$F(1)=11.051/(2\pi*1.444*0.781)*\sqrt{(2060.4/3.784)}=36.4 \text{ Hz}$$
The total mass of the solar array structure is now approximately 9.0 kg. With table 7.8 this results in a design mass of 34.2 kg. When contingency is taken into account (6%) the total mass is 36.3 kg.

remarks.
   -The design of the solar array is quite good. This is so because reference 7.8 is very accurate. Also detailed information is used from reference 7.5.
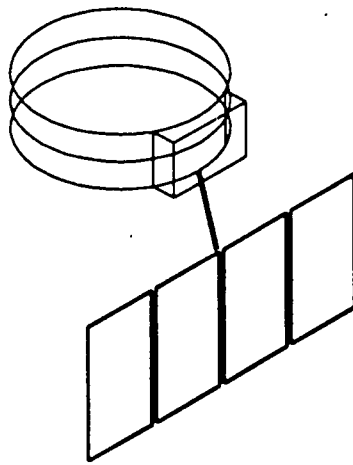
figure 7.40
The solar array under the Hitch-Hiker.

upper platform

hinge

reflector

ribs

hold down points
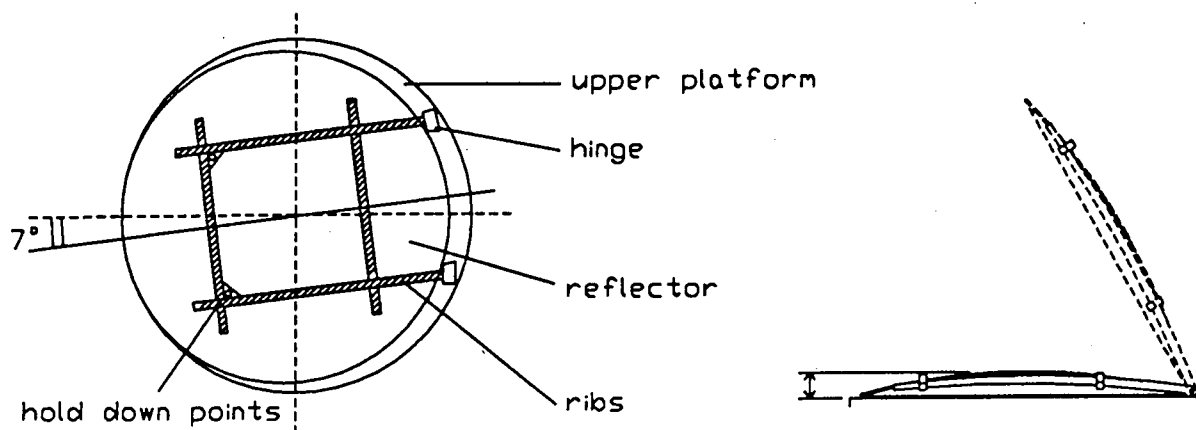
figure 7.41
Rib-stiffened antenna reflector.
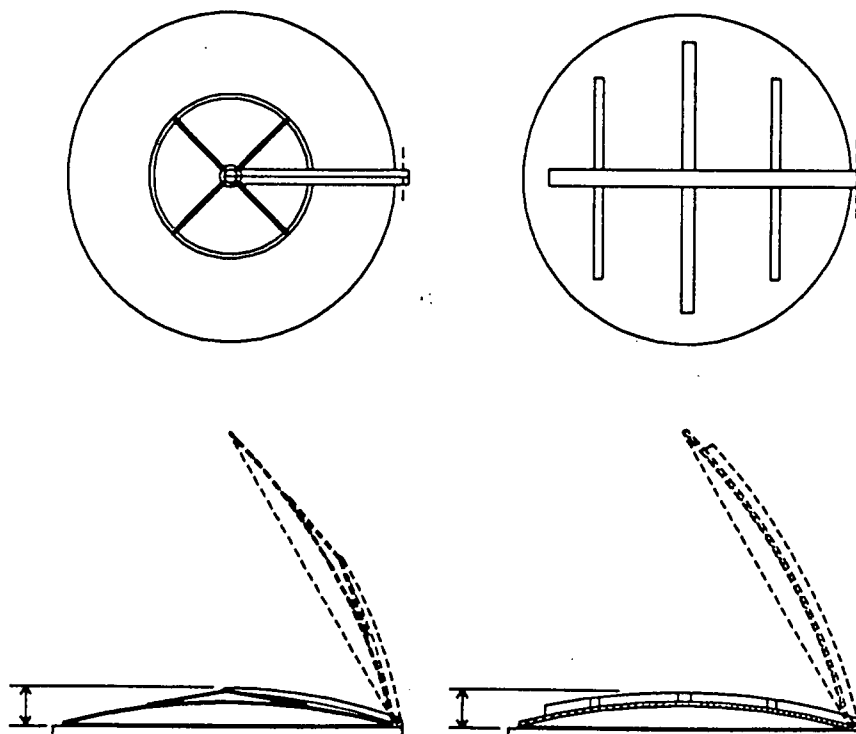
figure 7.42
Classical deployment arm.

figure 7.43
One deployment "rib" in the middle.

-The length of the yoke is determined in figure 7.39. It must be of such
length that no shadow can fall on the array. In this case, the dish
antenna must not be hit. It shows that the yoke must be at least 300 mm
long. However this gives some difficulties in the stowage so the length
of half a panel is used (1444/2= 722 mm).
-The used equipment for release, hold-down and latching is not designed
because there is not enough time to do so. Only the hold-down system is
used because the available literature was sufficient.
-Another solution might gain some mass because only one BAPTA is used
(figure 7.40). But it would also require an extra moving part namely the
BAPTA. Extra moving parts have to be avoided. And in this case all the
solar array would be situated on one side of the satellite so there is no
symmetrical design anymore. So this alternative was abandoned.

7.4.7 The dish antenna.

A stiff, lightweight dish antenna is designed for the Hitch-Hiker. The
configuration consists of a thin honeycomb sandwich with stiffening back-up
rib structure on the rear of the reflector dish (figure 7.41). Two of the
stiffening ribs extend beyond the edge of the dish for deployment. The antenna
reflector has a parabolic surface. It is held into position during launch and
transfer orbit by two pyrotechnic activated release mechanisms and by the
deployment arm attachment mechanisms.

design requirements
-The projected aperture dimension is a circle with a diameter of 1800 mm.
-The maximum deviation from parabola in orbit (best-fit rms) is 1.4 mm.
-The resonance frequency in a stowed configuration must be higher than
40 Hz.

From these requirements it follows that a high stiffness and a low
coefficient of thermal expansion are needed. An extra requirement for the
reflector and the support structure is that it must be as flat as possible.
Namely the height of these elements is decisive for the height of the extra
ring (see configuration chapter). To get a flat reflector it follows that the
distance between the feed, which is placed in the focus of the parabola, and
the reflector must be as big as possible. The maximum distance is 1800 mm. The
feed is placed in the platform itself else the reflector can't be stowed in
its most flat position. The minimum depth (or height) is 120 mm (see payload
chapter).

From AOCS comes the requirement that the antenna must be rotated $7°$
because the antenna must be pointed to Western Europe.

The support structure must give the reflector a stiff support. The most
flat configuration is gained by a rib structure on the rear of the reflector.
Other solutions need more height (figure 7.42 and 7.43).

To calculate the dimensions of the ribs a model is made. Due to the
symmetry of the antenna, the antenna is split into two pieces and is
considered to be a beam of uniform section and uniformly distributed load
(figure 7.44). From reference 7.9 it follows that the angular resonance
frequency ω_n is given by:
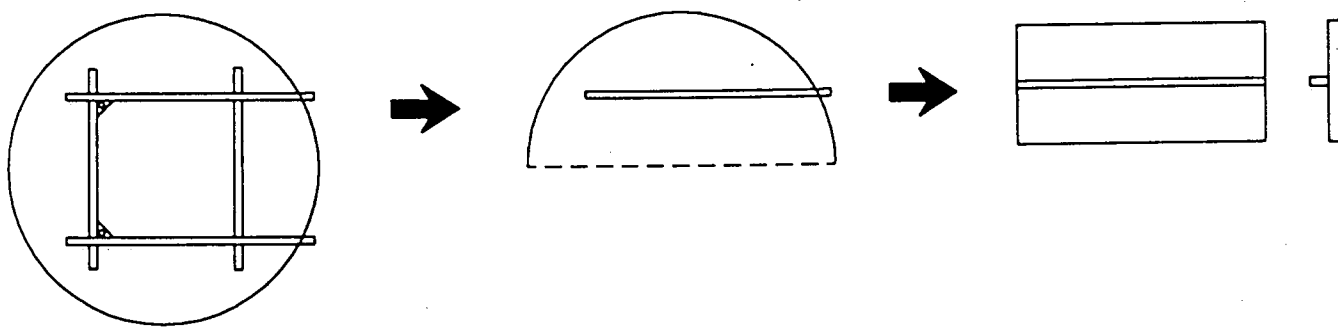
figure 7.44
Natural frequency modelizing of the reflector.
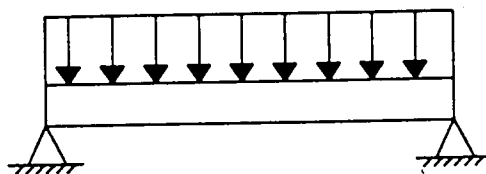
figure 7.45
Simply supported beam (A=9.87).
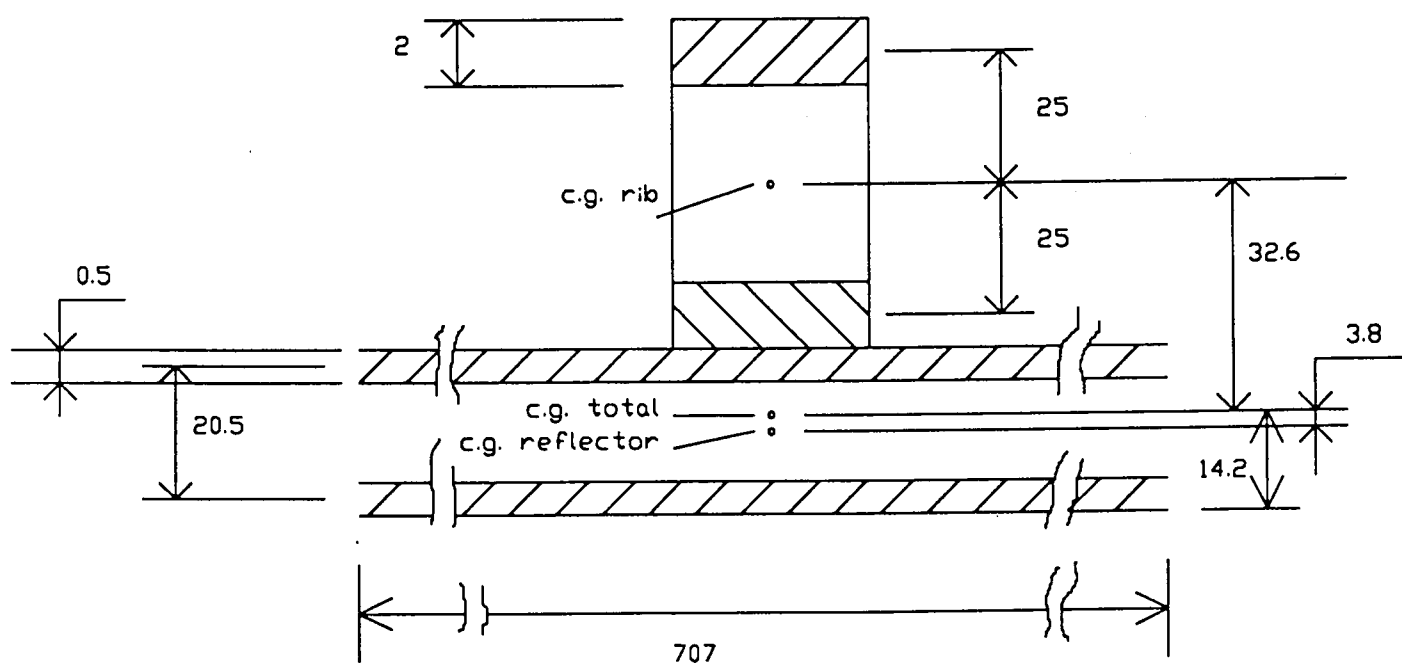
figure 7.46
Model for calculation of moment of inertia.

$$\omega_n = A/(2\pi)\sqrt{(EI/\mu l^4)} \quad \text{(in Hz)} \qquad (7.16)$$

Where: A = constant dependent of the sort of support and the number of waves

E = Young's modulus
I = area moment of inertia of beam cross section
l = length of beam
μ = mass per unit length of beam

For a simply supported beam A=9.87 (figure 7.45). Other estimations are;

for the reflector: aluminum core ρ_c =   32 kg/m³,   20 mm thick,

                CFRP sheets ρ_s = 1600 kg/m³, 0.5 mm thick,

                adhesive ρ_a = 0.10 kg/m²,

for the ribs: aluminum core ρ_c =   32 kg/m³,   30 mm thick,

                CFRP sheets ρ_s = 1600 kg/m³, 2 mm and 0.15mm,

                adhesive ρ_a = 0.10 kg/m²,

for CFRP sheets: E= 50,000 * 10⁶ N/m².

With figure 7.46 follows for the moment of inertia, I. (center of gravity on 14.2 mm). The effect of the core and vertical sheets on the moment of inertia is negligible.

$$I = b*t^3/12 + b*t*(\text{distance to center of gravity})^2 = \qquad (7.17)$$

$30*(2)^3/12 + 30*2*(32.6+25)^2 +$
$30*(2)^3/12 + 30*2*(32.6-25)^2 +$
$(707*(0.5)^3/12)*2 +$
$707*0.5*\{(20.5/2-3.8)^2 + 20.5/2+3.8)^2\} = 285297.8 \text{ mm}^4 =$
$\underline{2.85298 * 10^{-7} \text{ m}^4}$

A calculation of the mass of the reflector is made:

-Core   surface*ρ*thickness=1/4π(1.80)²*   32*   0.020=1.63 kg
-Sheets   2*surface*ρ*thickness=2/4π(1.80)²*1600*0.5*10⁻³ =4.07 kg
-Adhesive 2*surface*ρ*thickness=2/4π(1.80)²*0.100   =0.51 kg
Total mass   6.21 kg

So for μ, the mass per unit length beam follows:

$$\mu = \frac{\text{total mass of reflector}/2}{\text{length of beam}} = 6.21/2 * 1/1.8 = 1.725 \text{ kg/m}$$

With expression (7.16) follows:

ω_n= 9.87/2 * $\sqrt{[50,000*10^6 * 2.85298 * 10^{-7}/1.725*(1.8)^4]}$ =

= $\underline{44.1 \text{ Hz}}$

This result shows that honeycomb ribs of 50 mm height and 30 mm width and CFRP sheets of two 2 mm, on top and under the rib, support the dish sufficiently (requirement is 40 Hz). It must be said that this calculation of the resonance frequency is rather rough, but for this kind of problems a good analytical model is not found (and probably does not exist).

For a thermal analysis see the thermal control chapter.
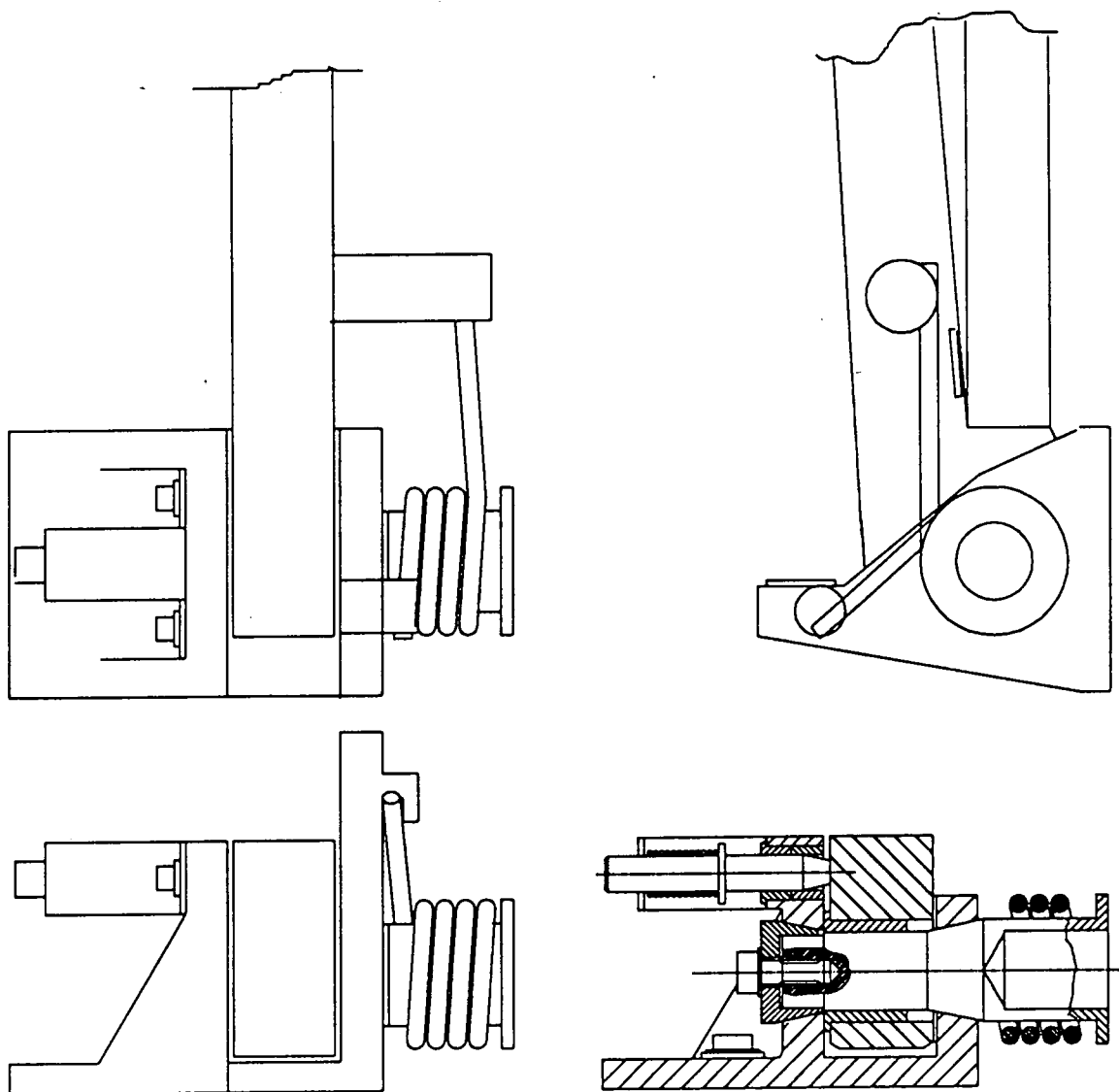
figure 7.47
Design of the hinge.
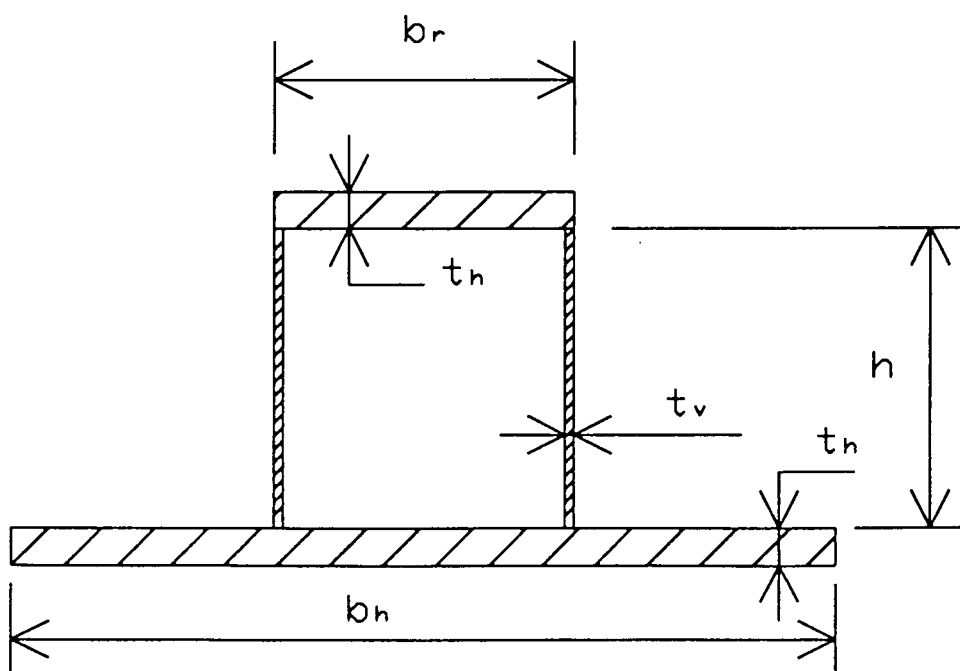
figure 7.48
Model for calculation of mass of rib.

The deployment mechanism consists of two hinges, placed on the upper platform, with torsion springs (figure 7.47). After the release of the antenna by the pyrotechnic bolts, the antenna will rotate until it reaches the end-stop. The pins (which ends are conical) will face a conical hole in the arm. Then a spring pushes the locking pin into this conical hole. The position of the conical hole is such that the pin makes contact only in one side of it. The arms (and antenna) will then be caught between the pin and end-stop without any play. The reason for this kind of hinge is the lack of room for another deployment mechanism at the upper platform. For heat-conductive reasons the hinges are mainly made of titanium.

Total mass calculation:
-mass of reflector (see above)   6.21 kg
-mass of ribs (figure 7.48)

sheets: $b_r * t_h * \rho_s = 30 * 2 * 10^{-6} * 1600$ = 0.096 kg

$b_h * t_h * \rho_s = 50 * 2 * 10^{-6} * 1600$ = 0.160 kg

$2 * h * t_v * \rho_s = 2 * 50 * 0.15 * 10^{-6} * 1600$ = 0.024 kg

core: $b_r * h * \rho_c = 50 * 30 * 10^{-6} * 32$ = 0.048 kg

adhesive: $2*(h + b_r) * \rho_a = 2*(50 + 30)*0.1*10^{-3} =$ 0.016 kg

total mass of rib per meter length   = 0.344 kg

total length of ribs 2*1.8+2*1.6= 6.8 m

total mass of ribs 6.8 * 0.344 = 2.34 kg

-hinges

rough estimation of volume of the two hinges:
$100 * 100 * 50 * 10^{-9} = 0.5 * 10^{-3}$ m³
density of titanium $\rho = 4.43 *10^3$ kg/m³
total mass hinges 2 * 0.5 * 4.43 = 4.43 kg

So the total mass of the antenna with deployment mechanisms is:
6.21 + 2.34 + 4.43 = 12.98 ≈ 13 kg.

This mass probably can be reduced by using thinner face sheets and a less heavy hinge.

7.4.8 The separation mechanisms.

The two extra rings are developed because the adaptor and the lower SPELDA cannot be changed to attach a separation mechanism. On these rings the separation mechanisms are attached (figure 7.49). The two separation mechanisms must provide separation after the launch and stiffness and support during launch. These last requirements follow from the Ariane IV user's manual.
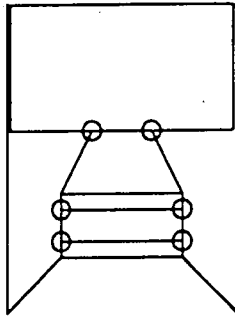
figure 7.49
Location of the separation mechanisms.
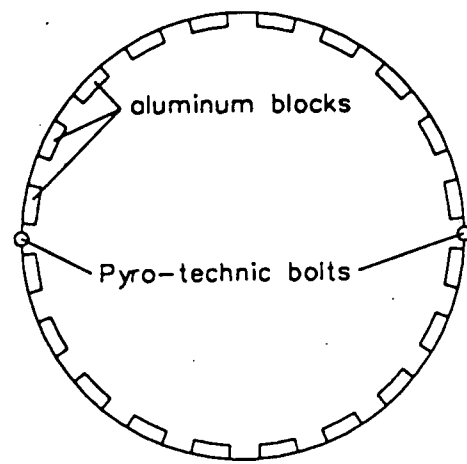
figure 7.50
The Marman clamp-band.
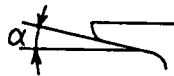
figure 7.51
The angle of the separation parts.

μ	α (°)	$T_{clamping}$ (N)	$T_{release}$ (N)
0.1	10	91222	- 24324
	20	156151	- 82600
	30	233127	-146357
0.5	10	240542	96464
	20	342523	3723
	30	491180	- 19466

Table 7.9 : $T_{clamping}$ and $T_{release}$

The separation mechanism itself consists of a spring mechanism and a Marman clamp band with pyrotechnic bolts like the one used in the Ariane IV on the upper side of the adaptor. (figure 7.50)

The clamp band provides the necessary stiffness during launch. It consists of a steel band that will be separated on two points with pyrotechnic bolts. Aluminum blocks are situated between the clampband and the cylinder edge (figure 7.50). The design is such that the heavy parts as the springs and the clamp band will not be a part of the satellite after the separation.

A rough analysis is performed to get an idea of the dimensions and the weight of the separation mechanisms. The expression used to calculate the clamping force is shown below together with an expression to calculate the release force (ref. 7.1):

$$T_{clamping}=2\sqrt{2}(M/(\pi R))(\sin\alpha+\mu\cos\alpha)/(\cos\alpha-\mu\sin\alpha) \qquad (21)$$

$$T_{release}=2\sqrt{2}(M/(\pi R))(\mu\cos\alpha-\sin\alpha)/(\cos\alpha+\mu\sin\alpha) \qquad (22)$$

Where: M = moment on the cylinder=35250 kgm
R = radius of the cylinder=960 mm
α = angle of separation parts (figure 7.51)
μ = coefficient of friction on the contact surface
between the structure and the Marman clamp band

While the momentum force on the cylinder and the radius are given the $T_{clamping}$ and $T_{release}$ are a function of α and μ. table 7.9 shows $T_{clamping}$ and $T_{release}$ for some values of α and μ. From these values the mass of the clamp band can be calculated as follows:

$$\sigma=F/A \text{ thus } A=F/\sigma, \text{with } W=2\pi RA\Upsilon \text{ follows } W=2\pi R\Upsilon F/\sigma. \qquad (7.20)$$

Where: A = crosssectional area of the ring
σ = yield stress of steel = 1000 MPa
Υ = mass density of steel = 7850 kg/m^3

For the adaptor 937B the angle of the separation parts has a value of $\alpha=20°$. From table 7.9 it shows clearly that a low value of μ gives a low value of T and thus a lower mass of the clamp band. So $\alpha=20°$ and $\mu=0.1$ is chosen. Using expression 7.20 this gives:

$$m=(2\pi*960*156151*7850*10^{-9})/1000= 7.4 \text{ kg}$$

There are some extra parts of the separation mechanisms:
-The aluminum blocks in the clamp band that have an estimated mass of 7 kg (ref. 7.1).
-The springs that keep the clamp band attached to the structure after the separation to prevent space debris or collision with other parts of the satellite.
-The springs that provide the separation and their support structure (figure 7.52). These are estimated on 5 kg.
-The microswitches that have to control wether the separation has been completed or not (figure 7.53).
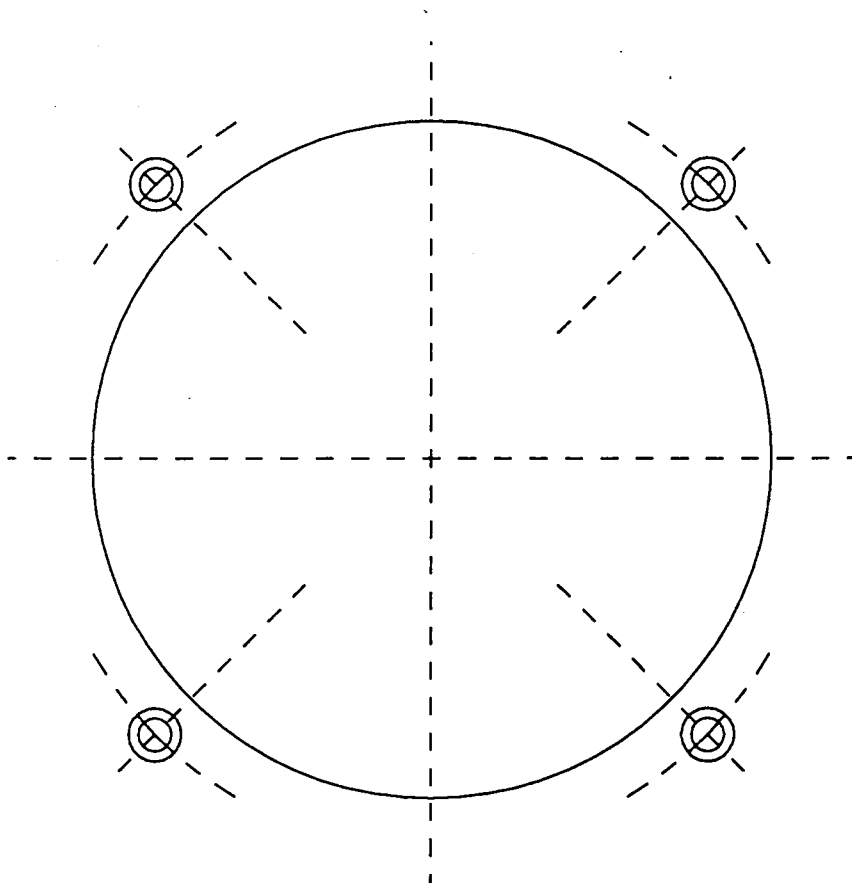
figure 7.52
Position of the separation springs.
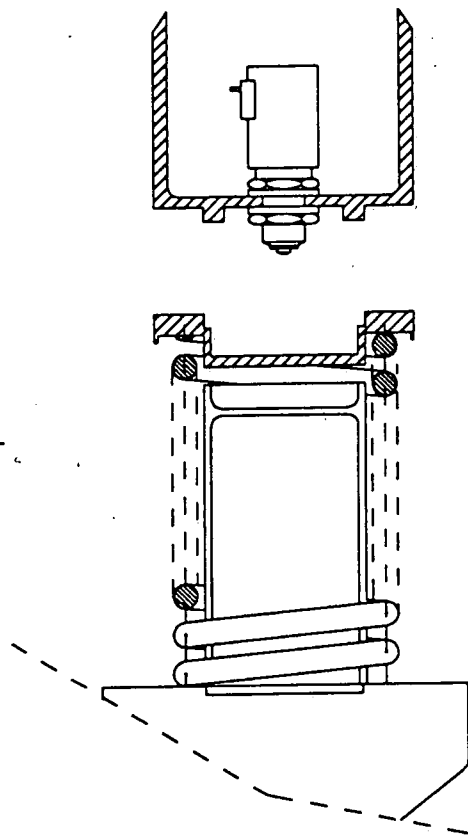
figure 7.53
Separation springs and microswitches.

cylinder	23.8 kg
platforms	23.8 kg
extra support structure	14.0 kg
tank support structure	13.0 kg
separation mechanisms	5.0 kg
mass after separation	79.8 kg ≈ 80 kg
extra mass during launch:	
separation mechanisms	35.0 kg
extra rings	10.0 kg
total launch mass	125.0 kg

Table 7.10 : mass budget

These parts together are estimated to have a mass of approximately 12 kg (ref. 7.1). So together the separation mechanism has a mass of 20 kg. The two separation mechanisms are the same because this design reduces the development costs. In the calculations above the highest loaded separation mechanism (the one just above the lower SPELDA) is dimensioned so the second one will certainly suffice.

The design is such that the heaviest part of the equipment is no part of the satellite after separation. At this point only one half of the separation springs is a part of the satellite. This is estimated at 5 kg. The rest of the both separation mechanisms remain attached to the adaptor and the SPELDA. Nevertheless this mass must be reckoned to the launch mass.

The extra rings on which the separation mechanisms are attached have an estimated mass of 10 kg. Again this mass is no part of the satellite after separation but still it is a part of the launch mass.

Remarks

The analysis made above is incomplete because of several reasons:
-The calculations take no account of imperfections. These have a great influence on the weight of the separation mechanism.
-The upper satellite shall require the same environment it would have had if the hitchhiker hadn't been there. So the stiffness requirements will be more severe than just preventing backlash.

conclusions

The analysis is a rough calculation, and it is not complete. Therefore a more detailed study has to be performed to optimize the design. Nevertheless it is used to get an idea of the weight of the separation mechanisms.

7.5 Remarks and conclusions.

The mass budget of the structure subsystem is given in table 7.10. The masses of the extra support structure and the tank support structure are estimated with the help of reference 7.1. The total launch mass of the subsystem is 124.4 kg. The structural mass after separation is 79.4 kg.

The maximum allowable mass of the structure subsystem is 80 kg, based on a 10% of 800 kg, being the maximum allowable mass of the Hitch-Hiker satellite. In the case of the Hitch-Hiker the structural system must also carry the adaptor and the upper satellite so the subsystem is heavier than in a normal design. This will increase the structural weight, compared to normal satellites. That is why the requirement of 10% mentioned above is too severe. In the calculations to estimate the allowable mass this is not taken into account.

The reliability of the design is not very high because only first-order calculations or even estimations have been made. Nevertheless the results are a reasonable guideline for a more detailed study because a margin of 20% is added (see chapter 2.3).

During the several discussions held during the final presentation some possibilities to reduce the weight of the structure subsystem were considered:
-To use a cylinder, made of CFRP instead of aluminum. It was estimated that the weight of the cylinder would decrease to approximately 16 kg, which is 7 kg less.
-To make a more acceptable analysis of the weight of the extra support structure and the tank support structure. This will in any case give a better estimation than the very rough one that exists at the moment.

8   AOCS.

8.1   Introduction.

In this chapter the attitude and orbit control subsystem (AOCS) will be described. At first shall be shown how the system is developed and why it is done in that way. After that the system is checked, whether it meets the requirements.
The specific requirements the AOCS subsystem have to meet are:

Orbit: -the S/C has to operate in a geostationary orbit.
         -the S/C needs to have a station keeping tolerance of ±0.1° NS/EW.
Attitude and orbit corrections:
         -the S/C must have "delta velocity" capability of up to 50 m/s per
          year over the mission lifetime.
         -attitude corrections needed to meet the performance requirements of
          the payload shall be minimized.
Unattended operation:
         -the S/C has to survive without degradation for periods up to 24
          hours without any RF uplink.
Stabilization:
         -the S/C has to be stabilized during all phases of the mission.
         -the antenna beam pointing (ABP) accuracy target is ±0.1° (1σ).
         -if the S/C is spin-stabilized, the ratio spin axis moment of inertia
          to maximum transverse moment of inertia has to be greater than 1.05.

The antenna beam pointing (ABP) accuracy target is later rectified to 0.3°. This is done because the ABP accuracy normally is about 10% of the antenna beam width.
The antenna beam width of the Hitch-hiker is about 4.55°, so an accuracy of 0.3° seems more realistic (see section 8.7.2: Antenna beam pointing error).

For the design of the AOCS subsystem during the operational phase of the mission, only a study is made on three-axis stabilized systems. The choice for a three-axis stabilized S/C is made at the beginning of the project, because no time was available to study all possibilities.

8.2   Trade off's.

A trade off is made for the transfer orbit and normal mode attitude control system.

8.2.1 Normal mode.

In the normal mode a three-axis stabilized system had to be designed. For a three-axis stabilized system there are different systems possible:
    - a system based on a momentum wheel with thrusters for roll-yaw control
      and desaturation of the momentum wheel. (momentum biased)
    - a system with reaction wheels (RW) with thrusters only for
      desaturation. (zero momentum)
    - a system based on control-moment gyros (CMG).
    - a combination of these three.
    - a system based on attitude control with thrusters. (cold-gas jets)

Wheel diameter	cm	20	26	35	50	60*)
Angular momentum range	Nms	1.8...6.5	5.0...20	14...80	50...300	200...1000
Max. reaction torque	Nm	0.2	0.2	0.2	0.3	0.3−0.6
Speed***)	min⁻¹	6000	6000	6000	6000	6000
Loss torque at max. speed**)	Nm	≤ 0.012	≤ 0.013	≤ 0.015	≤ 0.022	≤ 0.07
Power consumption:						
− steady state (depending on speed)	W	2...7	2...8	2...10	3...15	10...50
− max. power rating	W	≤ 60	≤ 80	≤ 100	≤ 150	≤ 500
Dimensions:						
− diameter A	mm	203	260	350	500	600
− height B	mm	75	85	120	150	180
Weight	kg	2.7...3.4	3.5...6.0	5.0...8.0	7.5...12	20...37
Environmental conditions:						
− operating temperature − vibration (sinusoidal) − vibration (random) − linear acceleration		suitable for satellites compatible with launchers such as ARIANE or Space Shuttle				

*) under development
**) with ironless motors
***) Max. speed of reaction wheels, nominal speed of momentum wheels (control range ± 10%)

Table 8.1
TELDIX wheels (ref. 8.2).
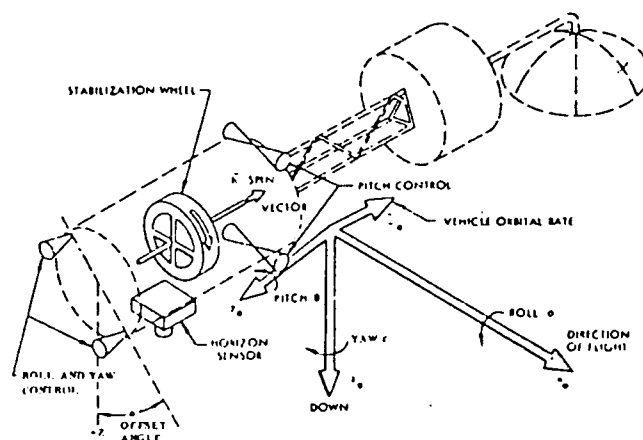
figure 8.1
Location and orientation of stabilization component of Whecon
(ref. 8.10).

In the trade off, only the first three options are really taken into account.

Beforehand, the idea about the cold gas jets system was that it will be too heavy, due to thrusters and propellant. Furthermore such a system will have a complex and expensive plumbing, which is subject to failure (ref. 8.1, page 19).

During the trade off, the attention is mainly based on the mass, required power and the complexity of the system.
The information about the RW and momentum wheels is taken from table 8.1 (ref. 8.2).

The system with one momentum wheel needs one wheel and thrusters with control over all axis. The thrusters are necessary for roll-yaw control and desaturation of the momentum wheel.
The rotation axis of the wheel is thought to be the pitch axis of the S/C (see also figure 8.1). For redundancy a second momentum wheel can be used.

The RW-system needs three RW, one for each axis, and thrusters with control over all axis.
Now the thrusters are only needed for desaturation. For redundancy a fourth wheel can be used. Mostly that wheel will stand skewed to the other wheels. In comparison with the momentum wheel this means a lesser increase of the total mass, because one momentum wheel weights more than one reaction wheel, for the needed angular momentum.

Because you don't need to have angular momentum when using RW, the nominal wheel speed of these wheels can be held low. This means also a lower steady state power. A momentum wheel needs more steady state power because it has to be held on a relatively high nominal wheel speed, to produce a big enough angular momentum. This also counts for the CMG-system.

With this CMG-system however there are three gyros (momentum wheels) to be held on high nominal wheel speed.
This system can give high torques and mostly has a high pointing accuracy (ref. 8.3). The steering laws are however much more complex than for the other two systems.

Because of the task, to keep the design simple, the CMG-system is not really attractive. The opinion is that the required accuracy can also be accomplished with one of the other systems. Besides that, the CMG-system will probably have more mass and need more power than the other systems. So the CMG-system hasn't been chosen.

Supposing that the disturbance torque works constantly $T_d = 10^{-6}$ Nms and assuming that after three orbits (=days) the angular error is no more than $0.1°$, it is possible to find the required angular momentum of the momentum wheel. With the angular momentum it is possible to estimate the mass and the required power of the momentum wheel.
With the impulse-momentum-law, the following can be obtained:

$$\Delta\psi.B = \int T_d dt = T_d.t \qquad (T_d = constant) \qquad (8.1)$$

$$\Rightarrow \quad B = \frac{T_d.t}{\Delta\psi} = \frac{72*3600*10^{-6}}{0.1*\pi/180} \approx 150 \text{ Nms}$$

where $\Delta\psi$ = angle error about z-axis after
three orbits (set at $0.1°$).

B = angular momentum of momentum wheel.

T_d = constant disturbance torque about z-axis.

t = 72*3600 (three orbits).
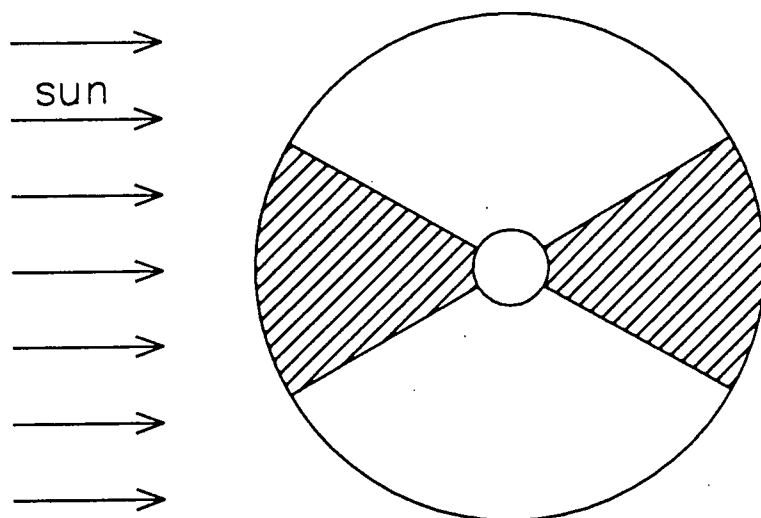
figure 8.2
Regions where the QSS can not see the sun and where the RIG are
needed.
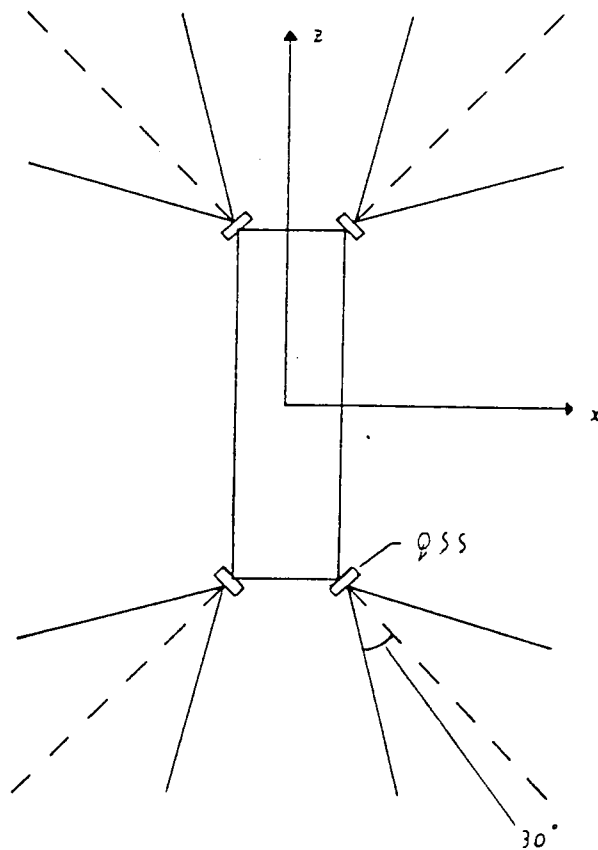
figure 8.3
A possible QSS configuration.

In table 8.1 can be seen that the momentum wheel then has a weight of about 10 kg and requires a steady state power of ± 7 W (d=50 cm).
For the RW the following can be obtained:

$$T_d = \frac{dB}{dt} = Iw.\frac{d\omega}{dt} \qquad\qquad (8.2)$$

where Iw = moment of inertia of the RW.
 ω = the angular speed of the RW.

If the maximum wheel speed is set at 2500 rpm and the wheel has to take the disturbance torque for three orbits (=days) before desaturation is needed, then the angular momentum at the end is: B = 10^{-6}*72*3600 = 0.26 Nms and Iw ≈ 0.05 kgm^2.
With this and table 8.1 it can be obtained that the reaction wheel weighs about 3 kg and needs a steady state power of 2 to 3 W.
For three wheels this means a weight of 9 kg and a steady state power of 6 to 9 W.

From this very rough estimation of the mass and power, can be seen that there is no big difference between the system with a momentum wheel and the system with RW.
The disadvantage of a momentum wheel is that it has an angular drift due to the disturbance torque. To keep the angle error within allowable limits, thrusters must be used.
This isn't necessary with RW. Because of this, and the knowledge that earlier designed reaction wheel systems have functioned well, the system with reaction wheel control is chosen for this S/C.
To measure the angle error, a sensor configuration is chosen. For the measurement of the roll and pitch angles an infrared earth sensor (IRES) is used, The summarized description of the IRES can be found in section 8.5.
For the measurement of the yaw angle, a two-axis sun sensor has to be used, like the coarse analog sun sensor (CASS) or the quadrant sun sensor (QSS). The choice has fallen on the QSS, because it has a better accuracy than the CASS. In principle two QSS will be used with a field of view FOV of 60° over two axis.
During the time the two QSS can't see the sun, the yaw control will be based on the rate integrating gyro (RIG). If one of the QSS can see the sun, the RIG is re-set (see also figure 8.2).
Because the FOV of one QSS (on the +x side) cannot be held totally unobscured by the structure of the satellite (the dish antenna), one extra QSS is placed (see configuration figure 8.11 in section 8.5).
Another possibility is to use four QSS and place them at an angle with the x-axis (see figure 8.3). The time the S/C is controlled with the RIG is shortened in this way. This possibility isn't worked out in this study, so it isn't known wether this is a better solution than the chosen configuration.

8.2.2 Transfer orbit.

During the transfer orbit, the S/C can be spin-stabilized or three axis stabilized.
For a three axis stabilized system, there is another sensor system needed for measuring the attitude of the S/C. Besides that, the wheels also require power, while the solar arrays are not entirely used yet.

PROCEDURE
(a) Despin and dewobble   (d) Earth acquisition
(b) Sun acquisition   (e) Pointing x-axis
(c) Depl. Solar arrays   (f) switch to normal mode
    and antenna   in drift orbit
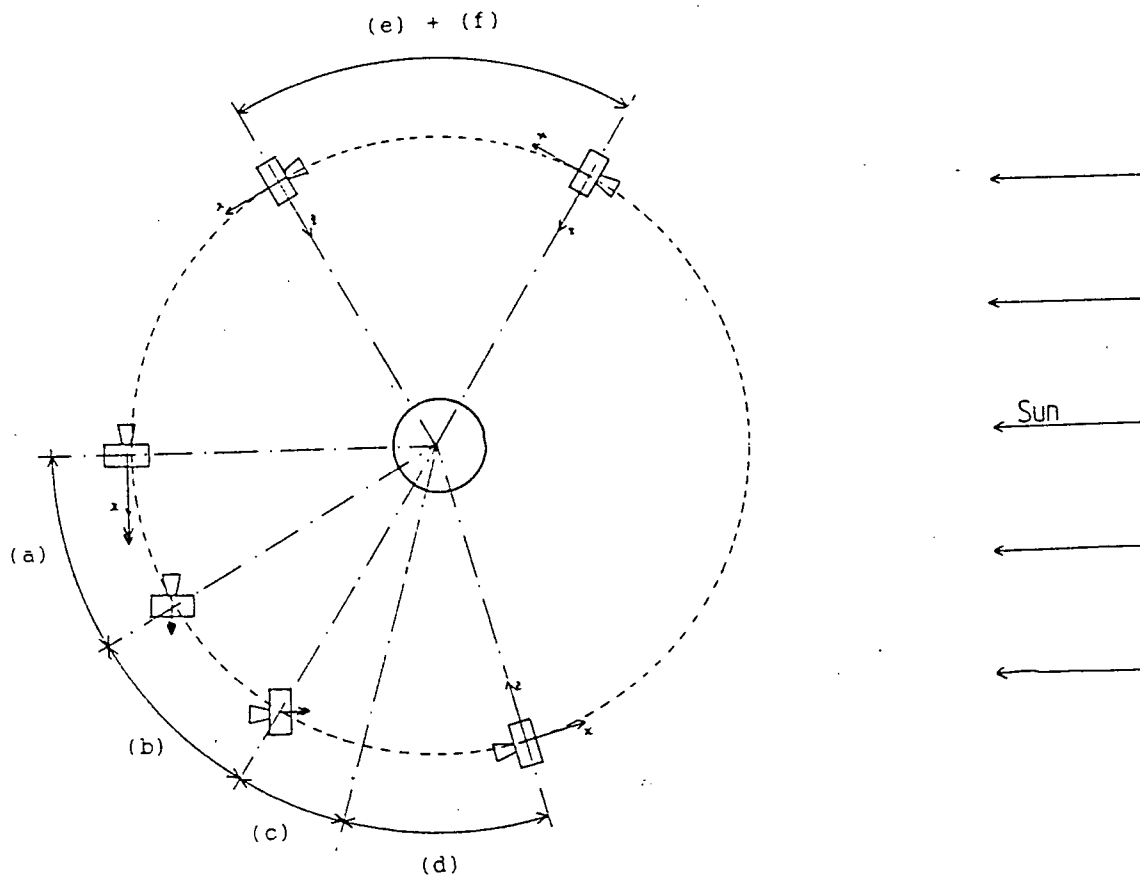
figure 8.4
Acquisition procedure.

Because the S/C won't have much room for extra equipment, and spin-stabilization is much more simple, the S/C will be spin-stabilized during the transfer orbit. The only sensor used during the transfer orbit, is the RIG in the x axis.

After separation from the ARIANE 4, the S/C is spinning with a spinrate of 5 rpm. For the spin-stabilization, a spinrate of about 40 rpm is needed. So the S/C has to be spun up by thrusters. This is done by the attitude control thrusters (ACT).

8.3 Acquisition procedure.

After the first apogee engine firing (AEF), which brings the S/C in a quasi-geostationary orbit with a very low eccentricity, the S/C has to change from a spin stabilized about the x-axis to a three-axis stabilized S/C with the z-axis fixed to the earth.
To do this, a complex procedure is needed. See also figure 8.4.

First the S/C must be despinned from a spinrate of about 40 rpm to about 1 rpm.

This is done with the attitude control thrusters (ACT), the same thrusters as for desaturation of the wheel in x-axis during normal mode. With thrusters of 4.45 N the time needed for despinning is approximately 3 min. A misalignment of 10% of the thrusters will result in a spin about an axis perpendicular to the x-axis with a spinrate of about 4 rpm.

So dewobble is needed. The spinrates are measured by the rate integrating gyros (RIG).

Now that the S/C is spinning with a low spinrate about the x-axis, it is possible to change the direction of the x-axis to the sun, using the ACT. This is called the sun acquisition.
Information about the sun is given by the sun acquisition sensors (SAS). They are positioned at both sides of the x-axis, giving an output zero when the sun is detected in the x-axis, otherwise giving information in which quadrant the sun is present.

Two SAS, one on each side, is normally enough, because each SAS has a field of view (FOV) of more than $180°$.

Because of obstruction of the FOV of the SAS by the nozzle and the antenna, four SAS are used, two on each side.

After sun acquisition, the solar arrays and the antenna dish are deployed.

Spinning with a low spinrate about the x-axis, a two-axis infrared earth sensor (IRES) pointing into the z-direction, will have the earth in it's FOV at a certain moment.

When the earth is within the FOV of the IRES, the z-axis is fixed to the earth. This is called the earth acquisition.

The S/C is now three-axis stabilized with the z-axis pointing to the earth and the x-axis pointing in the ecliptic plane, which makes an angle with the equatorial plane (except in vernal and autumnal equinox). The desired position of the S/C is with the x-axis pointing to the east, and the solar arrays perpendicular to the orbit plane.

The SAS can not be used to point the x-axis to the east (in the orbit plane). Two-axis sun sensors must be used, like the coarse analog sun sensor (CASS) or the quadrant sun sensors (QSS), positioned in the same direction as the SAS.

The choice has fallen on the QSS because it has a better accuracy than the CASS.

At this point the three reaction wheels (RW) are started to keep the S/C in position.

During the drift orbit i.e station aquisition mode (about 23 days) it is not necessary to have a pointing accuracy of $0.3°$.
After the second apogee kick (using the ACT) however, the pointing accuracy must be $0.3°$, ending the acquisition procedure.
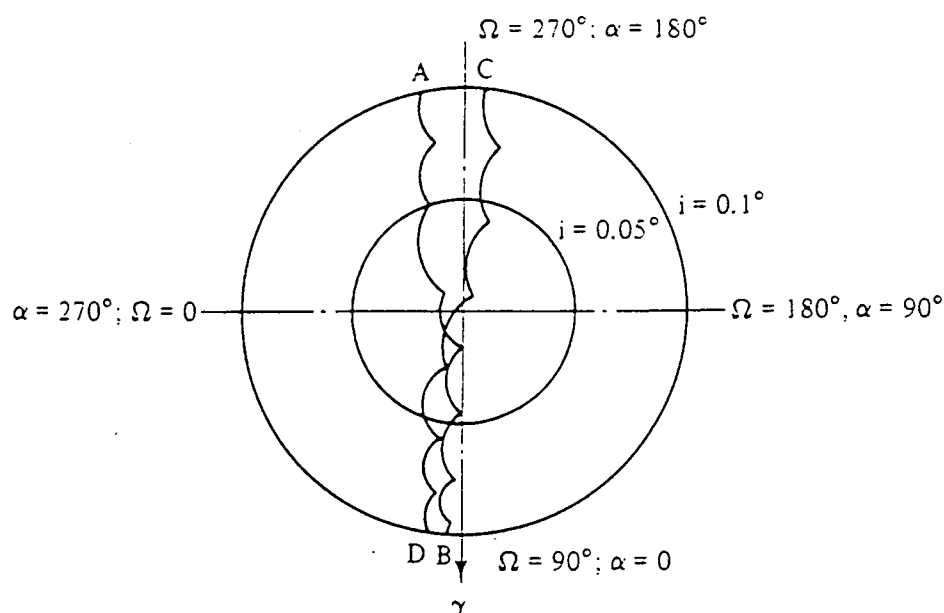
figure 8.5
Orbit pole trajectories (ref. 8.5).
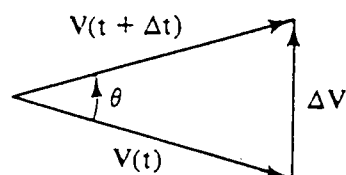
figure 8.6
Velocity vector diagram for inclination correction (ref. 8.5).

Date January 1	Ω moon (Deg.)	$i_,$ (Deg.)	$\Omega_,$ (Deg.)	$\dfrac{di}{dt}\Big\|$ moon (Deg./Yr.)	$\dfrac{di}{dt}\Big\|$ Total (Deg./Yr.)
1979	171.332	18.375	2.459	0.480	0.749
1980	152.004	19.049	7.417	0.491	0.760
1981	132.623	20.300	10.975	0.513	0.782
1982	113.295	21.902	12.769	0.542	0.811
1983	93.966	23.627	12.910	0.574	0.843
1984	74.638	25.279	11.694	0.607	0.876
1985	55.257	26.703	9.447	0.636	0.905
1986	35.929	27.776	6.489	0.657	0.926
1987	16.601	28.422	3.089	0.671	0.940
1988	357.273	28.595	− 0.511	0.674	0.943
1989	337.892	28.284	− 4.088	0.668	0.937
1990	318.563	27.511	− 7.388	0.652	0.921
1991	299.235	26.330	− 10.171	0.628	0.897
1992	279.907	24.830	− 12.155	0.598	0.867
1993	260.526	23.135	− 13.023	0.565	0.834
1994	241.198	21.423	− 12.436	0.533	0.802
1995	221.870	19.898	− 10.138	0.506	0.775
1996	202.542	18.793	− 6.132	0.487	0.756
1997	183.161	18.311	− 0.903	0.479	0.748
1998	163.833	18.557	4.504	0.483	0.752
1999	144.505	19.476	8.993	0.498	0.767
2000	125.177	20.888	11.875	0.523	0.792
2001	105.796	22.568	13.006	0.554	0.823
2002	86.468	24.287	12.581	0.587	0.856
2003	67.139	25.865	10.929	0.619	0.888

Table 8.2
Inclination drift rates (ref. 8.5).

8.4 Station keeping.

By disturbance forces, due to the sun and the moon, the inclination of the orbit of the S/C will be changed. Also the longitude λ of the S/C will be changed, due to the ellipticity of the earth.

Because of this there are corrections needed to place the S/C back on its original position.

The allowable errors, given in the requirements, are $\pm 0.1°$ in NS and EW direction. To keep the S/C between these limits, there can be chosen between two methods of station keeping:

-The corrections can be made automatically in a fixed cycle time (ref. 8.4, page 620), or

-the corrections can be made on command by the ground control when the S/C is reaching the limits (ref. 8.5).

There is chosen for the last option because in that case less corrections are needed during the lifetime of the S/C. Besides that, it has more flexibility in unforeseen situations. This of course, means an extra task for the ground control, but because the S/C has to be watched in any case, it won't be much work extra.

The drift of the inclination i and the right ascension of the ascending node Ω can be shown in a correction cycle (see figure 8.5)

The line from point A to B gives the drift of the pole of the orbit of the S/C. In point B a pulse can be given with the ACT in the north direction. The angle Ω will approximately change $180°$.

The pole of the orbit goes to point C in the figure, and will drift to point D. When it has come in that point, again a pulse will be given, etc.

The needed "delta velocity" for this corrections is:

$$\Delta V = 2V \cdot \sin\left(\frac{\theta}{2}\right) \quad \text{(see figure 8.6)} \tag{8.3}$$

For $\Omega = 180°$ this gives :

$$\Delta V = 2V \cdot \sin(i) \tag{8.4}$$

Where V is the orbit velocity of the S/C. So for each correction a delta velocity of 10.33 m/s is needed. Because the drift of the inclination is about $0.85°$ per year (see table 8.2), this correction has to take place each 2.8 months.

For a lifetime of 10 years this means a total delta velocity of about 461 m/s.

The east-west drift of the longitude of the S/C can be described by a formula that approximates the real drift.

For the acceleration of the longitude can be written as function of the longitude λ where the S/C is standing (see ref. 8.5):

$$\ddot{\lambda} = -0.00168 * \sin 2(\lambda - \lambda_s) \quad °/\text{day}^2 \tag{8.5}$$

Where λ_s = stable longitude $75°$ E and $255°$ E

The period between two EW-corrections is (see figure 8.7):

$$T = \frac{2 * \lambda_0}{\text{abs}(\ddot{\lambda})} \quad \text{or} \quad T = 4 \sqrt{\frac{\Delta\lambda}{\text{abs}(\ddot{\lambda})}} \tag{8.6}$$
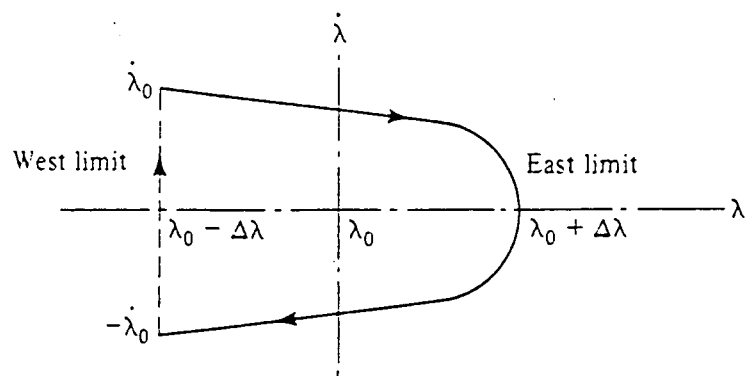
figure 8.7
Longitudinal station keeping (ref. 8.5).

For ∆λ = 0.1° and λ = 12° these periods is about 34 days.

The delta velocity, needed for this correction is about 0.13 m/s. For a lifetime of 10 years this means a total delta velocity of about 14 m/s.

Together with the NS-station keeping delta velocity, the total delta velocity for station keeping becomes 475 m/s.
This is below the 50 m/s per year allowed by the requirements

A point of attention is the time in orbit when station keeping takes place. As already told in section 8.3, there are two periods in the orbit where the sun sensors (QSS) don't see the sun (see figure 8.2). The S/C is then using a gyro (RIG) for measuring the yaw-error.

The station keeping-maneuvers better cannot take place during these periods in connection with the accuracy of the RIG (see also ref. 8.4).

If the NS-maneuvers and the EW-maneuvers have to take place at almost the same time, then the NS-maneuver has to be done at first. This is because the NS-maneuver influences the EW-position of the S/C. The influence of the EW-maneuver on the NS-position, is however neglectible (see also ref. 8.4).

The NS and EW corrections will be done with the ACT. This means a maneuvering time for the NS-correction of about 8 minutes and for EW-correction of about 6 seconds.
Assuming a misalignment of the ACT, the ACT will cause too large disturbing torques for the RW. So during station keeping the attitude control will be done by the ACT also.

8.5   Subsystem architecture.

8.5.1 Equipment list.

The equipment used for the attitude and orbit control subsystem (AOCS) can be divided into three categories, namely the sensors, the actuators and the electronics.

The elements of each category are as follows:

SENSORS: elements which sense the attitude of the S/C.

2	sun acquisition sensors	(SAS)	+x axis
2	sun acquisition sensors	(SAS)	-x axis
2	quadrant sun sensors	(QSS)	+x axis
1	quadrant sun sensor	(QSS)	-x axis
1	infrared earth sensor	(IRES)	-z axis
4	rate integrating gyros	(RIG)	x,y,z,z axis

ACTUATORS: elements which give torque about the centre of gravity (c.o.g.).

3	reaction wheels	(RW)	x,y,z axis
12	attitude control thrusters	(ACT)	x,y,z axis

ELECTRONICS: elements which use and convert information to control the actuators.

1	wheel drive electronics	(WDE)
1	on board computer	(OBC)
1	A/D converter	
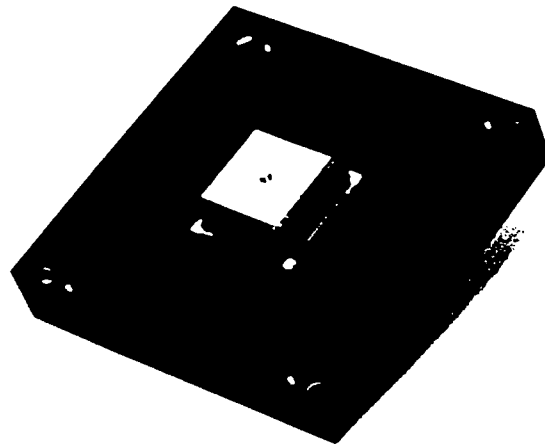
SUN ACQUISITION SENSOR FOR HEMISPHERIC FOV

(For specific mission requirements light-weighing baffles
for obscuration of a part of the FOV can be attached to
this structure)

figure 8.8.a
Sun acquisition sensor (SAS) (ref. 8.6).
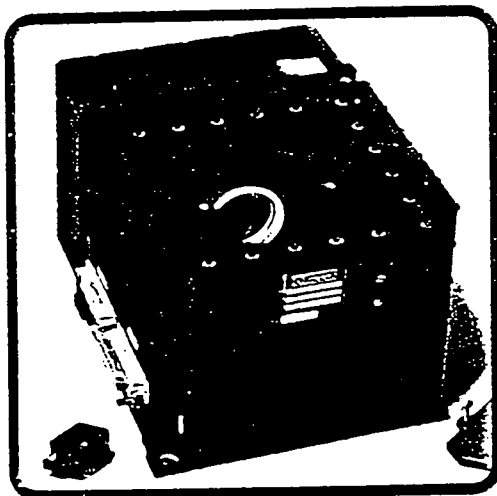
(a) IRES box
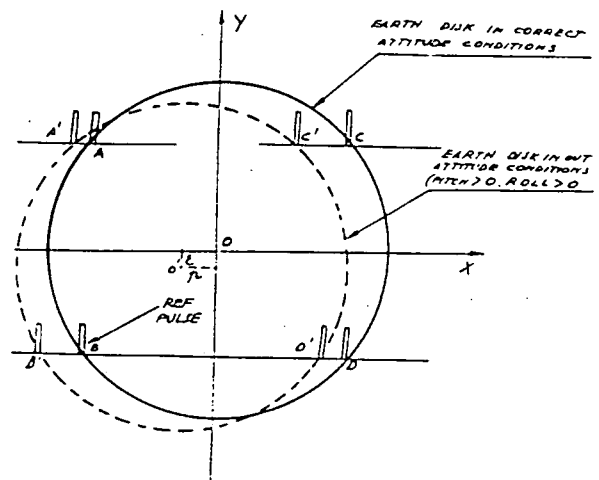
(b)

Earth disk as seen from the geostationary altitude with the sensor in correct and out-of-null attitude conditions.

figure 8.9
Infrared earth sensor (IRES) (ref. 8.8).

8.5.2 Element description.

In this section summarized descriptions of the different elements will be given, (for more elaborate descriptions of the elements references will be given).

SAS

Sun acquisition sensors (see figure 8.8.a) are used during the acquisition mode to point the x axis to the sun. The SAS gives an output zero when the sun is in the boresight of the sensor, otherwise it gives the quadrant in which the sun is present.

It consists of an aluminum structure with an outer knife-edge rim and a central pyramid to which solarcell type of silicon light detectors are attached.The sensor has a field of view (FOV) of more than 180°, so with two sensors (one on each side) the whole hemisphere can be covered.

When a part of the FOV is obscured, two sensors on one side is possible by using baffles, so that two sensors together function as one.

An A/D converter is necessary to convert the analog output of the sensors into digital information.
More information about the SAS can be found in reference 8.6.

QSS

Quadrant sun sensors (see figure 8.8.b) are used during normal mode. It sets the RIG about the y axis used for yaw control. Three QSS are used, one on the -x side and two on the +x side. On the +x side it is impossible to reach the FOV because of the dish antenna, so two sensors must be used. On the -x side however, there is no obstruction, so one sensor is enough.

This fine sun sensor employs silicon quadrant detectors placed behind a square diaphragm. It is connected to an electronics box, which processes the individual quadrant output and transfers it to the OBC.

The accuracy and the FOV depends on the distance the diaphragm is placed from the detector. The FOV is set at 60°, giving a measurement accuracy of about 0.06°.

More information can be found in reference 8.7.

IRES

The two-axis scanning infrared earth sensor (see figure 8.9) is used for pitch and roll control.
It is based on the electromechanical modulation of the incidence energy from the earth horizon in the 14 to 16 μ wavelength band.

Four pencil beams scan the earth horizon along a scan path at 45 degrees latitude north and south.

The E/S S/E radiance discontinuities are detected and the relevant pulses are compared in phase with an internal reference.

The resulting information is electronically processed to obtain the pitch and roll outputs.

The FOV of the sensor are ±12 degrees in pitch and ±14 degrees in roll. See also reference 8.8.

RIG

Rate integrating gyros are used for spinrate measurement during the acquisition mode and for yaw-angle measurement during normal mode.

Ferranti 125 (see figure 8.10) are chosen as the RIG, because they have a proven reliability with a high accuracy (there was not a real trade off because of lack of knowledge and information about RIG). It consists of two boxes, making up the gyro package. The sensors are separated from the electronics to simplify the mechanical and thermal design of the units, running at 70 or 55 degrees Celsius.
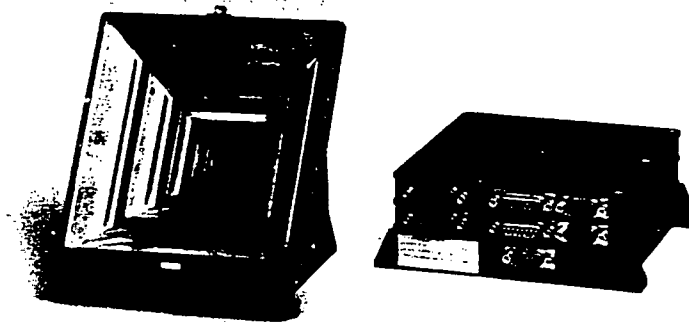
QUADRANT SUN SENSOR : OPTICAL UNIT AND ELECTRONICS BOX

$$S_y(\alpha') = \frac{tg\,\alpha'}{tg\,\alpha'_{max}} = \frac{Q_1 + Q_2 - Q_3 - Q_4}{\Sigma Q}$$
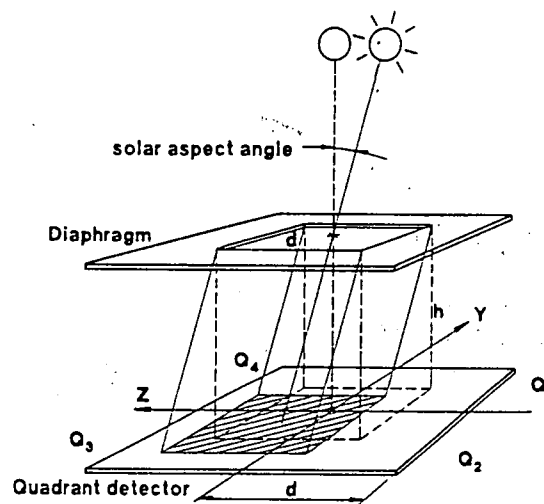
$$S_z(\beta) = \frac{tg\,\beta}{tg\,\beta_{max}} = \frac{Q_1 + Q_4 - Q_2 - Q_3}{\Sigma Q}$$

Operating principle Quadrant sun sensor

figure 8.8.b
Quadrant sun sensor (QSS) (ref. 8.7).

FLUID EXPANSION BELLOWS

TEMPERATURE SENSOR

MAGNETIC SHIELD

MOTOR BEARING

MOTOR STATOR

FLOAT BALANCE NUT

ADJUSTABLE JEWEL

TORQUE MAGNET ASSEMBLY

PICK-OFF STATORS

MAGNET COVER

FLOAT BALANCE ADJUSTOR

FLOAT BALANCE SCREW

GYRO HEATER

GYRO HOUSING

BERYLLIUM FLOAT

FLOAT PIVOT

FLYWHEEL

TORQUE/PICK-OFF ROTOR

INNER RETURN PATH

CAP ASSEMBLY

FIGURE 1

FERRANTI TYPE 125 GYRO

INERTIAL QUALITY FLOATED RATE INTEGRATING GYRO

INERTIAL SYSTEMS DEPARTMENT

FERRANTI   EDINBURGH

Z-GYRO

Z-GYRO

X-GYRO

Y-GYRO

figure 8.10
Rate integrating gyros (RIG) (ref. 8.9).

Number	ELEMENT	MASS (Kg)	POWER (W)	DIM. (mm)	Op.Temp.(°C)	FOV (°)	ACC. (°)	RELIAB.
3	QSS	5.4	4.8	Optical unit 103*83*28.5 Electr. unit 164*139*58.5	-20 to +60	60	0.06	0.976
4	SAS	0.62	-	110*110*42	-80 to +80	>180	0.2 in boresight	0.995
1	IRES	2.55	2.3	139*190*158	-20 to +45	±12 pitch ±14 roll	0.020	0.972
4	RIG	4.5	40.0	d=150;h=100	+70	-	0.025/n	?
1	RIG-el.	2.0		200*100*100	-20 to +50	-	-	?
3	RW	9.0	9.0 Steady state	d=200;h=75	-10 to +50	-	0.01	?
1	WDE	3.5	5.0	210*150*150	-20 to +50	-	-	?
1	A/D conv.	0.250	0.5	50*100*15	-20 to +50	-	-	?

Table 8.3
EQUIPMENT LIST.
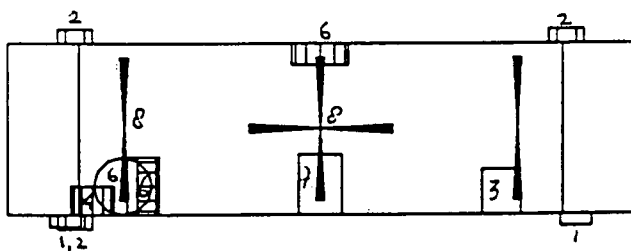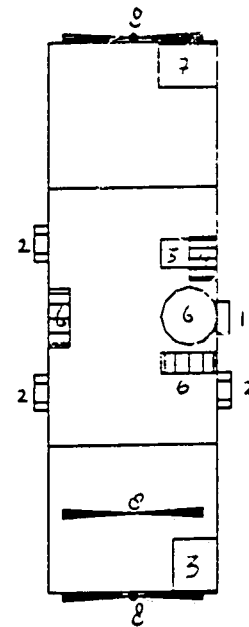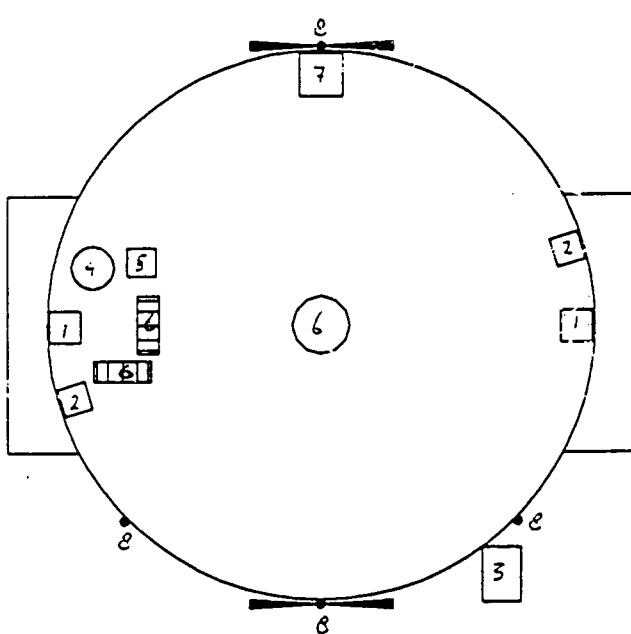
1. SAS
2. QSS
3. IRES
4. Ferranti-box
5. RIG-electronics
6. RW
7. WDE
8. ACT

figure 8.11
Configuration of the elements

RW

Reaction wheels are used to store momentarily angular momentum, caused by external disturbance torque, like solar radiation pressure and thruster misalignment.

Chosen are the RW of TELDIX with a momentum storage of 1.8 Nms with maximum wheel speed of 6000 rpm. Its maximum reaction torque is 0.2 Nm, with a power consumption of 60 W (see table 8.1).

Because 60 W is too high, the maximum reaction torque our attitude controller can use is set at 0.1 Nm, with a power consumption of about 30 W.

ACT

Attitude control thrusters are 4.45 N bi-propellant thrusters used to dump the angular momentum of the RW when it reaches the limit of storage capability by giving torques about the axis.

For every axis, four thrusters are needed, making in total 12 thrusters (see configuration figure 8.11).

The ACT are also used for the second apogee kick, for the spinning up and down of the S/C and for the NS/EW station keeping.

WDE

The wheel drive electronics constitutes the interface between the OBC (the satellite's attitude control electronics) and the RW. It receives the commands from the OBC and determines the torque, speed and speed directions of the wheels.

OBC

The centralized on board computer is the satellite's attitude control electronics. It gets sensor information with which it determines the commando's for the WDE and the ACT.

It can also receive and send information and commando's from and to the ground via the TT&C.

The OBC is an element of the data-handling subsystem.

The dimensions, the operating temperature, the mass and the power of the different elements are given in table 8.3.

A configuration figure of the elements is given in figure 8.11., and a blockdiagram of the AOCS subsystem is given in figure 8.12.

8.5.3 Subsystem budget.

A mass and power budget of the AOCS subsystem can be made from the mass and power of the different elements.

The OBC is not included because it is accounted for in the mass and power budget of the data-handling subsystem.
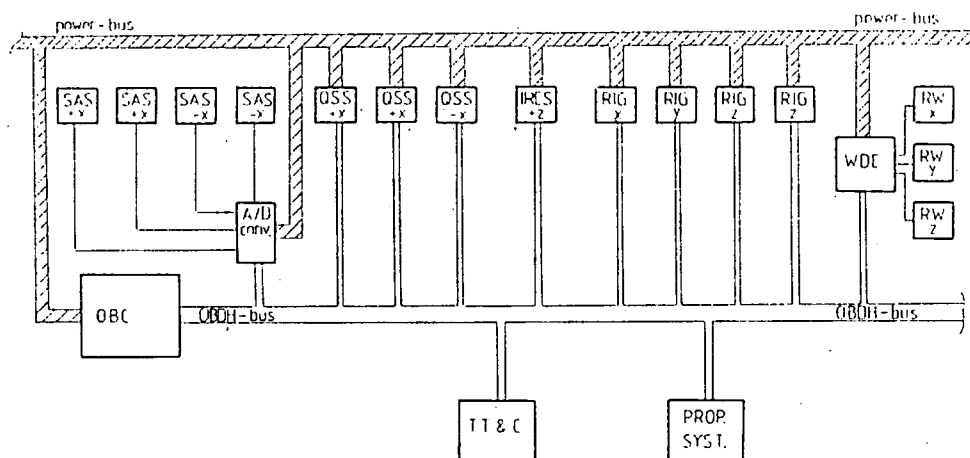
figure 8.12
Block diagram of the AOCS subsystem.

ELEMENT	MASS(kg)	POWER(W)
3 x QSS	5.4	4.8
4 x SAS	0.62	0.0
1 x IRES	2.55	2.3
4 x RIG	2.5	
1 x RIG electronics	2.0	40.0
3 x RW (steady state)	9.0	9.0
1 x WDE	3.5	5.0
1 x A/D converter (4 inputs)	0.250	0.5
SUBTOTAL	25.8	61.6
MARGIN of 10%	2.6	6.2
TOTAL	28.4	67.8

A margin of 10% is for:
- additional equipment
- minor modifications
- cabling mass

The above value of the total mass of the AOCS subsystem is below the allowable mass, given by the system-engineering team.

The allowable power the AOCS subsystem could use is set at 110 W.

The estimated total steady state power is 67.8 W ,so the rest, 42.2 W, can be used to accelerate the RW.

8.6 Reliability and redundancy.

The reliability of the designed AOCS subsystem isn't really studied. This is mainly due to a lack of knowledge c.q information, and to the lack of time.

Because the used instruments are already used in other missions, and have functioned well, they probably have a good reliability. For a higher reliability, it is possible to place some instruments double for redundancy.

This is already done with the yaw-RIG, because this is a very important instrument.

Other instruments, that could be double placed for redundancy are for example the IRES and the reaction wheels (by placing a fourth wheel). If doing so, it has to be studied how great the advantages are in comparison with the increment of weight, power, cost and complexity.

The big question is, what reliability do you want and what are you prepared to pay for.

As a matter of fact, despite a very high reliability, there always can occur a failure.
Some failures can be expected i.e. they are predictable.

For example the failure of getting out of the FOV of one of the sensors. Two possible failure modes, for being able to react on the failures, are an automatic detection and reconfiguration or a ground based failure identification and recovery.

For the given example the RIG can be used as a backup reference on which the S/C can be reconfigured to its required position. So an automatic detection and reconfiguration mode is used in this case.
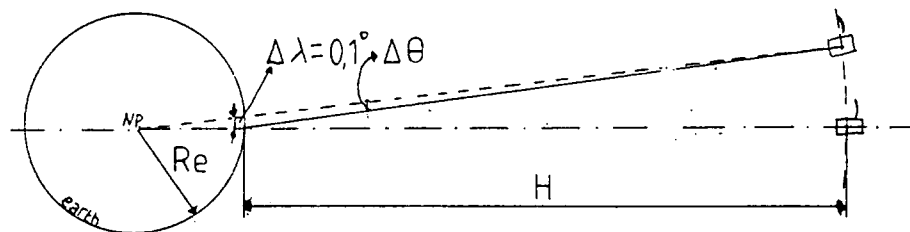
(a)
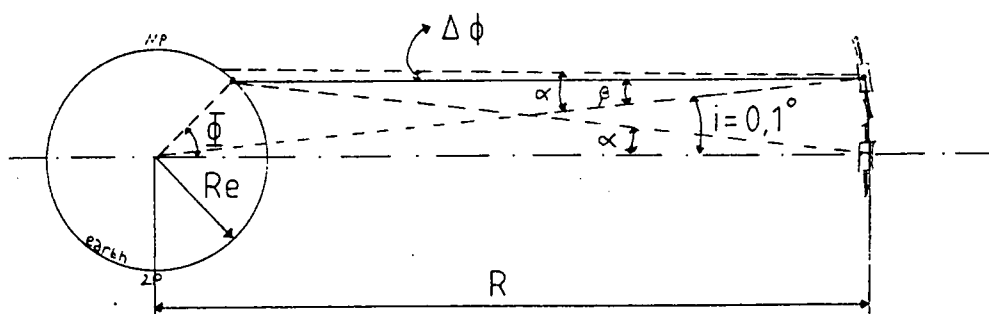
(b)

figure 8.13
a) Pitch error due to east-west orbit error of 0.1°;
b) Roll error due to north-south orbit error of 0.1°.

8.7   System error.

The S/C is controlled by measurement of the difference between the actual attitude and the desired attitude.

Errors in the measurement are unavoidable, so that the actual attitude is not perfectly known.

Additional to these errors, errors are caused by limitation of the actuators (the RW), making the real attitude errors greater than the measurement errors.

Errors can be classified according to their temporal behaviour:

- Systematic errors: errors which are constant in time.
- Pseudo-systematic errors: errors which change slowly in time. Random drift of the RIG can be classified as pseudosystematic errors.
- Random errors: Errors which vary randomly in time. These are in principle unpredictable.

The systematic and the pseudo-systematic errors are sometimes identified as one class, called the deterministic errors.

There are several ways of finding a total error, namely direct addition, root-sum-squaring or a combination of the two.
The method used here is the method usually called the pseudo-exact error combination method.

It is a combination, where errors of the same class are root-sum-squared and the totals for the different classes added linearly.

8.7.1 Error sources.

There are different error sources, namely:

- Sensors
- Wheel speed/torque
- Electronics effects
- Solar arrays perturbation
- Thermal distortion
- S/C alignment
- Error due to the controller
- Orbit errors

Sensors are the major source of errors in equipment.

Solar arrays perturbation errors are caused by the flexibility of the arrays. Thermal distortion errors consist of errors due to distortion of the structure, caused by temperature changes.

The S/C alignment errors are due to misalignment of the sensors and the actuators.

Errors due to the controller are caused by the limitation of the actuators.

Orbit errors, north-south and east-west, cause errors in pitch and in roll. See figure 8.13.

Pitch error due to east-west orbit error:
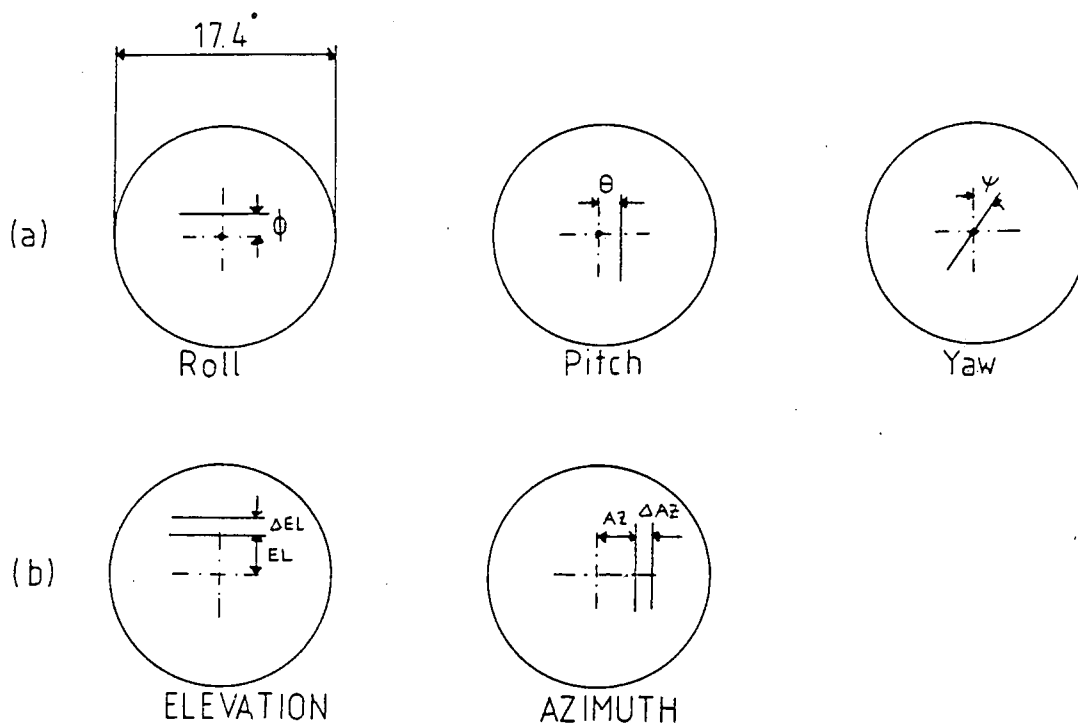
figure 8.14
ABP error expressed in terms of
a) roll, pitch and yaw and
b) elevation and azimuth.

ERROR SOURCE	ROLL		PITCH		YAW	
	RANDOM	DETERM.	RANDOM	DETERM.	RANDOM	DETERM.
SENSORS	± 0,010	± 0,020	± 0,010	± 0,020	OSS ±0,006	± 0,060
					Gyro	±0,025×δk
WHEEL SPEED / TORQUE ERROR		± 0,010		± 0,010		± 0,010
ELECTRONICS EFFECTS		±0,010		±0,010		±0,010
SOLAR ARRAY PERTURBATION	± 0,010		± 0,010		± 0,010	
SUBTOTAL ATT. CONTROL	± 0,014	± 0,024	± 0,014	± 0,024	±0,012	± 0,210
ORBIT ERROR	± 0,010		±0,018		—	
THERM. DIST. + S/C ALIGNMENT	± 0,252		± 0,188		± 0,150	
TOTAL S/C ERROR	± 0,30		± 0,245		± 0,372	
ANTENNA BEAM POINTING ERROR	ELEVATIE : ± 0,30		AZIMUT : ± 0,30			

(in degrees)

Table 8.4
ERROR LIST.

$$\Delta\theta = \frac{\Delta\lambda . Re}{H} \qquad\qquad (8.7)$$

Where $\Delta\theta$ = pitch error
      Re = radius of the earth
      H = height of S/C from earth surface
      $\Delta\lambda$ = east-west orbit error

Roll error due to north-south orbit error:

$$tg\alpha = \frac{Re.sin\Phi}{R - Re.cos\Phi} \qquad tg\beta = \frac{Re.sin(\Phi-i)}{R - Re.cos(\Phi-i)} \qquad (8.8)$$

$$\Delta\Phi = \alpha - \beta \qquad\qquad (8.9)$$

Where $\Delta\Phi$ = roll error
      Φ = latitude of ground target
      R = radius of the S/C orbit
      α, β = angles, see figure 8.13
      i = north-south orbit error

8.7.2 Antenna beam pointing error.

The antenna beam pointing (ABP) error can be expressed in terms of roll, pitch and yaw or it can be expressed in terms of azimuth (east-west) and elevation (north-south).
See figure 8.14.
The contribution of the pitch and roll error transforms directly into ABP error in azimuth and elevation.
The contribution of the yaw error depend on the location of the ground target.
The error in azimuth and elevation can be expressed as:

$$\Delta AZ = \theta + \frac{AZ}{57.3} . \psi \qquad\qquad (8.10)$$

$$\Delta EL = \Phi + \frac{AZ}{57.3} . \psi \qquad\qquad (8.11)$$

Where $\Delta EL, \Delta AZ$ = elevation and azimuth errors in degrees
      Φ, θ, ψ = roll, pitch and yaw errors in degrees
      EL, AZ = elevation and azimuth of the ground target in degrees with respect to S/C axis.
      (EL = ±6.8° ; AZ = ±0°)

From the last expressions it is clear that only a part of the yaw error is contributed to antenna beam errors.
At first an ABP accuracy of 0.1° was required.
Because normally 10% of the antenna beam width (4.55°) is required, an ABP accuracy of 0.3° seems more realistic. Furthermore, the requirement to the structure-subsystem (±0.02° for thermal distortion and S/C alignment), was too severe to achieve the 0.1° accuracy.
With an accuracy of 0.3° the requirements to the structure-subsystem are less severe, namely ±0.252° in roll, ±0.188° in pitch and ±0.150° in yaw. So with authorization of the system-engineering team the requirement of the ABP accuracy was set at 0.3°.

In table 8.4 an error budget is given for an ABP accuracy of $0.3°$, whereby is assumed the north-south and the east-west orbit error to be $0.1°$. The latitude of the ground target is assumed to be $45°$, so that the elevation of the ground target with respect to the S/C axis is $6.8°$. The azimuth is assumed to be $0°$.

Only random and deterministic errors are considered.

8.8 Modelling.

8.8.1 Dynamics.

To model the dynamics of the S/C, the following linear moment equation is used: (from ref. 8.5, page 131)

$$\bar{M} \cong \begin{cases} \dot{h}_x + I_{xx}(\ddot{\phi} - \omega_0\dot{\psi}) + h_z(\dot{\theta} - \omega_0) - h_y(\dot{\psi} + \omega_0\phi) \\ \quad - (I_{zz} - I_{yy})\omega_0(\dot{\psi} + \omega_0\phi) \\ \\ \dot{h}_y + I_{yy}\ddot{\theta} + h_x(\dot{\psi} + \omega_0\phi) - h_z(\dot{\phi} - \omega_0\psi) \\ \\ \dot{h}_z + I_{zz}(\ddot{\psi} + \omega_0\phi) + h_y(\dot{\phi} - \omega_0\psi) \\ \quad - h_x(\dot{\theta} - \omega_0) - (I_{yy} - I_{xx})\omega_0(\dot{\phi} - \omega_0\psi) \end{cases} \qquad (8.12)$$

Where

$\bar{M} = \bar{M}_g + \bar{M}_s + \bar{M}_c$

$\bar{M}_g =$ gravity-gradient torque

$\bar{M}_s =$ solar radiation pressure torque

$\bar{M}_c =$ control torque (by thrusters)

$I_{xx}, I_{yy}, I_{zz} =$ principal moments of inertia of the S/C

$h_x, h_y, h_z =$ angular momentum of the reaction wheels

$\phi, \theta, \psi =$ attitude error angles, known as roll, pitch and yaw error respectively

$\omega_0 =$ orbital rate

The disturbance torque consists of gravity-gradient torque, solar radiation pressure torque and control torque.

The gravity-gradient torque however, is much smaller than the solar radiation pressure torque. So in the model this torque is neglected.

After some rearrangements, the moment equations become:

$$\bar{M} = \bar{M}_s + \bar{M}_c = \begin{cases} I_{xx}\ddot{\phi} + [\omega_0^2(I_{yy} - I_{zz}) - \omega_0 h_y]\phi \\ \quad -[h_y + \omega_0(I_{xx} - I_{yy} + I_{zz})]\psi + \dot{\theta}h_z - \omega_0 h_z + \dot{h}_x \\ \\ I_{yy}\ddot{\theta} + \omega_0 h_x\phi - h_z\dot{\phi} + \omega_0 h_z\psi + h_x\dot{\psi} + \dot{h}_y \\ \\ I_{zz}\ddot{\psi} + [\omega_0^2(I_{yy} - I_{xx}) - \omega_0 h_y]\psi \\ \quad +[h_y + \omega_0(I_{xx} - I_{yy} + I_{zz})]\phi - \dot{\theta}h_x + \omega_0 h_x + \dot{h}_z \end{cases} \qquad (8.13)$$

These equations are coupled. But because h_x, h_y, h_z and ω_0 are small, the coupling terms can (in the beginning) be neglected. The equations of motion then become independent.

The coupling terms can be regarded as an external torque.
The coupling torque then becomes:

$$\bar{M}_{coupl} = \begin{vmatrix} \omega_0 h_y \phi + [h_y + \omega_0(Ixx - Iyy + Izz)]\psi - \theta h_z + \omega_0 h_z \\ -\omega_0 h_x \phi + h_z \phi - \omega_0 h_z \psi - h_x \psi \\ \omega_0 h_y \psi - [h_y + \omega_0(Ixx - Iyy + Izz)]\phi + \theta h_x - \omega_0 h_x \end{vmatrix} \qquad (8.14)$$

and the linear equations become:

$$\bar{M} = \bar{M}_s + \bar{M}_c (+ \bar{M}_{coupl}) = \begin{vmatrix} Ixx\ddot{\phi} + \omega_0^2(Iyy - Izz)\phi + \dot{h}_x \\ Iyy\ddot{\theta} + \dot{h}_y \\ Izz\ddot{\psi} + \omega_0^2(Iyy - Ixx)\psi + \dot{h}_z \end{vmatrix} \qquad (8.15)$$

The terms $\omega_0^2(Iyy - Izz)\phi$ and $\omega_0^2(Iyy - Ixx)\psi$ are so small that they can be also neglected. This gives three identical equations.

For the solar radiation pressure torque the following equations are used: (from ref. 8.5, page 135)

$$\bar{M}_s = PA(\bar{n} \cdot \bar{S})\bar{r} \times \{(1 - \rho_s)\bar{S} + 2(\rho_s + \frac{1}{3}\rho_d)\bar{n}\} \qquad (8.17)$$

$$\bar{S} = (\sin\alpha\cos\delta, \sin\delta, \cos\alpha\cos\delta) \qquad (8.18)$$

Where
P = solar radiation pressure $(4.644 * 10^{-6})$
A = area
$\bar{n}$ = normal vector of the area
$\bar{S}$ = unit vector along the direction of the incoming photons
$\bar{r}$ = vector from center of mass of S/C to the center of pressure of area
α = orbit angle measured from S/C local noon
δ = declination of the sun
ρ_s = specularly reflection coefficient
ρ_d = diffuse reflection coefficient

The solar radiation pressure torque, $\bar{M}_s$, is mainly due to the solar arrays and the dish antenna. Other sources are neglected.

For the solar arrays the vector $\bar{n}$ is $(\sin\alpha, 0, \cos\alpha)$ and for the dish antenna $\bar{n}_a$ is $(0, -\sin(EL), \cos(EL))$. The dish antenna is assumed to be a flat dish. EL is the angle of the dish about the S/C x-axis.
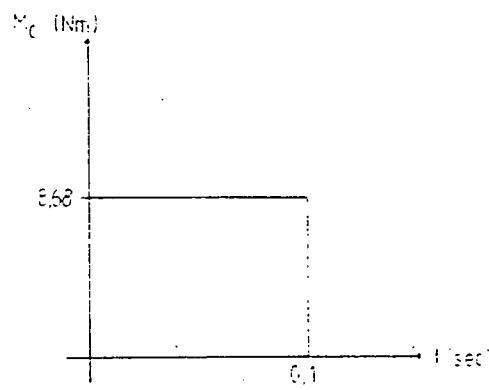
figure 8.15
Block signal representation of the desaturation torque.

For the solar radiation pressure torque $\bar{M}_s = \bar{M}_{s,s} + \bar{M}_{s,a}$,
we get

$$\bar{M}_{s,s} = \begin{matrix} PA(yK_1\cos\alpha - zK_2) \\ PA(zK_1\sin\alpha - xK_1\cos\alpha) \\ PA(xK_2 - yK1\sin\alpha) \end{matrix} \qquad (8.19)$$

where $K_1 = [(1 - \rho_s)\cos\delta + 2(\rho_s + \frac{1}{3}\rho_d)]\cos\delta$
$\qquad K_2 = (1 - \rho_s)\cos\delta\sin\delta$

and

$$\bar{M}_{s,a} = \begin{matrix} y_a L_3 - z_a L_2 \\ z_a L_1 - x_a L_3 \\ x_a L_2 - y_a L_1 \end{matrix} \quad PA_a[(\cos(EL)\cos\alpha\cos\delta - \sin(EL)\sin\delta)] \qquad (8.20)$$

where $L_1 = (1 - \rho_{s,a})\sin\alpha\cos\delta$
$\qquad L_2 = (1 - \rho_{s,a})\sin\delta - 2(\rho_{s,a} + \frac{1}{3}\rho_{d,a})\sin(EL)$
$\qquad L_3 = (1 - \rho_{s,a})\cos\alpha\cos\delta + 2(\rho_{s,a} + \frac{1}{3}\rho_{d,a})\cos(EL)$

The x,y,z are the components of vector $\bar{r}$, the index a stands for the antenna.

Because the values of reflection coefficients and areas are not exactly known, some values are assumed.

$\bar{M}_c$ is the torque due to the thrusters (ACT).

In the normal mode, these are used for desaturation. Because the maximum impuls moment of the wheels is set at 1 Nms, the thrusters have to give an angular momentum change of ±0.9 Nms (not 1 Nms to avoid stiction).

The thrust of the ACT is 4.45 N. So they will give a torque of magnitude $M_c = 1.95$ m $*$ 4.45 N = 8.68 Nm.

If the ACT works for 0.1 sec, the angular momentum change is 0.868 Nms. In the model this will be represented by a block signal (see figure 8.15).

8.8.2 The control loop.

The control loop that is used is given in figure 8.16.
The equation of motion about one axis (for example x-axis) is:

$$M = Ixx\ddot{\phi} + \dot{h}_x \qquad (8.21)$$

For the wheel torquer a PD-controller is used. The equation then becomes:
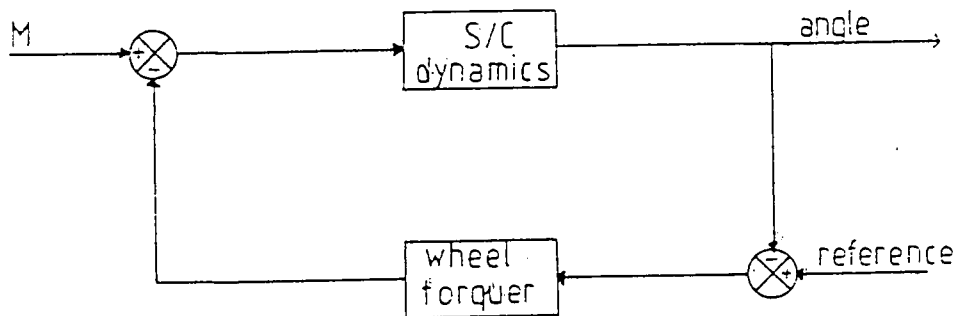
figure 8.16
Control loop for one axis control.
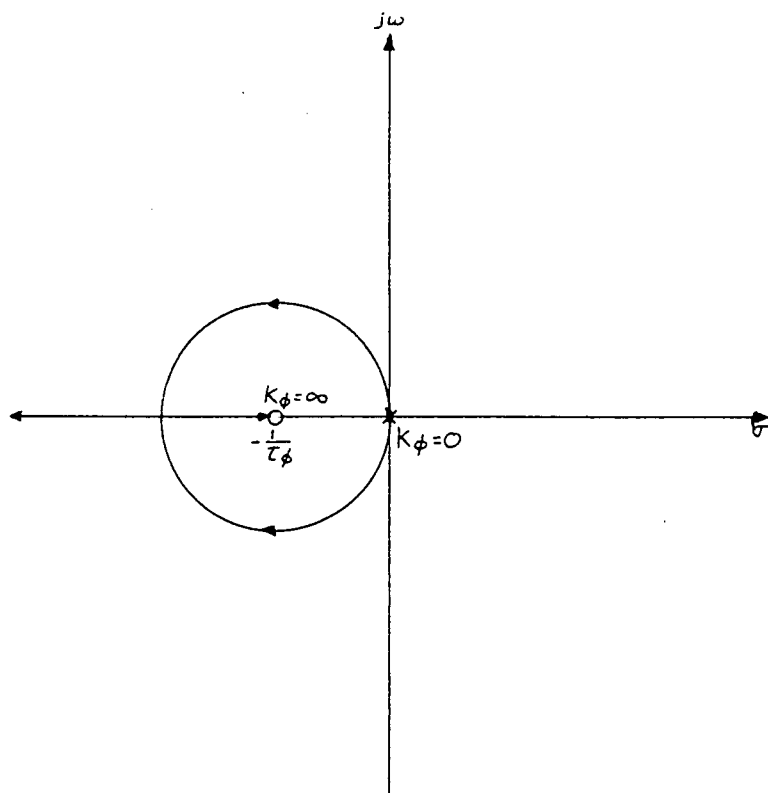
figure 8.17
Root-locus plot for roll axis control.

$$M = Ixx\ddot{\phi} + K_\phi \tau_\phi \dot{\phi} + K_\phi \phi \qquad (8.22)$$

The equation of motion becomes a damped second-order system for $K_\phi, \tau_\phi > 0$.
The natural frequency and the damping ratio are respectively:

$$\omega_\phi = \sqrt{\frac{K_\phi}{Ixx}} \quad \text{and} \quad \xi_\phi = \frac{\tau_\phi}{2}\sqrt{\frac{K_\phi}{Ixx}} \qquad (8.23)$$

The transfer function of the closed loop is:

$$\phi(s) = \frac{H(s)}{1 + G(s)H(s)} M(s) \qquad (8.24)$$

in which $H(s) = 1/(Ixxs^2)$; S/C dynamics
$\qquad G(s) = K_\phi(\tau_\phi s + 1)$; wheel torquer

The root-locus of the closed loop is given in figure 8.17.
Usually, the damping ratio is taken at about 0.7.

If τ_ϕ is set at 15 sec, then K_ϕ becomes ± 9.5 (Ixx = 1096 kgm^2).

For the z-axis K_ψ becomes ± 9.5 (τ_ψ = 15;Izz = 1082 kgm^2), and for the y-axis K_θ becomes ± 1.7 (τ_θ = 10;Iyy = 87 kgm^2).

The values of Ixx, Iyy and Izz are estimated values, based on the expected configuration and mass distribution.

8.9 Simulation.

The simulation-programme PSIE is used for the simulation of the Hitch-Hiker AOCS-subsystem. The programme based on the equations that are previously shown is given in appendix A. In this programme the AOCS-system is considered as a continuous system. Actually the system is a discrete system. Because the used integration interval is of the same amount of the sampling rate of the OBC, this probably won't lead to very different results.

The following situations are simulated:

-the normal mode: a) without coupling terms
                   b) with coupling terms
-the desaturation of the wheels

THE NORMAL MODE

During the normal mode the only disturbance torque working on the s\c is the solar radiation pressure torque(M_s). M_s is dependent of the declination of the sun. So M_s is calculated for three situations, namely for δ=23,5°, δ=0° and δ=-23,5°. As can be seen from fig 8.18, 8.19, 8.20 the disturbance torque is the greatest for a declination of δ=-23,5°, specially for the x-axis and the z-axis. So the simulation is done for this declination, taking a worst case. From fig. 8.21 can be seen that the antenna is the greatest source of the disturbance torque.
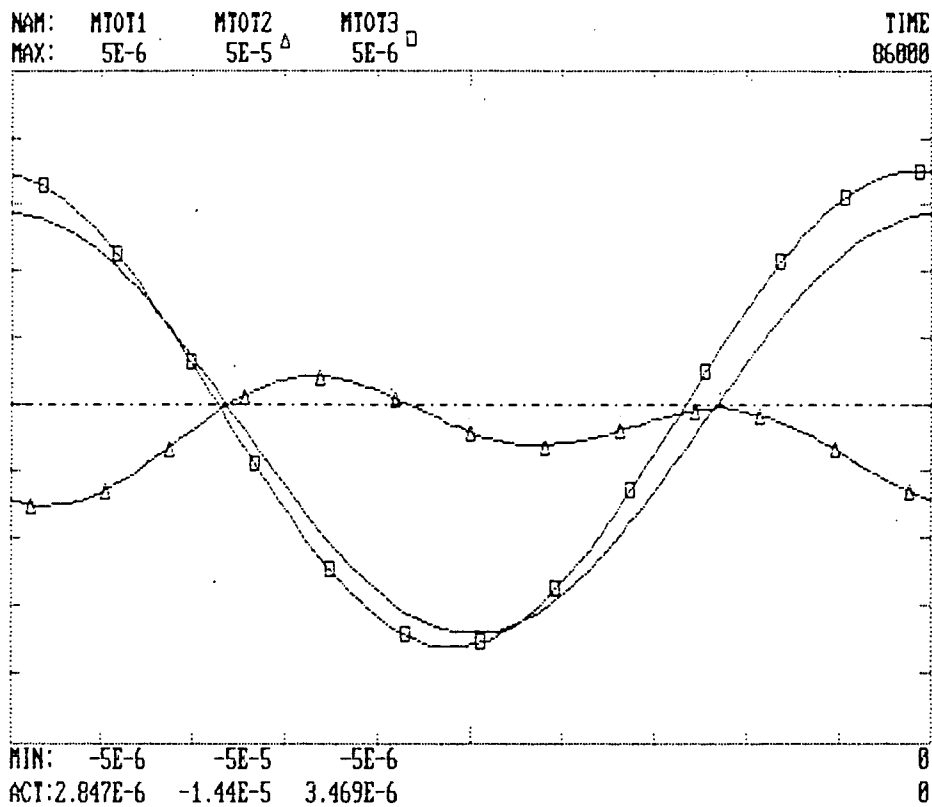
figure 8.18
Disturbance torque with declination δ = 23.5°.
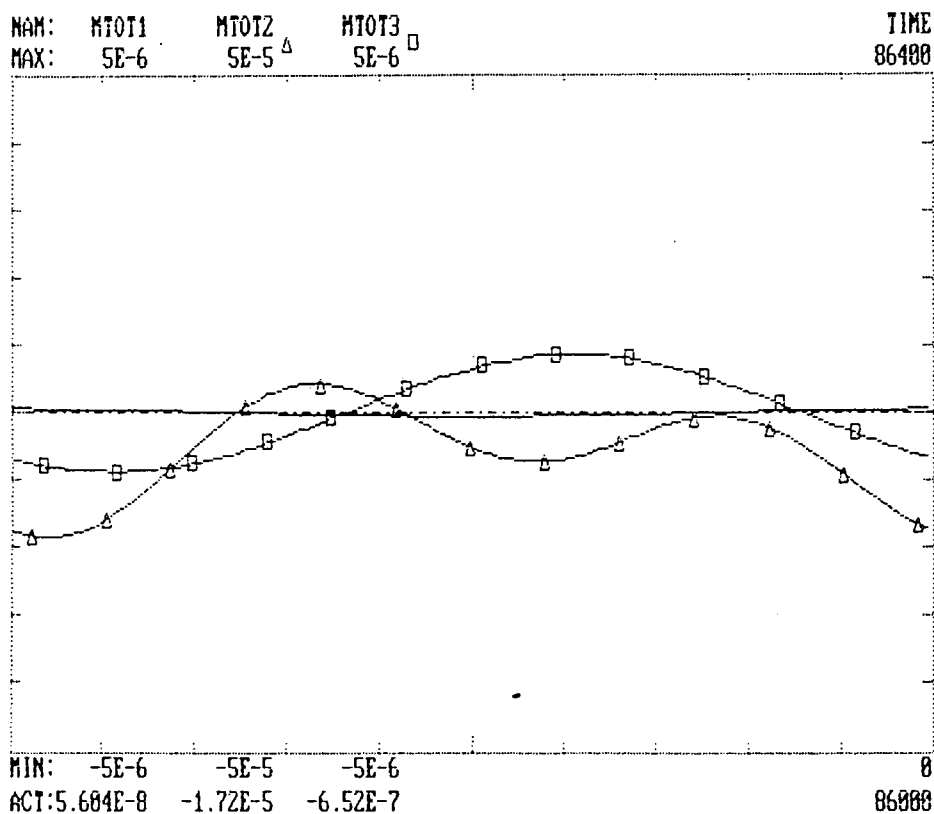
figure 8.19
Disturbance torque with declination δ = 0°.

In fig. 8.22 and 8.23 can be seen how the paths of the angle errors phi, teta, psi and the angular momentums of the wheels h1, h2, and h3 are developed over one orbit. As expected, the angle errors are following the disturbance torques. This is due to the used PD-regulator. The greatest angle occurs over the y-axis. Teta then has an amount of about $6*10^{-6}°$. This is small enough to neglect in comparison to the errors in the error-list shown in section 8.7.

After one orbit the angular momentum of all the three wheels has increased (figure 8.23). Because the disturbance torque is cyclic over one orbit, the angular momentum of the wheels will increase with the same amount after each orbit. So we can see that after about two orbits the wheel of the y-axis has to be desaturated (because h has to stay below 1 Nms). For the z-axis this would be after about 25 orbits and for the x-axis after about 200 orbits.

If the coupling terms are taken into account, however, can be seen from figure 8.24 that after one orbit the coupling terms are of the same magnitude as M_s (or even greater). These coupling terms are mainly due to the rotation of the S/C about the y-axis as a result from focalizing on the earth. So, as can be seen, these coupling terms only occur over the x- and z-axis and the development of the teta-error isn't really influenced.

The developments of the angles phi and psi, however, are certainly influenced, as can be seen from figure 8.25 compared to figure 8.22.

Naturally, the developments of h1 and h3 are also changed (see figure 8.26). But the path of the total disturbance torque (i.e. M_s+M_{couple}) isn't cyclic anymore. So little can be said about the time after which the wheels of the x- and z-axis has to be desaturated. This probably is less than 25 or 200 days, but not less than 2 days. To simulate more than one orbit would take very much calculation time, so that wasn't done.

Another aspect that can be seen in figure 8.26 is, that h1 and h3 are negative and positive in the same amount during one orbit. This means that it will be very difficult to keep the wheel speed of these wheels in one direction, even when the wheels start with a non-zero wheel speed. So the wheel speed will pass the zero speed several times,where the torque given by the wheels is influenced by stiction. The results of that stiction aren't studied in this project.

DESATURATION

As described before, the desaturation of the wheels is done with the ACT, which have a thrust of 4.45 N and are standing ~ 1.95 m out of each other. So the torque they give is (see note at the end of this section):

$$M_c = 1.95*4.45 = 8.68 \text{ Nm} \tag{8.25}$$

Because the thrusters are working during a very short time (namely 0.1 sec), this pulse can be simulated as a sudden increase of the angular speed of the satellite:

$$\omega = \frac{M_c}{I} \tag{8.26}$$

Where I = angular momentum of the axis
       ω = angular speed of the S/C over that axis
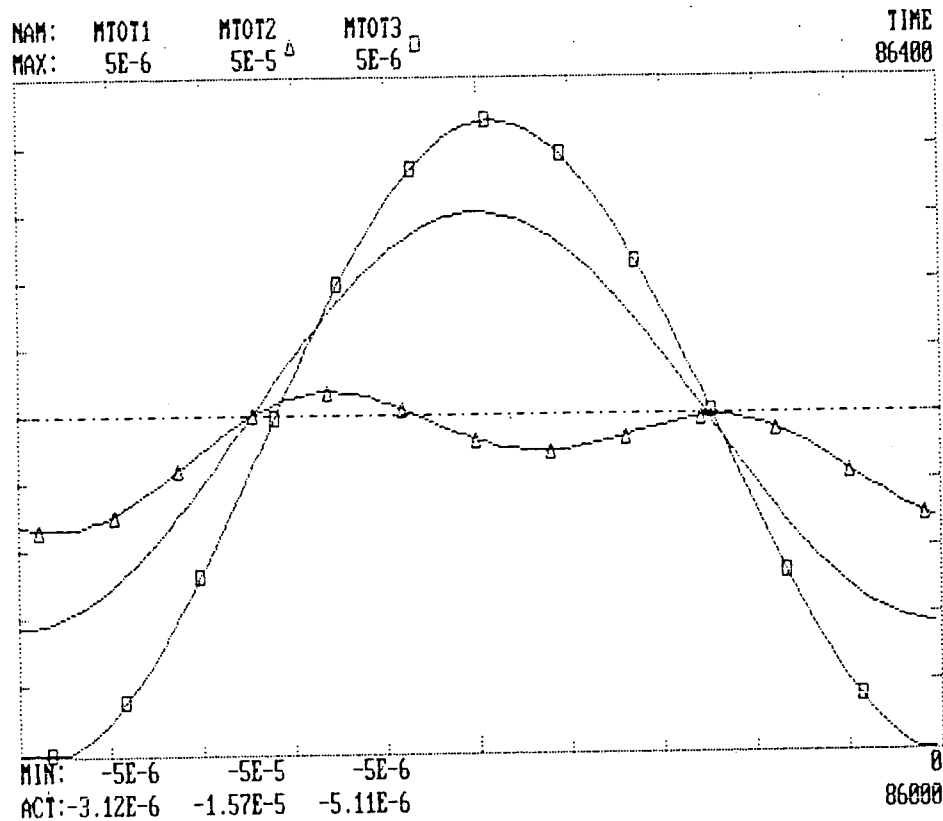
figure 8.20
Disturbance torque with declination δ = -23.5°.
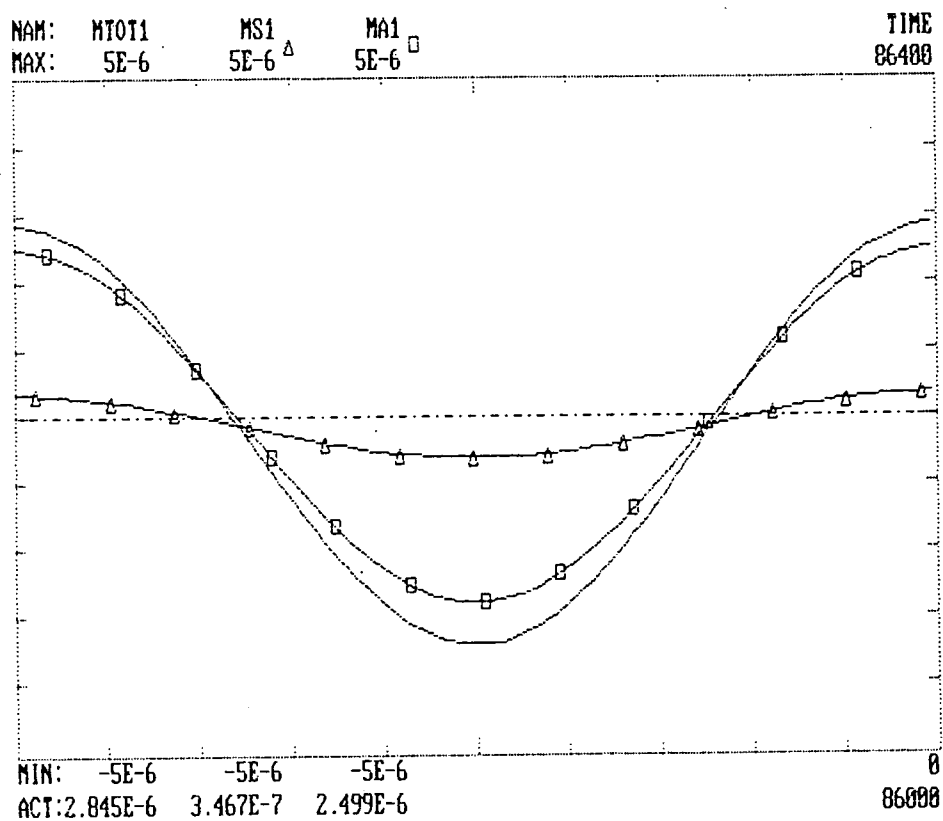
figure 8.21
Disturbance torque; Antenna is the greatest
source (MTOT1 = MS1 + MA1).

MIN: -1E-6   -1E-5   -1E-6   0
ACT: -5.41E-7   0
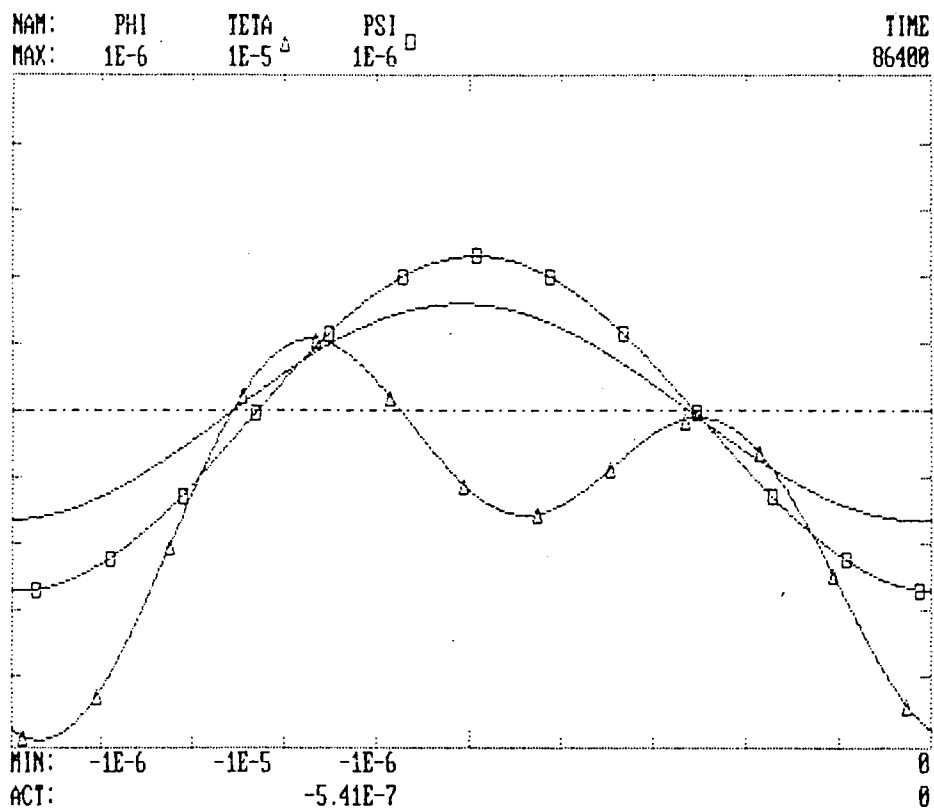
figure 8.22
Angle error roll (PHI), pitch (TETA) and yaw (PSI) (no coupling).

MIN: -0.1   -1   -0.1   0
ACT: -0.00129   0
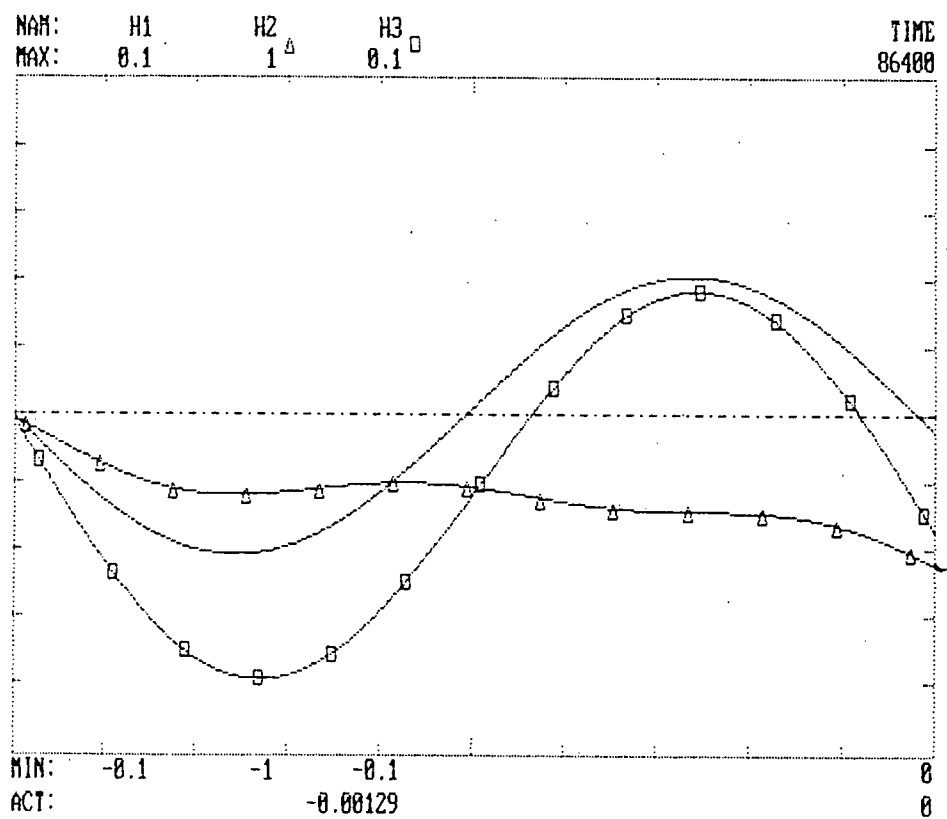
figure 8.23
Angular momentum of the wheels, H1, H2 and H3 in x, y and z
direction (no coupling).

MIN: -5E-5   -5E-5   -5E-5   0
ACT: 4.383E-8   0
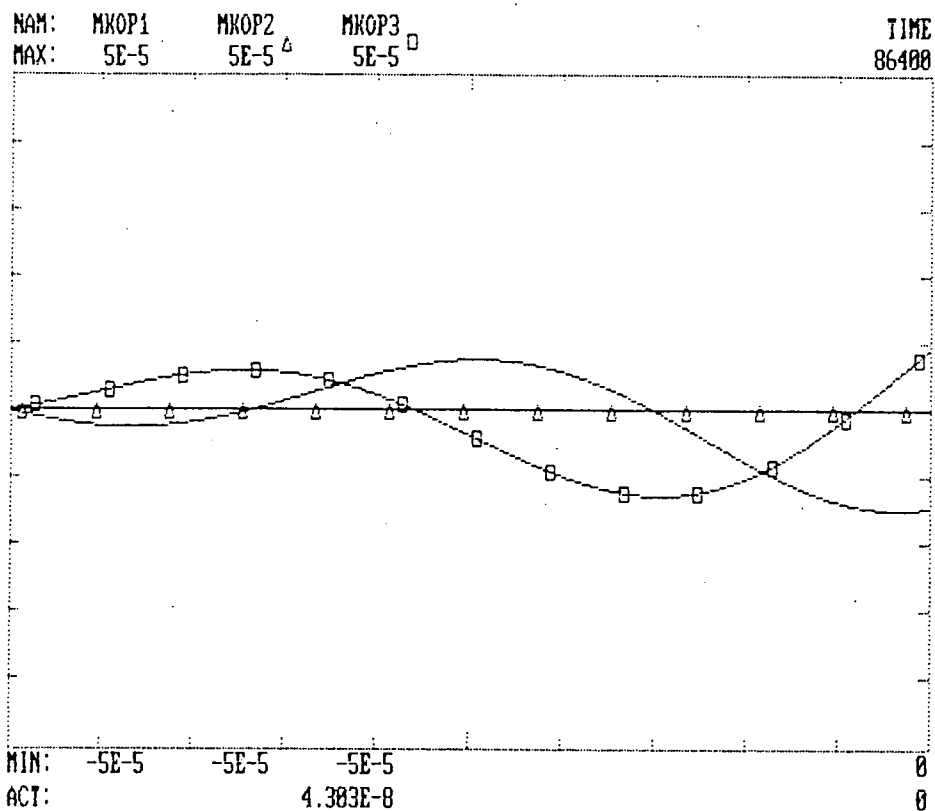
figure 8.24
Coupling terms MKOP1, MKOP2 AND MKOP3.

MIN: -5E-6   -1E-5   -5E-6   0
ACT: -5.41E-7   0
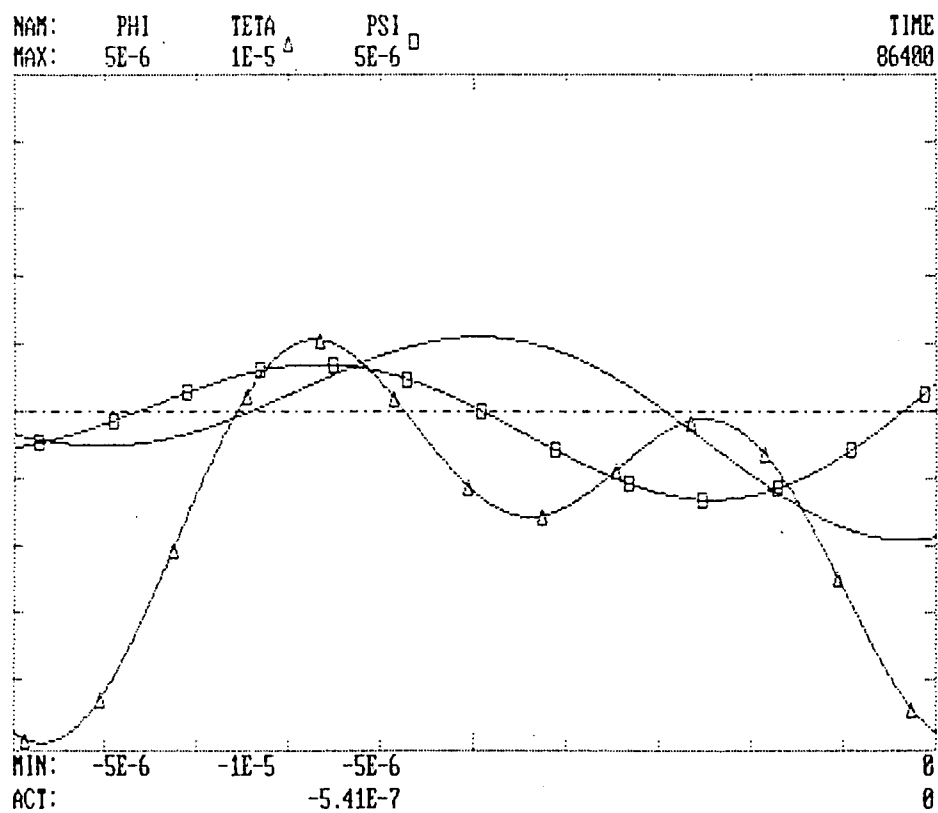
figure 8.25
Angle error roll (PHI), pitch (TETA) and yaw (PSI) with coupling
terms.

The results can be seen in figure 8.27, figure 8.28 and figure 8.29. Because the wheels have a maximum reaction torque of 0.1 Nm, they can not compensate immediately the applied torque M_c. So the error angles are increasing very rapidly to very high amounts of about 0.3° to 0.4°, over the y-axis even to 2°.
After 40 sec the angles have again allowable values. So during a short time the required accuracy isn't achieved.

There are some options to get a, probably, better desaturation procedure; for example:

- Other thrusters can be used, like cold gas jets, with a lower thrust. The wheels then keep the angle errors within a smaller limit because they can better react on the given torque M_c. This, of course has great consequences for the propulsion subsystem and with that, also for the total configuration.

- The thrusters "can" be placed closer to each other. In this way they give a smaller torque then before. This, however, also has great consequences for the total configuration.

- The given torque can be made twice as small as before by using only one thruster. Now, the wheels are more capable to keep the angle errors within smaller limits because they can better react on the given torque (however, M_c is still greater than the maximum reaction torque).

By using one thruster, the orbit of the S/C is disturbed also. But, because the thruster is working for a very short time, this is probably acceptable. For the configuration it doesn't have really consequences.

- As said before in section 8.6, the maximum reaction torque is set at 0.1 Nm. The wheels, however are capable to give a torque of 0.2 Nm maximal,
So the maximum reaction torque can be set at a higher level. But, as a result, the reaction wheels will consume more power during desaturation. This can have serious consequences for the power subsystem.

NOTE:

The configuration of the thrusters is changed after the simulation of this subject.
In this configuration the thrusters for yaw-control are standing closer to each other (about 1 m). This means, they give a smaller torque. So they have to burn for circa 0.2 sec. For the accuracy of the system this only can give a better result, so it isn't worked out in this report.

MIN: -0.5   -1   -0.5   0
ACT: -0.00129   0
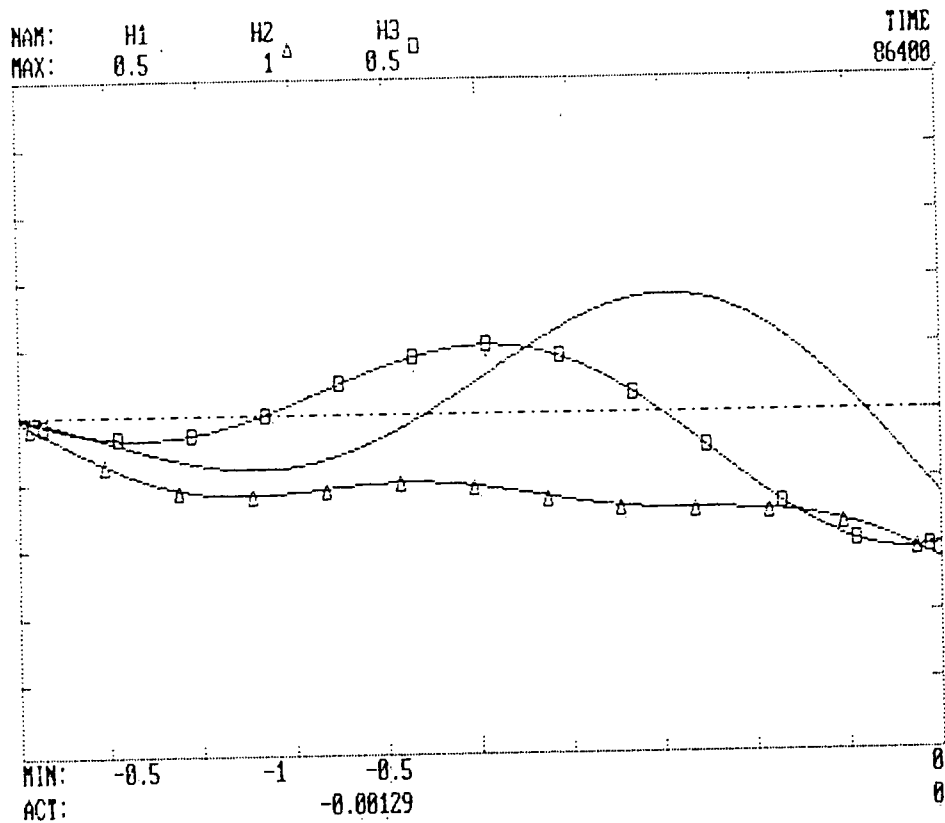
figure 8.26
Angular momentum of the wheels. H1, H2 and H3 with coupling
terms.

MIN: -0.01   -1   -0.1   0
ACT: 0.1   0
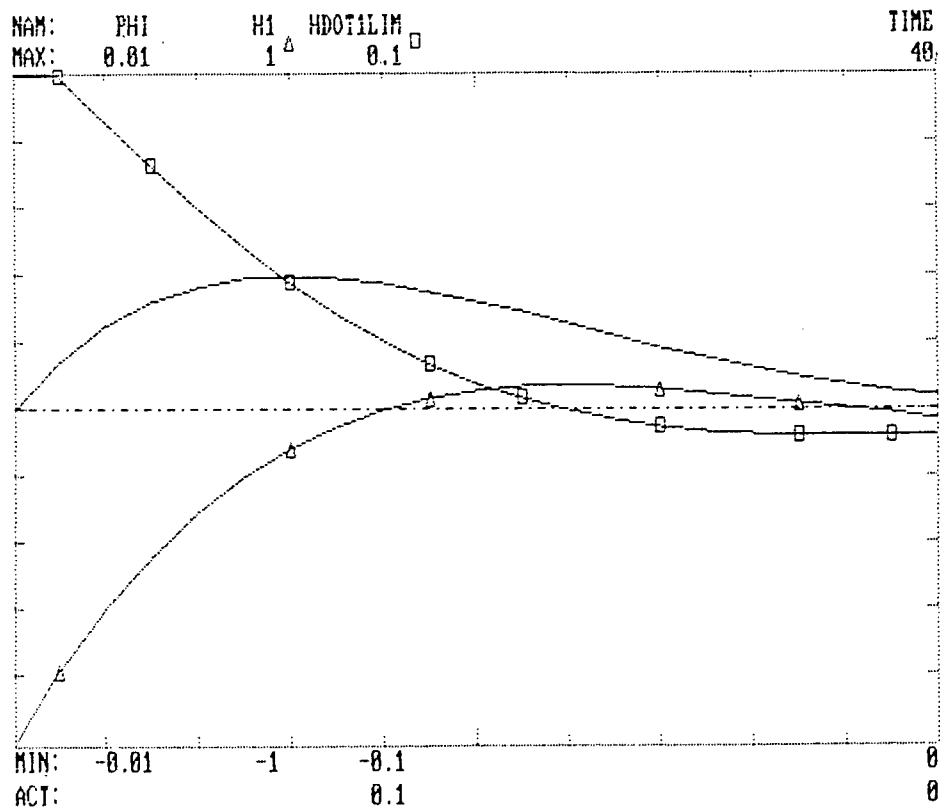
figure 8.27
Desaturation of RW in x-axis (PHI = angle error, HDOT1LIM =
reaction torque with max. 0.1 Nm, H1 = angular momentum of RW).

8.10   Conclusions.

From the results of the simulations, some conclusions can be made. At first can be said that the subsystem is working good in the normal mode. It is advisable, however, to study on the effects of stiction on the attitude of the S/C.

In the desaturation mode there are troubles. The amount of the error-angles is in principle unacceptable. In a further development of this project it is important that a solution for this problem will be found. Some options are given in the previous section.

In the station keeping mode, the attitude control is done by the ACT. Because also in this mode relatively large torques are used, it is advisable to study how this system has to be controlled.

Another subject for further study is the reliability of the subsystem and the capability of the subsystem to react on some predictable failures.

Assuming that the previous problems can be solved and looking at the given error list (Table 8.4), it can be said that the described AOCS-subsystem in this chapter is capable to ensure a ABP-accuracy of $\pm 0.3^\circ$.

The demands made upon the structure are then realistic.

```
NAM:    TETA        H2   HDOT2LIM              TIME
MAX:    0.05         1      0.1                 40
```

```
MIN:   -0.05        -1     -0.1                  0
ACT:                        0.1                  0
```
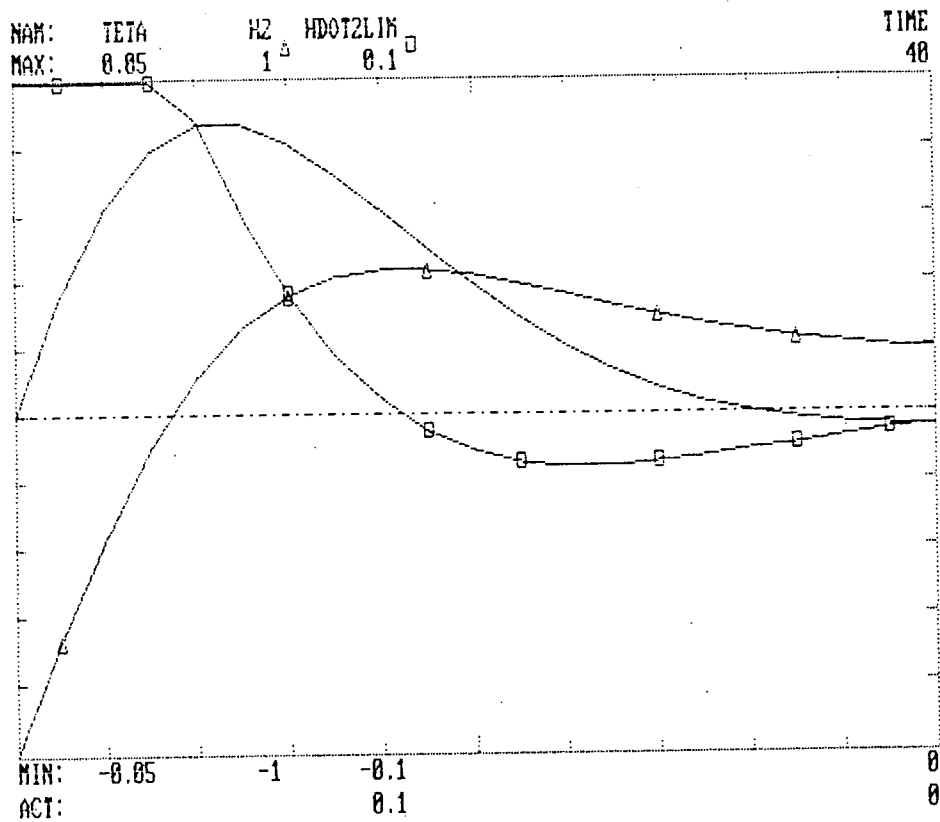
figure 8.28
Desaturation of RW in y-axis (TETA = angle error, HDOT2LIM =
reaction torque with max. 0.1 Nm, H2 = angular momentum of RW).


```
NAM:    PSI         H3   HDOT3LIM              TIME
MAX:    0.01         1      0.1                 40
```

```
MIN:   -0.01        -1     -0.1                  0
ACT:                        0.1                  0
```
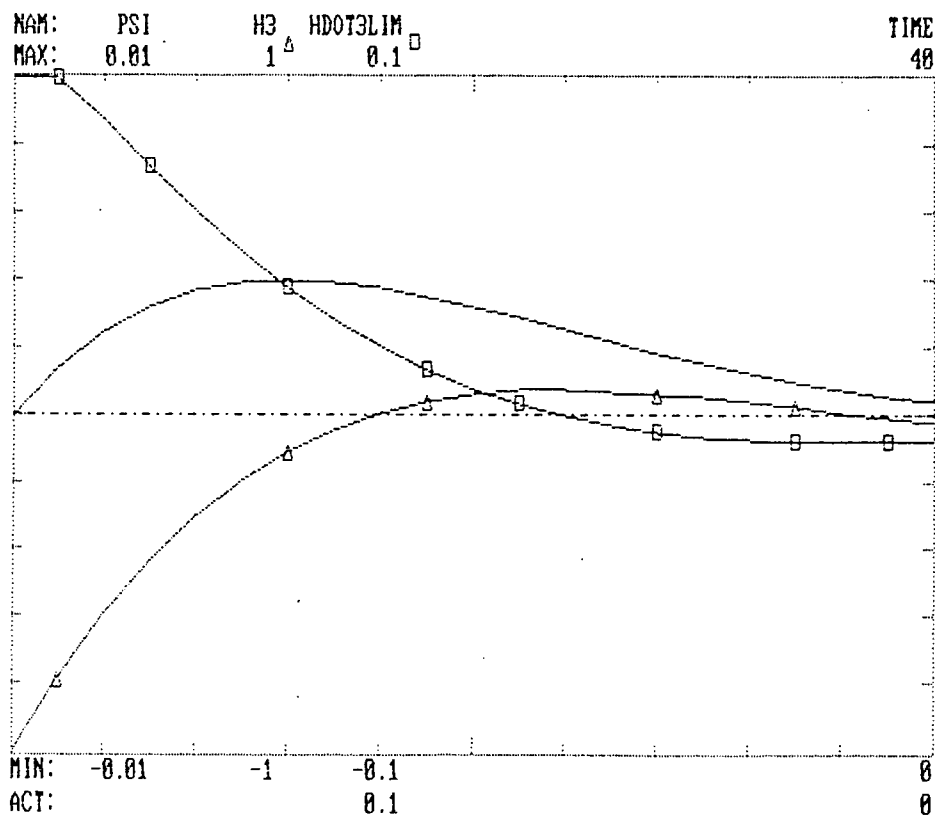
figure 8.29
Desaturation of RW in z-axis (PSI = angle error, HDOT3LIM =
reaction torque with max. 0.1 Nm, H3 = angular momentum of RW

N

TITANIUM INSULATED
SUPPORTS +

MLI +
TITANIUM LAYER

S

23°
S

MULTILAYER
INSULATION = ML

S

BLACK PAINT
e=0.95
S

OPTICAL SOLAR
REFLECTOR = OSR
a=0.08 BOL
a=0.15 EOL

HEATERS +
THERMISTORS

S

INSULATION

Z

WHITE PAINT
a=0.2 BOL - a=0.6 EOL
e=0.85

HEAT PIPES
HEAT SINKS

MLI

HEAT SHIELD
(TIODIZED TITANIUM)
a=e=0.6

INSULATED TITANIUM SUPPORT

e=0.22
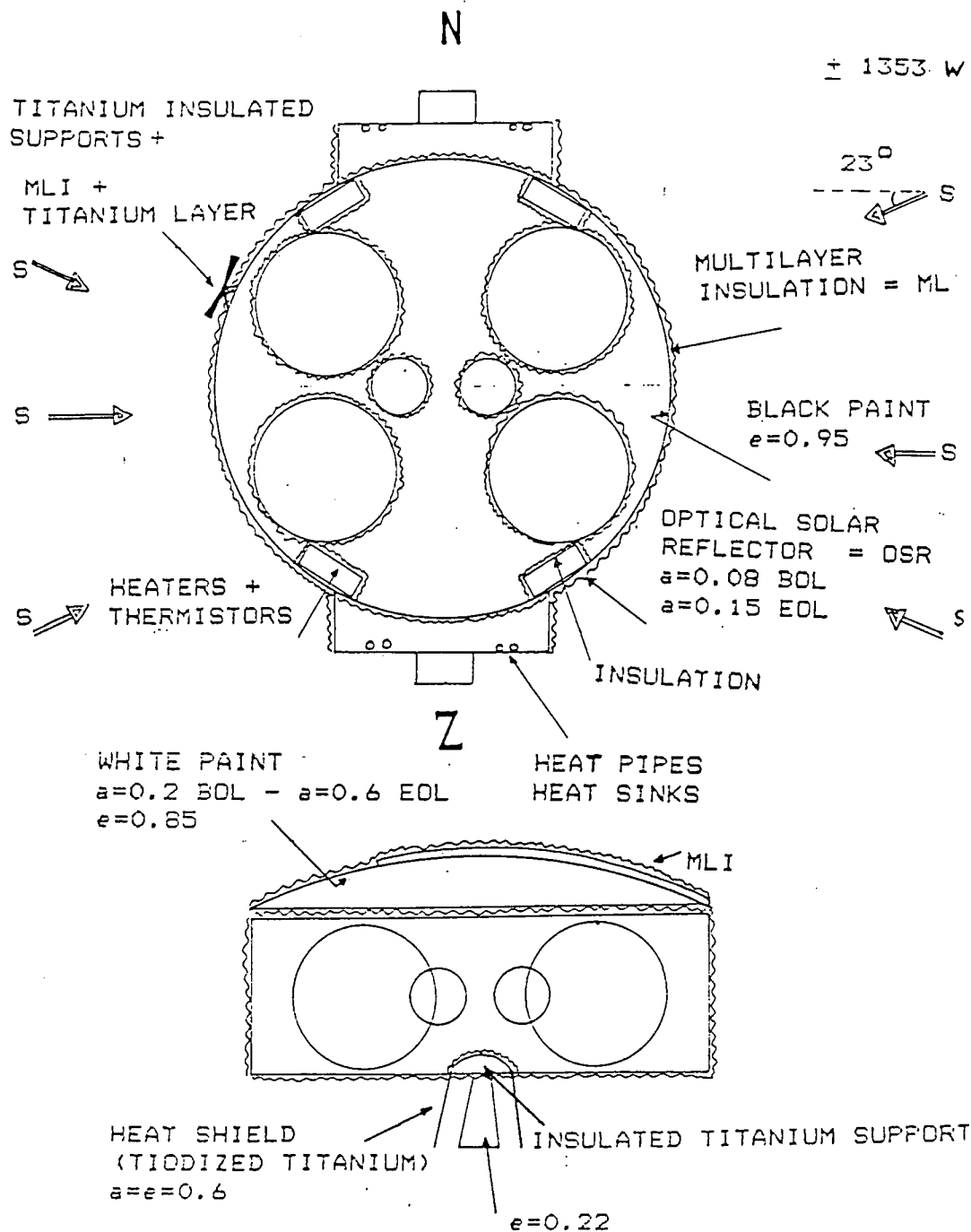
figure 9.1
Thermal subsystem.

9   Thermal control.

9.1   Introduction.

The following handles about the thermal control during the operational phase, the transfer orbit and in-orbit storage. Unfortunately there is no time to look at all aspects of thermal control. For instance no study has been done about manufacturing, or about the MLI-suport structure.

Mainly the operational phase of the batteries, antenna, thrusters, main engine, solar panels, TWT's and EPC's is studied, also a massbudget and an overall design was made.

During the operational phase the thermal loads are the highest. The sun shines most of the time fully on the satellite, and the payload dissipates a lot of heat. Other principal phases of the mission are pre-launch and launch. Before launch the temperature can be regulated by airconditioning. During launch the temperature in the fairing is influenced by the rocket motors, by dynamic pressure and by friction heat. But the temperature in the fairing changes with a certain inertia, so it will not reach extreme values. During separation the satellite will be protected from aerodynamic flux by the upper satellite.

9.2   Subsystem design.

See figure 9.1

9.3   Specification and requirements.

The specification is to design and analyze the thermal control subsystem for the principal phases of the mission assuming a payload heat disipation of 70 % of the power.

The satellite design shall be such that satisfactory temperature environments shall be maintained for all components during pre-launch operation, launch, separation sequences, pre-operational and operational stages of the mission including eclipse periods plus in orbit storage. The thermal control shall be by passive means, i.e. excluding moving parts, but may include heaters with automatic control with ground command override capability. The thermal system shall be designed to maintain all equipments within operating in-orbit temperature units with a design margin of 10 degrees Celsius between these ranges and those over which the equipments are to be qualified.

The optimum operating temperatures of the equipment are given in table 9.1.

RECEIVER
MULTIPLEXER
TWT's
EPC's
ANTENNA
BATTERIES
OTHER ELECTRICAL UNITS
SAS
OSS
CASS
GYRO
REACTION WHEELS
WHEEL DRIVE ELECTRONICS,
FUEL AND OXIDIZER AND PIPES
AND APOGEE MOTOR
HELIUM TANKS
SOLAR PANELS   SUMMER/WINTER
                   SPRING/AUTUMN
                        ECLIPS
STRUCTURE MECHANISM

-160 -140 -120 -100 -80 -60 -40 -20 0 20 40 60 80

(^{o}C)

figure 9.2
Operating temperatures of the subsystem.
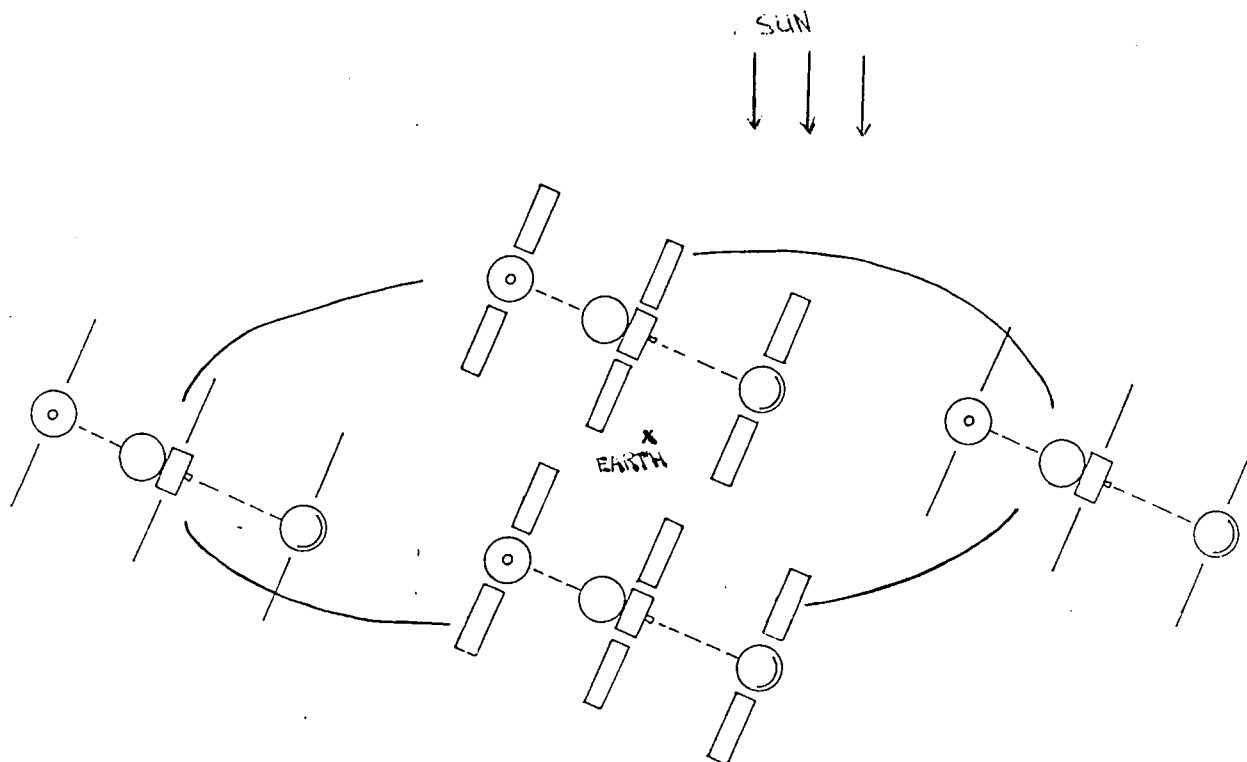
figure 9.3
Satellite position with respect to the sun.

9.4 Heat input.

EXTERNAL HEAT INPUT:

SPACE TEMPERATURE	T	$= 4$ K
SOLAR RADIATION	S	$= 1353 \pm 13.5$ W/m2
		(seasonal variation)
ALBEDO	I_a	$= IaO \ (R/r)^2$ W/m2
	I_{aO}	$= 420$ W/m2
	r	$= 42241.08$ km
	R	$= 6378.139$ km
	I_a	$= 9.579$ W/m2
EARTH RADIATION	I_e	$= IeO \ (R/r)$ W/m2
	I_{eO}	$= 300$ W/m2
	I_e	$= 6.840$ W/m2

INTERNAL HEAT INPUT:

PAYLOAD	340 W	*	70 %	=	315	W
OTHER SUBSYSTEMS	300 W	*	10 %	=	30	W
	750 W				345	W

Consider an infinitely conductive and therefore isothermal, cylindrical shaped spacecraft in a geosynchronous orbit.

This cylinder has a diameter of 1920 mm and a height of 650 mm.

The albedo and earth radiation is negligible compared to the solar heat flux. The solar input on this cylinder depends on the radiated surface As. (figure 9.3)

1. As $= 0.65 * 1.92 = 1.25$ m2
2. As $= \pi * 0.96^2 * \cos 23^\circ + 0.65 * 1.92 * \sin 23^\circ = 3.15$ m2
3. in eclipse As $= 0$, else As is 1.25 m2
4. As $= 3.15$ m2

The total radiating surface is

$$At = 2 * \pi * 0.96^2 + 2 * \pi * 0.96 * 0.65 = 9.71 \text{ m2}$$

With the formula

$$\alpha_s * S * As + P = \epsilon * \sigma * Tb^4 * At$$

we can calculate a body temperature.

a = solar absorption coefficient
S = solar flux = 1353 W/m2
P = dissipated heat = 345 W
ϵ = emission coefficient
σ = Stephan Boltzmann constant = 5.6703e-08 W/Km2

Suppose the outside of the cylinder is covered with a thermal insulation layer of aluminized kapton $\epsilon = 0.1$ and the with optical solar reflector (OSR) $\alpha_s = 0.15$ EOL, you get a maximum body temperature Tb = 365 K.

1.Coatings

	BOL		EOL	
	α	ϵ	α	ϵ
BLACK PAINT	0.9	0.9	0.9	0.9
WHITE PAINT	0.2	0.85	0.6	0.85
OSR	0.08	0.8	0.2	0.8
AL. TAPE	0.12	0.06	0.18	0.06
ANODIZED AL.	0.2	0.8	0.6	0.8
SOLAR CELLS	0.7	0.8		
TIODIZED TITANIUM	0.6	0.6		

2.MLI

T<150°C   : 22 SHIELD DOUBLE SIDED ALUMINIZED MYLAR WITH
                 "SUPERFLOC" SPACER

$$K_{eff}=1.5*10^{-4}$$

T>150°C,T<350 C : 22 SHIELD DOUBLE SIDED ALUMINIZED MYLAR WITH
                  "SUPERFLOC" SPACER
                  WITH AN OUTER LAYER OF D.S.A. KAPTON

T>350°C,T<1200 C: 22 SHIELD DOUBLE SIDED ALUMINIZED MYLAR WITH
                  "SUPERFLOC" SPACER
                  WITH AN OUTER LAYER OF TITANIUM

ALL MLI. BLACK PAINTED ACCEPT THE FIRST ONE.

3. INSULATION

- TITANIUM : K= 7.4 W/m²
- FOAM   : K= 0.1 W/m²

Table 9.6: Thermal control materials.

This is far above the desired temperature of ca. 293 K.
If the whole outside of the satellite would be a better radiating surface this
temperature can be reached. With As = 3.15 m2, ε = 0.24

This can be reached, but it means that for instance in the eclipse when
the solar radiation is zero, there has to be a lot of heat input by heaters to
keep the body at a reasonable temperature, because with ε = 0.24 the body is
not so well isolated.

There are some remarks on this solution. The heat is not spread equally
over the cylinder. Locally very high and very low temperatures will be
reached.
The side radiated by the sun will be much warmer than the other side, and
some of the equipment radiates much more heat than others.

DISSIPATED HEAT

		(WATT)	EFFICIENCY
PAYLOAD			
RECEIVERS		2.5	
MAIN AMPLIFIERS	10 *	3.0	
CONTROL BOX		1.2	
ALC,FET AMPL.DRIVE-ADJUST	10 *	2.1	
TWT 'S	10 *	16.0	n=55%
EPC 'S	10 *	4.0	
CABLING		0.3	
ISOLATOR,MULTI-PLEXING FILTER	10 *	2.2	
SUBTOTAL		277.0	
TELEMETRY,TELECOMMAND		27.6	n=90%
PROPULSION (apogee kick)		5.3	n=90%
ELECTRIC POWER			
PCU,PCDU,BAPTA,CABLES		1.0	n=90%
AOCS			
IRES		2.2	n=90%
GYRO		3.5	n=90%
THERMAL CONTROL		2.0	n=90%
BATTERY CHARGING		49.0	n=70%
DISCHARGING		16.8	
SUBTOTAL (charging)		90.6	
TOTAL		367.6	

Most of the heat comes from the payload, specially from the TWT's .It is
better to separate these from the other equipment.
This other equipment not dissipating so much heat can be put in a well
isolated place with a constant temperature and must be as less as possible
influenced by solar radiation. The most dissipating elements should be placed
on the north and south side of the satellite. These sides have the lowest
solar input, so a good radiating surface can be made there. If the TWT's are
placed against the cylinder wall there will not be enough space in the
cylinder to place all the equipment in. As a solution for this problem the
extra support structures are made on the cylinder. The batteries have the most
critical temperature range of all. The best is to hold them as near as
possible at a temperature of 15 C.

SUMMER/WINTER   AUTUMS/SPRING
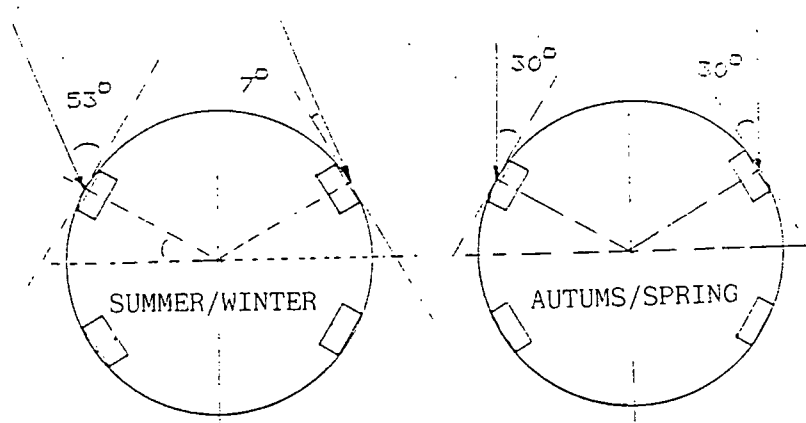
$$a*So*\sin\beta*Arad + Q_b = \varepsilon*\sigma*T_b^4*Arad$$
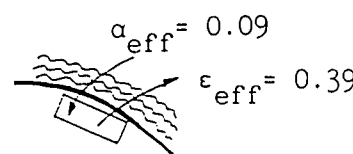
$Arad = 0.0832 \ m^2$ (no conductions)

POWER (W)	T(K)
$Q_b = 0$ $S = 0$	–
$Q_b = 0$ $S = 0$	218
$Q_b = 4.2$ $S = 8.3$	288
$Q_b = 0$ $S = 8.3$	259
$Q_b = 12.5$ $S = 0$	288

$\alpha_{eff} = 0.09$

$\varepsilon_{eff} = 0.39$

MAXIMUM HEATER POWER $\pm$ 40 WATT

figure 9.4

9.5 Thermal control materials and techniques.

The choice of thermal control materials is based on only a few material properties. These properties are the solar absorptance, the emittance, the conductivity k and the thermal capacity. These properties are used in several thermal control techniques.

The techniques used in this design are coatings, insulations, heatsinks and heaters.

The use of coatings is based on the solar absorptance and the emittance. By using a coating we can change the surface conditions. There is an immense variety of coatings. The most commonly used are mentioned in Table 9.1.

Insulations can be subdivided in single homogeneous materials and multilayer insulations. The single homogeneous materials used are foams which have a conductivity of 0.03-0.6 W/m.K. In the insulated supports, titanium is used. Titanium has a very low conductivity of 7.4 W/m.K.

The MLI used, for normal temperatures (< 150 C), is a 22 shield double-sided aluminized mylar with "superfloc" spacer. For higher temperatures (<350 C) an outer aluminized kapton layer is used. For extreme temperatures an outer layer of titanium or stainless steel with a coating is used. The MLI is defined by the coefficient k_{eff} which can be used in the formula:

$$Q = k_{eff} \cdot (T_H - T_C) * A/l$$

Q : transferred heat.
$T_{C,H}$: boundary temperatures.

The coefficient k_{eff} depends not only on the used materials but also on the effect of joints, evacuation holes, support structures etc. In Table 9.1 the used MLI are mentioned. The MLI are chosen after a detailed literature study. The mentioned values of k_{eff} are average values including the effects of evacuation holes, joints and support structure.

Materials with a large thermal capacity are used as heatsinks. These materials are placed in thermal contact with the temperature controlled component. The heatsink absorbs the heat from the component and transfers it to low temperature components or heat radiators. In this design aluminum alloys are used as heatsinks.

Heaters are used to keep specific elements above a required minimum temperature.

9.6.1 The batteries.

The north and south sides of the satellite are the best locations to place the batteries. These sides have the least change in solar input, so they have the most constant temperature. But on the north and the south side the extra support structure is placed to put the TWT's and EPC's in. The batteries can not be placed behind this structure, for that means that they don't have a radiation surface, which they need to get rid of the produced heat during charge and discharge.

As a solution for this problem there are four batteries placed in on the cylinder wall as shown in figure 9.1.

The solar input on the radiation surfaces is seen in figure 9.4.

There are 5 critical phases the battery can be in. These phases are given in the table below. To calculate the battery temperature the following formula has been used.
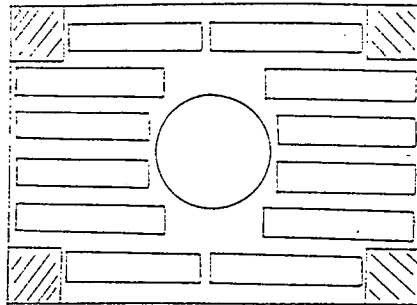
TWT 5*16 WATT
EPC 5* 4 WATT

1 TWT   16.0 + a*A*S*sin23° = e*s*Tb^{4}*Aeff*0.94

a=0.15
e=0.9
Tb=317-377 K
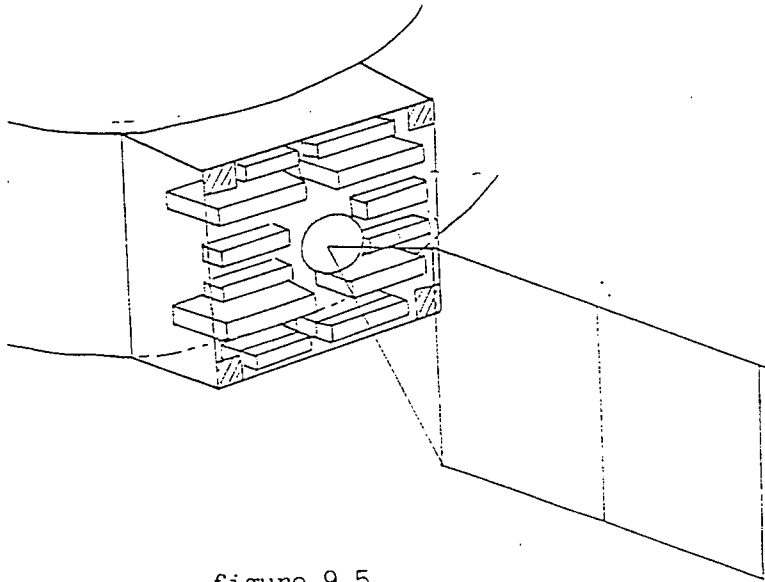
figure 9.5

$$\alpha * So * \sin 53^{O} * Ar + Qb = \epsilon * \sigma * (T + \Delta T)^{4} * A$$

α = solar absorption coefficient
Ar = radiator surface
A = total battery surface
Qb = dissipated heat of the batteries
$\Delta T = \frac{Qb*t}{k*Ar}$ = temperature difference in\outside radiator
k = 0.121 W/mmK
t = 1 mm

ΔT is neglectible compared to T
Ar is a variable. It should be taken so that a temperature of ca. 288 K is reached.

Heater power needed is maximal 4 * 12.5 = 50 W

9.6.2 The TWT'S and EPC'S.

To radiate the heat, dissipated by the TWT's an extra support structure is placed at the north and south side of the cylinder. The EPC's are placed close to the TWT's to avoid power loss. The radiating surfaces have an emission coefficient ϵ = 0.9. Between the extra support structure and the cylinder there is an insulation layer.

The TWT's and the EPC's are placed in the extra support structure as shown in figure 9.5 The extra support structere has a maximum size because there has to be a free piece of the cylinder to make a radiator surface for the batteries (see figure 9.4). The maximum size of this surface can be 0.65 * 0.9 m2. There are several possibilities to place the TWT's and the EPC's on this surface, only one is shown in figure 9.5.

```
TWT  5 *  16.0 WATT
EPC  5 *   4.0 WATT+
          100.0 WATT
```

The maximum solar input on the box is

$$S = So * \sin 23^{O} * \alpha_s * As$$

Sizes of a TWT : 50 * 60 * 300 mm3
Sizes of an EPC : 330 * 60 * 150 mm3
Bapta diameter : 250 mm
conductioncoefficient of AlMg k= 1.55 W/cm C

Only 10 of 12 TWT's operate at the same time. The others are for redundancy. Every TWT has a certain surface That can be used as a radiation surface. For one TWT this is ca.0.120*0.325 = 0.039 m2. For one EPC this is 0.330*0.0060= 0.020m2.

With the radiation formula we get for the highest solar radiation
$$16.0 + \alpha * A * S * \sin 23^{O}= \epsilon * \sigma * Tb^{4} * A * 0.94$$

Tb = 317 K
Without sun radiation Tb = 361 K
(6 % radiation loss because of the solar panels).

MLI → White paint (α=0.2 (BOL) - 0.6 (EOL), ϵ=0.85)

Q_1

Q_2

Q_4

Q_3

INSULATED TITANIUM SUPPORTS

Q_5
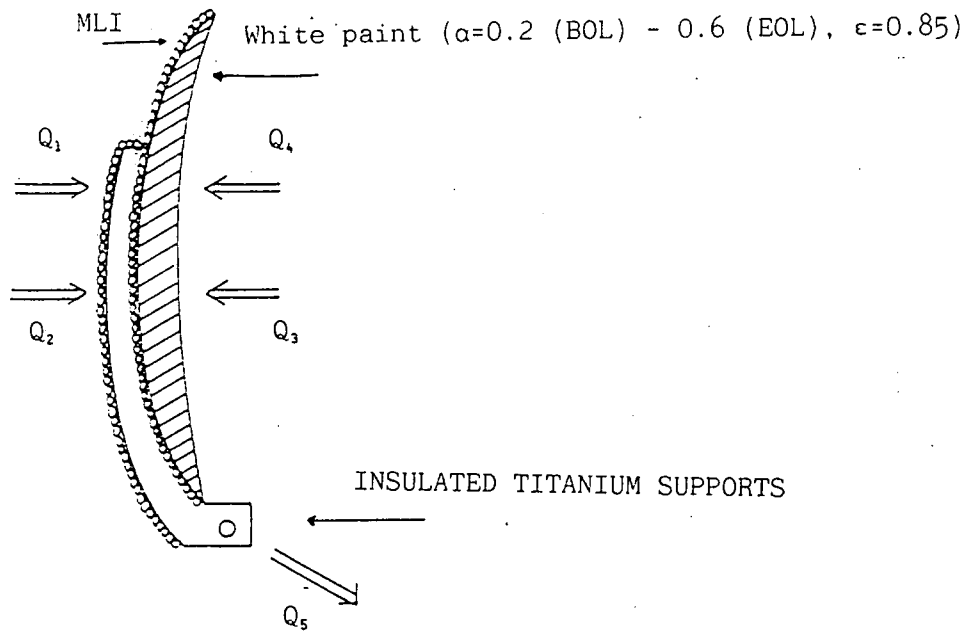
$Q_1 = Q_2 = 0$

$Q_3 = \alpha*S*A$

$Q_4 = \epsilon*\sigma*T^4*A$

$Q_5 = k*(T_{sat}-T)/A$

$A = 2.5$ m^2

$A = 3.0$ m^2

$T_{sat} = 288$ K

figure 9.6
Antenna model.

But because the heat doesn't spread equally, the effective radiation surface is only half of the available surface. Near to the collector of the TWT there is a peak temperature.

Now the temperature Tb is 377 K!

To reduce this peak temperature and to make the effective radiation surface higher than 0.5, the heat has to be spread by use of two methods:

- The wall can be made thicker
- Heat pipes can be placed

For the EPC's the formula is

$$4.0 + \alpha * Ar * So * \sin 23^\circ = \varepsilon * \sigma * Tb^4 * A * 0.94$$

A=0.020 m2	Tb = 276 K
Aeff=0.010 m2	Tb = 316 K
Shadow	Tb = 254 K

Because a margin of 10 K is needed the EPC's too will be too warm and the effective radiator surface has to increase. In the shadow heaters are needed to keep TWT's and EPC's at the right temperature.

The heater power in the shadow

3.1 W per TWT *5
1.6 W per EPC *5
23.5 W + 20 % = 28.2 W

9.6.3 The antenna.

To keep the temperature of the antenna within the temperature limits the following measurements are taken:
1. The front side is painted white.
2. The rear side is covered with MLI.
3. Insulated supports.
The temperatures were calculated for the model in figure 9.6 in eclipse and in maximum sunlight and both for BOL and EOL.

A. in eclipse.
The temperature of the dish must be higher than 110 K this means that from the equation:

$$\varepsilon * \sigma * T^4 * A = k * \Delta dT * A/l \qquad A : \text{insulated support surface.}$$
$$l : \text{Length of A.}$$
$$0.85 * 5.67 * 10^{-8} * 110^4 * 2.5 = 7.4 * 178 * A/l$$
$$A/l = 0.014$$

So if the titanium isolated supports have an A/l = 0.014 then the temperature of the antenna will not be lower then 110 K
This temperature will be the same at EOL as at BOL.

MAIN ENGINE

INSULATED SUPPORTS
(titanium struts)
1. L = 0.1 - 0.2 M
2. t = 1 mm
3. A = 0.002 m²

MAIN ENGINE (T=338 K)

PLATFORMS (T=288 K)

A_1

Q_1

A_3

Q_2

A_2

Q

A_4

NOZZLE (α=0.22 ; T=1200 K)

HEATSHIELDS (α=ε=0.6)
A_1 = 0.14 m²
A_2 = 0.35 m²
A_3 = 0.13 m²
A_4 = 2.2 m²
Q_1 = 3400 W
Q_2 = 790 W (eclips)
       1681 W (sun)

MLI (α=ε=0.9)
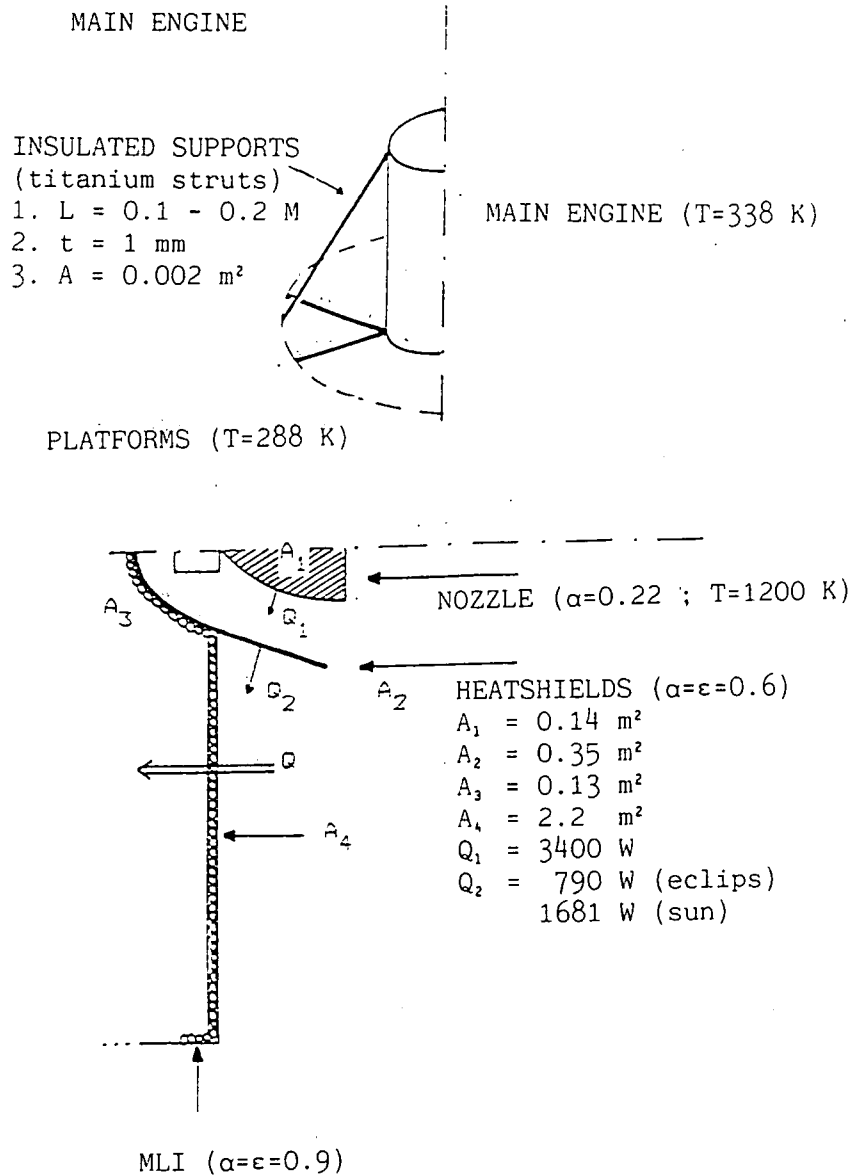
figure 9.7
A main engine model.

B. in sun.
The temperatures can be calculated from the Equilibrium equation:

$$\alpha * S * A = \epsilon * \sigma * T^4 * A + k * \Delta T * A / l$$

BOL: $0.2*1350*2.5=0.85*5.67*10^{-8}*T^4*3.0 +7.4*dT*0.014$
T = 264

EOL $0.6*1350*2.5=0.85*5.67*10^{-8}*T^4*3.0 + 7.4*dT*0.014$
T = 350 K

These temperatures are within the required temperature limits.

9.6.4 Thrusters and main engine.

During the operational phase of the main engine and the thrusters, energie in the form of heat is produced. To avoid heattransfer to the rest of the satellite the engines must be isolated. To give an impression of the temperatures and dissipated heat calculations were made for the models in figures 9.7 and 9.8.

1.CONDUCTION
To avoid heat conduction the engines are placed on insulated supports. For these supports, titanium is used. The heat conduction for the model of the main engine then becomes approximately with the formula for conduction:

$$Q=k*(T_H-T_C)*A/l$$

$$Q=7.4*40*8*0.0002/0.1 + 7.4*40*4*0.0002/0.2 = 6.0 \text{ W}$$

and for each thruster:

$$Q=7.4*40*4*0.0002/0.12 = 2.0 \text{ W}$$

To avoid high temperatures at the fastening points at the satellite the heat has to be spread out. The thrusters are fastened on the aluminum ring. The aluminum ring has a high conductioncoefficient and works as a heatsink so the heat is not concentrated at the fastening points. The main engine is fastened in the middle of the satellite. The ring where the titanium bars are attached to is also made of aluminum so the heat can spread trough the platform.

2.RADIATION
To avoid heat radiation to the satellite, the satellite must be protected with MLI and radiation shields. There is already a MLI around the outside of the satellite. In the neighborhood of the thrusters, this MLI only has to be adjusted to the higher temperatures of the thruster.Around the main engine a heatshield is placed and the MLI near the heatshield must be adjusted to the higher temperatures. These temperatures can be calculated for the models in figures 9.7 and 9.8 with the equations for the radiation and absorbtion.

Main engine: Temperature A_2:

Eclipse: $0.6*Q_{1-2} = 0.6*5.67 \; 10^{-8}*T^4*2A_2$

$0.6*2625=0.6*5.67*10^{-8}*T^4*2*0.35$
T=507 K

INSULATED SUPPORTS

THRUSTERS

TITANIUM l = 0.12   m
          t = 1   mm
MLI   A = 0.0002 m²

T_{sat} = 288 K

γ_1 = 10°
γ_2 = 71°
Q_1 = 500 W
Q_1-_2 = 3.8 W
Q_1-_3 = 175 W
A_2 = 2.4*10^{-4} m²
A_3 = 0.28 m²

Q_1

γ_2 γ_1 Q_1-_3

A_2 Q_1-_2

A_3
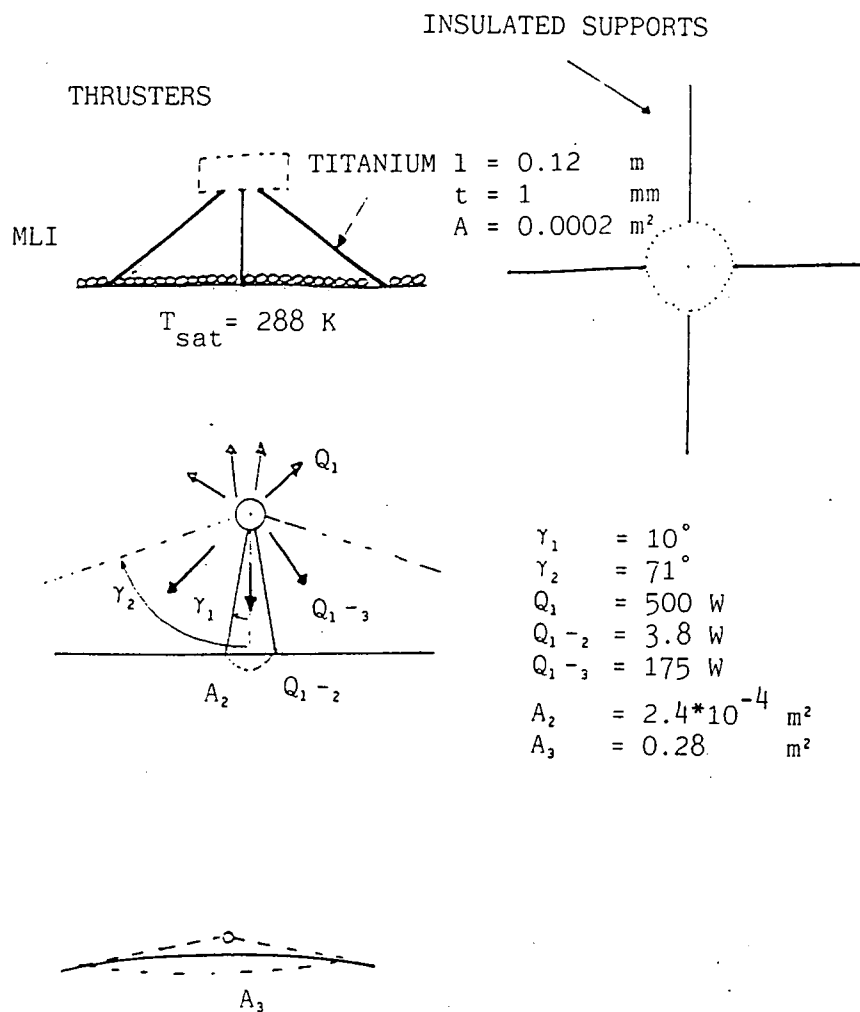
figure 9.8
A thruster model.

Sun : $0.6*Q_{1-2} + 0.6*Q_s*A_s = 0.6*5.67*10^{-8}*T^4*2A_2.$

$0.6*2625 + 0.6*1350*0.125 =$

$0.6*5.67*10^{-8}*5.67*10^{-8}*T^4*2A_2$

$T=515$ K

Main engine: Temperature A_3:

Eclipse: $0.9*Q_{1-3} = 0.9*5.67*10^{-8}*T^4*A_3$

$0.9*450 = 0.9*5.67*^{-8}*T^4*0.14$

$T=485$

Sun : $0.9*Q_{1-3} + 0.9*Q_s*A_s = 0.9*5.67*10^{-8}*T^4*A_3$

$0.9*450 + 0.9*1350*0.045 = 0.9*5.67*10^{-8}*T^4*A_3$

$T=504$ K

Temperature A_4:

Eclipse: $0.9*Q_{2-4} = 0.9*5.67*10^{-8}*T^4*A_4$

$0.9*480 = 0.9*5.67*10^{-8}*T^4*2.2$

$T=282$ K

Sun : $0.9*Q_{2-4} + 0.9*Q_s*A_s = 0.9*5.67*10^{-8}*T^4*A_4$

$0.9*480 + 0.9*1350*2.1 = 0.9*5.67*10^{-8}*T^4* 2.2$

$T= 404$ K

Thrusters: Temperature A_2:

Eclipse: $0.9*Q_{1-2} = 0.9*5.67*10^{-8}*T^4*A_2$

$0.9*175 = 0.9*5.67*10^{-8}*T^4*0.28$

$T= 324$ K

Sun : $0.9*Q_{1-2} + 0.9*Q_s*A_s = 0.9*5.67*10^{-8}*T^4*A_2$

$0.9*175 + 0.9*1350*0.22 = 0.9*5.67*10^{-8}*0.28$

$T=415$ K

Temperature A_3:

Eclipse: $0.9*Q_{1-3} = 0.9*5.67*10^{-8}*T^4*A_3$

$0.9*3.8 = 0.9*5.67*10^{-8}*T^4*2.4*10^{-4}$

$T= 727$ K

Sun : $0.9*Q_{1-3} + 0.9*Q_s*A_s = 0.9*5.67*10^{-8}*T^4*A_3$

$0.9*3.8 + 0.9*1350*2.3*10^{-8} = 0.9*5.67*10^{-4}*T*2.4*10^{-4}$

T=741 K

The temperatures calculated are average temperatures over the regarded surfaces. The temperature of surface A_4 in the main engine model is higher than 150 C so the MLI must have an outer layer of double sided aluminized kapton. The temperature of surface A_2 in the thruster model is higher than 350 C so the MLI must have an outer layer of titanium or stainless steel.

The extra dissipated heat through the MLI follows from the temperature raise and is for the calculation models :

Thrusters $\Delta(T_3) = 415 - 370 = 45$

$\Delta(Q_3) = k_{eff}* dT * A/1 = 1.5*10^{-4}*45*0.28/0.02 = 0.1W$

Main engine $\Delta(T_4) = 404 - 370 = 34$

$\Delta(Q_4) = 0.72$ W

$\Delta(T_2) = 504 - 296 = 208$

$\Delta(Q_2) = 0.22$ W

This is not as much as the heat dissipation due to conduction.

9.6.5 Solar panels.

For the solar panels again the same radiation formula can be used to calculate the temperatures.

Solar radiation on one side of the panels is on three extreme cases (A=9.026 m^2, α=0.05 , β=0.03)

summer/winter S = α * A * So * cos 23° = 563 W
spring/autumn S = α * A * So = 611.5 W
eclipse   S = 0 W

With The formula:
$S = \epsilon * \sigma * Tb^4 * 2 * A$

the temperatures can be calculated. The temperatures are:
summer\winter: T_b= +46 C

spring\autumn: T_b= +56 C .

eclipse: T_b= -100 C
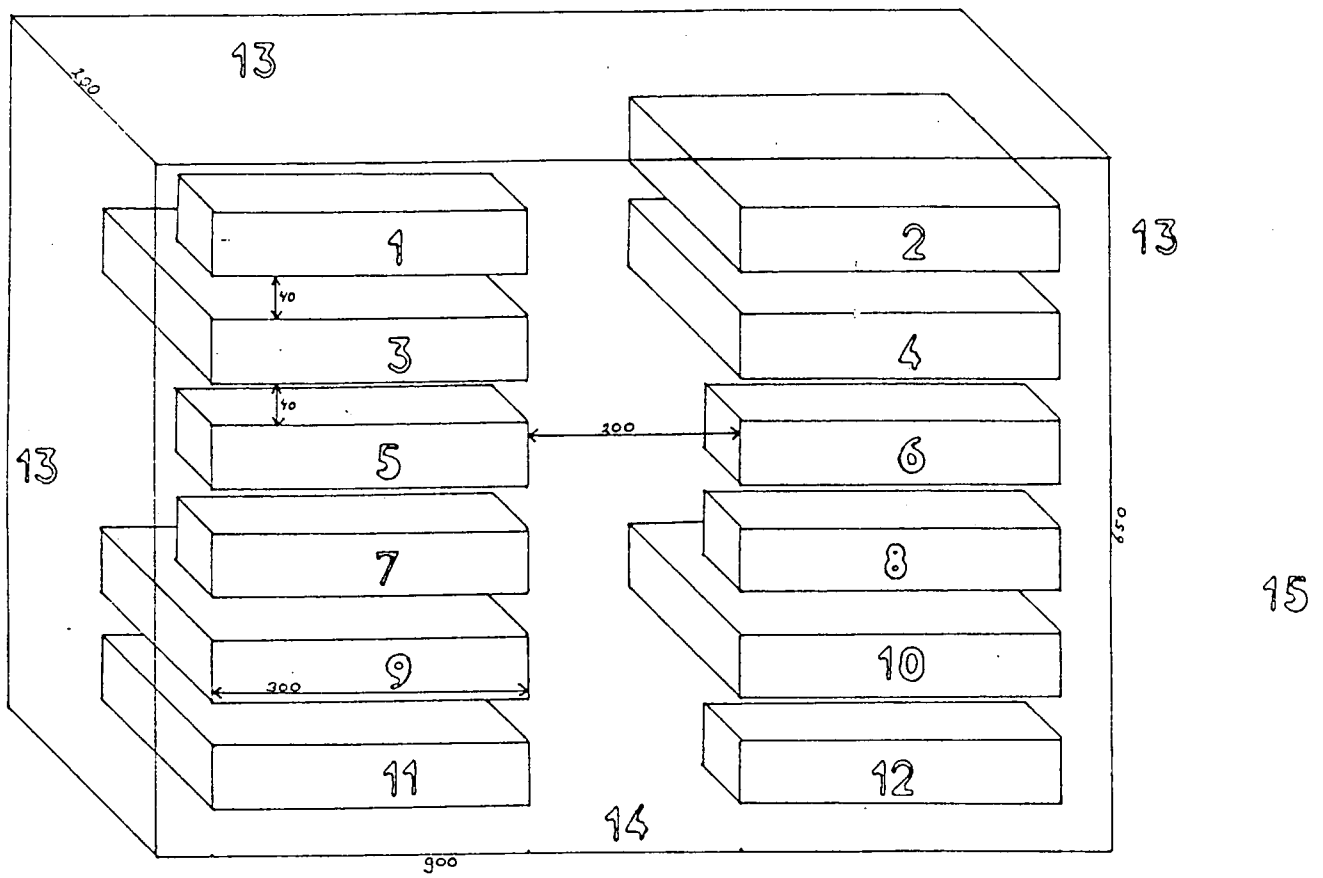
figure 9.9
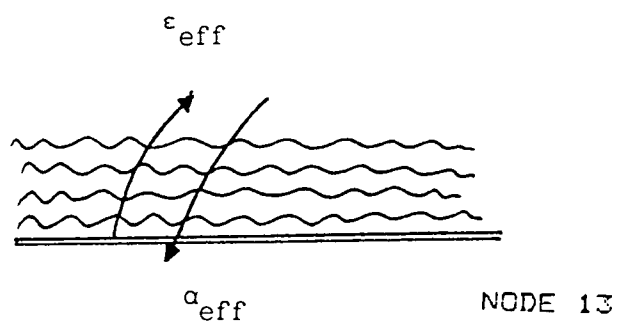
figure 9.10

9.7 Mass calculation.

Blankets:
tanks 0 760 mm * 4	: 7.26 m2
He tanks 0 280 mm * 2	: 0.49 m2
body	$\pi * r^2 * 2$	: 5.09 m2
body	$2 * \pi * r * 0.6$	: 3.39 m2
antenna	$\pi * r^2$	: 2.54 m2

total surface 18.77 m2 a 250 gr/m2 = 4.69 kg

	other blankets	= 3.00 kg
Heat pipes:	5.2 meter a 0.335 kg/m	= 1.74 kg
Painting:	total surface 30 m2 a 40 gr/m2	= 1.20 kg
Heaters:	a 0.369 kg/m2	= 1.00 kg
OSR + hanging		= 8.37 kg
		20.00 kg

9.8 Subsystem verification.

With the aid of a thermal analyzer program the subsystem has been verificated on two areas.
1. The TWT-EPC box
2. The cylinder with the two platforms and the batteries.

To use this program the Gebhard factor (B_{12}) between the several nodes (1->2) should be calculated. This Gebhard factor is defined as the total part of the radiation from node one that falls on node two, with all the reflections. Since this is a very difficult calculation the Gebhard factor has been replaced by the view factor F_{12}. This is the Gebhard factor without the reflection part. This can be done by assuming that the equipment is painted black. The emission coefficient than is $\epsilon = 0.95$, and the reflection can be neglected.

1. The TWT-EPC box

To be able to calculate the view factors, a model has been made from this part of the satellite (see figure 9.9). The made assumptions are:
1. All TWT's and EPC's have the same height and length.
2. There are only radiation couplings in horizontal and vertical directions between the EPC's and TWT's. So node 3 has radiation coupling with node 1,4,5,13 and 14.
3. The outer box (node 13) is assumed to be isolated on all sides except for the frontside (node 14). This is a radiator surface.
4. Node 13 has on the backside a connection with the remaining satellite. Therefore there will be some heat input from the cylinder to node 13, but on the other hand there also will be some heat transfer the other way around. The assumption is that the total heat transfer will be zero, so has not been taken in the program.
5. The TWT's and the EPC's have a full conductive coupling with the radiator (node 14).
6. For node 13 an effective emission coefficient and an effective absorption coefficient have been taken. Node 13 represents the inner side of the blankets (See figure 9.10).

The viewfactors of two surfaces of different sizes are calculated with the following method. (see figure 9.11)
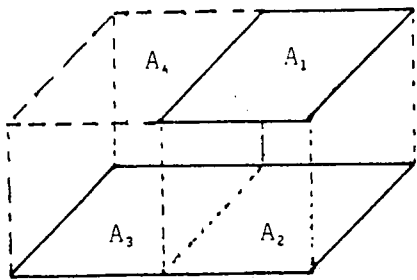
figure 9.11
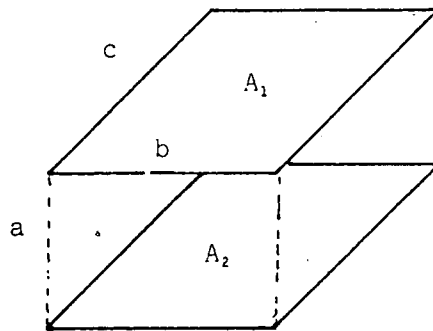
figure 9.12
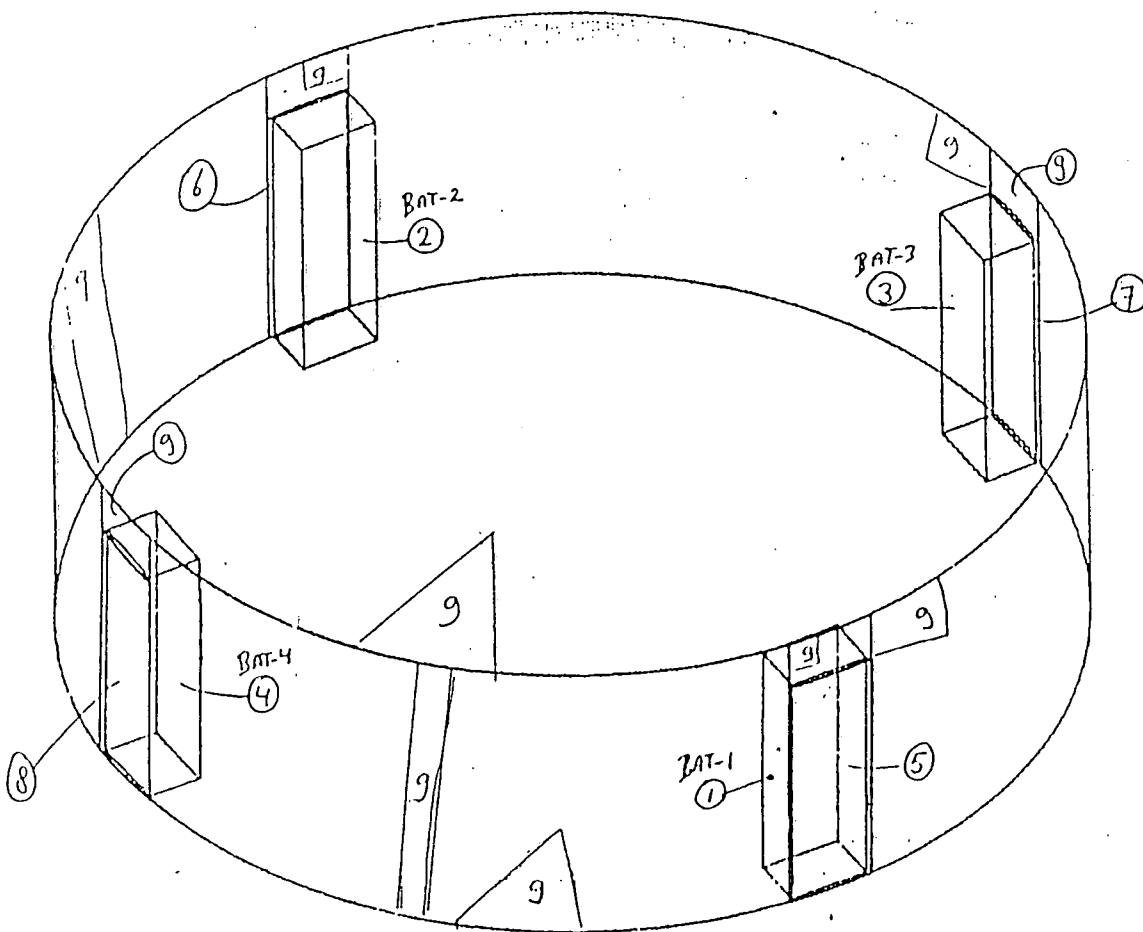
figure 9.13

$$A_1F_{1-23} = A_1F_{1-2} + A_2F_{1-3}$$

$$A_4F_{4-23} = A_4F_{4-2} + A_4F_{4-3}$$

$$\overline{(A_1 + A_4)F_{14-23} = A_1F_{1-2} + A_4F_{4-2} + A_1F_{1-3} + A_4F_{4-3}}^{+}$$

$$F_{4-2} = F_{1-3}$$

$$F_{1-23} = \frac{A_4}{A_1+A_4} F_{1-2} + F_{14-23} - \frac{A_4}{A_1+A_4} F_{4-3}$$

For two parallel surfaces at a certain distance the literature gives the following formula for the view factor (see figure 9.12).

$$F_{1-2} = \frac{1}{\pi} * [\frac{1}{BC} * \frac{\ln XY}{(X+Y+1)} + \frac{2\sqrt{X}}{B} * \tan^{-1}(\frac{C}{\sqrt{X}}) + \frac{2\sqrt{Y}}{C} * \tan^{-1}(\frac{B}{\sqrt{Y}})$$

$$- \frac{2}{C}\tan^{-1}(B) - \frac{2}{B}\tan^{-1}(C)$$

$$B = \frac{b}{a} \ ; \ C = \frac{c}{a} \ ; \ X = 1+B^2 \ ; \ Y = 1+C^2$$

The results of these calculations are given in figure C.1 (see appendix C).

Node 13 receives all the radiation of the TWT's and EPC's that does not go to an other node.

Node 13 and node 14 have radiation couplings with space (Node 15) with respectively $\epsilon = 0.08$ and $\epsilon = 0.5$.

One EPC and one TWT are redundant (node 3 and 8). They have no internal power. The results of the thermalanalyzer program are given in figure C.2.

2. The platform, cylinderwall and batteries.

This model can be seen in figure 9.13. The viewfactors of this model have been calculated with the help of a viewfactor program.

The model contains 10 nodes. Node 9 yields the cylinder wall, the platforms, all the equipment connected to the platforms and the tanks except for the batteries. Node 5,6,7 and 8 are radiators. They are covered with optical solar reflectors.

The radiation coupling is given in figure C.3 and the calculated temperatures are given in figure C.4.

9.9   Conclusions.

From the calculations in paragraph 9.6.1-9.6.5 we see that the temperatures for the models are within the required limits.

There are two reasons why the temperatures in a real-life situation differ from the calculated temperatures. First we calculated with estimated values of α and ϵ. Small changes of these values give relatively great changes for the temperatures.

The second reason why the temperatures will differ is because the calculated temperatures are steady-state temperatures and in a real-life situation it will take some time before these temperatures are reached. In most cases the calculated temperaturelimits aren't reached at all. What the effect will be on the real temperatures follows from a testprogramm.

In paragraph 9.8 we see that there are some temperatures outside the limitvalues. For the same reason as mentioned above the temperatures probably will stay within the limits. Only a testprogramm will show if the temperatures really stay within the temperaturelimits.

From above follows that an intense testprogramm is necessarily to check and correct the thermal control system before it is good enough to be used in a real-life situation.

This thermal control design is however a good system to start with.

From paragraph 9.7 follows that in this stadium of the design the total mass of the system is still within the required budget.

10 Telemetry and telecommand.

10.1 Introduction.

Because datahandling and TTC go hand in hand, it is difficult to clearly distinguish between them. Nevertheless an attempt has been made to divide this chapter into three main parts. Part one called DATAHANDLING (paragraphs 10.2.1 to 10.2.4) gives an impression on the datahandling subsystem which will turn out to be a computer. Part two called TELEMETRY (paragraphs 10.3.1 and 10.3.2) is concerned with an example of the telemetry format and also gives a functional description of the telemetry encoder. The third part called TELECOMMAND (paragraphs 10.4.1 and 10.4.2 gives a brief discussion on the subject of decoding after the ESA command frame has been explained.

In general, a small communications satellite such as the Hitch-Hiker spacecraft, can be functionally divided into two blocks ; basic spacecraft and telecommunications payload, the first representing all the support functions which are needed to allow the operation of the second. Considering both, basic satellite functions as well as payload functions, one may conclude that the subsystem which has to be developed, should be able to perform the following:

- station keeping
  - -attitude control
  - -thermal control
  - -power control

- telemetry data
  - -housekeeping data as listed below, formatting temperatures (structure, equipment, solar arrays) pressures (fuel tanks, plenum chambers)equipment power supply (rail voltages and currents) deployment of mechanisms (parabolic dish, solar arrays, separation from launcher) redundancy status (main or standby equipment in use) operating status of equipment (on or off, operational mode selected)

  - -attitude data
    earth sensors
    gyroscopes

  - -housekeeping check data, used to generate alarms

  - -memory data, to verify whether data coming from ground have been received correctly or not

- telecommand
  - -interpretation and distribution of ground commands
  - -storage of time-tagged commands

As far as TTC is concerned, certain subsystem requirements specified by ESA, have to be met. A summary of these requirements is given below.

- The TTC subsystem shall provide the necessary monitoring and control of the satellite throughout all mission phases including ground system testing, injection into orbit, and operation. The system shall be designed to permit the detection of satellite degradation and anomalous performance during all phases of the mission.

- The TTC subsystem shall retain maximum operational capability under abnormal or emergency conditions including any anomalous attitude.

- The frequencies for the TTC system shall be within the payload frequencies.

- The telecommand format shall provide a means of uniquely addressing each spacecraft of a series so that the probability of commanding another spacecraft of the same series when illuminated by equivalent RF flux density is less than one part in 10e-9. The decoded bit error rate for both telemetry and telecommand services shall be superior to one part in 10e-7 over the nominal range of RF flux to be specified.

- The design of the satellite shall preclude the accidental execution of any hazardous command. Initiation of one shot operations involving hazardous commands shall require at least two separate actions, command and execution, each being verifiable by telemetry.

10.2   Datahandling.

10.2.1 Centralized datahandling versus hardware-orientated approach.

If one makes a comparison between a computer-orientated approach where each function listed in the previous paragraph is performed by the same centralized general purpose equipment (i.e. centralized datahandling), and a hardware-orientated approach where the spacecraft has to perform each one of the functions by means of special-purpose hardware (i.e. decentralized datahandling), it soon becomes clear that both approaches offer their own advantages and disadvantages.

In the case of a hard-ware orientated system, the loss of one function due to equipment failure, does not necessarily have to affect the others, still allowing operation of the spacecraft, although degraded.

On the other hand, the flexibility of such a system is very limited due to the presence of special-purpose equipment, which means the hardware developed can only be used to serve this particular satellite.

This special equipment might lead to prohibitive mission (i.e. development) cost and hardware weight.

In a computer-orientated approach, advantages in flexibility and mission cost can be achieved, provided the Central Processing Unit (CPU) is made reliable enough to guarantee its operation during the mission lifetime of 10 years. The computer's reprogrammability and its modular expandable structure, ensure " easy matching" to other satellites of a series and can also cope with late changes of payload operations, not only during the satellite's development, but also during its orbital lifetime (by means of sending new programmes via telecommand).

From the considerations in this paragraph it can be easily derived that the use of an on-board computer (OBC) can be advantageous, (flexibility, less development cost and weight), provided the problem of reliability is solved. For these reasons and also cause of the fact that centralized datahandling is a commonly used and well established technique, it is decided to provide the Hitch-Hiker spacecraft with an on-board computer.

10.2.2 Computer design goals.

To fully exploit the advantages offered by the use of an OBC, some design goals have been taken into account.
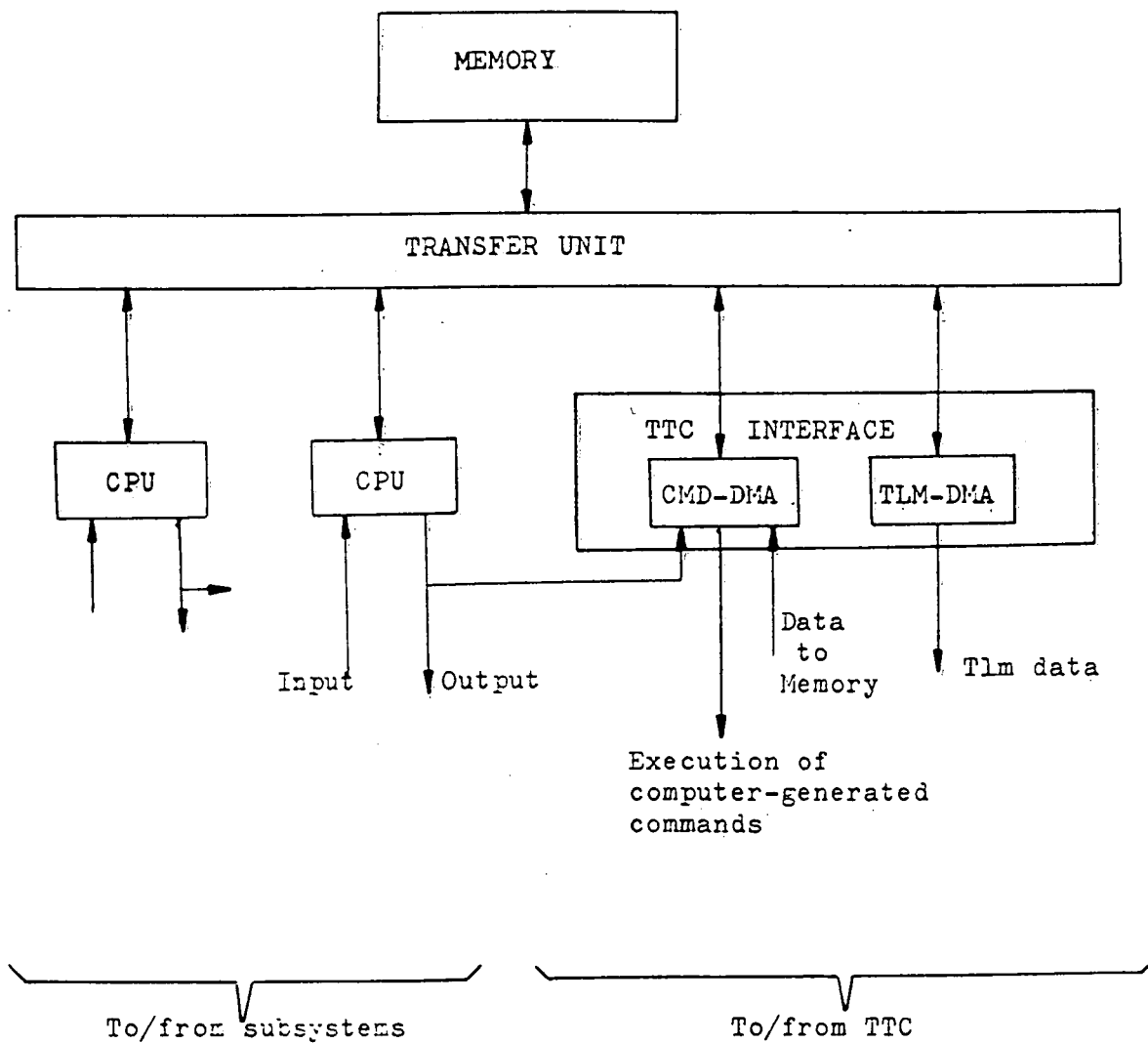
figure 10.1
OBC general block diagram.

Achievement of high operational flexibility and the ability to reduce the mission cost can both be ensured by means of easily expandable computer hardware, allowing various system configurations to suit the various mission requirements.

Standardization of the interfaces, which is more or less common practice with designing communications satellites, will also reduce mission cost as it helps to reduce the on-board hardware complexity.

As reliability is of great importance, one has to provide the OBC with redundant hardware, such as a standby CPU and redundant circuits for the encoder and decoder.

Of course while designing the OBC, one should not loose sight of goals as low volume, weight, and power consumption.

10.2.3 Functional description of the OBC.

Before any further discussion, it might be useful to "draw a picture" of the OBC, without going into details such as computer electronics. Therefore figure 10.1 only shows the essential components which form a typical on-board computer used in a small spacecraft. The main purpose of this paragraph is not only to describe the functions of each component as shown in figure 10.1, but also to point out in which way they enable the computer, and thus the total subsystem, to meet the two predominant goals mentioned in paragraph 10.2.2, reliability and flexibility. For this reason to each component a subparagraph has been dedicated, in which it is briefly illustrated.

10.2.3.1 Memory.

Memory can be divided into two different types. Firstly there is Main Memory, used to store:

- Processor Computer Programme, with instructions for generating control signals to command all subsystem functions

- Time-tagged commands

 Secondly there is Data Memory, used for storing:

- Programmes used for Attitude Control, Thermal Control, Power Control, and Housekeeping

- Housekeeping check data

Because it is not likely that the Processor Computer Programme will be reprogrammed during the mission lifetime, it is preferred to store this programme in a non-destructive Read Only Memory (ROM). However, to keep open the possibility to change instruction sets if necessary, Erasable Programmable Read Only Memory (EPROM) is used in stead of ROM. This EPROM should be made random accessible because the Processor Computer Programme will not always make use of the instructions in the same sequence they are stored in Memory. All remaining contents of Memory need to be stored in a read/write Memory, for which random access is not a necessity because all data are fetched in the same sequence they are stored.

Data source	Computer input	Computer task	Computer output	Memory size	
				Tables	Programmes
Attitude Control	Sensor & gyro outputs	Attitude data processing & maneuver logic	Commands	5 kbit	14 kbit
Housekeeping check	Output from multiplexers	Compare with stored limits, generate alarms	Commands to subsystems, alarms to ground	5 kbit	3 kbit
Telemetry	Output from multiplexers	Data formatting, encoding	Telemetry format	Instructions (part of Processor Prog.)	
Telecommand	Time-tagged commands from decoder	Execution of time-tagged commands, pro- gramme update	Commands to subsystems via decoder	Instructions (part of Processor Prog.)	

Processor Computer Programme	Memory size
Arithmetic Logic Transfer (table look up) Loop control Instructions	12 kbit.

To give an estimate of the required memory, one could make use of tables given in reference 11.2. In these tables figures are listed for three different missions, of which one of them is a small communications satellite, comparable to the Hitch-Hiker spacecraft. Tables 10.1 and 10.2, derived from reference 11.2 and based on the assumption that memory required for Thermal and Power Control is negligible, therefore only show figures which are of importance within the scope of this project.

As can be derived from tables 10.1 and 10.2, total memory required for this project is quite small (approximately up to 40 kbit). For the reason it is decided to make all cells random accessible, taking extra cost for granted in favour of avoiding hardware complexity.

Comparing different technologies (Bipolar, MOS, Junction FET), it soon becomes obvious that MOS, especially C-MOS, will best suit this mission. This technology namely offers the advantages of:

- Low Power consumption

- Almost no standby power is required (microwatts), which means memory expansion does not have to result in extra power consumption

- Low weight and volume

Problems like volatility and low resistance to radiation, can be easily avoided because all essential instructions are stored in a non-destructive EPROM which is non-volatile, whereas Memory could be protected against radiation by shielding the cells with a thin layer of aluminum.

In order to achieve flexibility (by means of growth potential), Memory could be built up of basic modules, each having a capacity of 40 kbit. By this means one also provides for low power consumption, because each memory module will contain switching circuitry that switches power on, only when that specific module is addressed. All at that time not addressed modules will only require for standby power, which is very low because MOS technology is used.

10.2.3.2 Central Processing Unit.

Functions the CPU should be able to perform are as follows:

- Execution of programmes by generating commands. The programmes are executd as a sequence of instructions, which are fetched in the proper order from Memory. The part of the CPU devoted to this function is called the Control Unit.

- To provide the OBC with arithmetic and logic functions. The portion of the CPU performing these functions, is called the Operating Unit

- Ability to handle programme interrupt requests. It is the Programme Interrupt Unit that gives the CPU the capability to modify the sequence in which programmes are being executed.

To achieve a feature like flexibility, the CPU makes use of a microprogrammed Control Unit. This means instead of discrete logic elements the Control Unit is stored as a Processor Computer Programme in an EPROM. By doing this one also increases flexibility because microprogramming offers the possibility of changing the EPROM. At the same time it reduces hardware, thus it's very likely that reliability and the required mission lifetime can be achieved without too many problems, because computer programmes won't suffer from degeneration or equipment failure.
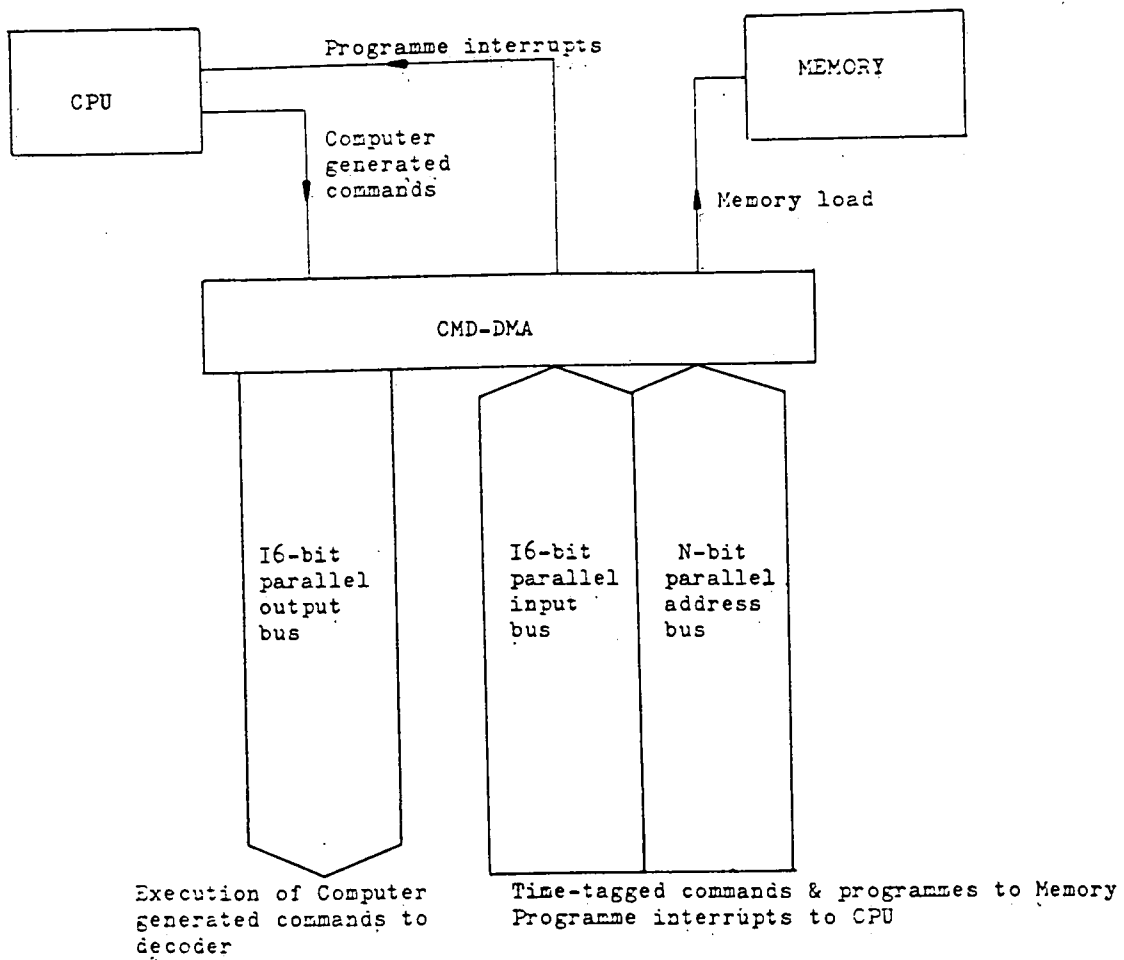
figure 10.2
Busstructure.

Because the CPU is the most important, complicated, and therefore most vulnerable component of the OBC, it should be made redundant. As can be seen in figure 10.1 a second CPU, connected with the same memory, could serve as a back·up operating in standby mode. As obvious, providing the OBC with a redundant CPU, one enormously increases its reliability.

CPU operation is started by means of a ground command.

10.2.3.3 Transfer Unit.

This component provides data transfer between Memory and other OBC components. It also avoids transfer conflicts to or from Memory.

10.2.3.4 Telemetry and Telecommand DMA's.

One must provide the OBC with Direct Memory Access units for telemetry and telecommand because programmes should be loaded and memory contents should be checked (to see whether data from ground have arrived correctly or not) without intervention of the Central Processing Unit.

Telecommand DMA unit

This unit performs the following two functions:

- Transfer of information from ground to Memory, such as computer programmes whenever reprogramming is required for, and time-tagged commands which will also enter Memory via this DMA.

- Execution of computer- generated commands, which is performed as follows: the command generated by the CPU will be loaded in the DMA unit after which the unit sends the command to be executed to the telecommand decoder.

Whenever programmes are loaded into Memory, data are processed at a much higher bit rate. Therefore the CMD-DMA must contain high efficiency circuitry capable to deal with high rate data. Time-tagged commands on the other hand will enter Memory via normal mode circuits.

Provided both functions will use the same message length of 24 bits, one establishes simplification of hardware and reduction in· weight because the same command decoder may be used to decode both, commands coming from ground and computer-generated commands.

Telemetry DMA unit

This unit also has two functions which are:

- Verification of memory contents by transferring the contents to be verified from Memory to ground. This process is initiated by means of a telecommand which defines the memory address and the memory data block to be transferred. After being initiated, the DMA unit automatically transfers the specified data block from Memory to the telemetry encoder.

- Transfer of housekeeping check data. Initiation and transfer are the same as with the verification process, only the command to initiate the DMA unit will come from the CPU.

Verification of memory contents requires for high rate data. For this reason, just like the command DMA, the telemetry DMA must also contain high efficiency circuits.

figure 10.3
System layout.
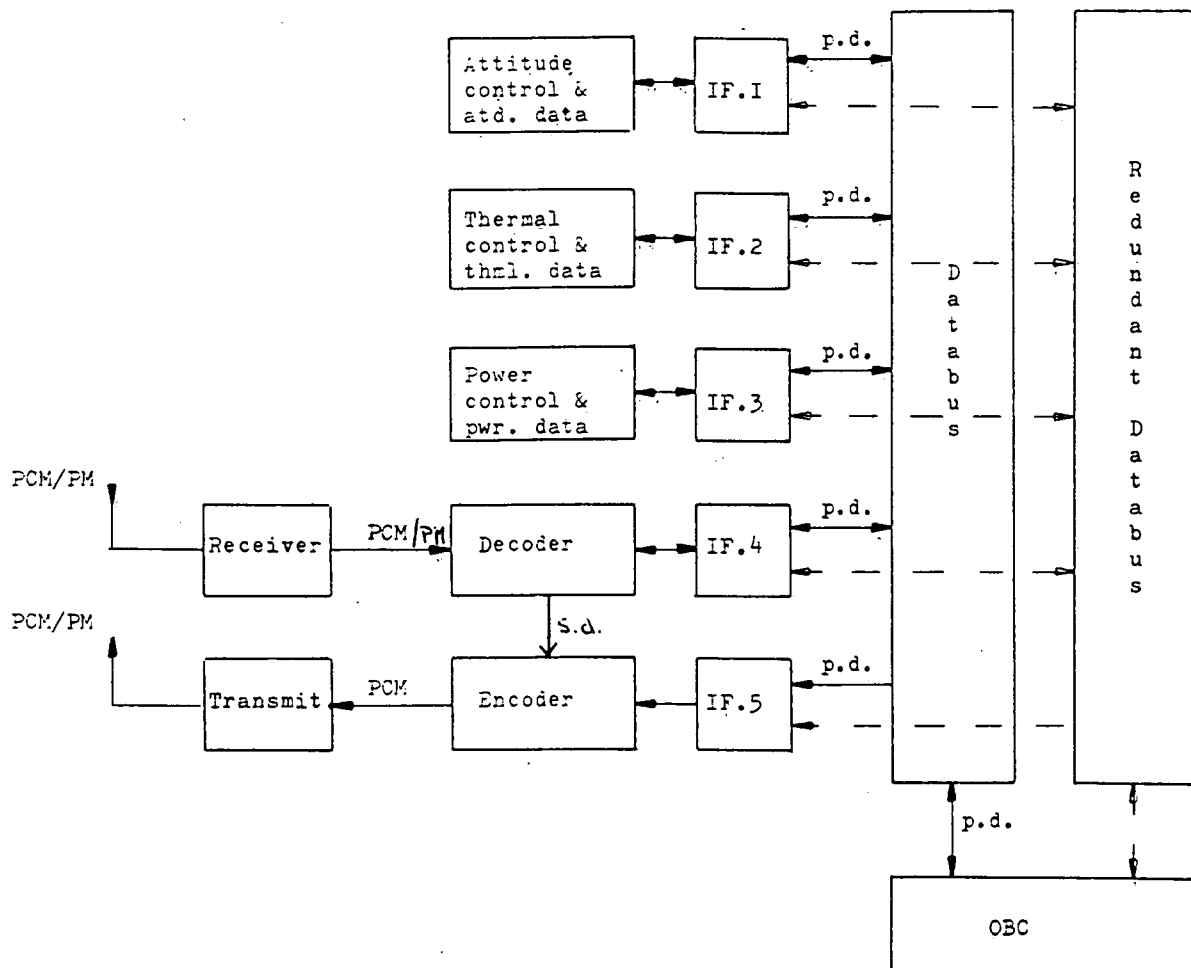
Legend

s.d.	:	serial digital
p.d.	:	parallel digital
PCM	:	Pulse Code Modulation i.e. serial digital
PCM/PM	:	Pulse Code Modulation/Phase Modulation
IF.	:	Inter Face

Inter Faces I to 3 contain parallel digital to analog converters
Inter Face 4 contains formatting circuits and a serial digital to parallel
digital converter
Inter Face 5 contains a parallel digital to serial digital converter

At fixed intervals the OBC starts a housekeeping check where all housekeeping parameters are stored in Memory and compared with fixed limits. As a result of these check cycles the computer produces diagnostic information representative of the satellite's health. This information is transferred to the telemetry encoder under computer control, by which means the DMA unit is enabled to alert the CPU at the moment transfer has been completed. The DMA unit can then be reactivated by the CPU for the transmission of another data block according to the telemetry format. For the bit rate at which housekeeping check data are processed, just like memory contents, high efficiency mode is required for.

10.2.4 Busstructure.

Through the years it has grown quite a tradition to equip on-board computers with a word length of 16 bits. Therefore it is obvious that computer-generated commands will always occupy two 16-bit words of which the first 8 bits contain a routing label, defining the equipment the command should be sent to, whereas the following 24 bits are used for the command code. Because data received from telecommand have the same structure, one enables the command decoder to decode both, computer generated commands and commands coming from ground, by means of the same hardware.

For the reasons mentioned above, the databus performing data transfer between the OBC and the subsystems, may have the following structure:

- 16-bit parallel input bus

- 16-bit parallel output bus

- N-bit parallel address bus where the parameter N depends on the exact number of subsystem parameters each having a memory address of its own. A reasonable value for N would probably be 8.

The busstructure is sketched in figure 10.2.   .

With a space-qualified computer it is desirable to process data in real time, which means that a command coming from ground or a computer-generated one is immediately executed (if not a time-tag is put on it) without a time delay. To accomplish this feature, data transfer between the OBC and the subsystems is in parallel, by which it becomes necessary to equip computer interfaces with parallel digital to analog converters which can also work the other way around. For the decoder and encoder interfaces, it is sufficient to be equipped with respectively a serial digital to parallel digital and a parallel digital to serial digital converter.

Data from a PCM telecommand link are generally received at a rate in excess of the rate at which the OBC can accept and make calculations on it. Therefore data arriving from ground should be reduced in speed before computer entry, which is accomplished in computer data formatting circuits contained by the decoder interface.

For a system layout the reader might refer to figure 10.3. This figure also shows that in order to provide for redundancy, all subsystems and the OBC are connected with two databuses of which one of them will function as a back up in case of anomalies should occur.

By giving the databus the structure as described in this paragraph, one also builds in flexibility because subsystems can be added or removed without influencing other subsystems.

Serial digital data from OBC, i.e. Memory
data to verify contents, and Housekeeping
check data

Analog and
serial digital
Housekeeping &
Attitude data

Digital
MPXR

Analog
MPXR

A/D

Signal Mixing
Gates

PCM to
Transmitter

Programmer

Synchr.
Generator

Digital Instructions

From CMD- Decoder
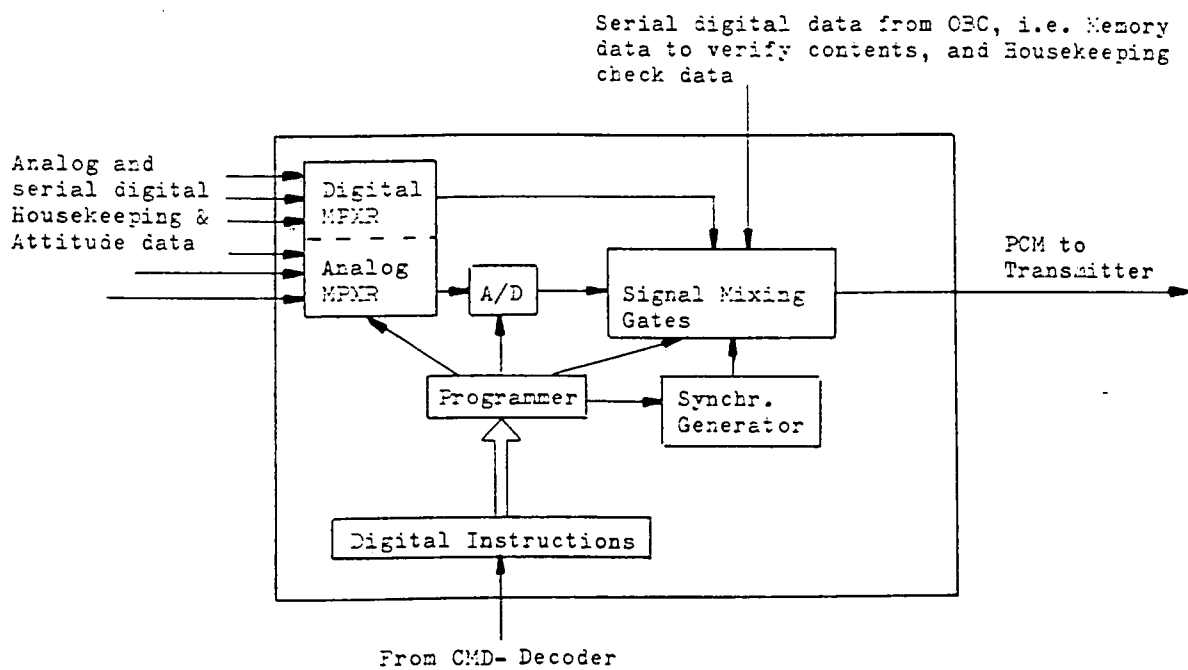
figure 10.4
Encoder block diagram.

10.3   Telemetry.

The functions a telemetry unit should be able to perform in a spacecraft where an OBC is used are relatively simple so that this unit may exist of a telemetry encoder and a transmitter. The main function of the encoder is to supply for synchronization and identification. Synchronization bits are used for separating the 8-bit data words, whereas synchronization words are used to define the beginning of each frame. Frame identification words enable the Ground Segment to identify messages, need to clarify whether the frame being received contains housekeeping data, housekeeping check data, attitude data, or memory contents.

The sequence of telemetry data, according to which the format is compiled, will be fixed in order to avoid complexity. In the following paragraphs the reader will find a functional description of the telemetry encoder and an example of the telemetry format.

10.3.1 Functional description of the telemetry encoder.

The main equipment needed to provide for the encoder functions (see figure 10.4) are:

- Analog multiplexers for sampling analog signals coming from subsystems.

- Analog to serial digital converters to generate the 8 information bits which describe analog signal levels as a percentage of full scale.

- Digital multiplexers for sampling subsystem interface gates in which analog signals have already been converted into digital.

- Synchronizer generator used to produce zero bits. These zero bits or word synchronization bits, will be placed in between 8-bit data words thus providing for word synchronization.

- Signal mixing gates that will mix digitalized subsystem data, already digital subsystem data, and digital data coming from the OBC, with synchronization bits according to the telemetry format.

- Computer-controlled programmer to generate timing pulses that command all decoder equipment. The programmer is driven by a digital instruction set which code determines the operation of the programmer according to a fixed frame. The instruction set is activated by means of a serial command from the CMD-DMA.

A brief illustration of the encoding process is given in the following.
In case of analog data, the analog multiplexer is commanded by the programmer to close one selected gating circuit and thus conduct the corresponding analog signal to the A/D converter. During the time interval the analog sample is present at the converter input gates, the A/D converter receives a series of timing pulses from the programmer.

	0	1	2	3 --	-- 32 or 64
S0	FSO	FSI	FIW	HOUSEKEEPING DATA	ATTITUDE DATA
S1	,,	,,	,,	HOUSEKEEPING DATA	
S2	,,	,,	,,	HOUSEKEEPING DATA	ATTITUDE DATA
S3	,,	,,	,,	HOUSEKEEPING DATA	
S4	,,	,,	,,	HOUSEKEEPING DATA	ATTITUDE DATA
S5	,,	,,	,,	HOUSEKEEPING DATA	
S6	,,	,,	,,	HOUSEKEEPING DATA	ATTITUDE DATA
S7	,,	,,	,,	HOUSEKEEPING DATA	

Legend

FSO   : first Frame Synchronization Word
FSI   : second Frame Synchronization Word
FIW   : Frame Identification Word
S-   : -th Telemetry Frame

figure 10.5
Possible telemetry format.

These pulses drive the converter through a complete cycle to generate the eight information bits which describe the present analog sample as a percentage of full scale by means of Pulse Code Modulation (PCM). This means the sample is copied as a combination of one and zero bits. By now the Programmer commands the Synchronizer Generator to produce a single zero bit, or if frame synchronization is required for a combination of one and zero bits, to be inserted with the data and thus provide for word or frame synchronization. The reader should notice that if digital data are presented to the encoder, the step of analog to digital conversion can be omitted because data are already in PCM. Therefore digital subsystem data and data coming from the OBC are directly gated to the signal mixing gates.

When the encoding process has been completed, the available PCM signal is used to phase modulate a RF carrier (pure sine wave), generated in the transmitter by an oscillator.

The encoder should be equipped with back up operating modes, allowing transmission of telemetry data independently of OBC operation in case of computer failure. If such a failure should occur, the encoder is controlled by means of telecommand (so-called "manual control").

10.3.2 Example of the telemetry format.

- Word length of 8 bits, 8th bit may be used for odd parity check

- Frame length of 32 or 64 words depending on the exact number of parameters to be transmitted (appr. a few hundred)

- Format length of 8 frames

As can be seen in figure 10.5 each housekeeping parameter is sampled at least twice per format whereas the more important Attitude Control parameters are sampled once per frame, thus four times per format.

Data originating from housekeeping check cycles probably will occupy two or more formats. These formats are sent down to Ground Segment once every sixteen formats.

If memory contents are to be checked, a telecommand initiating memory unloading is sent up. Memory contents probably also will occupy two or more formats (new programmes and tables).

The bit rate at which the telemetry format is being transmitted varies from appr. 256 b.p.s. in case of housekeeping and attitude data up to appr. 1024 b.p.s. in case of memory contents and housekeeping check data.

The reader should notice that somewhere near the beginning of each format a code must be inserted which identifies the satellite originating the telemetry. This code is left out in figure 10.5.

10.4   Telecommand.

Broadly speaking sending telecommands is the reverse process of receiving telemetry from a satellite, however the telecommand structure is quite different from the telemetry format. There are many ways of structuring a telecommand and several space organizations have developed their own different standards.

Word length (bits)

```
   16         4  4     8    4     8    4     8    4    8    4     8    4     8    4    = 96 bits
 ┌───────────┬──┬──┬──────┬────┬──────┬────┬──────┬────┬──────┬────┬──────┬────┬──────┬────┐
 │           │  │  │      │    │      │    │      │    │      │    │      │    │      │    │
 │    ASW    │M │  │      │    │      │    │      │    │      │    │      │    │      │    │
 │           │o │  │      │    │      │    │      │    │      │    │      │    │      │    │
 │           │d │  │      │    │      │    │      │    │      │    │      │    │      │    │
 │           │e │  │      │    │      │    │      │    │      │    │      │    │      │    │
 └───────────┴──┴──┴──────┴────┴──────┴────┴──────┴────┴──────┴────┴──────┴────┴──────┴────┘
```

Mode repeated   Hamming   2nd   3rd   3rd
                  code   Data word   Data word Data word
                                                          repeated
        1st   1st   2nd
        Data word   Data word   Data word
                      repeated   repeated

ASW: Address and Synchronization Words

ESA standard telecommand frame.

```
              ◄ First on/off ►  Second on/off    Third on/off
 ┌───────────┬──┬──┬──────┬────┬──────┬────┬──────┬────┬──────┬────┬──────┬────┐
 │           │  │  │      │    │      │    │      │    │      │    │      │    │
 │    ASW    │M │de│      │    │      │    │      │    │      │    │      │    │
 │           │o │  │      │    │      │    │      │    │      │    │      │    │
 └───────────┴──┴──┴──────┴────┴──────┴────┴──────┴────┴──────┴────┴──────┴────┘
```

figure 10.7.a
On/off telecommand.

```
            Routing label    ◄ First half of ►  Second half of
                               ML command         ML command
 ┌───────────┬──┬──┬──────┬────┬──────┬────┬──────┬────┬──────┬────┬──────┬────┐
 │           │  │  │      │    │      │    │      │    │      │    │      │    │
 │    ASW    │M │de│      │    │      │    │      │    │      │    │      │    │
 │           │o │  │      │    │      │    │      │    │      │    │      │    │
 └───────────┴──┴──┴──────┴────┴──────┴────┴──────┴────┴──────┴────┴──────┴────┘
```

figure 10.7.b
Memory load telecommand.

```
            ◄ First part of ►  Second part of   Third part of
              CL command         CL command       CL command
 ┌───────────┬──┬──┬──────┬────┬──────┬────┬──────┬────┬──────┬────┬──────┬────┐
 │           │  │  │      │    │      │    │      │    │      │    │      │    │
 │    ASW    │M │de│      │    │      │    │      │    │      │    │      │    │
 │           │o │  │      │    │      │    │      │    │      │    │      │    │
 └───────────┴──┴──┴──────┴────┴──────┴────┴──────┴────┴──────┴────┴──────┴────┘
```

figure 10.7.c
Computer load telecommand.

Nevertheless all these standards have been derived from one shared concern, namely that a command should be only received by the addressed satellite, and once received it should be correctly executed. To avoid mishaps such as addressing the wrong satellite, various space organizations have established telecommand standards which contain data redundancy and error detection or Hamming codes. The European Space Agency (ESA) has developed one of the most widely used standards which this project will adopt because it offers the possibility to make use of an ESA standard PCM command decoder. This decoder is generally described in paragraph 10.4.2 whereas paragraph 10.4.1 is concerned with an explanation of ESA standard telecommand frame.

10.4.1 ESA command frame.

Before analyzing the structure it might be useful to note that operating the Hitch-Hiker spacecraft requires for three commonly used types of command which are listed below.

- 8 bit On/off commands used for simple equipment reconfiguration such as throwing a switch.

- 16 bit Memory Load commands for inserting binary numbers into equipment registers. It is emphasized that the word "memory" in Memory Load refers to equipment registers and not to main or data memory. Therefore memory load commands are immediately executed and do not require for CPU intervention.

- 24 bit Computer Load commands used to programme the OBC (programmes and tables)

The general structure of 96 bits standard ESA telecommand frame is shown in figure 10.6. Satellite addressing and synchronization occupy the first 16 bits followed by a 4 bit mode selection word which advises the telecommand decoder what type of command is being received. To detect bit corruption the mode selection word is repeated once. If the two mode selection words are different the decoder rejects the entire command and Ground Segment has to transmit it once more.

The real command instruction is contained in one or more (up to three) 12 bit data words of which each word is repeated, also for detecting bit corruption. Again, if one of these words does not resemble its repeated version, the command will be neglected. The first 8 bits of each data word are occupied by the actual instruction while the last 4 bits constitute an error detecting or Hamming code derived from the preceding 8 bits.

A complete ESA telecommand frame is thus made up of 96 bits. Frames may be linked together into strings whereby each frame begins with 16 satellite addressing and synchronization bits.

Because an On/off command is made up of 8 bits, three different commands may be included in a single frame (figure 10.7a).
A Memory Load command is accommodated by placing an 8 bit routing label defining equipment the command should be sent to. The 16 bit numerical content is spread over the two remaining 8 bit words (figure 10.7b).
Computer Load commands need all three available data words to hold 24 bit messages. This type of command is shown in figure 10.7c.
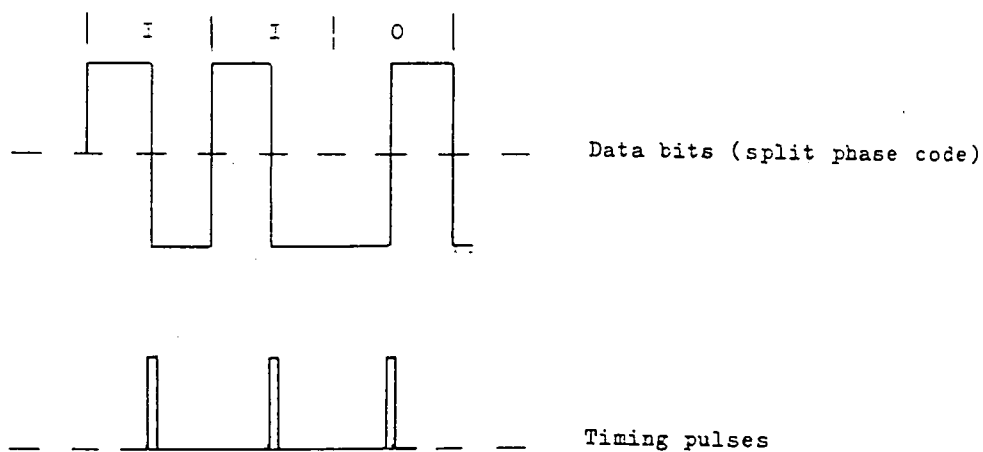
figure 10.8
Bit synchronization process.
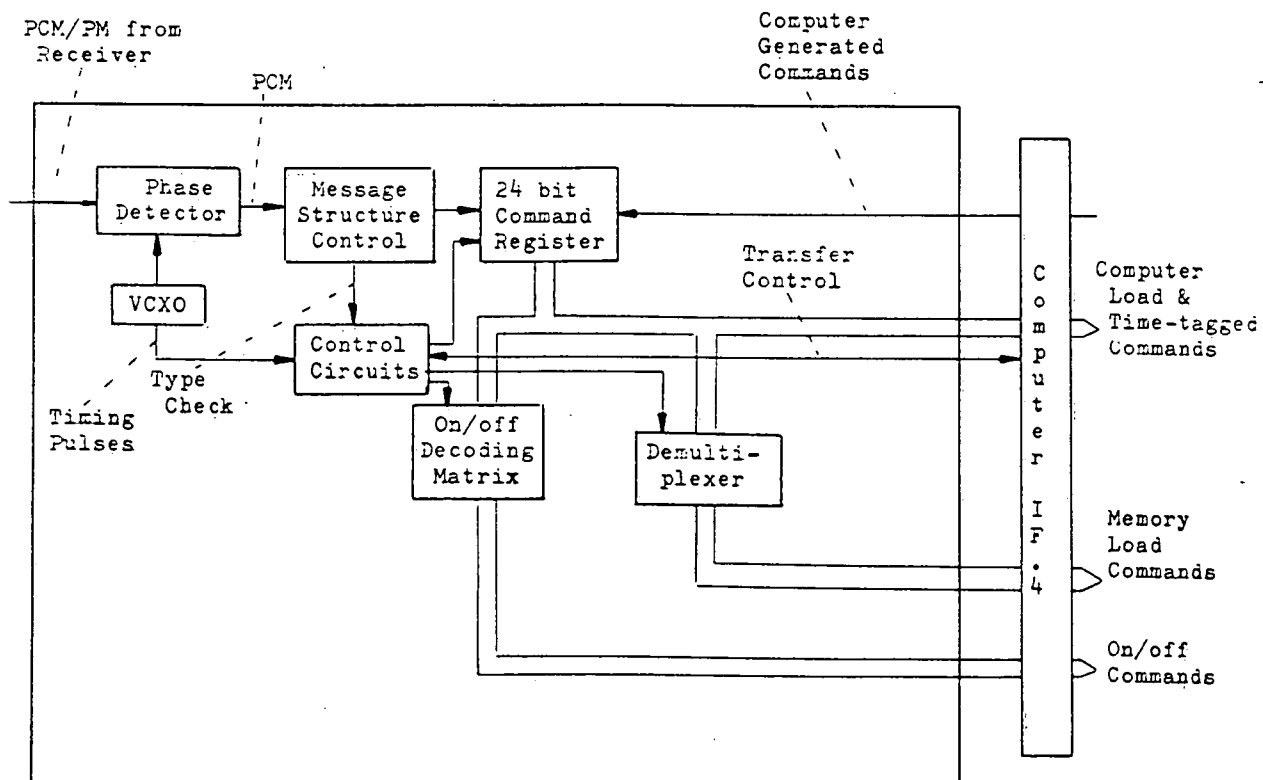
figure 10.9
Decoder block diagram.

Besides the types of telecommand previously mentioned, another type is needed for controlling the spacecraft namely Time-tagged commands. Strictly speaking Time-tagged commands are not a type by themselves but they consist of two linked frames in which the first frame is a Memory load containing memory address (first word) and the time tag (second and third word). The second frame contains the actual command to be executed at a given moment in time.

Strictly speaking, time-tagged commands are used whenever a command should be executed out of view of a ground station, e.g. firing the thrusters in Geostationary Transfer Orbit (GTO). On the other hand one could also put a time tag on commands which require for CPU intervention. Cause of this reason it is decided to also consider more complicated commands such as deployment of dish and arrays as time-tagged commands to be executed by the OBC at a specified moment in time.

10.4.2 Functional description of the telecommand decoder.

Because the data received are still phase modulated, the decoder should provide for phase demodulation equipment. After 12 bit data words have been phase demodulated each bit is accompanied by a timing pulse placed in the middle, thus bit synchronization has been accomplished (see figure 10.8). For both functions, phase demodulation and bit synchronization, one may use one and the same "phase lock loop". This loop principally consists of a phase detector and a Voltage Controlled Crystal Oscillator (VCXO) running at bit rate or a multiple thereof. To regenerate the PCM signal, the loop first locks on and then tracks the bit rate which is accomplished by the phase detector that compares the incoming PCM/PM signal with its own oscillator and adjusts to produce negligible phase differences. Because the oscillator is running at bit rate (or a multiple there of), the pulses it produces can also be used as timing pulses needed to command decoding equipment.

For a brief discussion on the decoder functions figure 10.9 is referred to. Coincident with each bit coming from the phase lock loop, the available timing pulses are gated to control circuits which command all functions of the decoder. If in Message Structure Control the Mode Word has been recognized and proved to be valid by resembling its repeated version, the decoder knows what type of command is being inserted (type check) and will accept the following 24 bits representing the first part of a command frame. At the same time bits are being accepted Message Structure Control runs a Hamming Code check and inspects "word resemblance" which are both performed three times because a command frame includes three parts. Only when the entire command frame has been approved, the original three 8-bit data words are stored in the command register from which they are transferred in serial to gate the proper circuits (Matrix Gates in case of On/off commands, Demultiplexer Gates in case of Memory Load commands, and Decoder Computer Interface Gates in case of Computer Load commands or Time-tagged commands).

The decoder directly takes care of real-time commands (On/off and Memory Load) whereas Computer Load Commands and commands with a time delay (Time-tagged) are stored in computer memory. When the satellite clock matches the time- tag the last mentioned type of command is routed back to the decoder as a computer-generated command.

As Time-tagged Commands, thus also more complicated commands which are also considered time-tagged, require for CPU intervention, the command decoder in case of computer failure must allow "switch over" to operate standby redundancy. Therefore, just like the telemetry encoder, one has created self-sufficient thus reliable equipment allowing "manual control" from Ground Segment.

PCM/PM

Receiver

Filter   Preamp.   Amp.   PCM/PM   Decoder   PCM to
                                                                     IF.4

-PCM/PM   PCM/PM   s.d.

                                                                     PCM &
        SSPA   X40   Phase   PCM   Encoder   analog
                       Modulator   from IF.5
Harmonic   Freq.
Rejection   Mult.   VCXO   f=98,75 MHz
Filter
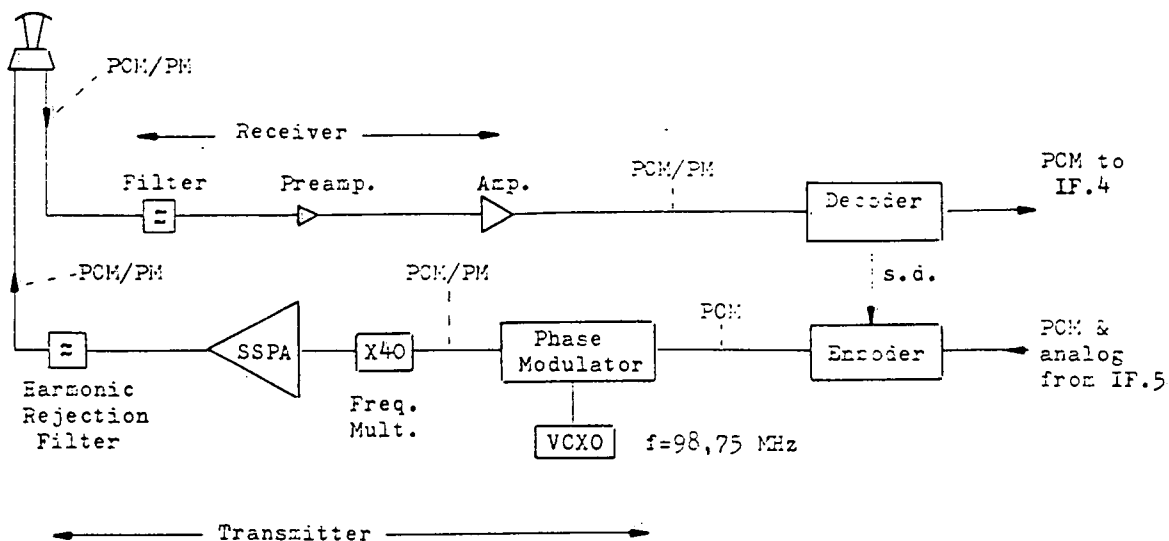
Transmitter

figure 10.10
Receiver/transmitter functional block diagram.

PCM from
Encoder

Phase   PCM/PM
Modulator

Carrier (pure sine wave)
from VCXO
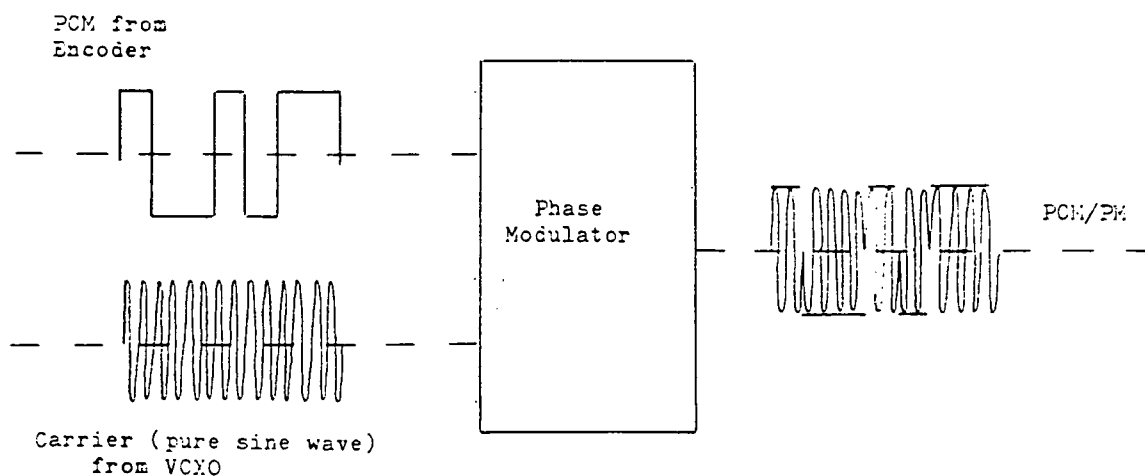
figure 10.11
Phase modulation.

10.5 The Telemetry-Telecommand receiver/transmitter.

As already mentioned before, this project makes use of a pulse code modulated signal (combined with a split phase code) to phase modulate the RF carrier. The main reasons for this decision are summed below:

- Pulse Code Modulation (PCM) because this kind of modulation limits the binary signal (e.g. between -4.5 Volt and +4.5 Volt) so that equipment used in the transmitter/receiver need only handle two levels thus avoiding hardware complexity.

- Split Phase Code (SPC). This type of bit representation provides for easy bit synchronization at Ground Segment. Also good system accuracy and possibility to sample at high rates are guaranteed.

- Phase Modulation (PM). Phase modulating the carrier offers good signal performance such as signal to noise ratio and carrier frequency stability.

With TTC it is common practice to use the same antenna for receiving and transmitting (see figure 10.10). The signal received by the antenna must be amplified to a level high enough in order to avoid detrimental effect on the system efficiency whenever long cables are being used. Therefore a preamplifier is mounted as close as possible to the antenna itself. A filter preceding the preamplifier rejects any other signal that may cause degradation to the PCM/PM signal being received. Because until now the signal strength is still very weak a second amplifier boosts the signal to such a level high enough that it can be gated to the phase lock loop contained by the telecommand decoder. In this loop the frequency of the phase modulated carrier is down converted to an acceptable level in order to restore the PCM signal. Notice that equipment needed for down conversion is not depicted in figure 10.9.

On the other hand to enable the transmitted signal to travel its long distance through space, the signal coming from the telemetry encoder is used to phase modulate a carrier after which the resulting PCM/PM signal is amplified. A Voltage Controlled Crystal Oscillator (VCXO) running at 98,75 MHz provides for the RF carrier whereas a Solid State Power Amplifier (SSPA) is used for amplification. In the Phase Modulator the carrier coming from the Xtal Oscillator is shifted by 180 degrees with every level change thus obtaining a phase modulated carrier (see figure 10.11). This phase modulated signal or PCM signal is fed to a frequency multiplier chain consisting of conventional transistor circuits. This chain may perform a X40 frequency multiplication obtaining the required down link frequency of 3,95 GHz. After being amplified the PCM/PM signal is ready for transmission.

As stated in the requirements, the frequencies used for TTC should be within the Payload frequencies and this offers some possibilities to "cut back" on weight and volume because certain functions such as filtering (Harmonic Rejection Filter) and to some extent down conversion of the carrier frequency (2,25 GHz) can be performed by already present Payload hardware thus giving a weight reduction, whereas the compactness of the combined TTC/Payload hardware may lead to a reduction in volume. In figure 10.12 a schematic description of the resulting combination is given whereas the reader may refer to chapter 5 for a more detailed configuration sketch.

Omni. ant.

To IF.4

From IF.5

| Decoder | | SSPA Filters | | Phase Modulator VCXO X40 | | Encoder |

Filters
Preamp.
Amp.
2,25 GHz down
conversion

TWTA's

DMPXR

MPXR

Dish ant.
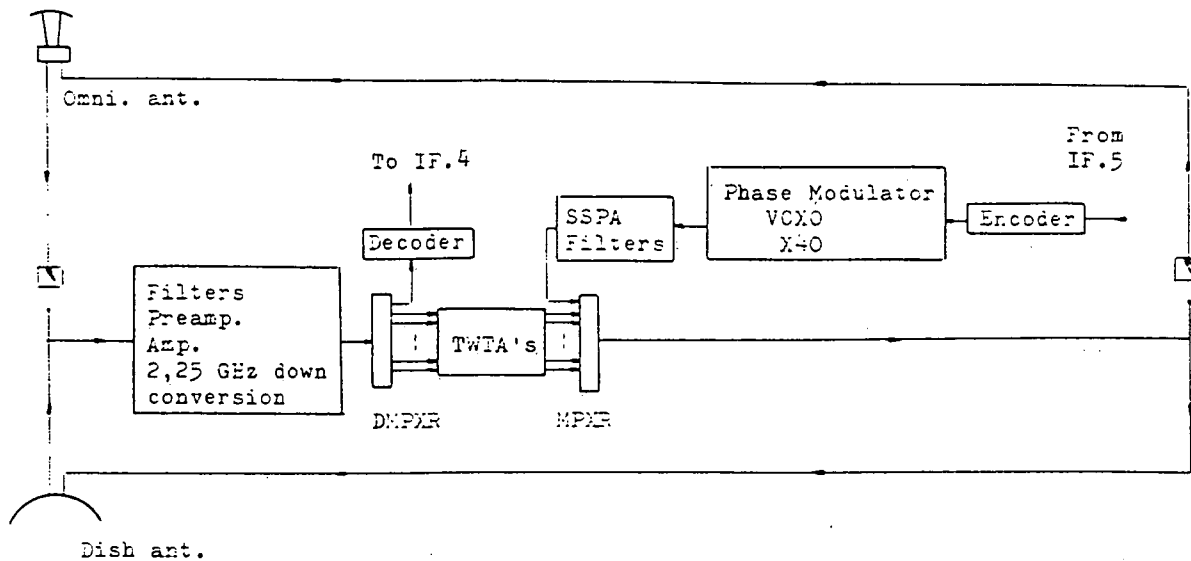
Legend

DMPXR : Demultiplexer
MPXR : Multiplexer
TWTA : Traveling Wave Tube Amplifier
VCXO : Voltage Controlled Chrystal Oscillator
X40 : X40 Frequency Multiplier

figure 10.12
Combined TTC/payload subsystem block diagram.
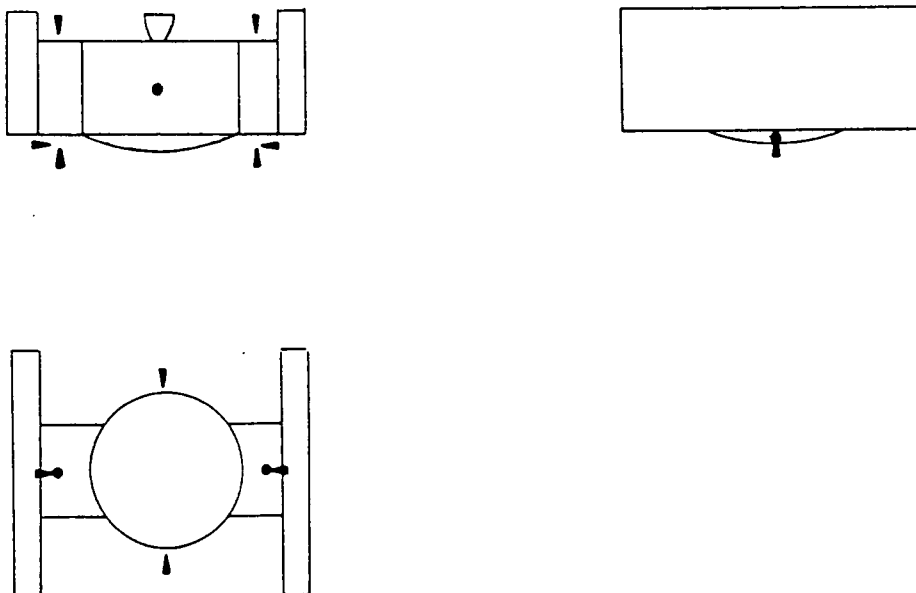
figure 10.13
Configuration during launch phase and transfer orbit.

To complete this paragraph, system operations are briefly described. During launch phase and transfer orbit the switching circuits will be closed thus enabling the system to make use of the omnidirectional antenna (8 flush-mounted horns as shown in figure 10.13). This type of antenna provides for the necessary monitoring and control of the satellite during the phases mentioned. When the satellite has reached its final (i.e. geostationary) orbit while the dish has been deployed, the switching circuits will be put" out of lock" and from that moment on TTC will start making use of the parabolic dish antenna providing the TTC signal with a much higher gain. The reader should notice that the omnidirectional antenna can still be used in case anomalies should occur, thus redundancy of TTC antenna has been obtained.

10.6 Tentative mass and power budgets.

For each unit its approximate mass and power consumption are listed in table 11.3 from which figures one may conclude that the total Datahandling/TTC subsystem mass and power consumption will appr. be 25,5 kg and 32,5 Watts respectively.

The following remarks should be placed:

- Cabling e.g. between filters and preamplifiers, has been taken into account with Payload Equipment. Other weight caused by cables running from one unit to another have been neglected which is a reasonable assumption because units like the Phase Modulator, VCXO, Frequency Multiplier, and Telemetry Encoder are mounted very close to each other.

- To give a rough estimation of the databus' weight, its length has been computed with a circumference of $2\pi R$, where for the parameter R 75% of the satellite's radius has been chosen. Knowing its length, one could make use of figures given in reference 10.10 where a databus with the same structure is being described.

- Figures for computer units (CPU, Transfer Unit, DMA's, and Memory) can be found in reference 10.1. According to this report, weight and power data have have been computed from typical data derived from a literature survey on technology and materials suitable for space applications. All power consumption figures are given for operational mode. If the computer units remain in standby mode power consumption amounts 2 Watts instead of 10 Watts. Notice that one of the two CPU's functions as a back up in standby mode, by which 3,5 Watts in Table 11.3 refer to one CPU in operational mode and the second standing by.

- To save mass (and volume) it is proposed to house all computer units as well as the encoder, decoder, and their Inter Faces in one aluminum box of which the measurements (in mm) are shown in figure 10.14. The given mass of 25,5 kg does not include this housing box for which 1 kg seems to be a reasonable value thus giving rise to a total mass of 26,5 kg.

10.7 Conclusions.

According to paragraphs 10.1 to 10.6 the following conclusions can be drawn.

Unit	Number	Mass(kg)	Power Consumption(W)	Volume
CPU	2	I,8	3,5	
Transfer Unit	I	0,2	0,2	
TLM-DMA	I	0,5	0,3	
CMD-DMA	I	0,5	0,5	
Memory(C-MOS)	One 40 kbit Module	I,5	5	
Inter Face switches	One Telemetry IF and one Telecommand IF	0,5	0,5	Appr. 4 litres excl. Databus Payload Eq. Horns
Encoder	I	I	I,5	
Decoder(incl. phase lock loop)	I	I	I,5	
Databus(4,3 metres)	2	4	--	
Phase Modulator X+O Freq. Mult. VCXO	One integrated chain	0,4	I	
Preamps SSPA Filters	Payload Equipment	8,5	I8,5	
Horns	8	5,6	--	
		Total mass (excl. Housing) 25,5 kg	Total Power Cons. 32,5 Watts	

Table 3
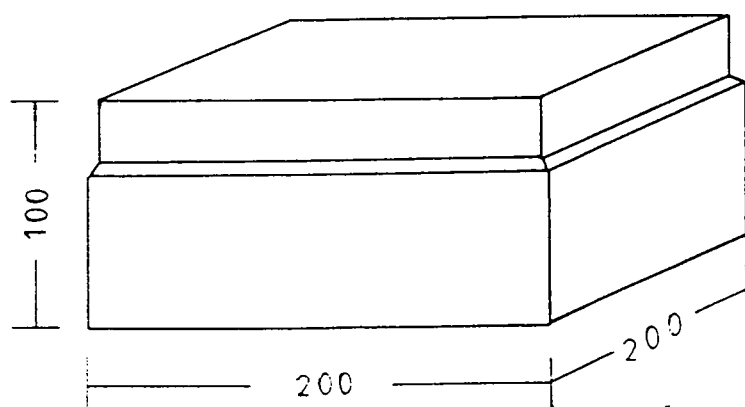
figure 10.14
OBC mechanical layout.
Upper part contains memory module.
Lower part contains electronics.

First of all it should be mentioned that due to lack of knowledge and experience, to the author this part of the project was more of a literature survey than coming up with tangible results. For this reason it probably would have been better to attract a student in the field of electrical engineering to take care of this part. As an example phase lock techniques without any foreknowledge are way above one's head whereas a requirement like "The probability to command another spacecraft when illuminated by equivalent RF flux should be less than 10e-9" was not clearly understood.

During the Midterm Review which took place at Delft University d.d. 11-4-'90, ESA's D.Brown explained that limiting the TTC frequencies to the Payload frequencies is quite a recently developed strategy. The combined TTC/Payload subsystem is therefore afflicted with a few uncertainties concerning the configuration and in particular hardware equipment.

As time was running out no further attention has been paid to ranging signals, needed to determine the satellite's orbital parameters, and polar patterns of the omnidirectional antenna. On the other hand ranging signals belong to Ground Segment activities while polar pattern determination without the proper mathematical background and test facilities seems almost impossible.

11 Propulsion.

11.1 Introduction.

In order to develop a propulsion system for a spacevehicle one has to describe to the system the realization of the following
three tasks:
1) The apogee kick
2) Station keeping
3) Attitude control
The apogee kick is realized by an apogee boost motor. Station keeping and attitude control by smaller thrusters.

In the next paragraphs the following aspects concerning the development of a propulsion system are considered:

1) Type of propulsion
2) Propulsion system mass
3) Possible configurations

11.2.1 Type of propulsion.

Choosing a suitable propulsion system the possibilities are first of all divided in three main categories:

1) Thermal nuclear
2) Chemical
3) Electric

Thermal nuclear propulsion and electric propulsion are both excluded from being a realistic possibility for this small communications satellite for thermal nuclear propulsion is :
- used for great forces
- dangerous
- still in an experimental stage
- very expensive
- too advanced

An electrical propulsion system creates small forces only and is dependent on a power supply.
Therefore these alternatives are not considered.
A lot of experience was obtained in the past with the chemical propulsion. This is the cheapest and most common kind of propulsion used in spacecrafts
Chemical propulsion can on its turn be divided in three seperate categories:
- solid
- liquid
- hybrid

The hybrid option is not taken into account because it is also in an experimental phase.
The last subdivision that can be made is between liquid propulsion systems namely:
- Mono-propellant (N_2H_4)

- Cold gas
- Bi-propellant (NTO/MMH)
Each of the systems given above has its own advantages and disadvantages compared with the other systems and a choice will be made in section 11.3 Trade-off.

Propulsion system using :	specific impulse (sec.)
Solid propellant	285
Mono-propellant	235
Bi-propellant	300

table 11.2.1
Specific impulse for different propulsion systems.

11.2.2 Propulsion system mass.

Since there are no requirements from the other subsystems concerning the propulsion system a mass calculation is made.
To make an accurate mass estimation however it is necessary to write a program for the numerous possiblities of propulsion system configurations as mentioned in the preceding paragraph. The program computes the total propulsion system mass given the dry mass of the satellite (construction mass of propulsion system excluded) or given the total maximum mass of the satellite for a certain choice of the type of propulsion (i.e. unified propulsion system or (solid/mono)-propulsion sytem).
The important term in these calculations is the propellant mass estimation by means of the formula (see lit.1):

$$M_p = M_i*(1-exp(-\Delta v/n*g*Isp)) \tag{11.1}$$

Given the initial mass of the satellite, the total velocity increment during the lifetime and the specific impulse of the propulsion type, this formula gives the propellant needed for this mission and a more extensive explanation of the mass calculation of the propulsion system is given in section 11.5.
The parameters for the mission are:

$$
\begin{aligned}
(\Delta v) \text{apogee} &= 1488 \text{ m/s} \\
(\Delta v) \text{orbit control} &= 50 \text{ m/s} \\
M_i &= 800 \text{ kg} \\
n &= 0.9
\end{aligned}
$$

These values are the same for all possible propulsion systems, so that the determining factor in formula (11.1) is the specific impulse and the values for the specific impulse for the different types of propulsion according to ref. 11.1 are given in table 11.2.1.

Since one is free to choose a configuration with one or more apogee engines this possibility has been examined too in order to obtain certain possible advantages such as a smaller weight and construction advantages.
The results for different values of (Mtot)sat and (Mdry)sat and for different types of propulsion are given in appendix 1.

11.2.3 Configuration.

Not to lose the overall picture an enumeration of the possible configurations for the small communications satellite is given below:

1) Solid apogee motor with mono-propellant or cold gas attitude control thrusters.
2) Bi-propellant.
3) Bi-propellant with cold gas RCS.
4) Bi-propellant apogee motor with mono-propellant RCS.

Besides the lower specific impulse the monopropellant system using N_2H_4
(Hydrazine) has the follwing property that it needs a catalyst of which the quality decreases during the lifetime and therefore also the performances.

engine thrust (N)	company	engine mass (kg)	spec.impulse (sec.)	propellant (kg)
490	Marquardt	3.76	312	210
111	MBB	2.04	280	227.5
400	MBB	1.95	305	213.6

table 11.2.2
Comparison of propellant mass for the different bi-propellant
engines from different companies.

	4 x 110 N	4 x 22 N	4 x 10 N
engine mass (kg)	+ 4.38	- 1.07	-1.23
2 stationkeeping thrusters less (kg)	-0.75	-0.75	-0.75
extra tubing & fitting (kg)	+ 2.00	+ 2.00	+2.00
total (kg)	+ 5.63	0	0

table 11.2.3
Comparison of the 490 N apogee engine with 4 smaller thrusters
(All thrusters are available at the Marquardt company).

Using the bi-propellant system four possible configurations concerning the amount of apogee motors were examined as mentioned before. To make this comparison one has to determine the most favourable engine when the configuration consists of only one apogee motor. A supply of existing thrusters with a high specific impulse is given in table 11.2.2.

As one can see the 490 N thruster from the Marquardt company has the highest specific impulse and has the lowest mass.

Knowing this one can make a comparison with smaller thrusters.

Possible configurations are using the existing engines of ref 11.6:

1) 1 490 N thruster   (I_{sp} = 312 sec)

2) 4 110 N thrusters   (I_{sp} = 280 sec)

3) 4 22 N thrusters   (I_{sp} = 289 sec)

4) 4 10 N thrusters   (I_{sp} = 285 sec)

The total mass of the propulsion system for each of the configurations is given in appendix 2, however one remark has to be made comparing the four engines with the 490 N thruster.
For example:

Comparing four 110 N engines with the 490 N engine there is a certain increase in engine mass and an increase in mass through the need of extra tubings and fittings. However there is also a small decrease in propulsion system mass, because using four apogee engines, one can also use the engines for stationkeeping so two stationkeeping thrusters can be dropped. Whether this fact leeds to certain advantages or disadvantages for the total propulsion system mass comparing the 490 N with the four engines case can be seen in table 11.2.3.

11.3 Trade-off.

From the mass calculations one can see that for the communications satellite the bi-propellant propulsion system is by far the most ideal system when no other requirements are made, then to design a propulsion system with a small mass. Reason for this favourable weight is the specific impulse as mentioned before.

Knowing that bi-propellant is to be used one can still choose out of existing thrusters having its own performances and coming from different companies.

First of all there are no requirements or whatsoever concerning the performances for the apogee engine such as max.thrust level, burntime, etc.. A lower thrust will lead to a greater burntime but is not a problem. A greater thrust will lead to a greater acceleration but is no probem either which can be understood easily when one considers the fact that the structure of the satellite has to endure much greater forces during launch and transfer orbit allready.

Thus is chozen for the 490 N thruster from the Marquardt company there by excluding the 111 N and 400 N engines from the MBB company (see table 11.2.2), for this engine has the highest specific impulse of all the engines.

For the AOCS-thrusters however the AOCS-subsystem demanded a thruster with the lowest thrust range. This engine was the 4.45 N thruster again from the Marquardt company (ref. 11.6).

Thus to conclude:

The propulsion system consists of one 490 N model R-4D apogee engine and twelve 4.45 N AOCS-thrusters both from the Marquardt company.

Using hypergolic bi-propellant thrusters one needs a feed system. This is discussed in the next section whereas the tanks of the propulsion system are discussed in 11.6.

PRESSURIZING
GAS
(HELIUM)

PRESSURE REGULATORS

← CHECK VALVES →

FUEL

OXIDIZER

← LATCHING VALVES →
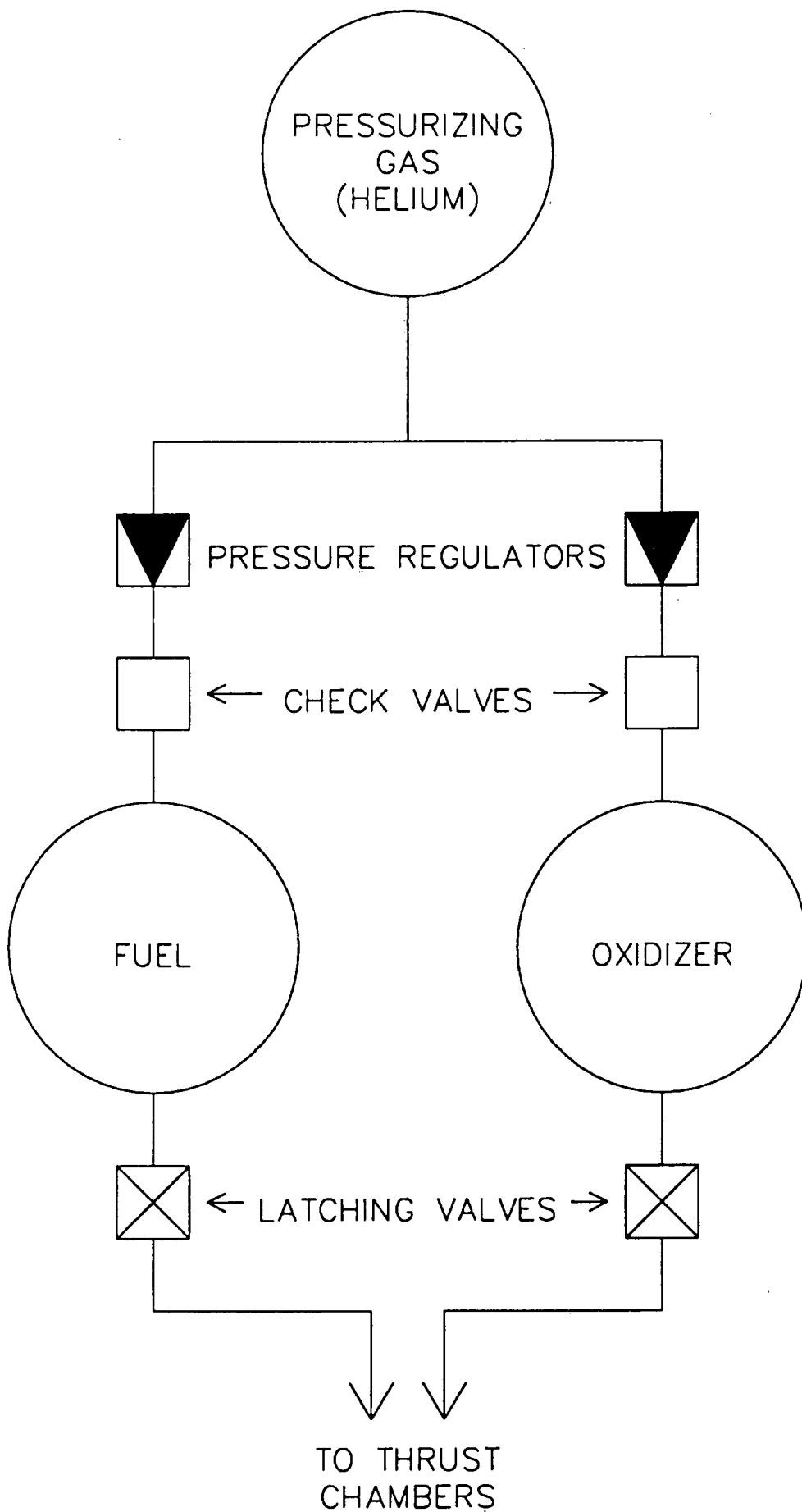
TO THRUST
CHAMBERS

figure 11.1
Schematic layout pressure-fed feed system.

11.4 Feed system.

An important component of a propulsion subsystem is the feed system for transfering propellants from the tanks to the thrust chambers.

The simplest form of a feed system is the pressure-fed system. Another possibility is the pump-fed system, which is used for high-thrust rockets, and is therefore not applicable in the Hitchhiker satellite.

In the pressure-fed system, a pressurant gas is used to force the propellants to flow from the tanks to the thrusters. The gas employed is generally helium or nitrogen, since these do not interact chemically with the propellants. From these two, helium has a lower density and is therefore chosen for pressurizing the propulsion system (a certain volume of pressurant is needed to pressurize the system).

Figure 11.1 shows a schematic representation of a pressurefed feed system. The helium is stored at a high pressure (300 bar) and is regulated to a lower pressure by means of pressure regulators. The check valves are used to prevent reverse flow of propellant tank fluids into the pressure regulators. Downstream of the propellant tanks are latching valves, which are used to control the fuel and oxidizer flow to the thrust chambers.

The lay-out shown in this figure is very schematic, and a more detailed diagram is presented in the last paragraph, in figure 11.2.

11.5 Calculations.

11.5.1 Propellant mass.

In this section the necessary amount of fuel (Monomethyl hydrazine, MMH) and oxidizer (Nitrogentetroxide, NTO) for the Unified Propulsion System (UPS) will be calculated. The total propellant mass consists of propellant for the:

1) apogee kick
2) orbit control
3) attitude control

To calculate these quantities Tsiolkovsky≈s equation is used:

$$M_p = M_i * (1 - e^{[-\Delta V/ngI]})$$ (11.2)

In which : M_p = necessary propellant mass

M_i = initial (satellite)mass

ΔV = velocity increment
n = efficiency factor   (= 0.9)
g = gravitational constant (= 9.8066 m/s²)
I = specific impulse

In order to find the apogee kick propellant mass (M_{ap}) is taken :

M_i = 786.6 kg.

ΔV_{ap} = 1488 m/s, which is a mission requirement.

I_{ap} = 312 sec, which is an engine specification.

With these values the M_{ap} follows : M_{ap} = 330.4 kg.
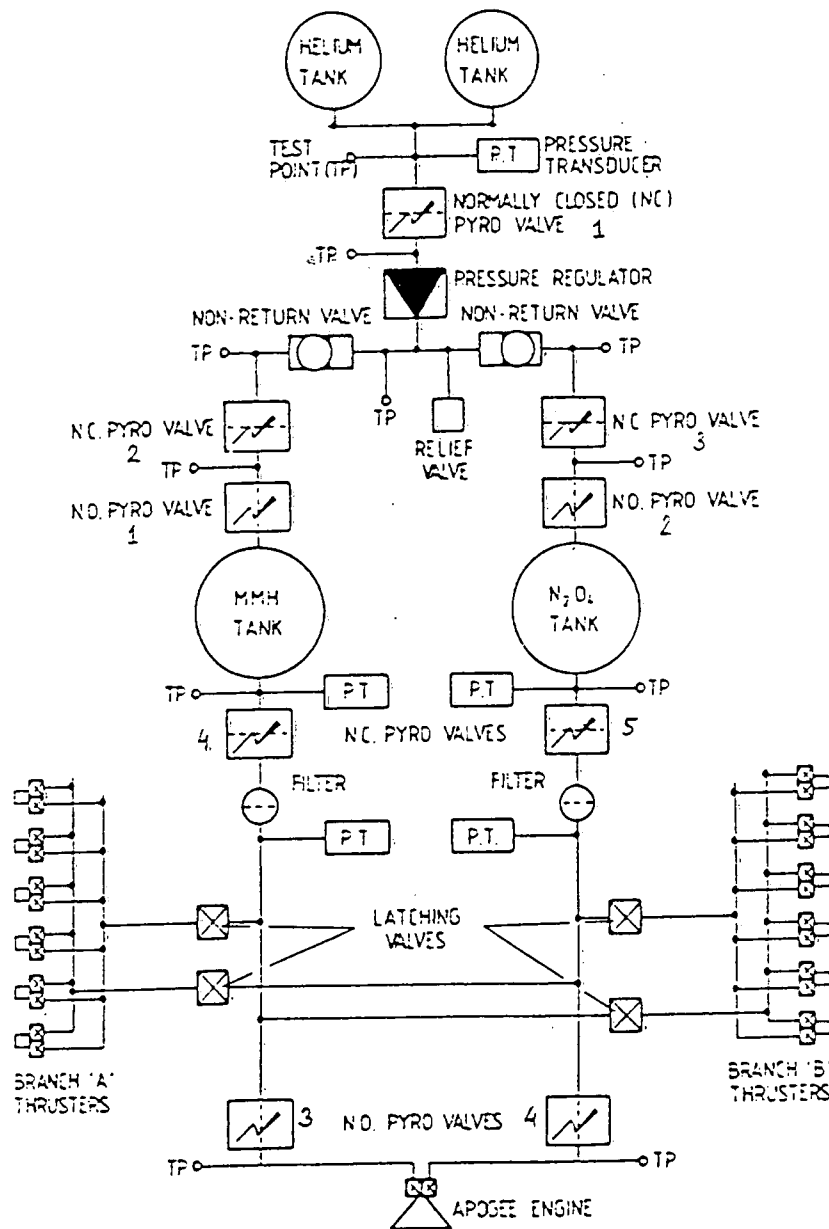
figure 11.2
CPS layout.

In a similar way the propellant masses for the orbit control (M_{oc}) and attitude control (M_{ac}) are obtained. In these cases the M_i's have got different values because of the fact, that from the start of using this part of the equipment the apogee kick propellant has been consumed. Also the values of ΔV and I are different :

$$M_i = 456.3 \text{ kg.}$$

ΔV_{oc} = 521 m/s, which is a mission requirement for the orbit control system during the lifetime of 10 years (an orbit correction of 50 m/s a year and 21 m/s which is necessary for the transfer orbit manoeuvering).

ΔV_{ac} = 20 m/s, which is an estimated necessary velocity increment for the attitude correction (2 m/s a year).

I_{oc} = 280 sec, which is a thruster specification.

I_{ac} = 200 sec, idem.

The values of the propellant masses are respectively :

$$M_{oc} = 83.6 \text{ kg.}$$

As the necessary mass for the spin-down comes on the account of the attitude control system a mass of M_{sd}= 0.31 kg (see section 11.5.3) has to be added to the mass which is a result of the formula above. In the M_{ac} as given below this M_{sd} is included.

$$M_{ac} = 5.45 \text{ kg.}$$

Also an estimation can be made for the needed construction mass of this UPS (ref. 11.1) :

$$M_{co} = 0.084 * M_{pt}$$

In which : M_{co} = the construction mass.

M_{pt} = the total propellant mass.

This means, that M_{co} = 35.2 kg. This value should be seen as a kind of mass budget for the several parts of the propulsion system. The dry mass ofsatellite propulsion system should not exceed this estimated value. Later on in this chapter an equipment list will be shown with the corresponding masses.

11.5.2 Pressurizing gas mass.

The amount of necessary Helium, which is used as a pressurizing gas in operation and is conserved in a high pressure tank, can be estimated by the following formula (ref. 11.7):

$$V_p = V_t ([n \cdot P_t]/[P_{ti} - P_{pe}]) \cdot (1 + res)$$

In which : V_p = pressurant tank volume.

V_t = propellant tank volume.

P_t = propellant tank pressure.

P_{pi} = initial pressure in Helium tanks (=300 bar).

P_{te} = final pressure in Helium tanks (= 25 bar).

n = polytropic exponent (= 1.2).

res = reserve (5%).

The value for the polytropic exponent is a safe one, which accounts for all the complex processes occure, like pressure losses and problems with emptying of the tanks. The reserve of 5% is taken because of safety reasons.

The propellant tank pressure is 17.5 bar, which is the maximum expected operating pressure (MEOP). The value of V_t = 0.0931 m³ (volume of one tank) as can be found in section 11.6 in which it is determined. This means that the two identical spherical Helium tanks need to have volume of V_p = 0.0134 m³.

As the density of the liquid Helium is ρ = 50.36 kg/m³, the required Helium mass is M_{he} = 1.35 kg.

11.5.3 Acceleration and burntime.

The minimum and maximum values of the acceleration, which will occure during the apogee engine firing, can be determined, for all the masses are known. The initial mass of the satellite with all the propellant on board is :
M_i = 786.6 kg.

The apogee engine produces a constant force of 490 N from what is concluded, that the minimum acceleration, which occurs at the start, is a_{min} = 0.62 m/s². The maximum acceleration occures at the end of the apogee engine firing when all of the apogee propellant mass (331.1 kg) has been consumed. Therefore the maximum acceleration is : a_{max} = 1.07 m/s².

The burntime and the necessary time for the required spin-down are calculated below.

To calculate the burntime of the apogee booster the average acceleration during this phase of the transfer orbit is used :

$$a_{av} = \frac{a_{max} + a_{min}}{2} = 0.845 \text{ m/s}^2 . \tag{11.3}$$

As mentioned before, the constant thrustforce is 490 N and the mission required velocity increment is 1488 m/s. This means, that the burntime (t_b) is:

$$t_b = \frac{\Delta V}{a_{av}} = \frac{1488}{0.845} = 1761 \text{ sec. (29.35 minutes)}. \tag{11.4}$$

The propellant massflow during this burning is :

$$m = \frac{M_p}{t_b} \ , \ m = 0.188 \ kg/s. \tag{11.5}$$

The burntime of the boost phase of the station keeping thrusters (2 * 4.45 N = 8.90 N), which is necessary to accomplish the required second velocity increment (21 m/s) is calculated in the same way.

The satellite mass at the time of ignition is $M_* = M_i - M_{ap}$. The estimated propellant mass for this part of the transfer orbit is: $M_{p*} = \frac{21}{521} * M_{oc} = 3.37$ kg ,because the total amount of orbit control propellant is based on the estimated necessary total velocity increment during ten years (521 m/s). Although this is not a lineary equation, the mass, which is needed for manoeuvres like this one, is calculated this way. Now the average acceleration is:

$a_{av*} = 0.195 \ m/s^2$. The burntime now is:

$$t_{b*} = \frac{21}{a_{av}} = \frac{21}{0.195} = 1074 \ sec \ (17.9 \ minutes).$$

Now the spindown time and the necessary amount of fuel for this manoeuvre is considered. The rate of rotation around the principal axis of inertia during the transfer orbit is : $\omega = 4.189$ rad/s (40 r.p.m.). This is also the rate of rotation decrement, which has to be done by the attitude control thrusters of 4.45 N.

$\Delta\omega = 4.189$ rad/s. The moment of inertia around the x-axis is: $I_{xx} = 400 \ kgm^2$. The moment generated by the thrusters is :

$M_{xx} = 2.0 * 4.45 = 8.90 \ Nm.$

With the formula : $M_{xx} = I_{xx} + \frac{d\omega}{dt}$ follows:

$\frac{d\omega}{dt} = \frac{8.90}{400} = 0.0223 \ rad/s^2$. The spin-down time therefore is:

$$t_{sd} = \frac{4.189}{0.0223} = 188.3 \ sec \ (3.13 \ minutes).$$

The extra quantity of propellant ,which is needed for the manoeuvre is : $\Delta M = 0.31$ kg. This follows from the relations:

$F = m + g_o + I_{sp}$ and $m = \frac{\Delta M}{t_b}$.

(F=4.45 N; g_o=9.8066 m/s^2 ; I_{sp}=280 sec.)

This amount comes on the account of the attitude control system as can be seen in section 11.5.1.

(

11.6 Tanks.

11.6.1 Propellant tanks.

The important specifications of the fuel and oxidizer tanks are given below. Some of these specifications are calculated in the Turbopascal computer program, which can be found in the appendix.

-Volume : As the necessary amount of propellant is known, it is possible to determine the volume of the tanks which is needed. The fuel (MMH) and oxidizer (NTO) are both stored at a temperature of 20°C. At this temperature the densities are repectively: ρ_{MMH}= 876.5 kg/m^3 and ρ_{NTO}= 1446.8 kg/m^3. In order to get identical tanks the combustion mixture ratio (r) has to be taken in accordance with the ratio of both densities :

$$r = \frac{\rho_{NTO}}{\rho_{MMH}} = \frac{1446.8}{876.5} = 1.65$$. Another aspect which is considered is, that the tanks cannot be filled totally. This means that a fill ratio has to be introduced. In this case it is possible to fill the tanks up to 97 %. Chosen is a configuration of 4 propellant tanks so the volume of each tank has been determined with these data : V_{prop}= 0.0931 m^3.

-Material : The Titanium alloy Ti-6Al-4V has been chosen for these tanks, because it is a light weight metal with a density of ρ = 4.43+10^3 kg/m^3 in connection with a rather high strength of σ = 1103+10^6 N/mm^2 and the highly agressive fuel and oxidizer do not affect this alloy.

-Shape : The 4 tanks are identical and their shape was decided to be spherical.

-Diameter : According to the chosen shape and necessary volume the diameter is: d = 562 mm.

-MEOP : The maximum expected operating pressure is : 17.5 bar

-Burst : The burst pressure is rather high because of the fact that the dimensioned burst pressure of 2*MEOP could not be realised. The required mininum wall thickness for this pressure is too little and a minimum wall thickness of 0.8 mm is required for reasons of production.

-PMD : A propellant management device is used for propellant draining.

-Sloshing : To handle the sloshing problems two baffles are assembled.

-Thickness: The wall thickness is 0.8 mm.

-Dry mass : The dry mass of the tank (baffles and PMD excluded) is: 3.52 kg.
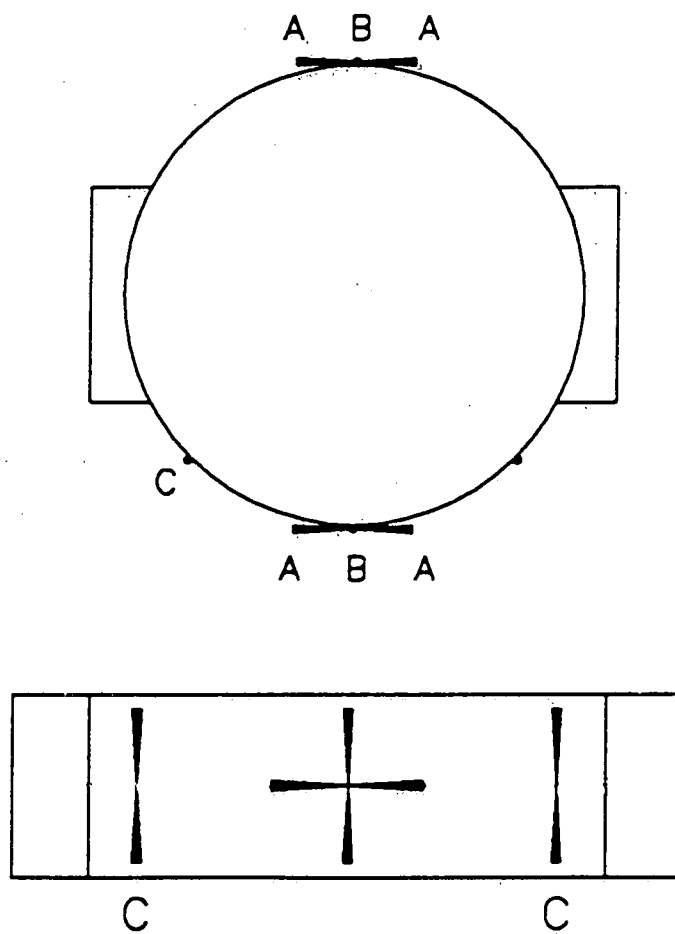
figure 11.6
Thrusters-configuration.

```
------------------------------------------------------
 | EQUIPMENT LIST                         MASS
 |_____
 |
 |  4 propellant tanks            4*3.52 =14.08
 |  2 pressurant tanks            2*2.20 =4.40
 |  1 apogee engine               1*3.76 =3.76
 | 12 attitude control thrusters 12*0.43 =5.16
 |  1 pressure regulator                 =0.230
 |  1 relief valve                       =0.050
 |  2 non-return valves           2*0.150=0.300
 |  2 filters                            =0.050
 |  3 n.c.gas pyro valves         3*0.055=0.165
 |  2 n.o.gas pyro valves         2*0.055=0.110
 |  2 n.c.liquid pyro valves      2*0.080=0.160
 |  2 n.o.liquid pyro valves      2*0.080=0.160
 |  5 pressure transducers        5*0.120=0.600
 |  4 latching valves             4*0.250=1.000
 |    helium (liquid)                     1.350
 |  7 prop/fill & drain valves    6*0.035=0.210
 |  2 He/fill & drain valves      2*0.080=0.160
 |    tubing/fitting                     =4.000
 |                               -----------------
 |              mass      :              35.90
 |              10% margin:               3.59
 |                               -----------------
 |              total mass:              39.49
 |
------------------------------------------------------
```

MODEL R-4D 110 LBf (490 N) BIPROPELLANT ROCKET ENGINE
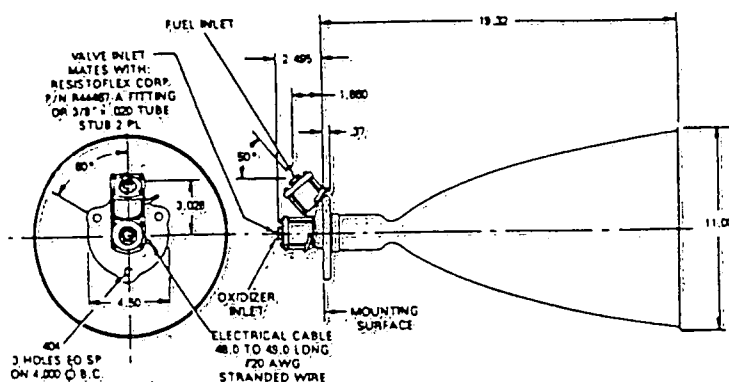
Dimensional Characteristics

FUEL INLET

VALVE INLET
MATES WITH:
RESISTOFLEX CORP.
P/N R44467-A FITTING
OR 3/8" x .020 TUBE
STUB 2 PL

60°

19.32

2.495

1.880

.77

3.028

OXIDIZER
INLET

MOUNTING
SURFACE

11.00

4.50

404
3 HOLES EQ SP
ON 4.000 Ø B.C.

ELECTRICAL CABLE
48.0 TO 49.0 LONG
#20 AWG
STRANDED WIRE

NOTE: DIMENSIONS ARE INCHES

Performance Characteristics

(ENGLISH UNITS)

	NOMINAL	RANGE
THRUST:	110 LBf	60-150 LBf
FEED PRESSURE:	220 PSIA	100-400 PSIA
MIXTURE RATIO	1.65	1.0-2.4
VOLTAGE RANGE:	28 VDC	18-50 VDC
WEIGHT:	8.3 LBm	
SPECIFIC IMPULSE:	311 SECONDS	

MINIMUM IMPULSE BIT:	0.6 LBf SEC
MAXIMUM FIRING TIME:	CONTINUOUS
POWER CONSUMPTION:	1-4 AMPS @ 28 VDC
PROPELLANTS	NITROGEN TETROXIDE/MONOMETHYLHYDRAZINE OR HYDRAZINE
USAGE:	APOGEE/PERIGEE MANEUVER; ORBIT ADJUST; ATTITUDE CONTROL
STATUS:	FLIGHT QUALIFIED

Thermal Characteristics

FUEL INLET

130/140°F
(54/60°C)

980°F
(527°C)

2300°F
(1260°C)

280/360°F
(138/182°C)

OXIDIZER
INLET

MOUNTING
SURFACE

XXXX/XXXX – STEADY STATE/SOAKBACK

DISTANCE FROM INJECTOR FACE (INCHES)

figure 11.4
Model R-4D engine.

11.6.2 Helium tanks.

The specifications for the pressurant tanks (2) follow below:

-Volume   : This has already been calculated in section 11.5.2:
$$V_p = 0.0134 \text{ m}^3.$$

-Material : As this tank has to withstand a very high pressure a combination
of the same Titanium alloy as for the propellant tanks and Kevlar
is used. The thin Titanium wall of 1.0 mm is needed for sealing
and the Kevlar for strength. The density of the Kevlar is ρ =
$1.38+10^3$ kg/m^3, the strength in longitudinal direction is $\sigma_{lo}=$
1378 N/mm^2 and in transverse direction $\sigma_{tr}=$ 29 N/mm^2.

-Shape   : These tanks are also spherical.

-Diameter : This is : d = 147 mm.

-MEOP   : 300 bar.

-Burst   : The burst pressure is 2*MEOP = 600 bar.

-Thickness: The wall of these tanks consists of : 1.0 mm of the Titanium alloy
Ti-6Al-4V and a layer of 4.63 mm of Kevlar.

-Dry mass : The dry mass of one tank is : 2.2 kg.

11.1   Configuration and operation.

The configuration of the propulsion subsystem is similar to the combined
propulsion subsystem (CPS), used in the Olympus satellite (ref. 11.3 and
11.4), because the Olympus satellite is in many ways similar to the Hitchhiker
satellite. Points of resemblance are:
   * communications satellite
   * geostationary orbit
   * Ariane launched
   * unified bi-propellant propulsion subsystem
   * 3-axis stabilized
   * 10 years lifetime

Figure 11.2 shows a schematic lay-out of the CPS. The changes made for the
Hitchhiker application are the number of the helium tanks (2 instead of 4),
the number of propellant tanks (4 instead of 2) and the number of reaction
control thrusters (12 instead of 16).

The operation of the Hitchhiker unified propulsion system (UPS) can be divided
into the following modes:
1. During ground operations and Ariane 4 launch, the normally closed (nc)
valves 1 to 5 (see figure 11.2) are closed in order to avoid leakage by
isolating the propellant tanks from the pressurization sub-system.

MODEL R-2 1 LBf (4.45 N) BIPROPELLANT ROCKET ENGINE

Dimensional Characteristics
(With Bipropellant Valve)
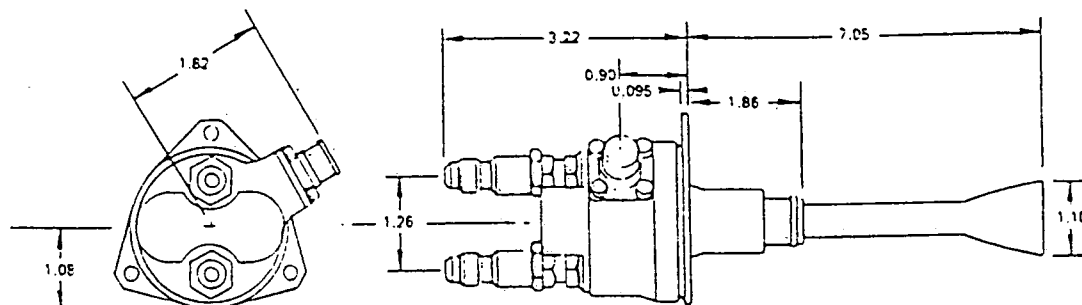
NOTE: DIMENSIONS ARE INCHES

Performance Characteristics
(ENGLISH UNITS)

	NOMINAL	RANGE
THRUST:	1 LBf	0.55-1.35 LBf
FEED PRESSURE:	220 PSIA	100-350 PSIA
MIXTURE RATIO	1.65	1.25-2.0
VOLTAGE RANGE:	28 VDC	18-32 VDC
WEIGHT:	0.95 LBm	
SPECIFIC IMPULSE:	280 SEC	

MINIMUM IMPULSE BIT: 0.003 LBf SEC @ 220 PSIA

MAXIMUM FIRING TIME: CONTINUOUS

POWER CONSUMPTION: 15 WATTS @ 28 VDC

PROPELLANTS: NITROGEN TETROXIDE/ MONOMETHYLHYDRAZINE

USAGE: ATTITUDE CONTROL/ STATIONKEEPING

STATUS: DEVELOPMENT

Thermal Characteristics

75°/95°F (24°/35°C)

150°/400°F (66°/204°C)

2300°F (1260°C)

°F

DISTANCE FROM INJECTOR FACE (IN)

XXX/XXX
STEADY STATE/SOAKBACK
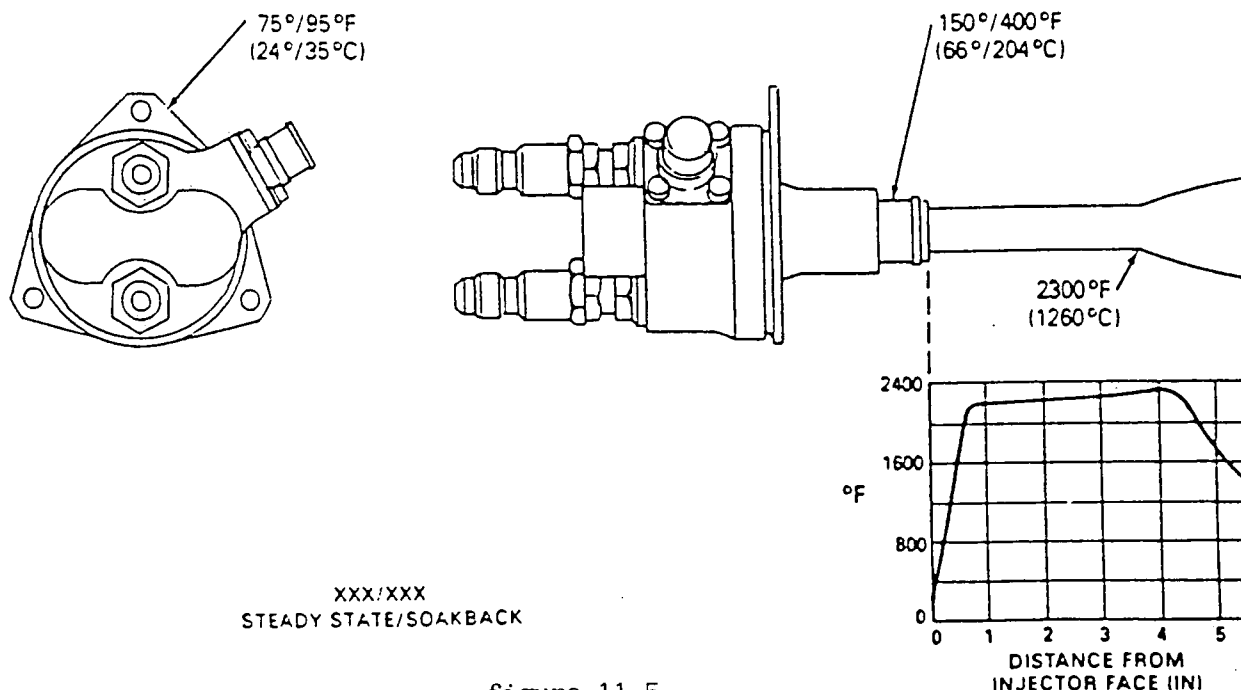
figure 11.5
Model R-2 engine.

2. During apogee motor firing (AMF), the nc valves 1 to 5 will be activated and will stay open. High-pressure helium (300 bar) is now fed to a single pressure regulator (since the pressure in the fuel and oxidizer tanks will be the same, the two pressure regulators presented in figure 11.2 can be replaced by one single pressure regulator). This pressure regulator controls the downstream pressure to 15.7 bar. The relief valve downstream of the regulator has the function of guarding against over-pressurisation of the propellant tanks. In the case of a fully open failure it will limit the tank pressure to 17.5 bar.

   Two non-return (check) valves prevent reverse flow of the propellants into the pressure regulator.

3. On completion of AMF, the normally open valves (no) 1 to 4 are fired, thereby isolating the pressurant tanks and apogee motor from the rest of the subsystem.

   The system now operates in the so-called "blow-down mode". The pressure in the propellant tanks is enough to force the propellant out of the tanks during reaction control manoeuvres.

Besides all the above mentioned elements, the UPS also consists of filters in the propellant feed line downstream of the nc-valves 4 and 5. Also several test points and pressure transducers are included to monitor the pressure.

A single apogee motor is used having a thrust level of 490 Newtons (110 Lbf).

Chosen is the Model R-4D built by the Marquardt Company (ref. 11.8). It has a high nominal specific impulse (312 sec) and the capability to fire continiously for more than one hour.

The dimensions and performance characteristics are shown in figure 11.3. The model R-4D engine has been in production for a lot of previuosly launched satellites and the performance characteristics are flight qualified.

The thermal characteristics of the apogee motor are also presented in figure 11.3. As can be seen from this figure, the maximum temperature in the nozzle is 1260°C.

The reaction control function is performed by 12 identical 4.45 N (1 Lbf) thrusters (Model R-2 ,Marquardt Company). The dimensional as well as the performance characteristics are shown in figure 11.4.

The model R-2 is capable of providing very small impulse bits while maintaining a relatively high steady state impulse (280 sec). The thermal characteristics are also shown in figure 11.4. The thrust chamber can be located within a heat shield for protection of sensitive devices on the satellite.

The thrusters are located on the satellite in such a manner, that all reaction control manoeuvres can be executed (see figure 11.5).

The thrusters for pitch control are not located on the inertial-axis of the satellite for structual reasons (they would otherwise be located too close to the bapta).

Thrusters #10 and #12 will also be used for East-West stationkeeping and thrusters #2 and #4 for North-South stationkeeping.

Finally, an equipment list is presented in table 11.7.1. The mass of the different valves and pressure regulator are copied from the equipmemt lists of comparable satellites and handbooks (ref 11.3 and 11.5).

With a 10% margin, the total dry mass of the propulsion subsystem will be 39.49 kg.

12   Conclusions.

The total massbudget of 936 kg exeeded the required total mass of 800 kg.
This mass-problem demonstrates one of the difficulties of designing a
satellite. Solutions have to be found to reduce the total mass. The total mass
could be reduced when the following points are used. This could be
demonstrated in a continued study.

- The application of SSPA's. This could mean a mass reduction of 20 kg.
  When using SSPA's less equipment is used, so the complexity of the system
  will be decreased. However, SSPA's are less efficient so the extra power
  needed could result in a higher total mass.
- The use of thinner solar cells means a reduction of 2 a 3 kg.
- The application of advanced materials such as carbon fiber would also
  reduce the mass considerably, when used in equipment like the cylinder.
- The batteries are designed for maximum power use for every subsystem at
  all times. When a power profile is studied this will probably lead to a
  more efficient use of power, so the battery capacity in the eclipse could
  be reduced. This would decrease the battery mass and possibly the amount
  of solar cells.

N.B. The propulsion system used here gives an extra 1.5 kg mass reduction
per saved kg. A mass reduction of 60 kg of equipment would mean an actual
saving of 140 kg in the total mass.

Some interesting point for further study, due to lack of available time
are:

- A detailed study of the requirement of the subsystems;
- A study of the power profile;
- The separation mechanisms;
- The extra support structure;
- The tank support structure;
- The desaturation procedure;
- The stationkeeping mode;
- The use of a higher frequency, since the use of the C-band needs special
  authorization;
- The reliability of all the subsystems.

Besides these points, a study could be performed to the tasks which were
neglected in the first stage of the design study, like:
- A trade-off study of the stabilization system: spin, dual-spin or three-
  axis stabilization.
- Manufacture & Test;
- Cost analysis.

Appendix A: Program to calculate moments of inertia and the location of the
            center of gravity.


```
program traagh(input,output);

{This programma computes the moments of inertia and the location of the center}
{of gravity for the Hitch-Hiker satellite.}
{Assumptions: -homogeneous massdistribution over the elements}
{             -a few simplified element models.}
{16 mei, Barendrecht, Albert-Jan Bunt}

var l,b,h,r,t,Ix,Iy,Iz,Cxy,Cyz,Cxz,x1,y1,z1,m1,xz,yz,zz,
    Ix1,Iy1,Iz1 : real;
    el,nr,i : integer;
    f,g : text;
    m,x,y,z : array[1..90] of real;

begin
    Ix:=0;
    Iy:=0;
    Iz:=0;
    nr:=0;
    assign(f,'traagHto.dat');
    reset(f);
    readln(f,el);
    while (el<>0) do
    begin
        nr:=nr+1;
        if el=1 then begin
            readln(f,l,b,h,m[nr],x[nr],y[nr],z[nr]);
            Ix:=Ix+m[nr]*(b*b+h*h)/12;
            Iy:=Iy+m[nr]*(l*l+h*h)/12;
            Iz:=Iz+m[nr]*(l*l+b*b)/12;
            end;
        if el=2 then begin
            readln(f,r,m[nr],x[nr],y[nr],z[nr]);
            Ix:=Ix+m[nr]*r*r*2/3;
            Iy:=Iy+m[nr]*r*r*2/3;
            Iz:=Iz+m[nr]*r*r*2/3;
            end;
        if el=3 then begin
            readln(f,r,m[nr],x[nr],y[nr],z[nr]);
            Ix:=Ix+m[nr]*r*r*2/5;
            Iy:=Iy+m[nr]*r*r*2/5;
            Iz:=Iz+m[nr]*r*r*2/5;
            end;
        if el=4 then begin
```

```pascal
          readln(f,t,r,m[nr],x[nr],y[nr],z[nr]);
          Ix:=Ix+m[nr]*t*t/12+m[nr]*r*r/4;
          Iy:=Iy+m[nr]*t*t/12+m[nr]*r*r/4;
          Iz:=Iz+m[nr]*r*r/2;
          end;
        if el=5 then begin
          readln(f,t,r,m[nr],x[nr],y[nr],z[nr]);
          Ix:=Ix+m[nr]*r*r/2;
          Iy:=Iy+m[nr]*t*t/12+m[nr]*r*r/4;
          Iz:=Iz+m[nr]*t*t/12+m[nr]*r*r/4;
          end;
        if el=6 then begin
          readln(f,t,r,m[nr],x[nr],y[nr],z[nr]);
          Ix:=Ix+m[nr]*t*t/12+m[nr]*r*r/4;
          Iy:=Iy+m[nr]*r*r/2;
          Iz:=Iz+m[nr]*t*t/12+m[nr]*r*r/4;
          end;
        if el=7 then begin
          readln(f,t,r,m[nr],x[nr],y[nr],z[nr]);
          Ix:=Ix+m[nr]*r*r*3/20+m[nr]*t*t*3/5;
          Iy:=Iy+m[nr]*r*r*3/20+m[nr]*t*t*3/5;
          Iz:=Iz+m[nr]*r*r*3/10;
          end;
        readln(f,el);
  end;
  Ix1:=Ix;
  Iy1:=Iy;
  Iz1:=Iz;
  close(f);

  for i:=1 to nr do
  begin
      Ix:=Ix+m[i]*(y[i]*y[i]+z[i]*z[i]);
      Iy:=Iy+m[i]*(x[i]*x[i]+z[i]*z[i]);
      Iz:=Iz+m[i]*(x[i]*x[i]+y[i]*y[i]);
      Cxy:=Cxy+x[i]*y[i]*m[i];
      Cyz:=Cyz+y[i]*z[i]*m[i];
      Cxz:=Cxz+x[i]*z[i]*m[i];
  end;
  writeln('The moments of inertia about the center are:');
  writeln('Ix=',Ix);
  writeln('Iy=',Iy);
  writeln('Iz=',Iz);
  writeln('Cxy=',Cxy);
  writeln('Cyz=',Cyz);
  writeln('Cxz=',Cxz);

  for i:=1 to nr do
```

```
      begin
          x1:=x1+x[i]*m[i];
          y1:=y1+y[i]*m[i];
          z1:=z1+z[i]*m[i];
          m1:=m1+m[i];
      end;
      xz:=x1/m1;
      yz:=y1/m1;
      zz:=z1/m1;
      writeln('The position of the center of gravity about the center is:');
      writeln('x=',xz);
      writeln('y=',yz);
      writeln('z=',zz);

      for i:=1 to nr do
      begin
          x[i]:=x[i]-xz;
          y[i]:=y[i]-yz;
          z[i]:=z[i]-zz;
      end;

      Cxy:=0;
      Cyz:=0;
      Cxz:=0;
      Ix:=Ix1;
      Iy:=Iy1;
      Iz:=Iz1;
      for i:=1 to nr do
      begin
          x1:=x1+1;
          Ix:=Ix+m[i]*(y[i]*y[i]+z[i]*z[i]);
          Iy:=Iy+m[i]*(x[i]*x[i]+z[i]*z[i]);
          Iz:=Iz+m[i]*(x[i]*x[i]+y[i]*y[i]);
          Cxy:=Cxy+x[i]*y[i]*m[i];
          Cyz:=Cyz+y[i]*z[i]*m[i];
          Cxz:=Cxz+x[i]*z[i]*m[i];
      end;
      writeln('The moments of inertia about the center of gravity are:');
      writeln('Ix=',Ix);
      writeln('Iy=',Iy);
      writeln('Iz=',Iz);
      writeln('Cxy=',Cxy);
      writeln('Cyz=',Cyz);
      writeln('Cxz=',Cxz);

      close(f);
end.
```

Appendix B: PSIE-program to simulate AOCS.

SYMBOLS USED IN PSI-PRGOGRAM

A	Total solar panels area
A_ANT	Area of the antenna
DECL	Declination of the sun
ELEV	Elevation of the antenna with respect of the S/C axis
IXX	Moment of inertia about x-axis
IYY	Moment of inertia about y-axis
IZZ	Moment of inertia about z-axis
KOP	KOP=0 if coupling terms neglected and KOP=1 if not
KPHI	Gain of the x-axis controller
KPSI	Gain of the z-axis controller
KTETA	Gain of the y-axis controller
OMEGA	Orbital rate
P	Solar radiation pressure
PHIRE	Reference angle of roll
PSIREF	Reference angle of yaw
RHOD	Diffuse reflection coefficient of solar arrays
RHODA	Diffuse reflection coefficient of antenna
RHOS	Specularly reflection coefficient of solar arrays
RHOSA	Specularly reflection coefficient of antenna
TETAREF	Reference angle of pitch
TOUPHI	Time constant of x-axis controller
TOUPSI	Time constant of z-axis controller
TOUTETA	Time constant of y-axis controller
X,Y,Z	Components of vector r of solar arrays
XA,YA,ZA	Components of vector r of antenna

** Structure and parameters of present model **
===

Block	Type Inputs/Comment	Par1	Par2	Par3
A	CON	10.00		
A_ANT	CON	2.550		
DECL	CON	-.4101		
EEN	CON	1.000		
ELEV	CON	.1187		
IXX	CON	1096.		
IYY	CON	87.00		
IZZ	CON	1082.		
KOP	CON	.0000		
KPHI	CON	9.500		
KPSI	CON	9.500		
KTETA	CON	1.700		
NUL	CON	.0000		
OMEGA	CON	7.2722E-05		
P	CON	4.6440E-06		
PHIREF	CON	.0000		
PSIREF	CON	.0000		

-140-

RHOD	CON		.0000		
RHODA	CON		.0000		
RHOS	CON		.2000		
RHOSA	CON		.2000		
TETAREF	CON		.0000		
TOUPHI	CON		15.00		
TOUPSI	CON		15.00		
TOUTETA	CON		10.00		
X	CON		1.0000E-02		
XA	CON		1.200		
Y	CON		1.0000E-02		
YA	CON		.0000		
Z	CON		1.0000E-02		
ZA	CON		-.9000		
Q12	DIV	M11, IXX			
Q15	DIV	M21, IYY			
Q18	DIV	M31; IZZ			
ALPHA	INO	OMEGA	.0000	1.000	
H1	INT	HDOT1LIM	.0000		
H2	INT	HDOT2LIM	.0000		
H3	INT	HDOT3LIM	.0000		
PHI	INT	PHIDOT	.0000		
PHIDOT	INT	Q12	.0000		
PSI	INT	PSIDOT	.0000		
PSIDOT	INT	Q18	.0000		
TETA	INT	TETADOT	.0000		
TETADOT	INT	Q15	.0000		
HDOT1LIM	LIM	HDOT1	-.1000	.1000	1.00(
HDOT2LIM	LIM	HDOT2	-.1000	.1000	1.00(
HDOT3LIM	LIM	HDOT3	-.1000	.1000	1.00(
C10	MUL	OMEGA, H3, PSI			
C11	MUL	H1, PSIDOT			
C13	MUL	PHIDOT, H3			
C14	MUL	C3, PHIDOT			
C15	MUL	OMEGA, H2, PSI			
C16	MUL	OMEGA, H1			
C18	MUL	TETADOT, H1			
C2	MUL	C1, OMEGA			
C4	MUL	C3, PSIDOT			
C5	MUL	OMEGA, H2, PHI			
C6	MUL	OMEGA, H3			
C8	MUL	TETADOT, H3			
C9	MUL	OMEGA, H1, PHI			
ERC	MUL	COSDECL, EENRHOS			
HDOT1	MUL	Q14, KPHI			
HDOT2	MUL	Q17, KTETA			
HDOT3	MUL	Q20, KPSI			
K1	MUL	Q2, COSDECL			
K2	MUL	SINDECL, ERC			
L1	MUL	EENRHOSA, SINALPHA, COSDECL			
L21	MUL	EENRHOSA, SINDECL			
L22	MUL	RHOMIX, SINELEV			
L31	MUL	EENRHOSA, COSALPHA, COSDECL			
L32	MUL	RHOMIX, COSELEV			
MA1	MUL	PA_ANT, NS, MA13			
MA11	MUL	YA, L3			
MA12	MUL	ZA, L2			

MA2	MUL	PA_ANT, NS, MA23			
MA21	MUL	ZA, L1			
MA22	MUL	XA, L3			
MA3	MUL	PA_ANT, NS, MA33			
MA31	MUL	XA, L2			
MA32	MUL	YA, L1			
MK1	MUL	KOP, MKOP1			
MK2	MUL	KOP, MKOP2			
MK3	MUL	KOP, MKOP3			
MS1	MUL	Q5, PA			
MS2	MUL	Q8, PA			
MS3	MUL	Q11, PA			
NS1	MUL	SINELEV, SINDECL			
NS2	MUL	COSELEV, COSALPHA, COSDECL			
PA	MUL	P, A			
PA_ANT	MUL	P, A_ANT			
Q10	MUL	Y, K1, SINALPHA			
Q13	MUL	PHIDOT, TOUPHI			
Q16	MUL	TETADOT, TOUTETA			
Q19	MUL	PSIDOT, TOUPSI			
Q3	MUL	Y, COSALPHA, K1			
Q4	MUL	Z, K2			
Q6	MUL	Z, K1, SINALPHA			
Q7	MUL	X, K1, COSALPHA			
Q9	MUL	X, K2			
COSALPHA	SIN	ALPHA	1.000	1.571	1.000
COSDECL	SIN	DECL	1.000	1.571	1.000
COSELEV	SIN	ELEV	1.000	1.571	1.000
SINALPHA	SIN	ALPHA	1.000	.0000	1.000
SINDECL	SIN	DECL	1.000	.0000	1.000
SINELEV	SIN	ELEV	1.000	.0000	1.000
C1	SUM	IYY, IXX, IZZ	-1.000	1.000	1.000
C12	SUM	C9, C10, C11	1.000	1.000	1.000
C17	SUM	C14, C15, C16	-1.000	1.000	-1.000
C3	SUM	C2, H2	1.000	1.000	
C7	SUM	C4, C5, C6	1.000	1.000	1.000
E1	SUM	PHIREF, PHI	1.000	1.000	
E2	SUM	TETA, TETAREF	1.000	1.000	
E3	SUM	PSI, PSIREF	1.000	1.000	
EENRHOS	SUM	EEN, RHOS	1.000	-1.000	
EENRHOSA	SUM	EEN, RHOSA	1.000	-1.000	
L2	SUM	L21, L22	1.000	-1.000	
L3	SUM	L31, L32	1.000	1.000	
M1	SUM	MTOT1, MK1	1.000	1.000	
M11	SUM	M1, HDOT1LIM	1.000	-1.000	
M2	SUM	MTOT2, MK2	1.000	1.000	
M21	SUM	M2, HDOT2LIM	1.000	-1.000	
M3	SUM	MTOT3, MK3	1.000	1.000	
M31	SUM	M3, HDOT3LIM	1.000	-1.000	
MA13	SUM	MA11, MA12	1.000	-1.000	
MA23	SUM	MA21, MA22	1.000	-1.000	
MA33	SUM	MA31, MA32	1.000	-1.000	
MKOP1	SUM	C8, C7	-1.000	1.000	
MKOP2	SUM	C12, C13	-1.000	1.000	
MKOP3	SUM	C17, C18	1.000	1.000	
MTOT1	SUM	MA1, MS1	1.000	1.000	
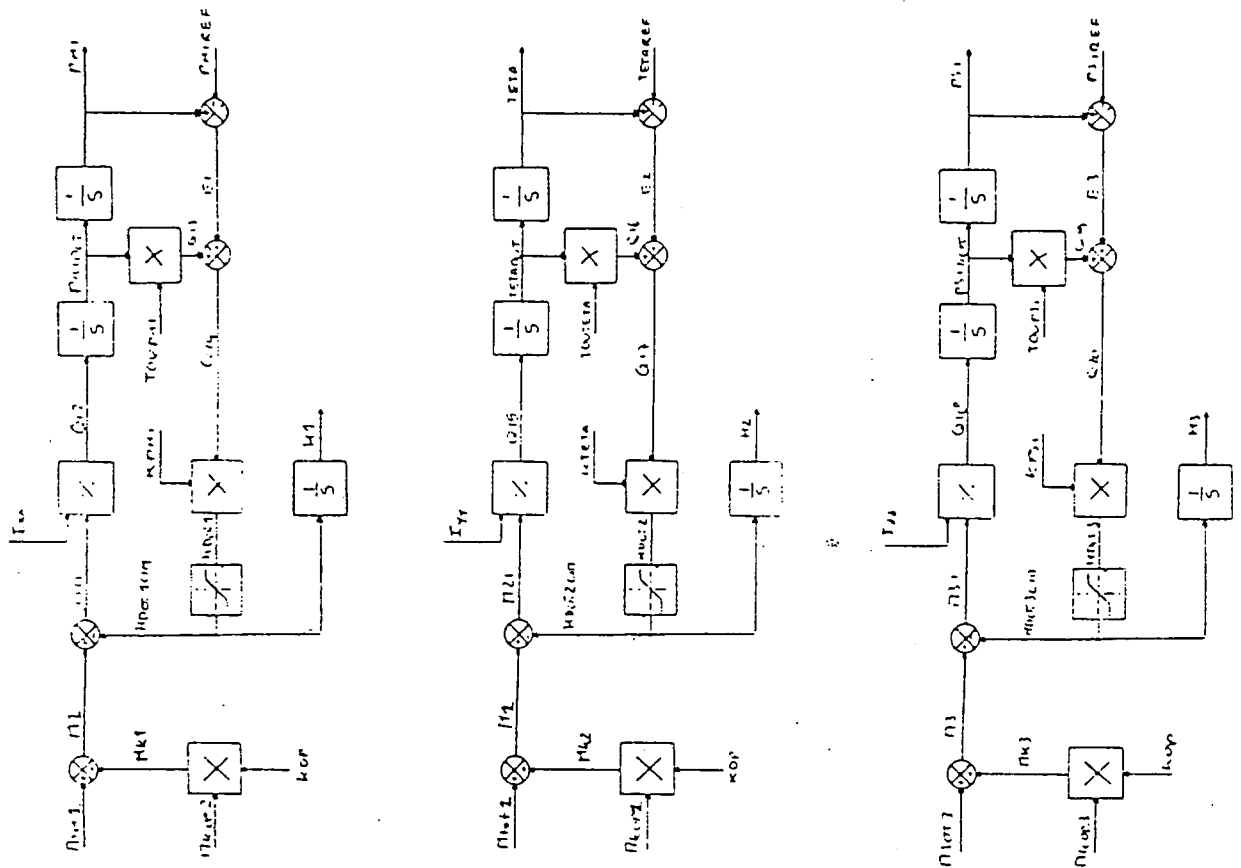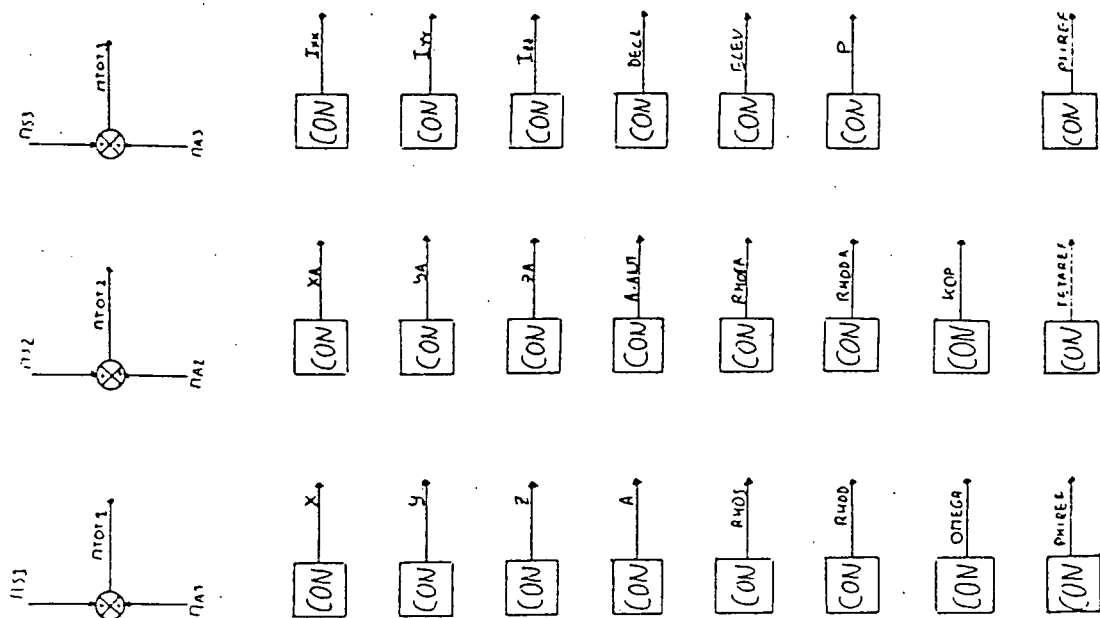
Appendix C: JASON output.

; RADIATIVE COUPLINGS ;

NODE I, NODE J, RAD. I->J:? 0,0,0
         1   2 .496500E-03   1   3 .816500E-02
         1   13 .426400E-01   2   4 .294300E-01
         2   13 .887700E-01   3   4 .160600E-02
         3   5 .816500E-02   3   13 .101800E+00
         4   6 .816500E-02   4   13 .805000E-01
         5   6 .647000E-04   5   7 .267600E-02
         5   13 .403900E-01   6   8 .267600E-02
         6   13 .403900E-01   7   8 .647000E-04
         7   9 .816500E-02   7   13 .403900E-01
         8   10 .816500E-02   8   13 .403900E-01
         9   10 .160600E-02   9   11 .294300E-01
         9   13 .805000E-01   10   12 .816500E-02
        10   13 .101800E+00   11   12 .496500E-03
        11   13 .887700E-01   12   13 .426400E-01
        13   14 .332100E+00   13   15 .496000E-01
        14   15 .292500E+00

figure C.1

-1001,   1,   2, 2.227E-07,   -1002,   1,   3, 6.150E-07
-1003,   1,   4, 6.107E-07,   -1004,   1,   5, 6.879E-02
-1005,   1,   9, 3.646E-03,   -1006,   2,   3, 6.107E-07
-1007,   2,   4, 6.149E-07,   -1008,   2,   6, 6.931E-02
-1009,   2,   9, 3.643E-03,   -1010,   3,   4, 2.227E-07
-1011,   3,   7, 7.043E-02,   -1012,   3,   9, 3.614E-03
-1013,   4,   8, 6.931E-02,   -1014,   4,   9, 3.643E-03
-1015,   5,   9, 3.720E-03,   -1016,   6,   9, 3.675E-03
-1017,   7,   9, 3.707E-03,   -1018,   8,   9, 3.674E-03

figure C.3

```
=======================================================================
maximum solar radiation on the box
rad-space=0.9*0.65*0.5     e blanket=0.08
=======================================================================
```

NODE NAME	TEMP.	TENVR	TENVC	SOL.INP.	INTPOW.	TOTPOW.	SIGMAT4
1 twt	35.45	28.59	27.83	.00	16.00	16.00	513.99
2 epc	29.73	28.96	27.83	.00	4.00	4.00	476.89
3 epc	28.35	29.60	27.83	.00	.00	.00	468.25
4 epc	29.85	29.38	27.83	.00	4.00	4.00	477.65
5 twt	35.51	28.96	27.83	.00	16.00	16.00	514.36
6 twt	35.49	28.80	27.83	.00	16.00	16.00	514.19
7 twt	35.54	29.19	27.83	.00	16.00	16.00	514.58
8 twt	28.03	29.19	27.83	.00	.00	.00	466.28
9 epc	29.86	29.40	27.83	.00	4.00	4.00	477.70
10 epc	29.76	29.09	27.83	.00	4.00	4.00	477.11
11 epc	29.73	28.96	27.83	.00	4.00	4.00	476.90
12 twt	35.49	28.82	27.83	.00	16.00	16.00	514.21
13 blankets	28.63	26.83	.00	12.95	.00	12.95	469.98
14 radiator	27.83	-15.46	31.90	46.38	.00	46.38	465.02
15 space	-270.00	.00	.00	.00	.00	.00	.00

```
=======================================================================
```
NR OF ITERATIONS: 35

```
=======================================================================
no solar radiation on the box
rad space=0.9*0.65*0.5 eblanket=0.08, ablanket=0.08
=======================================================================
```

NODE NAME	TEMP.	TENVR	TENVC	SOL.INP.	INTPOW.	TOTPOW.	SIGMAT4
1 twt	2.75	-5.61	-5.05	.00	16.00	16.00	328.38
2 epc	-3.34	-5.09	-5.05	.00	4.00	4.00	300.32
3 epc	-4.93	-4.52	-5.05	.00	.00	.00	293.30
4 epc	-3.22	-4.55	-5.05	.00	4.00	4.00	300.85
5 twt	2.80	-5.15	-5.05	.00	16.00	16.00	328.62
6 twt	2.79	-5.31	-5.05	.00	16.00	16.00	328.54
7 twt	2.83	-4.89	-5.05	.00	16.00	16.00	328.76
8 twt	-5.03	-4.90	-5.05	.00	.00	.00	292.85
9 epc	-3.21	-4.52	-5.05	.00	4.00	4.00	300.88
10 epc	-3.34	-5.08	-5.05	.00	4.00	4.00	300.33
11 epc	-3.34	-5.09	-5.05	.00	4.00	4.00	300.33
12 twt	2.78	-5.35	-5.05	.00	16.00	16.00	328.52
13 blankets	-5.77	-5.77	.00	.00	.00	.00	289.64
14 radiator	-5.05	-44.83	-1.04	.00	.00	.00	292.77
15 space	-270.00	.00	.00	.00	.00	.00	.00

```
=======================================================================
```
NR OF ITERATIONS: 36

figure C.2

===

NODE NAME	TEMP.	TENVR	TENVO	SOL.INP.	INTPOW.	TOTPOW.	SIGMAT4
1 bat1	6.38	6.46	6.31	.00	.00	.00	345.96
2 bat2	6.37	6.45	6.31	.00	.00	.00	345.96
3 bat3	6.37	6.45	6.31	.00	.00	.00	345.95
4 bat4	6.37	6.46	6.31	.00	.00	.00	345.96
5 rad1	6.31	2.70	7.82	.00	.00	.00	345.63
6 rad2	6.31	2.70	7.82	.00	.00	.00	345.63
7 rad3	6.31	2.73	7.82	.00	.00	.00	345.63
8 rad4	6.31	2.70	7.82	.00	.00	.00	345.63
9 body	9.26	-130.84	6.31	39.17	113.30	152.47	360.49
10 space	-270.00	.00	.00	.00	.00	.00	.00

===
NR OF ITERATIONS: 23

===
===

NODE NAME	TEMP.	TENVR	TENVO	SOL.INP.	INTPOW.	TOTPOW.	SIGMAT4
1 bat1	28.32	27.81	28.85	.00	.00	.00	468.10
2 bat2	2.61	2.69	2.55	.00	.00	.00	327.70
3 bat3	6.58	6.55	6.61	.00	.00	.00	346.97
4 bat4	2.61	2.69	2.55	.00	.00	.00	327.70
5 rad1	28.85	23.18	16.84	13.48	.00	13.48	471.37
6 rad2	2.55	-1.02	3.99	.00	.00	.00	327.41
7 rad3	6.61	2.73	5.97	2.05	.00	2.05	347.11
8 rad4	2.55	-1.02	3.99	.00	.00	.00	327.41
9 body	5.36	-128.60	10.14	16.07	113.30	129.37	340.96
10 space	-270.00	.00	.00	.00	.00	.00	.00

===
NR OF ITERATIONS: 27

===
===

NODE NAME	TEMP.	TENVR	TENVO	SOL.INP.	INTPOW.	TOTPOW.	SIGMAT4
1 bat1	46.15	32.67	33.60	.00	12.50	12.50	589.01
2 bat2	46.16	32.69	33.61	.00	12.50	12.50	589.08
3 bat3	46.11	32.71	33.61	.00	12.50	12.50	588.77
4 bat4	46.16	32.69	33.61	.00	12.50	12.50	589.08
5 rad1	33.60	40.36	29.65	.00	.00	.00	501.71
6 rad2	33.61	40.39	29.65	.00	.00	.00	501.79
7 rad3	33.61	40.39	29.63	.00	.00	.00	501.84
8 rad4	33.61	40.39	29.65	.00	.00	.00	501.80
9 body	13.14	-113.70	33.61	.00	113.30	113.30	380.71
10 space	-270.00	.00	.00	.00	.00	.00	.00

===
NR OF ITERATIONS: 25

figure C.4

LEFT INTENTIONALLY BLANK

LEFT INTENTIONALLY BLANK

LEFT INTENTIONALLY BLANK

Appendix D: The TSAT.PAS program.

The iterative routine given below was written to save time, because during the phase A study the values of the masses of the different subsystems, on which the propulsion system is dependent, changed all the time.
The program has been written in turbopascal.

```
PROGRAM PROG1(INV,UITV);
CONST g = 9.8066 ;                  {GRAVITY}
CONST n = 0.9 ;                     {EFFICIENCY}
CONST pi= 3.141592654;
CONST fr= 0.97;                     {FILL RATIO OF TANKS}
VAR MPA,MPAC,MPOC,MC,MPT,MD,MTOT,MPS,A,B,s   :REAL;
    MPL,C,D                                  :REAL;
    RO,RF,r,MOX,MFU,V,TV,RT,GH               :REAL;
    VP,Pt,VT,RP,HM                           :REAL;
    t,VMP,Pp,SIGP,RTI,MMP                     :REAL;
    tf,tm,Ph,SIGL,SIGT,SIGM,RKEV,MMH         :REAL;
    Rf1,Rf2                                  :REAL;
    DV,Is:ARRAY[1..3] OF REAL;
    I,Q,H,qw                                 :INTEGER;
    INV,UITV                                 :TEXT;
FUNCTION MATV(Ra,t: REAL): REAL;
  BEGIN
    MATV := 4*pi*Ra*Ra*t;
  END;
FUNCTION TH(P,Ra,SIG: REAL): REAL;
  BEGIN
    TH := (P*1.0E+05/1.01325)*Ra/(2*SIG);
  END;

{MASS CALCULATIONS}

FUNCTION FC(X,Y: REAL): REAL;
  BEGIN
    FC := 1-EXP(-X/(n*g*Y));
  END;
BEGIN
  ASSIGN(INV,'INV1.DAT');
  ASSIGN(UITV,'UITV1.DAT');
  REWRITE(UITV);
  CLRSCR;
  RESET(INV);
  WRITELN;
  WRITE('UNIFIED PROPULSION SYSTEM(=1),SOLID/MONO(=2) ? ');READLN(QW);
  WRITELN;
  WRITELN('A calculation can be made with a specified total- (Mtot) ');
  WRITELN('or dry satellite mass (dry propulsion mass not included) (MPL).');
  WRITELN;
  WRITELN(UITV);
  WRITE('Which specification will you use ? (MPL=1/Mtot=2) ?  ');READLN(H);
  WRITELN;
  WRITE('Give the specific impulse of the apogee engine : Is = ');READLN(GH);
  WRITELN;
  FOR Q:= 1 TO 3 DO
  BEGIN
    READLN(INV,DV[Q],Is[Q]);
  END;
```

```pascal
Is[1] := GH;
IF H=1 THEN
BEGIN
   WRITE('Give the dry mass of the satellite (without dry propulsion mass) : MPL=
');READLN(MPL);
   MC   := 30.0;
   C    := MC;
   MTOT := 600.0;
   A    := MTOT;
   REPEAT
     REPEAT
        MPA  := MTOT*(FC(DV[1],Is[1]));
        MPOC := (MTOT-MPA)*(FC(DV[2],Is[2]));
        MPAC := (MTOT-MPA)*(FC(DV[3],Is[3]));
        MPT  := MPA+MPOC+MPAC;
        MTOT := MPT+MPL+MC;
        IF QW=1 THEN MC := 0.084*MPT ELSE
        IF QW=2 THEN MC := 0.07*MPA + (0.01+0.0115*SQRT(10))*(MTOT-MPT);
        B := MTOT-A;
        A := MTOT;
        IF B < O THEN B:=-B;
     UNTIL B < 1.0E-03;
     D := MC-C;
     C := MC;
     IF D < O THEN D:=-D;
   UNTIL D < 1.0E-03;
   MD := MPL + MC;
END
ELSE IF H=2 THEN
BEGIN
   WRITE('Give the total mass of satellite Mtot= ');READLN(MTOT);
   MPA   := MTOT*(FC(DV[1],Is[1]));
   MPOC  := (MTOT-MPA)*(FC(DV[2],Is[2]));
   MPAC  := (MTOT-MPA)*(FC(DV[3],Is[3]));
   MPT   := MPA+MPOC+MPAC;
   MD    := MTOT-MPT;
   if qw=1 then mc := 0.084*mpt else
   if qw=2 then mc := 0.07*MPA + (0.01+0.0115*sqrt(10))*(mtot-mpt);
END;
MPS := MTOT-MD+MC;
IF QW=1 THEN
BEGIN
   WRITELN(UITV,'UNIFIED PROPULSION SYSTEM with specific impulses of: ');
   WRITELN(UITV);
   WRITELN(UITV,'a) apogee engine                      : Iap  = ',Is[1]:4:1,'sec');
   WRITELN(UITV,'b) orbit control thrusters            : Ioc  = ',Is[2]:4:1,'sec');
   WRITELN(UITV,'c) attitude control thrusters         : Iac  = ',Is[3]:4:1,'sec');
END
ELSE
BEGIN
   WRITELN(UITV,'SOLID/MONO with specific impulses of: ');
   WRITELN(UITV);
   WRITELN(UITV,'a) apogee engine                      : Iap  = ',Is[1]:4:1,'sec');
   WRITELN(UITV,'b) orbit control thrusters            : Ioc  = ',Is[2]:4:1,'sec');
   WRITELN(UITV,'c) attitude control thrusters         : Iac  = ',Is[3]:4:1,'sec');
END;
```

```
WRITELN(UITV);
WRITELN(UITV,'The dry mass of the satellite is      : Mdry  = ',MD:5:2,' kg');
WRITELN(UITV,'The total mass of the satellite is   : Mtot  = ',MTOT:5:2,' kg');
WRITELN(UITV,'The apogee propellant mass           : Map   = ',MPA:5:2,' kg');
WRITELN(UITV,'The orbit control propellant mass    : Moc   = ',MPOC:6:2,' kg');
WRITELN(UITV,'The attitude control propellant mass : Mac   = ',MPAC:6:2,' kg');
WRITELN(UITV,'The estimated construction mass      : Mcon  = ',MC:6:2,' kg');
WRITELN(UITV,'The total propulsion system mass is  : Mpro  = ',MPS:5:2,' kg');
IF QW=1 THEN
BEGIN

{TANK VOLUME}

  READLN(INV,RF,RO);
  r   := RO/RF;
  MOX := (r/(r+1))*MPT;
  V   := MOX/RO;
  WRITELN(UITV);
  TV  := (V/2)/fr;
  RT  := EXP((1/3)*LN((3/(4*pi))*TV));
  WRITELN(UITV,'The volume of each propellant tank is: Vprop = ',TV:6:5,' m^3');
  WRITELN(UITV,'This means a radius of               :     r = ',RT:4:3,' m');
  WRITELN(UITV);

  {PRESSURANT TANK VOLUME}

  READLN(INV,Pt);
  VP := 2*TV*(1.2*Pt/(275))*(1.05);
  WRITELN(UITV,'The volume of each pressurant tank is: Vpres = ',VP:6:5,' m^3');
  RP := EXP((1/3)*LN((3/(4*pi))*VP));
  HM := 2*VP*50.3597;
  WRITELN(UITV,'This means a radius of               :     r = ',RP:6:5,' m');
  WRITELN(UITV);
  WRITELN(UITV,'The required Helium mass is           :   Mhe = ',HM:3:2,' kg');

  {WEIGHT OF THE PROPELLANT TANKS}

  READ(INV,Pp,SIGP,RTI);
  t   := TH(Pp,RT,SIGP);
  IF t < 0.0008 THEN t := 0.0008 ;
  VMP := MATV(RT,t);
  MMP := RTI*VMP;
  t   := 1000*t;
  WRITELN(UITV,'Wallthickness of the propellant tanks:    t = ',t:3:2,' mm');
  WRITELN(UITV,'The mass of each propellant tank is  :   Mpt = ',MMP:4:3,' kg');

  {WEIGHT OF THE PRESSURANT TANKS}

  READ(INV,Ph,SIGL,SIGT,SIGM,tm,RKEV);
  tf  := (1/(SIGL+SIGT))*((Ph*1E+05*RP/1.01325) - 2*SIGM*tm);
  Rf1 := RP + tm/2;
  RF2 := RP + tm + tf/2;
  MMH := RKEV*(MATV(Rf1,tm) + MATV(Rf2,tf));
  tm  := 1000*tm;
  tf  := 1000*tf;
```

```
      WRITELN(UITV);
      WRITELN(UITV,'The wall thickness of the Helium tanks consists of ');
      WRITELN(UITV,'a)  t = ',tm:3:2,' mm  of TI-6A1-4V');
      WRITELN(UITV,'b)  t = ',tf:3:2,' mm  of Kevlar');
      WRITELN(UITV,'The mass of each Helium tank is       :  Mhet = ',MMH:4:3,' kg');
  END
  ELSE
  CLOSE(INV);
  CLOSE(UITV);
END.
```

The input.

The computer program TSAT.PAS can be used to calculate the important specifications of the system such as the radii of the tanks, the weight of the several parts. To use the program the input has to be in the format which follow below. The text between the parentheses may not be written in the input file INV1.DAT.


```
1488                     {apogee velocity increment}
300                      {specific impulse apogee kick}
521                      {orbit control velocity increment}
280                      {specific impulse orbit control}
20                       {attitude control velocity increment}
200                      {specific impulse attitude control}
0.8765E+03               {density of MMH}
1.4468E+03               {density of NTO}
15.7                     {normal operating pressure}
35 1103.0E+06 4.43E+03   {data concerning the propellant tanks}
600 1378E+06 29E+06 1103E+06 0.001 1.38E+03   {data concerning
                                               the pressurant
                                               tanks}.
```

The output.

The format of the output file UITV1.DAT is as follows :

UPS with specific impulses of:

a) apogee engine	: Iap	= 312.0 sec
b) orbit control thrusters	: Ioc	= 280.0 sec
c) attitude control thrusters	: Iac	= 200.0 sec

The dry mass of the satellite is	: Mdry	= 458.24 kg
The total mass of the satellite is	: Mtot	= 984.96 kg
The apogee propellant mass	: Map	= 411.18 kg
The orbit control propellant mass	: Moc	= 109.06 kg
The attitude control propellant mass	: Mac	= 6.46 kg
The estimated construction mass	: Mcon	= 44.24 kg
The total propulsion system mass is	: Mpro	= 570.96 kg

The volume of each propellant tank is:	Vprop	= 0.11686 m^3
This means a radius of	: r	= 0.303 m

The volume of each pressurant tank is:	Vpres	= 0.01681 m^3
This means a radius of	: r	= 0.15892 m

The required Helium mass is	: Mhe	= 1.69 kg
Wallthickness of the propellant tanks:	t	= 0.80 mm
The mass of each propellant tank is	: Mpt	= 4.097 kg

The wall thickness of the Helium tanks consists of
a) t = 1.00 mm of TI-6A1-4V
b) t = 5.12 mm of Kevlar
The mass of each Helium tank is   : Mhet = 2.785 kg

Trade-off.

The choice of the propulsion system in favour of the UPS is based on the data given below which are 2 outputs of the TSAT.PAS computer program. The differences were caused by the changed values of the specific impulses. The specific impulses of the UPS given below are different from the ones which were given above, because these are average (general) values and the other ones were specifications of a UPS with thrusters delivered by the Marquardt company.

UPS with specific impulses of:

a) apogee engine	: Iap	= 300.0 sec
b) orbit control thrusters	: Ioc	= 285.0 sec
c) attitude control thrusters	: Iac	= 175.0 sec

The dry mass of the satellite is	: Mdry	= 460.09 kg
The total mass of the satellite is	: Mtot	= 1008.76 kg
The apogee propellant mass	: Map	= 433.69 kg
The orbit control propellant mass	: Moc	= 107.59 kg
The attitude control propellant mass	: Mac	= 7.40 kg
The estimated construction mass	: Mcon	= 46.09 kg
The total propulsion system mass is	: Mpro	= 594.76 kg

<u>SOLID/MONO with specific impulses of:</u>

a) apogee engine   : Iap   = 285.0 sec
b) orbit control thrusters   : Ioc   = 235.0 sec
c) attitude control thrusters   : Iac   = 135.0 sec

The dry mass of the satellite is   : Mdry   = 470.75 kg
The total mass of the satellite is   : Mtot   = 1117.35 kg
The apogee propellant mass   : Map   = 498.94 kg
The orbit control propellant mass   : Moc   = 137.37 kg
The attitude control propellant mass : Mac   = 10.29 kg
The estimated construction mass   : Mcon   = 56.75 kg
The total propulsion system mass is   : Mpro   = 703.35 kg

As can be seen, these results all point in the direction of the UPS.

Number of apogee engines.

A trade-off among several possibilities for the number of apogee engines has been made with the help of the TSAT.PAS program. The options are as mentioned in section 11.2.3 with the belonging specific impulses.

<u>a) 1 * 490 N</u> : These specifications can be found in this appendix
                  in "**The output**"

<u>b) 4 * 110 N</u> : UPS with specific impulses of:

        a) apogee engine   : Iap   = 280.0 sec
        b) orbit control thrusters   : Ioc   = 235.0 sec
        c) attitude control thrusters   : Iac   = 135.0 sec

        The dry mass of the satellite is   : Mdry   = 469.12 kg
        The total mass of the satellite is   : Mtot   = 1125.30 kg
        The apogee propellant mass   : Map   = 509.03 kg
        The orbit control propellant mass   : Moc   = 136.89 kg
        The attitude control propellant mass : Mac   = 10.26 kg
        The estimated construction mass   : Mcon   = 55.12 kg
        The total propulsion system mass is   : Mpro   = 711.30 kg

<u>c) 4 * 22 N</u> : UPS with specific impulses of:

        a) apogee engine   : Iap   = 289.0 sec
        b) orbit control thrusters   : Ioc   = 235.0 sec
        c) attitude control thrusters   : Iac   = 135.0 sec

        The dry mass of the satellite is   : Mdry   = 467.14 kg
        The total mass of the satellite is   : Mtot   = 1099.73 kg
        The apogee propellant mass   : Map   = 486.06 kg
        The orbit control propellant mass   : Moc   = 136.31 kg
        The attitude control propellant mass : Mac   = 10.21 kg
        The estimated construction mass   : Mcon   = 53.14 kg
        The total propulsion system mass is   : Mpro   = 685.73 kg

<u>d) 4 * 10 N</u> : UPS with specific impulses of:

a) apogee engine	: Iap	= 285.0 sec
b) orbit control thrusters	: Ioc	= 235.0 sec
c) attitude control thrusters	: Iac	= 135.0 sec

The dry mass of the satellite is	: Mdry	= 468.00 kg
The total mass of the satellite is	: Mtot	= 1110.81 kg
The apogee propellant mass	: Map	= 496.01 kg
The orbit control propellant mass	: Moc	= 136.56 kg
The attitude control propellant mass	: Mac	= 10.23 kg
The estimated construction mass	: Mcon	= 54.00 kg
The total propulsion system mass is	: Mpro	= 696.81 kg

As can be seen, the masses are highly dependent on the specific impulses. It is clear that the 1 * 490 N configuration should be taken if there are no other requirements than that the mass should be as low as possible.

REFERENCES.

1 Management.

1.1 Brown, D.;
   Design of modular spacecraft, SOW & SPEC.
   Noordwijk, 1989, ESTEC.

1.2 Van Dolder, N.E.;
   Syllabus Project Operations,
   Amsterdam, 1990, Fokker Space & Systems B.V.

2 System engineering.

2.1 Brown, D.;
   Design of modular spacecraft, SOW & SPEC.
   Noordwijk, 1989, ESTEC.

3 Launcher and orbit dynamics.

3.1 Wakker, K.F.;
   Inleiding Ruimtevaarttechniek,
   Delft, may 1987.

3.2 Berlin, Peter;
   The geostationary satellite,
   Cambridge, 1988.

3.3 Agrawal, Brij N.;
   Design of geosynchronous spacecraft,
   Prentice Hall, 1986.

4 Configuration.

4.1 ARIANE IV user's manual.
   Arianespace.

4.2 Nieuwenhuizen, M.P.;
   lr37 Ruimtevaartconstructies.
   TU Delft, 1988.

5 Payload.

5.1 Agrawal, Brij N.;
   Design of Geosynchronous Spacecraft.
   Prentice-Hall, 1986.

5.2 Berlin, Peter.;
   The Geostationary Applications Satellite.
   Cambridge University Press, 1988.

5.3 Spacecraft engineering course notes.
   University of Southampton, Department of Aeronautics and
   Astronautics, July 1985.

5.4 Pritchard, Wilbur L. and Sciulli, Joseph A.;
     Satellite Communication System Engineering.
     Prentice-Hall, 1986.

5.5 Martin, James.;
     Communications Satellite Systems.
     Prentice-Hall, 1978.

5.6 Beni, P.;
     Determination of the G/T Figure of Merit of Ground Receiving
     Stations for Meteorological Satellites.
     ESA Journal, Volume 13, Number 2, 1989.

5.7 Maral, G and Bousquet, M.;
     Satellite Communications Systems.
     John Wiley & Sons Ltd., 1986.

6   Power.

6.1 Agrawal, Bry N.;
     Design of Geosynchronous Spacecraft,
     1986.

6.2 Rauschenbach, H.S.;
     Solar Cell Array Design Handbook,
     1980.

6.3 European Space Power,
     proceedings of the European space power conference in Madrid,
     ESA-SP-294, 1989.

6.4 Fourth ESTEC spacecraft power-conditioning seminar in Noordwijk,
     ESA-SP-186, 1982.

6.5 Photovoltaic Generators in Space,
     proceedings of the fourth European symposium in Cannes,
     ESA-SP-210, 1984.

6.6 Curtin, D.J.;
     Trends in Communications Satellites,
     1980.

6.7 Bargellini, P.L.;
     Communications Satellite Systems,
     1982.

7   Structure.

7.1 Nieuwenhuizen, M.P.;
     lr37 Ruimtevaartconstructies.
     TU Delft, 1988.

7.2 ARIANE IV user's manual.
     Arianespace.

7.3 Bruhn, E.F.;
     Analysis and design of flight vehicle structures.
     Tri State Offset Company, 1973.

7.4 Leissa, A.W.;
   Vibration of shells.
   Ohio State University, 1973, Columbus.

7.5 Leissa, A.W.;
   Vibration of plates.
   Ohio State University, 1969, Columbus.

7.6 Cruijssen, H.;
   Solar array subsystem design description.
   Amsterdam, Fokker Space & Systems B.V.

7.7 Kerstens, J.;
   Determination of the first eigenfrequencies and the optimal holddown point
   position for a four-point supported rectangular plate using the Rayleigh-
   Ritz method.
   Fokker, 1988, Amsterdam.

7.8 Harris, C.M. and Crede, C.E.;
   Shock and vibration handbook.
   Mac Graw-Mill book company, 1961.

7.9 Agrawal, Brij N.;
   Design of geosynchrous spacecraft.
   Prentice-Hall, Inc., 1986.

8   AOCS.

8.1 Wertz, James R.;
   Spacecraft attitude determination and control,
   Dordrecht, 1978, Computer Science Operations.

8.2 Teldix reaction and momentum wheels paper.

8.3 Flook, H.;
   Control moment gyro (CMG) application to spacecraft control and
   stabilization.
   Stevenage, England, august 1970, ESTEC.

8.4 Space dynamics for geostationary satellites,
   CNES, pg 620 and further.

8.5 Agrawall, Brij N.;
   Design of geosynchronous spacecraft,
   Prentice Hall, Inc., Engle wood cliffs, 1986.

8.6 Memorandum attitude sensors,
   Delft, 1988, TPD.

8.7 TPD.
   New sensors for attitude determination;
   Advanced technologies for spacecraft attitude control navigation and
   guidance,
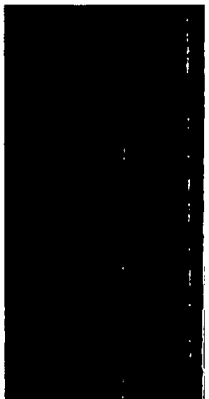   ESA workshop, 11, 12, 13, oct 1984, ESTEC.

8.8 2-Axis IRES for three-axis stabilized satellites,
ESA, SP-128.

8.9 Ferranti;
Trade off's in gyro package design using Ferranti 125 gyros,
ESA workshop, 11, 12, 13, oct 1988, ESTEC.

8.10 SAAB-SCANIA
Satellite attitude control and stabilisation using on-board computers
Goteborg, Sweden, july 1973, ESTEC.

9 Thermal control.

9.1 Wakker, K.F.;
Ruimtevaart techniek deel2.
TU Delft.

9.2 Agrawall, Brij N.;
Design of geosynchronous spacecraft,
Prentice Hall, Inc., Engle wood cliffs, 1986.

9.3 Gray, W.A., Muller, R.;
Engineering calculations in radiative heat transfer,
1974.

9.4 Olstad, Walter B.;
Heat transfer, thermal control and heat pipes,
1979.

9.5 Wiebelt, J.A.;
Engineering radiation heat transfer,
1966.

9.6 Collicott, H.E.;
Spacecraft thermal control, design, and operation.

9.7 Wong, H.Y.;
Handbook of essential formulae and data on heat transfer.

9.8 Lucas, J.W.;
Heat transfer and spacecraft thermal control; AIAA.

10 Telemetry and telecommand.

10.1 Study and simulation of an on-board computer for a satellite
volume 1.
ESRO-CERS contractor report March 1972.

10.2 Study and simulation of an on-board computer for a satellite
volume 2.
ESRO-CERS contractor report March 1972.

10.3 Transponder/receiver study for the NEMD project spacecraft.
ESRO-CERS final report Sept. 1973.

10.4 Study on omnidirectional satellite antenna for telemetering and tracking
in the UHF band.
ESRO-CERS final report May 1972.

10.5 Design, construction, and testing of an S-band telemetry transmitter.
ESRO-CERS final report Sept. 1973.

10.6 Stiltx, Harry L.;
Aerospace Telemetry vol 1.
Prentice-Hall Space Technology series.

10.7 Stiltz, Harry L.;
Aerospace Telemetry vol 2.
Prentice-Hall Space Technology series.

10.8 Regtien, P.P.L.;
Instrumentele Electronica.
Delftse U.M. 1987.

10.9 Prof. ir. Reyns;
Lecture notes on "Informatiesystemen en electrische energievoorziening in
de ruimtevaart".
Juni 1983.

10.10 Report LR 558, Project Aeneas.
Delft University of Technology, July 1988.

10.11 Berlin, P;
The Geostationary Applications Satellite.
Cambridge Aerospace series 1988.

10.12 Spacecraft Engineering Course Notes.
University of Southampton.
Department of Aeronautics and Astronautics, July 1985.

11   Propulsion.

11.1 Agrawal Brij N.;
Design of Geosynchronous Spacecraft.
Prentice-Hall Inc., Englewood Cliffs, 1986.

11.2 Anderson J.E. and Dugan D.W.;
"A feasibility of developing toroidal tanks for a spinning spacecraft".
AIAA, 1974-1154, p.3.

11.3 Bassewirz H.V.;
Ariane-Passenger-Experiment (APEX), Planungsstudie,
MBB, M+nchen, oktober 1976.

11.4 Bonhomme R. and Steels R.,
"Development and application of new technologies in ESA's Olympus
programme".
ESA journal, vol.8, 1984, p.358-363.

11.5 Bouloumi+ J.P. and Cable N.;
Catalogue of European pyrotechnic devices for use in space,
ESA Scientific Technical Publications Branch,
Noordwijk, Netherlands, 1982.

11.6 Hearn H.C.;
     "Evaluation of bipropellant pressurization concepts for spacecraft".
     Journal of spacecraft and rockets, vol.19, p.323.

11.7 Jansen D.P.L.F. and Kletzkine Ph.;
     "Preliminary Design for a 3 kN Hybrid Propellant Engine".
     ESA Journal,vol.88/4, 1988, p.421-439.

11.8 Rocket engines and propulsion systems. '
     The Marquardt Company (Ferranti Defense & Space),
     Van Nuys, California, 1985.

11.9 Rollins J.R. and Hobbs L.W.;
     "Design and qualification of the EUROSTAR propellant tank".
     AIAA, 1986-1659, p.2.

907230